MONASH University

INVESTIGATION OF NEUROPROTECTIVE AND NEUROTROPHIC EFFECTS OF EDIBLE BIRD'S NEST IN PARKINSON'S DISEASE MODELS

YEW MEI YENG

Bachelor of Science (Honours) Biomedical Science

A thesis submitted for the degree of Doctor of Philosophy at

Monash University in 2018

Jeffrey Cheah School of Medicine and Health Sciences

SUPERVISORS

Main supervisor: **Dr. Ng Khuen Yen**

Brain Research Institute Monash Sunway,

Jeffrey Cheah School of Medicine and Health Sciences,

Monash University Malaysia,

Jalan Lagoon Selatan,

47500 Bandar Sunway,

Selangor Darul Ehsan, Malaysia.

Co-supervisors: **Professor Dr. Iekhsan Othman**

Jeffrey Cheah School of Medicine and Health Sciences,

Monash University Malaysia,

Jalan Lagoon Selatan,

47500 Bandar Sunway,

Selangor Darul Ehsan, Malaysia.

Dr. Koh Rhun Yian

Division of Applied Biomedical Science and Biotechnology,

School of Health Sciences,

International Medical University,

No.126, Jalan Jalil Perkasa 19,

Bukit Jalil, 57000 Kuala Lumpur,

Wilayah Persekutuan Kuala Lumpur, Malaysia.

COPYRIGHT NOTICE

© The author (2018).

I certify that I have made all reasonable efforts to secure copyright permissions for third-party content included in this thesis and have not knowingly added copyright content to my work without the owner's permission.

THESIS INCLUDING PUBLISHED WORKS DECLARATION

I hereby declare that this thesis contains no material which has been accepted for the award of any other degree or diploma at any university or equivalent institution and that, to the best of my knowledge and belief, this thesis contains no material previously published or written by another person, except where due reference is made in the text of the thesis.

This thesis includes one original papers published in peer reviewed journals and three manuscripts (under review). The core theme of the thesis is the investigation of neuroprotective and neurotrophic effects of edible bird's nest in the interest of treatment of Parkinson's disease. The ideas, development and writing up of all the papers in the thesis were the principal responsibility of myself, the student, working within the Jeffrey Cheah School of Medicine and Health Sciences under the supervision of Dr. Ng Khuen Yen.

The inclusion of co-authors reflects the fact that the work came from active collaboration between researchers and acknowledges input into team-based research.

In the case of Chapter 3-6, my contribution to the work involved the following:

Thesis Chapter	**Publication Title**	**Status**	**Nature and % of student contribution**	**Co-author name(s) Nature and % of Co-author's contribution**	**Co-author(s), Monash student**
3	Edible bird's nest ameliorates oxidative stress-induced apoptosis in SH-SY5Y human neuroblastoma cells	Published	55%. Conception of study, experimentation, data collection, preparation of manuscript.	1) RhunYian Koh, Conception of study, data analysis, input into manuscript 20% 2) Iekhsan Othman, Conception of study, input into manuscript 5% 3) SoiMoi Chye, Conception of study 5% 4) KhuenYen Ng, Conception of study, data analysis, input into manuscript 15%	1) No 2) No 3) No 4) No

4	Edible bird's nest extracts confer neurotrophic effects by enhancing proliferation, migration and neurogenesis of neural stem cell *in vitro*	Submitted	55%. Conception of study, experimentation, data collection, preparation of manuscript.	1) RhunYian Koh, Conception of study, data analysis, input into manuscript 20% 2) Iekhsan Othman, Conception of study, input into manuscript 5% 3) SoiMoi Chye, Conception of study 5% 4) KhuenYen Ng, Conception of study, data analysis, input into manuscript 15%	1) No 2) No 3) No 4) No
5	Edible bird's nest improves motor behavior and protects dopaminergic	Submitted	55%. Conception of study, experimentation, data collection, preparation of	1) RhunYian Koh, Conception of study, data analysis, input into manuscript 10%	1) No 2) No 3) No 4) No 5) No 6) No

	neuron in Parkinson's disease mouse model against oxidative and nitrosative stress		manuscript.	2) Iekhsan Othman, Input into manuscript 5% 3) SoiMoi Chye, Conception of study 5% 4) Tomoko Soga, Experimentation, input into manuscript 15% 5) Ishwar Parhar, Input into manuscript 5% 6) KhuenYen Ng, Conception of study, data analysis, input into manuscript 5%	
6	*De novo* sequencing-assisted peptide profiling and antioxidant	Submitted	55%. Conception of study, experimentation, data collection, preparation of	1) RhunYian Koh, Conception of study, data analysis, input into manuscript 10%	1) No 2) No 3) No 4) No

	study of edible bird's nest extracts		manuscript.	2) Iekhsan Othman, Conception of study, input into manuscript 15% 3) Syafiq Asnawi Zainal Abidin, Experimentation, input into manuscript 5% 4) SoiMoi Chye, Conception of study 5% 5) KhuenYen Ng, Conception of study, data analysis, input into manuscript 10%	

I have not renumbered sections of submitted or published papers in order to generate a consistent presentation within the thesis.

Student signature: [redacted] **Date:** 15th May 2018

The undersigned hereby certify that the above declaration correctly reflects the nature and extent of the student's and co-authors' contributions to this work. In instances where I am not the responsible author I have consulted with the responsible author to agree on the respective contributions of the authors.

Main Supervisor signature: 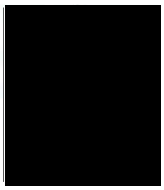 **Date:** 15th May 2018

ACKNOWLEDGEMENT

I would like to thank my supervisory panel, including main supervisor Dr. Ng Khuen Yen, and co-supervisors Professor Iekhsan Othman and Dr. Koh Rhun Yian, for their relentless efforts in guiding, advising and encouraging me throughout the candidature period. Their insightful feedbacks on my work have improved my research output significantly, hence the production of this important piece of thesis. Their professionalism at work has shaped me into an independent and focussed person with critical-thinking skill. These attributes will be my biggest takeaway values after the candidature. I would also like to express my gratitude to the reviewer panels, Dr. Tang Kim San, Associate Professor Md Ezharul Hoque Chowdhury, Associate Professor Tomoko Soga and Associate Professor Rakesh Naidu who have selflessly contributed their feedback during the annual progress review session.

I also appreciate the scholarship granted from Monash University Malaysia, which definitely has given me the financial flexibility to pursue postgraduate study by research. Many thanks to the technical and administrative support given by the staffs and officers from the Jeffrey Cheah School of Medicine and Health Sciences, and School of Pharmacy, who have helped me numerous times in ensuring swift experiment and timely completion of administrative work.

I am truly grateful for having friendly, supportive and helpful lab mates; Saatheeyavaane, Sonia Phang, Felix Kevin, Vanessa Lee, Alexis, Nur Izyani, Adzzie, Pei

Ling, Pei Ying, Owen Teo, Yi Yang and many others, thank you for being with me all these while and I wish you all the best in your candidature.

Lastly, I would like to dedicate my deepest appreciation to my dearest family. Thank you for your timeless patience and encouragement as I stumbled across many challenges during my candidature. I would not have completed this thesis without your unconditional love and support.

TABLE OF CONTENTS

Supervisors i

Copyright ii

Thesis including published works declaration iii

Acknowledgement ix

List of figures xv

List of tables xviii

Abbreviations xix

Abstract xxii

Chapter 1: Introduction and general objectives 1

1.1 Introduction 2

1.2 General objectives of the study 5

1.3 References 6

Chapter 2: Literature review 8

2.1 Parkinson's disease 9

2.1.1 Introduction 9

2.1.2 Progression and staging of PD 10

2.1.3 Aetiology and pathogenesis of PD 11

2.1.3.1 Oxidative stress 15

2.1.3.2 Neuroinflammation 17

2.1.3.3 Mitochondrial dysfunction 18

2.1.3.4 Apoptosis 20

2.1.3.5 Proteinopathy 21

2.1.3.6 Ferroptosis 22

2.1.4 Changes in motor circuitry in PD 23

2.1.5 Current treatment options for PD: Pitfalls and future 26

2.1.6 The need for multifaceted treatment in PD 30

2.2 Edible bird's nest 32

2.2.1 Production and origin 32

2.2.2 Traditional value of EBN 33

2.2.3 Compositional make-up of EBN 34

2.2.4 Bioactivity studies of EBN 34

2.2.5 EBN as a natural source of bioactive compounds 37

2.2.5.1 Bioactive compounds identified in EBN 38

2.2.5.1.1 Sialic acid 38

2.2.5.2 Potential neuroprotective and neurotrophic compounds in EBN 39

2.2.5.2.1 Epidermal growth factor 39

2.2.5.2.2 Melatonin 40

2.2.5.2.3 Vascular endothelial growth factor 43

2.3 Tandem mass spectrometry for proteomic study 45

2.3.1 Database search versus *de novo* sequencing 45

2.3.2 Proteomic studies of EBN 48

2.4 References 51

Chapter 3: Edible bird's nest ameliorates oxidative stress-induced apoptosis in SH-SY5Y human neuroblastoma cells 74

3.1 Summary of Chapter 3 75

3.2 Published paper 77

Chapter 4: Edible bird's nest extracts confer neurotrophic effects by enhancing proliferation, migration and neurogenesis of neural stem cell *in vitro* 89

4.1Summary of Chapter 4 90

4.2 Manuscript 91

4.3 References 114

Chapter 5: Edible bird's nest improves motor behavior and protects dopaminergic neuron in Parkinson's disease mouse model against oxidative and nitrosative stress 120

5.1 Summary of Chapter 5 121

5.2 Manuscript 123

5.3 References 157

Chapter 6: *De novo* sequencing-assisted peptide profiling and antioxidant study of edible bird's nest extracts 163

6.1 Summary of Chapter 6 164

6.2 Manuscript 165

6.3 References 221

Chapter 7: Discussions, general conclusion, future works and recommendations 268

7.1 Discussion 269

7.1.1 Possible links between EBN protein and effects seen in NSC and animal studies 269

7.1.2 Rationale of using EBN as a nutraceutical option for PD 270

7.1.3 Protein across blood-brain-barrier? 271

7.2 General conclusion of the study 272

7.3 Future works and recommendations 273

7.3.1 Purification of bioactive compound and characterization of novel compound 273

7.3.2 Study on alternative PD model 275

7.4 References 277

Publication 282

Appendix **283**

LIST OF FIGURES

Chapter	Figure Number and Title	Page Number
2	Figure 2.1. Schematic diagram of molecular mechanisms underlying the pathogenesis of PD	15
	Figure 2.2. Partial reduction of oxygen leads to formation of ROS	20
	Figure 2.3. The direct and indirect pathway of the basal ganglia motor circuit	25
	Figure 2.4. Basal ganglia-thalamo-cortical circuit under normal condition and PD	26
3	Figure 1 Cytotoxic effect of EBN extracts on SH-SY5Y cells	81
	Figure 2 Effect of EBN extracts on morphological and nuclear changes of 6-OHDA-challenged SH-SY5Y cells	82
	Figure 3 Effect of EBN extracts on 6-OHDA-challenged SH-SY5Y cell viability	83
	Figure 4 Effect of EBN extracts on intracellular reactive oxygen species (ROS) production in 6-OHDA-challenged SH-SY5Y cells	83
	Figure 5 Effect of EBN extracts on 6-OHDA-induced apoptosis	84
	Figure 6 Effect of EBN extracts on mitochondrial membrane potential (MMP) in 6-OHDA-challenged SH-SY5Y cells	85
	Figure 7 Effect of EBN extracts on cleavage of caspase-3 in SH-SY5Y cells challenged with 6-OHDA	86

4	Fig.1 Cytotoxic effect of EBN extracts on NE-4C	100
	Fig.2 Cell cycle profiling of EBN-treated NE-4C	102
	Fig.3 BrdU incorporation in EBN-treated NE-4C	104
	Fig.4 Cell migration studies in EBN-treated NE-4C	105
	Fig.5 Cell differentiation studies in NE-4C	107
	Fig.6 Neuronal differentiation in retinoic acid-primed NE-4C	108
	Fig.7 Neuronal differentiation after EBN extract treatments in retinoic acid-primed NE-4C	109
5	Fig. 1. Body weight of animal subjects across 4 weeks of oral treatment with EBN	135
	Fig. 2. H&E staining of lung, heart, liver, kidney and spleen sections from control mice, mice fed with S1 at 20 mg/kg, S1 at 100 mg/kg, S2 at 20 mg/kg and S2 at 100 mg/kg	139
	Fig. 3. Behavioral tests were applied to examine the locomotor activity of treated mice	141
	Fig. 4. Immunohistological studies of dopaminergic neurons in substantia nigra	145
	Fig. 5. Immunohistological studies of GPX1-positive and CD11b-positive neurons in substantia nigra of PD mice	146
	Fig. 6. NO production and lipid peroxidation assessment in PD cell model	147
6	Fig.1. Venn diagram of proteins identified from raw EBN powder and water extract of EBN	205
	Fig.2. Antioxidant capacity of EBN and standard as evaluated by	217

	(A) DPPH radical scavenging assay, (B) FRAP assay and (C) metal chelating assay	

LIST OF TABLES

Chapter	Table Number and Title	Page Number
5	Table 1. Blood biochemistry of animal subjects after 28 days of treatment with EBN crude and water extracts	136
	Table 2. Organ weight of animal subjects	139
	Table 3. Number of grid crossing and number of rear bouts of mice in open field test	143
6	Table 1. List of proteins detected in the in-solution digests of raw EBN	175
	Table 2. List of proteins detected in the in-solution digests of water extract of EBN	191
	Table 3. Proteins identified in EBN, their biological function and (possible) implication in other EBN studies	211
	Table 4. Matched information from Swiss-Prot for uncharacterized EBN proteins predicted by *de novo* sequencing	215
	Supplementary File 1 - complete list of peptide sequences and m/z values of raw EBN powder	228
	Supplementary File 1 - complete list of peptide sequences and m/z values of EBN water extract	251

ABBREVIATIONS

6-OHDA: 6-hydroxydopamine

ATP: Adenosine triphosphate

BBB: Blood-brain-barrier

BDNF: Brain-derived neurotrophic factor

BrdU: 5-bromo-2′-deoxyuridine

DBS: Deep brain stimulation

DJ-1: Parkinson disease protein 7.

DNA**:** Deoxyribonucleic acid

EBN: Edible bird's nest

EGF: Epidermal growth factor

EGFR: Epidermal growth factor receptor

FDA: Federal Drug Administration

FDR: False discovery rate

GDNF: Glial cell-derived growth factor

GNPS: Global Natural Products Social Molecular Networking

GPe: External globus pallidus

GPi: Internal globus pallidus

GWAS: Genome wide association studies

H_2O_2: Hydrogen peroxide

IFN: Interferon

IL: Interleukin

MAO: Monoamine oxidase

MAPK: Mitogen-activated protein kinases

MPTP: 1-methyl-4-phenyl-1,2,5,6-tetrahydropyrine PD

MS/MS: Tandem mass spectrometry

NCAM: Neural cell adhesion molecules

Neu5Ac: N-acetyl-D-neuraminic acid

NMR: Nuclear magnetic resonance

NSC: Neural stem cell

PINK1: PTEN-induced putative kinase *1*

PTM: Post-translational modifications

RNS: Reactive nitrogen species

ROS: Reactive oxygen species

SNCA: Alpha-synuclein

TNF: Tumor necrosis factor

UCH-L1: Ubiquitin carboxy-terminal hydrolase L1

UPS: Ubiquitin-proteasome system

VEGF: Vascular endothelial growth factor

Abstract

Parkinson's disease (PD) is the world's second most common progressive neurodegenerative disorder characterized by the loss of nigrostriatal dopaminergic neurons and intra-neuronal presence of protein inclusions known as Lewy bodies. PD impacts the quality of life in elderly due to deterioration of motor and cognitive skills. Public interest in complementary medicine has prompted the exploration of natural product for therapeutic application. Edible bird's nest (EBN), product made of swiftlet's saliva, is investigated herein due to potential presence of neuroprotective and neurotrophic bioactive compounds. Using neuronal cell model of PD, we demonstrated that EBN ameliorated degeneration of dopaminergic neurons by counteracting with the apoptosis caused by oxidative stress and nitrosative stress. EBN also possessed neurotrophic effect by promoting proliferation, migration and neurogenesis of neural stem cell. Our experiment with PD mouse model further illustrated the benefits of EBN in improving motor functions through antioxidative and anti-inflammatory mechanisms. Comprehensive protein profile of EBN acquired with bioinformatics tools have identified potential bioactive compounds implicated in immunity, extracellular matrix formation, neurodevelopment, cell survival and apoptosis, cell proliferation and migration, antioxidation, and common cellular processes. The study suggests that EBN may be further investigated for its nutraceutical application on neurodegenerative diseases.

Chapter 1

Introduction and general objectives

1.1 Introduction

Parkinson's disease (PD) is a progressive neurodegenerative disease affecting more than 1% of the population over 60 years of age (Farrer, 2006). Pathologically, there is loss of dopaminergic neurons in the substantia nigra which subsequently causes dopamine depletion in the striatum of the midbrain (Dauer and Przedborski, 2003). Dopamine depletion ultimately leads to deterioration of motor function, as seen in most PD patients (Snyder and Adler, 2007). For instance, patients of this disorder are manifested with clinical signs such as tremor, rigidity and bradykinesia. In addition, aggregation of abnormal α-synuclein protein known as Lewy bodies is also detected in surviving neurons (Przedborski, 2005). In Malaysia, around 15,000 individuals are affected by PD (Malaysian Parkinson's Disease Association, 2010). The disease itself is not fatal, yet the country's economic burden due to medical care and morbidity associated with the disease has raised much concern from the public.

Several etiologies have been proposed for the pathogenesis of PD including oxidative stress, neuroinflammation, mitochondrial dysfunction, failure of ubiquitin-proteasome system (UPS), apoptosis and proteinopathy. To date few conventional treatments have been made available to PD patients, namely the use of drug Levodopa and surgical manipulation through deep brain stimulation. However, these treatment options are prone to drug-induced side effects, and have limited application due to inconsistent clinical outcome. Despite a variety of therapies are available, the progressive nature of PD is yet to be tackled. As such, current strategy for treatment development focuses on slowing down disease progression through the promotion of neuroprotective mechanism and neuron regeneration.

Edible bird's nest (EBN) is natural food product made from saliva of the swiftlets, specifically by the genus Aerodramus. Chinese being the largest consumer usually prepared EBN in soup and regard it as delicacy with substantial medicinal value. Traditionally, EBN has been used for its tonic effect towards complications in the respiratory airways and gastrointestinal system. In addition to that, EBN is also well-sought after for claims such as ability to enhance skin complexion, immunity, growth, metabolism and blood circulation (Lim and Cranbrook, 2002).

Increasing public interest on the benefits of EBN has prompted evidence-based research on its bioactivity. Notably, numerous *in vitro* and *in vivo* studies have shown that EBN was able to boost immunity, promote cell division and proliferation, neutralize influenza activity, as well as prevent osteoporosis (Ng et al., 1986, Kong et al., 1987, Guo et al., 2006, Matsukawa et al., 2011). The bioactive compounds responsible for some of the effects mentioned were suggested and identified. This indicates that EBN may be a rich source of animal-derived natural compound that may offer health advantage.

EBN consists mainly of proteins, carbohydrates, ash, lipid and impurities (Marcone, 2005). Studies have reported that protein is the major content of EBN, which represents around 60% of the net weight (Kathan and Weeks, 1969, Marcone, 2005). Protein in EBN exists in two forms: simple protein and glycoprotein. A total of eighteen types of amino acids with aspartic acid and serine as the major amino acids were found in EBN (Kathan and Weeks, 1969). Studies have also discovered potent compound such as epidermal growth factor (EGF)-like compound and sialic acid in EBN (Kong et al., 1987, Yagi et al., 2008). Both EGF and sialic acid are neurotrophic factors known to promote neuron and brain development. Nonetheless, neuroprotective compound may also present because

animal saliva was previously found to contain vascular endothelial growth factor (VEGF) and melatonin (Voultsios et al., 1997, Pammer et al., 1998a). These are compounds powered with anti-apoptotic and antioxidant properties.

Overall, literature suggests that EBN might confer neuroprotective and neurotrophic effects due to possible presence of a number of bioactive compounds. Hence this study aimed to investigate the neuroprotective effect of EBN in *in vitro* neuronal cell model of PD, and its potential to affect proliferation and migration as well as to stimulate neurogenesis in cultured neural stem cell. The study also evaluated the effect of EBN oral supplementation on motor function and neurochemistry in PD mouse model. Lastly, proteomic study of the EBN was carried out to identify bioactive proteins that may be relevant to the effect of EBN in current study. The findings of this study will support the potential nutraceutical application of EBN in favour of the treatment of PD.

1.2 General objectives of the study

The study was carried out with the following objectives:

1. To evaluate the neuroprotective effects of EBN on 6-hydroxydopamine (6-OHDA)-challenged neuronal cell line.

2. To investigate the neurotrophic effects of EBN on the proliferation, migration and differentiation of neural stem cells.

3. To investigate the effects of EBN on the motor behaviour and neurochemistry in PD mouse model.

4. To identify bioactive compound from EBN relevant to its neuroprotective and neurotrophic effects.

1.3 References

DAUER, W. & PRZEDBORSKI, S. 2003. Parkinson's Disease: Mechanisms and Models. *Neuron,* 39**,** 889-909.

FARRER, M. J. 2006. Genetics of Parkinson disease: paradigm shifts and future prospects. *Nat Rev Genet,* 7**,** 306-18.

GUO, C. T., TAKAHASHI, T., BUKAWA, W., TAKAHASHI, N., YAGI, H., KATO, K., HIDARI, K. I., MIYAMOTO, D., SUZUKI, T. & SUZUKI, Y. 2006. Edible bird's nest extract inhibits influenza virus infection. *Antiviral Res,* 70**,** 140-6.

KATHAN, R. H. & WEEKS, D. I. 1969. Structure studies of collocalia mucoid. I. Carbohydrate and amino acid composition. *Arch Biochem Biophys,* 134**,** 572-6.

KONG, Y. C., KEUNG, W. M., YIP, T. T., KO, K. M., TSAO, S. W. & NG, M. H. 1987. Evidence that epidermal growth factor is present in swiftlet's (Collocalia) nest. *Comp Biochem Physiol B,* 87**,** 221-6.

LIM, C. K. & CRANBROOK, E. O. 2002. *Swiftlets of Borneo – Builders of edible nests* Sabah, Malaysia, Natural History Publication (Borneo) SDN., B.H.D. .

MARCONE, M. F. 2005. Characterization of the edible bird's nest the "Caviar of the East". *Food Research International,* 38**,** 1125-1134.

MATSUKAWA, N., MATSUMOTO, M., BUKAWA, W., CHIJI, H., NAKAYAMA, K., HARA, H. & TSUKAHARA, T. 2011. Improvement of bone strength and dermal thickness due to dietary edible bird's nest extract in ovariectomized rats. *Biosci Biotechnol Biochem,* 75**,** 590-2.

NG, M. H., CHAN, K. H. & KONG, Y. C. 1986. Potentiation of mitogenic response by extracts of the swiftlet's (Collocalia) nest. *Biochem Int,* 13**,** 521-31.

PAMMER, J., WENINGER, W., MILDNER, M., BURIAN, M., WOJTA, J. & TSCHACHLER, E. 1998a. Vascular endothelial growth factor is constitutively expressed in normal human salivary glands and is secreted in the saliva of healthy individuals. *J Pathol,* 186**,** 186-91.

PRZEDBORSKI, S. 2005. Pathogenesis of nigral cell death in Parkinson's disease. *Parkinsonism Relat Disord,* 11 Suppl 1**,** S3-7.

SNYDER, C. H. & ADLER, C. H. 2007. The patient with Parkinson's disease: part I-treating the motor symptoms; part II-treating the nonmotor symptoms. *J Am Acad Nurse Pract,* 19**,** 179-97.

VOULTSIOS, A., KENNAWAY, D. J. & DAWSON, D. 1997. Salivary Melatonin as a Circadian Phase Marker: Validation and Comparison to Plasma Melatonin. *Journal of Biological Rhythms,* 12**,** 457-466.

YAGI, H., YASUKAWA, N., YU, S. Y., GUO, C. T., TAKAHASHI, N., TAKAHASHI, T., BUKAWA, W., SUZUKI, T., KHOO, K. H., SUZUKI, Y. & KATO, K. 2008. The expression of sialylated high-antennary N-glycans in edible bird's nest. *Carbohydr Res,* 343**,** 1373-7.

Chapter 2

Literature review

2.1 Parkinson's disease

2.1.1 Introduction

Neurodegenerative diseases are the disorders of the nervous system characterized by progressive loss of structure or function of the neurons. Degeneration or death of the neurons gradually causes down-sizing of the neuronal network. Alzheimer's disease, PD and Huntington's disease are some of the most well-known neurodegenerative diseases that share some common pathologies, such as the presence of abnormal protein aggregates and the atrophy of the affected brain region due to structural loss of neurons (Ross and Poirier, 2004).

As an age-related disease, PD affects primarily people of 60 years old and above. Global prevalence of PD is only second to the top-listed neurodegenerative disorder, the Alzheimer's disease. According to the estimation by Malaysian Parkinson's Diseases Association, around 15,000 Malaysian is affected by PD. PD affects neurons project from substantia nigra in the midbrain to the striatal caudate-putamen in the forebrain, particularly dopaminergic neurons (Dauer and Przedborski, 2003). Another pathological hallmark of PD is the presence of Lewy bodies, an intraneuronal inclusion or aggregate of mutated protein. Specific to the disease's progression, Lewy bodies reside in the cytoplasm. They result from aggregation of several different proteins namely Parkin, ubiquitin and neurofilaments, but they mainly consist of mutant α-synuclein (Przedborski, 2005).

Patient of PD suffers from resting tremor, rigidity, slow movement and response, as well as postural instability (Snyder and Adler, 2007). The main

cause for impairment in motor skills is claimed by a significant drop in the dopamine pool, the neurotransmitter that relays electrochemical signals between nerve cells and promotes movement, in the striatum of the midbrain. When 60-80% dopamine-secreting neuron in the substantia nigra pars compacta is degenerated, respective nerve terminals in the striatum is subsequently affected. Involvement of the dopaminergic nigrostriatal pathway is not alone in the pathogenesis of PD, as non-dopaminergic systems such as noradrenergic, serotonergic and cholinergic systems may be affected as well, which contributes to non-motor symptoms experienced by PD patients (Ziemssen and Reichmann, 2007). Olfactory dysfunction, cognitive impairment, depression, dysautonomia and sleep disturbances are some of the examples. These complications have significant impact on health and life quality on not just the patients itself, but also on their family due to the enormous financial medical burden.

2.1.2 Progression and staging of PD

Progressive degeneration of neuromelanin-containing neurons in the dopaminergic-concentrated region of the brain is age-related and the manifestation of motor syndromes in PD patient follows marked loss of neurons (Reeve et al., 2014). According to Braak staging, distribution of Lewy bodies can be used as a parameter to determine severity of PD (Braak et al., 2003, Braak et al., 2004). Stage 1 and 2 are considered preclinical stages whereby the disease only affects olfactory bulb and PD is less likely to be diagnosed as early as at this stage. As neurodegeneration develops in lower brain stem, patients will experience autonomic disturbances and sleeplessness.

Then, as PD enters stage 3 and 4 patients will develop neuronal loss in substantia nigra follows by further loss in deep nuclei of the midbrain and the forebrain, which significantly affect their motor skill. At stage 5 and 6, or generically known as advanced PD, as limbic system and neocortex are involved, cognitive and psychiatric symptoms often appear alongside severe motor disability.

2.1.3 Aetiology & pathogenesis of PD

About 95% of PD cases are idiopathic while familial PD is only recognized recently after it was noticed that first degree relatives of PD patients had two-fold risk to develop the same disorder (Tan and Skipper, 2007). It is evident, although in rare cases, that genetic linkage plays a part in PD pathogenesis. Specifically, five genes have been extensively studied and mutations at these gene loci are directly associated with protein abnormalities, which include α-synuclein, Parkin, LRRK2, DJ-1 and PINK1 (Ross and Poirier, 2004).

Missense mutations in the α-synuclein gene (SNCA), including A30P, E46K and A53T, have been linked to autosomal dominant form of PD, a rare early-onset PD. Triplication of the SNCA gene was found to be associated with rapid progression and more extended neurodegeneration in PD (Venda et al., 2010). Lately, genome wide association studies (GWAS) has revealed strong correlation of common single nucleotide polymorphism within the SNCA locus and PD incidence (Saiki et al., 2012). At the molecular level, aggregates of mutant α-synuclein have been detected in neuronal cells both in *in vitro* and *in vivo* settings whilst transgenic mice has demonstrated signs of

neurodegeneration, which includes neuronal inclusions and mitochondrial abnormalities (Giasson et al., 2000, Kruger et al., 2002, Saiki et al., 2012). It is suggested that mutant α-synuclein-induced macroautophagy may have caused both non-cell autonomous cell death and cell autonomous cell death in dopaminergic neurons of the substantia nigra(Saiki et al., 2012)

On the other hand, mutation in the Parkin (PARK2) gene is linked to a form of autosomal recessive juvenile PD (Kitada et al., 1998). The patient of this form of PD develops dystonia as part of the clinical symptoms and Lewy bodies are not commonly found pathologically (Eriksen et al., 2003). Parkin is essentially an E3 ubiquitin ligase which helps to bind substrates for the UPS during the process of protein degradation. Interestingly, Parkin was found to associate with the maintenance of mitochondrial function. Specifically, Parkin and PINK1 work synergistically to label functionally impaired mitochondria for degration by autophagy (Saiki et al., 2012).

LRRK2 or the leucine rich repeat kinase 2 (PARK8) gene is implicated in the most common hereditary form of PD. At least 20 missense or nonsense mutations have been identified for this autosomal dominant disease, in which G2019S mutation represented a major pool of both hereditary and sporadic late-onset PD (Cookson, 2010, Saiki et al., 2012). The mutation was hypothesized to cause neurite retraction via actin cytoskeleton remodeling (Chan et al., 2011). Furthermore, G2019S mutation inhibited activity of human peroxiredoxin 3, a mitochondrial member of antioxidant family of thioredoxin

peroxidases, consequently leading to ROS production and mitochondrial-mediated cell death mechanism (Angeles et al., 2011).

Three missense mutations in the DJ-1 (PARK7) gene, including L166P, M26I and E64D, have been implicated in an early onset autosomal recessive juvenile form of parkinsonism presented with scoliosis, blephalospasm and psychiatric symptoms. DJ-1 is a protein that attenuates mitochondrial oxidative stress by up-regulating the expression of the antioxidant enzyme superoxide dismutase (Bonifati et al., 2003). It has been demonstrated in knockdown experiments that, loss of function of DJ-1 exposed neuronal cells to oxidative stress-induced mitochondrial damage (Yokota et al., 2003, Bonifati et al., 2003).

An early-onset, autosomal recessive form of PD may also be associated with loss of function in PINK1 (PTEN-induced putative kinase 1 or PARK6) gene (Valente et al., 2004). PINK1 is a serine–threonine kinase involved in regulating mitochondrial dynamics (Eriksen et al., 2005). Pathological mutations in PINK1 have been reported to render cell susceptible to oxidative stress and subsequently resulting in mitochondrial elimination via macroautophagy (Pridgeon et al., 2007, Saiki et al., 2012).

Several mechanisms at the cellular and molecular level have been explored in depth to better understand PD, as illustrated in Figure 2.1. Among all, oxidative imbalance, neuroinflammation, mitochondrial dysfunction, apoptotic events and proteinopathy are the proposed cardinal causes of PD.

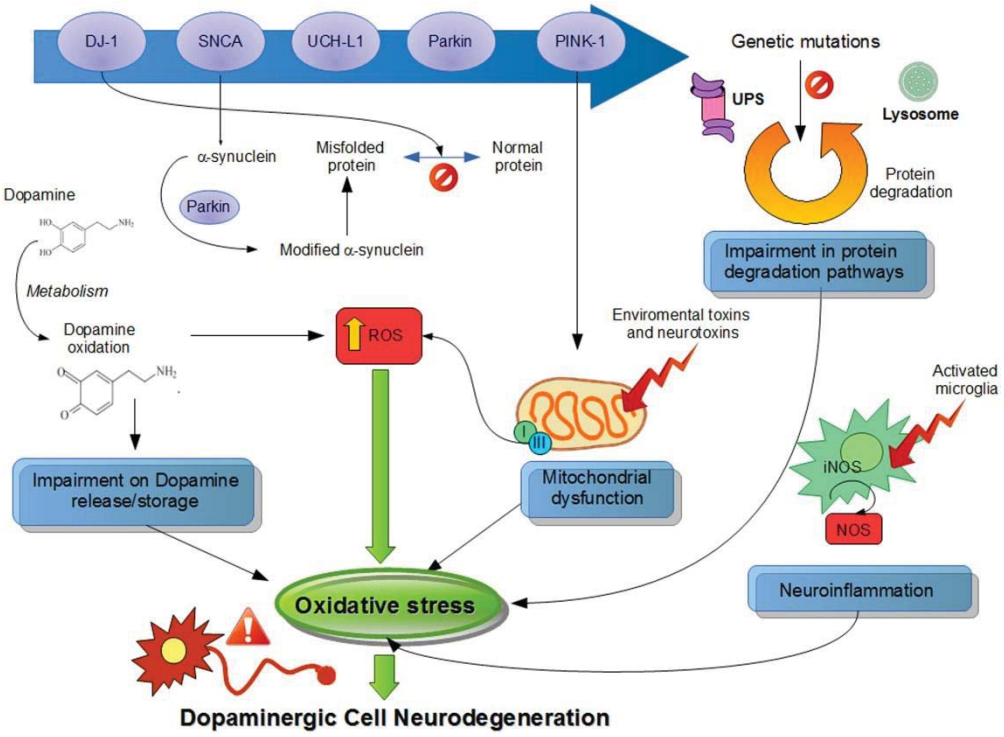

Figure 2.1. Schematic diagram of molecular mechanisms underlying the pathogenesis of PD. DJ-1: Parkinson disease protein 7. SNCA: alpha-synuclein gene. UCH-L1: Ubiquitin carboxy-terminal hydrolase L1. PINK1: PTEN-induced putative kinase 1. UPS: ubiquitin–proteasome system. iNOS: Inducible nitric oxide synthase. NOS: Nitric oxide synthase. Adapted from published image (Blesa et al., 2015).

Oxidative stress is commonly known to be involved in many pathological conditions including neurodegenerative diseases. Post-mortem analysis of brains in PD patients showed significantly higher degree of oxidative damage as confirmed by the presence of lipid peroxidation products such as malondialdehyde and 4-hydroxy-2-nonenal (Farooqui and Farooqui, 2011).

Moreover, local inflammation in the brain mediated by reactive microglia can cause widespread degeneration of dopaminergic neurons. Upon release of pro-inflammatory cytokines such as tumor necrosis factor (TNF)-α, interleukin (IL)-1β, interferon (IFN)-γ and prostaglandin E_2, large amount of reactive oxygen species (ROS) and reactive nitrogen species (RNS) are generated. These then become cytotoxic to neighboring cells (Zaitone et al., 2012). On the other hand, mitochondrial complex I deficit prompts apoptotic event in dopaminergic neurons (Banerjee et al., 2009) whereas genes encoding important member in UPS was found mutated in PD. The finding of abnormal accumulation of mutated protein in brain sample of PD patient may be attributed to the defective UPS protein degradation mechanism (Davie, 2008).

2.1.3.1 Oxidative stress

Oxygen is essential for biological functions in living organisms, such as to ensure survival as well as for metabolism. In the brain, there is high oxygen demand from neurons and astrocytes, which accounts for 20% of total oxygen consumption of the body (Eggers, 2009). ROS are collection of free radicals and non-radicals which generated as a result of partial reduction of oxygen. These include superoxide ($O_2^{\bullet-}$), hydrogen peroxide (H_2O_2), and the hydroxyl radical ($OH^{\bullet}$) (Nohl et al., 2005). They are unstable and highly reactive due to unpaired electron in their electrochemical structure and thus interact chemically with biological molecules particularly through oxidation-reduction. In normal cell, there is a network of systems to maintain the balance of pro-oxidant and antioxidant. These are enzymes and antioxidant mechanisms

including the glutathione, catalase, superoxide dismutase and heme oxygenase (Masella et al., 2005b). However, under some circumstances these members from the antioxidant system may fail to balance upon the accelerated generation of pro-oxidants. An excess of pro-oxidants accumulation results in a state called oxidative stress, whereby ROS attacks macromolecules such as proteins, lipids and DNA (Farooqui and Farooqui, 2011). Altered structure of the macromolecules, or known as oxidative adducts, are associated to development of various human diseases (Moon and Shibamoto, 2009).

Indeed, brain tissue is highly susceptible to oxidative stress because of its high polyunsaturated fatty acids content. Furthermore, it was reported that the brain has 7-10 fold lower concentrations of antioxidant enzymes compared to the liver, which may leave brain more susceptible to oxidative damage under oxidative stress (Reddy and Clark, 2004, Crichton et al., 2002). In addition, mutations in several genes implicated in neurodegenerative diseases, such as the Parkin gene in PD, huntingtin gene in Huntington disease and Battenin gene in Batten's disease, are involved in mechanisms that regulate intracellular oxidative status (Melo et al., 2011).

There are evidences to suggest the involvement of oxidative stress in PD. Firstly, catecholamines such as dopamine in the brain is itself unstable (Asanuma et al., 2003). It is easily metabolized by endogenous enzymes such as monoamine oxidases or through auto-oxidation. Metabolism of dopamine evokes the production of toxic quinones, peroxides and other ROS, which initiate oxidative cell injury. Secondly, markers for lipid peroxidation and

protein carbonyls are found to be significantly higher in PD brain compared to the healthy subject (Dalfó et al., 2005, Beal, 2002, Bender et al., 2006) . Seet et al. found that a series of lipid and DNA oxidation products including plasma F_2-isoprostanes, hydroxyeicosatetraenoic acid products, 7β-and 27-hydroxycholesterol, 7-ketocholesterol, neuroprostanes and urinary 8-hydroxy-2′-deoxyguanosine were elevated in PD patients, thus further established the relationship between oxidative damage and PD (Seet et al., 2010).

Moreover, there are reduced levels of antioxidant enzymes catalase and glutathione in PD brains, indicating that higher oxidative status may render brain more vulnerable to neurodegeneration (Masella et al., 2005a). Furthermore, various PD models, be it *in vitro* or *in vivo*, are established by introducing ROS releasing-neurotoxin into the cells or animals (Bové et al., 2005). These neurotoxin-based models are able to recapitulate some pathological features exhibited by PD, either via direct induction of ROS or inhibition of mitochondrial function. Free radicals were also shown to induce lipid peroxidation on cellular membrane. It is thus believed that redox balance is critically involved in maintaining neuron survival in the brain.

2.1.3.2 Neuroinflammation

Microglia, the resident innate immune cell of the central nervous system, coordinates immunological function of the brain and confers protection against foreign material infiltration (Li, 2016). Upon stimulation, activated microglia initiates acute inflammatory response which release cytokines and chemokines to sequester neurotoxin, hence prevents possible adverse chronic inflammation.

However, persistent and exaggerated inflammatory response will cause irreversible damage and mutation to biomolecules, leading to pathogenesis of many chronic diseases such as cancer and neurodegenerative disease.

In PD, studies showed that activated microglia concentrate around degenerated neurons at substantia nigra of the brain (Tansey and Goldberg, 2010). It was found that inflammatory mediators released from microglia contribute to the accumulation of free radicals and pro-inflammatory neurotoxic compounds which causes death of dopaminergic neurons (Ferrari and Tarelli, 2011). Beraud and Maguire-Zeiss added that α-synuclein, the protein of the Lewy bodies, directly binds to Toll-like receptors on cell surface to activate microglia, which then incite the production of pro-inflammatory molecules (Beraud and Maguire-Zeiss, 2012). The role of inflammation in PD has also been cited extensively in clinical studies. Post-mortem studies of the substantia nigra of PD patient have previously revealed evidence of activated microglia and pro-inflammatory cytokines including IL-1β, TNF-α, and IL-6 (Mogi et al., 1994). Clinically, the serum levels of TNF-α and TNF-α receptor 1 were significantly higher in PD patient compared to control, while IL-1β, and IL-2 were found elevated in both serum and cerebrospinal fluid of PD patients, signifying a distinctive change in inflammatory response during the course of PD (Dobbs et al., 1999, Blum-Degena et al., 1995, Scalzo et al., 2009).

2.1.3.3 Mitochondrial dysfunction

Under normal physiological condition, endogenous ROS is generated from the process of energy production by mitochondrial respiratory chain reaction

(Schapira, 2010). During oxidative phosphorylation, the energy molecule adenosine triphosphate (ATP) is produced and hydrogen ions are transferred across the inner mitochondrial membrane. This is facilitated by rigorous redox reactions occurring at the protein level to create pH and electrical potential gradient across the inner and outer mitochondrial membrane, which involves five major protein complexes I, II, III, IV and ATP synthase. In the end, electrons are transferred to an electron acceptor, such as the oxygen respired into the cell. The oxygen is then reduced to produce water that is harmless to the cell. However, a small percentage of electrons leaks from the electron transport chain, causing oxygen molecule to be incompletely reduced, thus generating superoxide radical (•O2-) and hydrogen peroxide as illustrated in Figure 2.2.

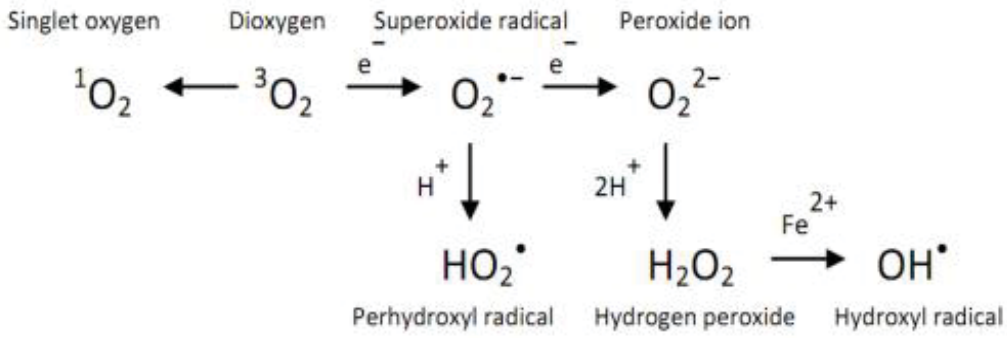

Figure 2.2. Partial reduction of oxygen leads to formation of ROS.
Adapted from published image (Gill and Tuteja, 2010).

Maintenance of mitochondrial integrity is crucial for cell survival. However, mitochondrial dysfunction can contribute to ROS outburst and is implicated in PD. Study by Bender et al. described a common deletion in mitochondrial DNA of neurons in the substantia nigra of PD patients, which is associated

with respiratory chain deficiency (Bender et al., 2006). In addition, it was shown that in PD, mitochondrial complex I activity of the substantia nigra was diminished (Keeney et al., 2006). Also, *in vitro* and *in vivo* models generated by inhibition of the mitochondrial complex I with the neurotoxins such as rotenone and 1-methyl-4-phenyl-1,2,5,6-tetrahydropyrine (MPTP) demonstrated biochemical and histopathological findings resembling that of PD (Bové et al., 2005). Many aspects of mitochondrial function other than the respiratory chain have been suggested for mitochondria-associated PD pathology. To name a few, calcium homeostasis, mitochondrial permeability and ATP production are affected in PD (Gandhi and Abramov, 2012). Moreover, several PD-related genes directly affecting the mitochondria such as PINK1, DJ-1, Parkin have also been identified for their role in contributing to oxidative stress.

2.1.3.4 Apoptosis

Apoptosis by definition is the programmed cell death, a tightly-regulated and energy-utilizing biological process essential for regulating cell growth, survival and homeostasis (Alenzi, 2004). There are two pathways down the apoptosis process, namely the intrinsic pathway and extrinsic pathway, which are mitochondria and death receptor-mediated, respectively. Yet, the downstream molecular events of the two pathways have been found to be inter-related and affecting one another, such as caspase activation which leads to final execution of cell death through DNA fragmentation and cytoskeletal breakdown. Other than that, other apoptotic mechanisms have been studied as

well, for example the perforin/ granzyme pathway mediated by T lymphocytes (cytotoxic T cell) and caspase-independent pathway (Elmore, 2007).

Substantial amount of studies have identified apoptosis as the major cell death mechanism accounted for pathology seen in PD. Apoptosis-related proteins including c-Jun, p53, GAPDH, bax, and caspases were up-regulated in post-mortem analysis of PD (Offen et al., 2000). The proteins mentioned above are also activated in experimental models of PD, particularly in MPTP-intoxicated mice (Tatton et al., 2003, Mattson, 2006).

2.1.3.5 Proteinopathy

Lewy bodies found in the degenerating neurons of the brain predominantly consist of oligomerized α-synuclein proteins. It is believed that the proteinopathy arises from diminished action of the UPS, which controls over the degradation of damaged and misfolded proteins. In addition, mutation in genes coding for the UPS enzymes such as Parkin and UCH-L1 are known to be associated with the familial form of PD (Klein and Westenberger, 2012). Meanwhile, due to the altered structure of the 26/20S proteasomes of the dopaminergic neuron, impaired enzymatic activities of the 20S are noted in the substantia nigra in sporadic PD (McNaught et al., 2003). These studies suggest that dysfunction of the protein degradation machinery UPS may lead to intracellular or extracellular protein deposition which could be noxious and toxic to the cell. Studies have shown that proteinopathy is linked to oxidative stress and mitochondrial dysfunction (Ganguly et al., 2017). Particularly, ROS exacerbates the formation of protein aggregates, and as these proteins

accumulate even more ROS is generated, hence leading up to oxidative imbalance. These protein aggregates are also known to cause disruption of mitochondrial bioenergetics, fusion/fission and mitophagy, all of which end up in ROS build up and the activation of apoptosis.

2.1.3.6 Ferroptosis

Despite being essential for many fundamental biological processes, such as in the metabolism of neurotransmitters and the myelination of oligodendrocytes iron is known to play a role in the pathogenesis of PD (Zucca et al., 2017). Therefore, the homeostasis of intracellular iron level is critical to the maintenance of cellular integrity (Medeiros et al., 2016, Zucca et al., 2017). In fact, post-mortem analysis of brain sample revealed that iron level in the substantia nigra and lateral globus pallidus regions was significantly higher in PD patients compared to age-matched controls (Griffiths et al., 1999). The study employed cryo-electron transmission microscopy to confirm that the iron may be stored as ferritin, which was found to be elevated in substantia nigra tissue of PD patient. Furthermore, the ferritin molecules in PD tissue were more heavily loaded with iron than in controls. Based on his study and previous literature, Griffiths et al. believed that excessive iron deposition may prompt free radical production, which will eventually lead to neuronal damage through the process of lipid peroxidation. Indeed, magnetic resonance imaging (MRI) scans showed that PD patients displayed excessive iron accumulation in the substantia nigra (Sian-Hulsmann et al., 2011).

On the other hand, significantly elevated level of hydroxyl radical has been found in post mortem substantia nigra samples of PD (Dexter et al., 1989). It is not surprising, as increased free iron concentration can exacerbate ROS production, especially the generation of toxic hydroxyl radical (OH·) via Fenton and Haber–Weiss reactions (Sian-Hulsmann et al., 2011). These radicals attack unsaturated fatty acids in cell membranes, causing oxidation of the lipid membrane through a process called lipid peroxidation. The term 'ferroptosis' explains an iron-dependent cell death mechanism, which is characterized morphologically by disappearing mitochondria membranes and smaller mitochondrial volume. Biochemically, ferroptosis is marked by accumulation of lipid peroxide released from peroxidation of polyunsaturated fatty acids on cell membrane (Doll et al., 2017, Yang et al., 2016). It is also accompanied by deficiency of the glutathione antioxidant system. Particularly the GPX4 is an enzyme responsible for the detoxification of lipid peroxides whereas GSH is important for iron-binding within the neurons. Hence, depletion of GSH and diminishing GPX4 activity may trigger ferroptosis (Wu et al., 2018). Apparently, dopaminergic neurodegeneration at the substantia nigra region in PD is where the iron is abundant (Ayton and Lei, 2014). Additionally, iron may cause aggregation of α-synuclein protein, which further aggravates generation of hydroxyl radical and promotes Lewy body deposition (Abeyawardhane et al., 2018). Interestingly, Do Van et al. suggested that ferroptosis in PD progression may be mediated via the activation of protein kinase Cα pathway (Do Van et al., 2016).

2.1.4 Changes in motor circuitry in PD

The motor system in the basal ganglia comprises the direct pathway and indirect pathways for precise control of movement (Obeso et al., 2008). The pathways are groups of neuronal projections which connect between the entry and the exit points of neuronal information, and relay electrical impulses between synapses and neurons in the motor-controlling center of basal ganglia. Corpus striatum is the entry point of the basal ganglia and receives stimulation from the cerebral cortex through the corticostriatal afferent neurons. These neurons are mainly responsible in inhibiting medium spiny neurons via the indirect pathway while providing support to the neurons via the direct pathway (Alexander et al., 1986, Alexander et al., 1990). At rest, input from nigrostriatal pathway binds to dopamine D_2 receptor in striatum to activate the indirect motor circuitry so as to keep muscle movement on hold and prevent mobility. The indirect pathway has neurons passing through the external globus pallidus (GPe) and subthalamic nucleus, and projects towards the internal globus pallidus or GPi (Wang and Han, 2015). From GPi, the thalamus receives GABAergic inhibition and leads to inhibition of movement (Merello and Cammarota, 2000). In contrast, when movement is desired the direct pathway, which consists of neurons project directly towards the GPi, is activated via the stimulation of the dopamine D_1 receptor in the striatum. When inhibitory action of the direct pathway acts on GPi, the neuronal information exits to the cortex through the thalamus in favor of movement.

Balance of activities from both pathways is the key to the state of movement, which otherwise will lead to abrupt output level from the basal ganglia and therefore abnormal movement (Figure 2.3). In case of PD, as dopamine level

drops significantly due to the degeneration of dopaminergic neuron, striatum receives less input hence there are increased activity of the indirect pathway and reduced activity in the direct pathway (Figure 2.4). As a result, excessive output from the GPi eventually leads to bradykinesia or akinesia, which refers to slowness or lack of movement, respectively.

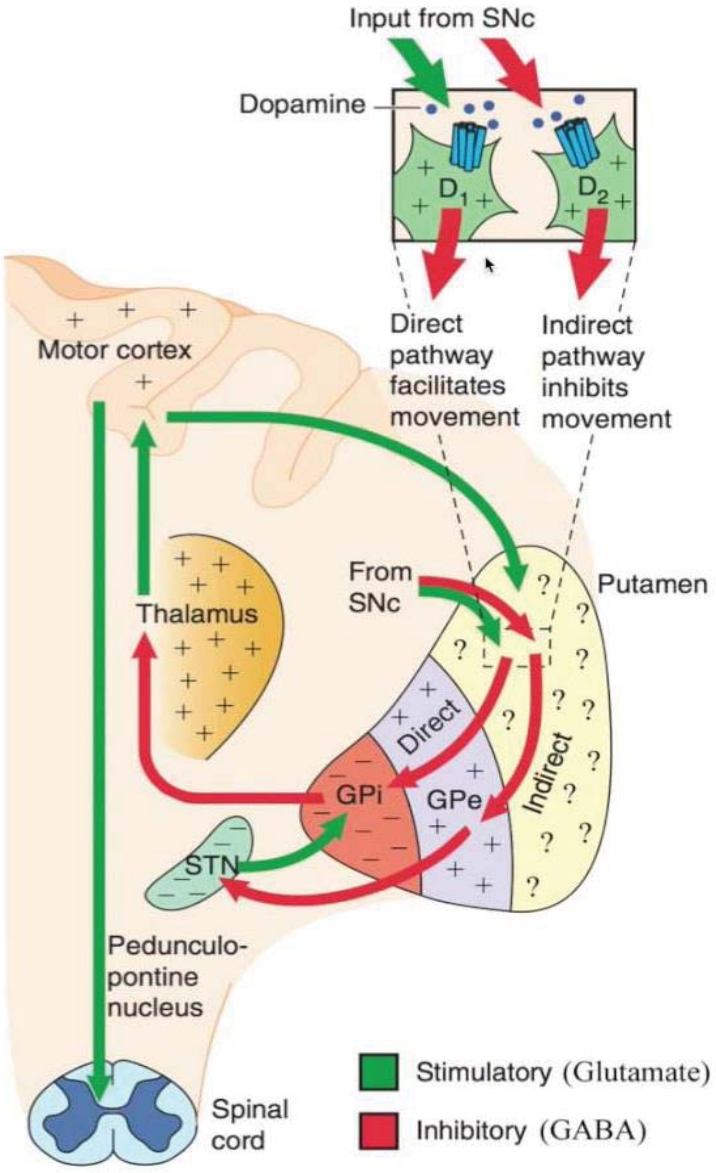

Figure 2.3. The direct and indirect pathway of the basal ganglia motor circuit. SNc: Substantia nigra pars compacta. GPe: External globus pallidus. GPi: Internal globus

pallidus. STN: Subthalamic nucleus. D_1: Dopamine D_1 receptor. D_2: Dopamine D_2 receptor. Adapted from published image (Le, 2015).

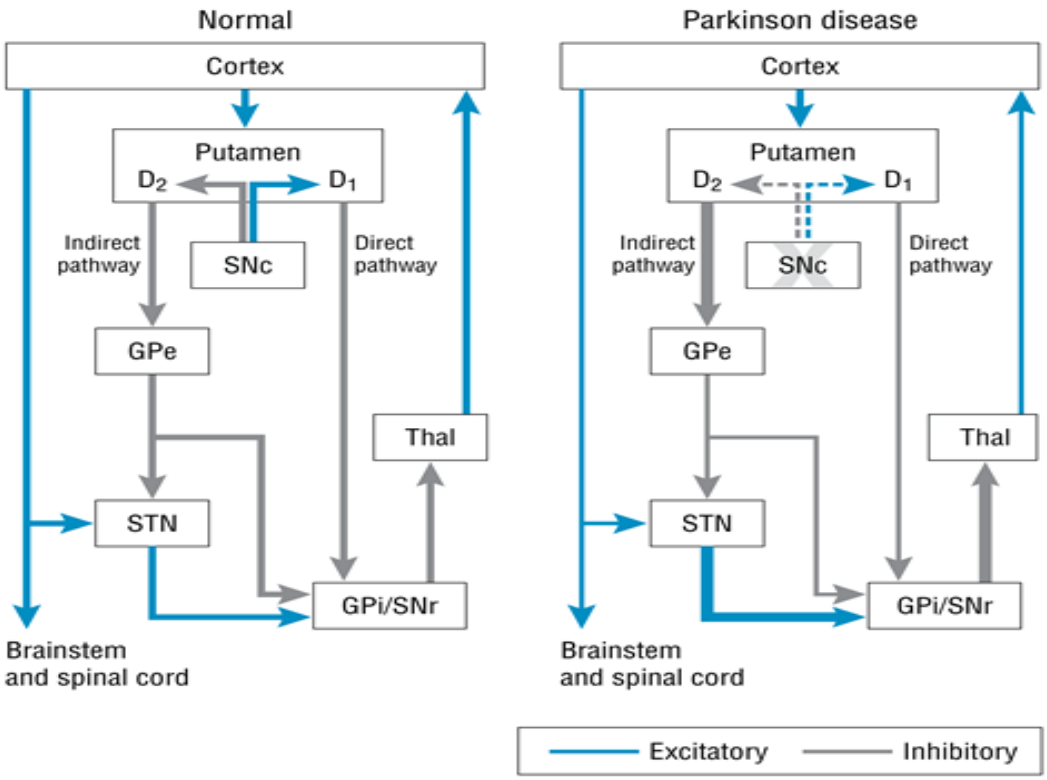

Figure 2.4. Basal ganglia-thalamo-cortical circuit under normal condition and PD. Thickness of the arrows represents relative strength of the excitation or inhibition. D_1: Dopamine D_1 receptor. D_2: Dopamine D_2 receptor; GPe: External globus pallidus; GPi: Internal globus pallidus; SNc: Substantia nigra pars compacta; SNr: Substantia nigra pars reticulata; STN: Subthalamic nucleus; Thal: Thalamus. Adapted from published image (Miocinovic et al., 2013).

2.1.5 Current treatment options for PD: Pitfalls and future

At present, the rule of thumb treatment for PD is dopamine-based as this approach is effective in improving symptoms arise from the loss of dopamine-

excitation of the basal ganglia, which mainly manifest as motor complications. Dopamine precursor such as levodopa is commonly prescribed to patient during early stage of diagnosis to replenish dopamine in the denervated striatum (Sullivan and Toulouse, 2011). Initially the treatment may be helpful despite adverse effect to the gastrointestinal system. However, nearly half of the patients developed refractory effect and complications known as dyskinesia within 5 years after initiated the treatment. Aberrant motor signs were also noticed in levodopa-induced dyskinesias including choreic, ballistic, or dystonic movements (Fahn, 2000). Li et al. and Pandey and Srivanitchapoom reviewed that such phenomenon may arise from altered firing pattern of neurons in the cortico-basal ganglia-thalamic loop which has important role in fine tuning motor skills, as a result of medication (Li et al., 2015, Pandey and Srivanitchapoom, 2017). On top of that, patients in late stage PD are often refractory to levodopa treatment due to emergence of non-motor symptoms which are dopamine-independent.

On the other hand, dopamine agonist is a more favorable choice of drug prescribed to younger PD patients by clinician compared to levodopa because of the intention to avoid adverse effects seen in chronic use of levodopa therapy including motor fluctuations and dyskinesias (Almeida and Hyson, 2008). Although treatment with dopamine agonist comes with side effects, it is still the mainstay of therapeutic option for younger patient who can tolerate symptoms including nausea, postural hypotension, hallucinations and drowsiness. Yet, it has been reported that drug efficacy of dopamine agonist was not on par with levodopa. To top it all off, it has been reported that

pharmacokinetic profile of levodopa and dopamine agonist can vary significantly between and within individuals, which make it difficult to determine the suitable dose for an effective treatment (Nomoto et al., 2006).

Drugs which inhibit enzymatic breakdown of dopamine have also demonstrated success in the management of PD. These drugs include selegiline, tolcapone, entacapone and rasagiline, and act as the inhibitor of monoamine oxidase (MAO), the enzyme that catalyzes oxidation of monoamine neurotransmitters. For example, selegiline has been shown to protect neuron against MPTP-induced neurotoxicity (Ebadi et al., 2002). Clinical trials showed that patients who took selegiline had delayed need for levodopa treatment, yet researchers are still doubtful regarding the true efficacy of selegiline as it is tricky to justify if patient's condition was improved due to symptomatic effect or neuroprotective effect of levodopa (Olanow et al., 1995). Neurotoxicity of metabolites from selegiline such as L-metamphetamine and L-amphetamine has also raised concerns regarding its safety use (Kupsch et al., 2001). On the contrary, rasagiline was found to be highly selective towards MAO-B instead of MAO-A, which is mainly found in the intestines (Guay, 2006). Rasagiline also does not produce toxic metabolite like selegiline does. It is thus expected to work better than selegiline due to higher drug selectivity, safer by-product and longer-lasting effect (Almeida and Hyson, 2008) . It was protective against glutamate and MPTP toxicity, but similar to selegiline, its mechanism of action is yet to be elucidated.

Deep brain stimulation (DBS) has received substantial attention as a viable option for patient with advanced PD since the approval from US Federal Drug Administration (FDA) in 2002. It is a surgical alternative to levodopa medication and in patient with severe tremor symptoms. By implanting brain stimulators at specific region of the brain, electrophysiological activity of various neuronal circuits can be manipulated to improve disease outcome. Health-related quality of life in PD patients generally has improved after DBS of subthalamic nucleus, thalamus or the GPi. This was mainly associated with enhanced motor skills, reduced systemic symptoms, and reduced depression and anxiety (Diamond and Jankovic, 2005).

However, the success of DBS depends on many factors such as screening of patient, placement of DBS electrodes, surgical techniques and stimulation technology (Picillo et al., 2016). Particularly, programming of the stimulation technology is a laborious process and may often result in poor clinical outcome due to the lack of established and validated programming protocols. Currently, the common practice after DBS surgery which includes optimization of stimulation parameters, medication adjustment and symptoms management is laborious and time consuming, which lasts for an average of 6 months (Wagle Shukla and Okun, 2014). PD patients who had no improvement and developed side effects from DBS surgery are known as 'DBS failures' and are required to visit advanced DBS centers for reevaluation. In one study, it was shown that DBS failures often linked to inadequate pre-operative screening, as well as surgical and device-related complications (Okun et al., 2005). On top of that, among PD patients who were 'DBS

failures', 51% of them benefited from reprogramming, indicating that carefully-planned optimization of a reliable and systematic algorithm-based DBS programming is pivotal to the success of the intervention. In fact, there has been growing interest in the customization of DBS treatment to make it more patient-focused and symptom-specific. For instance, the stimulation target can be tailored to patient's major concern; GPi DBS is recommended for patient with severe dyskinesias, cognitive disability and psychological disturbances whereas subthalamic nucleus DBS is preferred for control over resting tremors and rigidity. Hence the future of DBS is evolving with the discovery of more stimulation targets to tackle various motor and non-motor symptoms associated with PD.

The current guidelines available for DBS set-up only involves determination of the lead type, electrode configuration, impedance check and battery check, but more importantly, DBS technology needs to be refined in terms of the control over the shape of electrical field and intensity of stimulation. This is essential to fine tune the level of electrical control, as well as to confine stimulation to the neuronal pathway of interest only while keeping the stimulation away from other unintended areas. Recent advances in DBS technology such as the development of fractionated current technology and directional lead have resolved some of the existing technical limitations in DBS therapy, therefore this approach will continue to see future for better treatment efficiency (Wagle Shukla et al., 2017).

2.1.6 The need for multifaceted treatment in PD

Majority of the current treatment options for PD is symptomatic treatment from which undesirable complications may arise, and has yet to achieve long term efficacy. In fact, certain features such as tremor, postural instability and cognitive impairment fail to respond to medications currently used for PD (Radhakrishnan, 2018). Although motor skills are primarily affected in PD, non-motor symptoms are also apparent in advanced PD and mostly are associated to impairment of other neurotransmission system on top of dopaminergic system (Braak et al., 2003). For example, serotonergic deficit is partially involved in depression, whereas cholinergic and noradrenergic deficits are implicated in cognitive impairment (Bonnet, 2000). Autonomic dysfunction, on the other hand, is caused by deficits in adrenergic and noradrenergic neurotransmission. Many of these symptoms are not properly addressed and treated by drugs for PD mainly because they are not responsive to dopamine-based treatment (Hou and Lai, 2007). There is a compelling need to strategize treatment towards an individual-based therapy on the basis of the symptoms manifested by the patient (Hung and Schwarzschild, 2014). Also, dopaminergic treatment has not been successful in combating the progressive nature of nigrostriatal degeneration in PD. New treatment is needed to slow down disease progression, to restore loss of dopaminergic neuron and to prevent from acquiring the disease (Tuite and Riss, 2003).

Intriguingly, there is immense public interest in considering natural product of the past and present time for the management of PD. Development of patentable novel product has ensued from herbal sources such as *Curcuma longa*, *Huperzia selago* and *Centella asiatica*, and from compounds including

echinacoside, oleuropein, ginsenosides, caffeine and resveratrol (Cacabelos, 2017). It was suggested that these natural products may be neuroprotective due to their neurotrophic, antioxidant and anti-inflammatory attributes, and selective protection of the dopaminergic neuron against cell death. Neuroprotection implies an approach which targets underlying pathogenic mechanism of a disease in order to halt progressive degeneration of the neurons (Sarkar et al., 2016). Growing effort has been invested in drug discovery platform using natural product as the great span of biodiversity provides a wealth of rare and novel active compounds that may be medically useful. For instance, E-PodoFavalin-15999, a biopharmaceutical compound derived from *Vicia faba* L. has been found to enhance efficacy of anti-parkinsonian drugs, exert neurotrophic effect, regulate plasma catecholamine level and neuroendocrine functions, therefore is suggested to alleviate both motor and non-motor symptoms of PD (Cacabelos, 2017). It is apparent that continuous search for a treatment option with multifaceted effect is needed to improve treatment efficacy for PD.

2.2 Edible bird's nest

2.2.1 Production and origin

EBN is a natural food product made from saliva of the swiftlets, specifically by the genus *Aerodramus* found predominantly around Southeast Asia. The type of EBN produced is dependent on the bird species, two of the most commonly known swiftlets are *Aerodramus fuciphogus* and *Aerodramus maximus*, which produce white and black EBN, respectively. EBN is harvested in the form of hardened piece of bird's nest-like structure consisting

of glutinous strands and has been studied as early as in 1920s to confirm its mucinous nature (Wang, 1921).

Although a swiftlet weighs less than 20g, it is capable of building nest up to 2 times of its body weight during breeding season owing to its active salivary secretion from a pair of sublingual salivary glands (Marcone, 2005). The raw bird nest, built high on the wall and roof of caves in the shape of a bowl, is often mixed with feathers and twigs. Extensive processing and cleaning are required before it is marketed to consumers.

2.2.2 Traditional value of EBN

Chinese has the longest history of consuming EBN, which could date back to the Tang dysnasty (618–907 AD) and it is still popular until nowadays (Lim and Cranbrook, 2002). EBN is usually prepared in soup and is highly regarded as delicacy with substantial medicinal value. EBN soup used to be a food privileged to the ancient emperors and the wealthy, but its market later extended to among convalescence, elderly people and now, to the common people. At present, Hong Kong and mainland China are the largest importers of EBN, and most of these products come from major EBN-producing countries like Malaysia, Indonesia, Thailand and Vietnam (Goh et al., 2001).

In Traditional Chinese Medicine, EBN is regarded as effective towards various complications in the respiratory airways and gastrointestinal system. It is known to cure dry cough and tuberculosis, supress coughs and phlegm-dyspnea, alleviate asthma and hemoptysis, and improve voice, stomach ulcers

and gastric problems. In addition to that, EBN gains popularity for being able to improve skin complexion, increase immunity, raise libido, promote growth, enhance metabolism and blood circulation as well as to nourish vital organs including kidney, lung and heart (Lim and Cranbrook, 2002). Due to these anecdotal benefits, EBN has received growing interest from western countries, though its medicinal value is not yet proven by scientific investigation (Goh et al., 2001).

2.2.3 Compositional make-up of EBN

Marcone et al. summarized that EBN contains predominantly proteins and carbohydrates (Marcone, 2005). Ash, lipid and water were found at minimal percentage while elemental analysis showed the presence of minerals. Although the protein content of EBN has been reported to be at various percentages, they are still the most abundant among all the other nutrients, reported at 60% in one study (Halimi et al., 2014, Wong et al., 2017, Ma and Liu, 2012). Amino acid analysis have detailed out the abundance of both essential and non-essential amino acids like serine, valine, tyrosine, phenylalanine, aspartic acid and glutamic acid in EBN. On the other hand, carbohydrate content is slightly over 27%, which includes 9% sialic acid, 7.2% galactosamine, 5.3% glucosamine, 16.9% galactose, and 0.7% fructose.

2.2.4 Bioactivity studies of EBN

Several significant studies have been carried out to suggest that EBN confers a wide range of bioactivities. Early studies showed that EBN exerted immune-enhancing property by stimulating the proliferation of human peripheral blood

monocytes following stimulation with Concanavalin A and Phytohemagglutinin A (Ng et al., 1986). EGF-like glycoprotein was purified in EBN and it contributed to DNA synthesis in quiescent 3T3 fibroblast culture (Kong et al., 1987). The latter therefore proposed EBN to be beneficial to cellular regeneration and anti-aging.

In 2006, Guo et al. demonstrated influenza-inhibiting effect of EBN extract prepared through pancreatin digestion in Madin-Darby Canine Kidney cell line (Guo et al., 2006). The viral neutralization effect stayed strong when tested against a total of 19 strains of influenza A from the human, avian and swine species. Hemaglutination to human O erythrocytes was reduced as well. However, the extract did not act through the viral neuraminidase but hemaglutinin. It was also reported that 5-N-acetyl-neuraminic acid residues of sialyl glycoconjugates was responsible for the anti-viral response.

Lately, it was shown that EBN extracted at low and high pH exhibited potent radical scavenging activity and reducing power (Lee et al., 2009). In support of that, another recent study found EBN attenuated oxidative stress and matrix metalloproteinase activity in human keratinocytes, an effect mediated by the mitogen-activated protein kinases (MAPK) pathway (Kim et al., 2012).

Both findings have pushed forward the value of EBN as a potent source of natural antioxidant. Interestingly, Matsukawa and co-workers' research on ovariectomized murine models showed that supplementation of pancreatin F-digested EBN to the animal's diet improved their bone strength and dermal

thickness without affecting serum estradiol level, and this effect was dose-dependent (Matsukawa et al., 2011). In addition, EBN improves stem cell potency by inducing 34% proliferation on mesenchymal stem cell derived from human adipocytes comparing to control (Roh et al., 2012). All the above discoveries suggest the potential of EBN to be explored as health food option in the interest of anti-aging, anti-osteoporosis and stem cell therapy.

EBN also demonstrated neuroprotective and cardiometabolic effect in ovariectomized rats. Zhiping et al. reported that EBN attenuated estrogen deficiency-induced cortical and hippocampal neurodegeneration by reducing advanced glycation end-products in the serum and down-regulating apoptosis-associated genes in the hippocampus and frontal cortex (Zhiping et al., 2015). Meanwhile, EBN was also shown to improve lipid profile and metabolic indices in ovariectomized rats by regulating genes in insulin signalling (Hou et al., 2015), as well as coagulation-related genes in rats fed with high fat diet (Yida et al., 2015).

To date, various biotechnology techniques have enabled the isolation and structural characterization of glycoprotein, one of the major constituents of EBN with the characteristics of both protein and carbohydrate. Anti-influenza activity of EBN has been previously attributed to sialylglycoconjugates, which is made up of the sialic residues and the glycosylprotein. The sialic side chain is recognized as the N-acetyl-D-neuraminic acid (Neu5Ac), while a more sophisticated mass spectroscopic analysis by Pozsgay et al. had characterized a 4, 8-anhydro derivative of Neu5Ac in EBN acid hydrolysate (Pozsgay et al.,

1987). On the other hand, both O-glycan and N-glycan structures have been described in the glycosylation profile of EBN (Wieruszeski et al., 1987, Yagi et al., 2008) . As influenza A, B and C viruses, parainfluenza virus, Newcastle disease virus, rotavirus, coronavirus and cholera bacteria recognize sialic acid as their receptors, sialylglycoconjugates in EBN may neutralize viral infections in the host cell by blocking viral binding to sialic acid receptors on human erythrocytes and cells in the upper respiratory tract (Goh et al., 2001).

Nakagawa et al. first reported the presence of proteoglycan in EBN (Nakagawa et al., 2007). By combining techniques including gel filtration, mass spectrometric and NMR analysis, non-sulfated chondroitin glycosaminoglycans has been identified. This compound is thought to contribute to increased bone strength and dermal collagen fibrils formation in murine model fed with enzyme-treated EBN in Matsukawa's study, though the abundance of glycosaminoglycans varied between studies and limited recovery was attained (Nakagawa et al., 2007, Matsukawa et al., 2011).

2.2.5 EBN as a natural source of bioactive compounds

Animal saliva contains a wide panel of biologically active compounds that exhibit anti-inflammatory, wound healing, neuroprotective, anti-microbial and immune-regulatory properties (Mathison et al., 2010, Marukawa et al., 1996, Tenovuo, 2002, Kemp et al., 1985). Other than EGF-like compound and sialic acid which have already been identified in EBN (Kong et al., 1987, Yagi et al., 2008), melatonin and VEGF may also be present in swiftlets' saliva as high concentration of these bioactive compounds have been detected in animal

saliva (Voultsios et al., 1997, Pammer et al., 1998b). As these compounds are known to exert neurogenic activity, it is proposed that EBN might possess neurotrophic and neuroprotective advantages, which might be of medicinal relevance to PD.

2.2.5.1 Bioactive compounds identified in EBN

2.2.5.1.1 Sialic acid

The N- or O-substituted derivatives of neuraminic acid, a monosaccharide of nine-carbon backbone, are generally termed as sialic acid. However, sialic acid often refers to N-acetylneuraminic acid (Neu5Ac or NANA), which has a wide range of biological activity. The high abundance of sialic acid in the brain (about 15-fold of other organs) may implicate its essential role in brain functions. Meanwhile, sialic acid is also an essential precursor of polysialic acid glycan, which post-translationally modifies neural cell adhesion molecules (NCAM) on cell membrane (Brunngraber et al., 1972). Both gangliosides and NCAM are important in mediating cell-to-cell interactions important for neuronal outgrowth, synaptic connectivity, and memory formation, as well as axonal formation and elongation (Wang, 2012).

Gangliosides is a complex sialic acid-containing glycosphingolipids that represents an important element in plasma membrane and synaptic membrane of nerve cells (McJarrow et al., 2009). Experiment with knockout mice showed that gangliosides synthesis defect had serious impact on brain function which may be fatal (Proia, 2004). Another cross-species study also proved that maturation of the brain is positively associated with total sialic acid

concentration in brain homogenates (Wang et al., 1998). Therefore, sialic acid is a very important nutrient to support brain growth, especially in infants where brain development and sialic acid recruitment for gangliosides formation are at their peaks (Wang and Brand-Miller, 2003).

Segler-Stahl et al. previously reported that concentration of ganglioside-bound sialic acid decreased following an age-dependent trend (Segler-Stahl et al., 1983). However, dietary supplementation of sialic acid can easily compensate body's demands for this brain-building moiety as it is rapidly absorbed by small intestines, transported through blood-brain barrier and assimilated into the brain especially at frontal cortex which is the active site of cognition. Wang et al. reported an up-regulated gene expression of α-2,8-sialyltransferase IV and UDP-N-acetlylglucosamine-2-epimerase, which are enzymes involved in sialic acid metabolism, as well as enhanced learning behaviour in developing piglets after being fed with sialic acid-supplemented milk (Wang et al., 2007). An exogenous supply of sialic acid might be beneficial to brain regeneration and cognition improvement in PD patient.

2.2.5.2 Potential neuroprotective and neurotrophic compounds in EBN

2.2.5.2.1 Epidermal growth factor

EGF is a single chain acid-stable polypeptide of 53 amino acids first detected in submandibular secretion of mouse and has high affinity towards the EGF receptor (Cohen, 1962). Major physiological roles of EGF include inhibition of gastric acid secretion, promotion of blood circulation, mucus production and also epithelial cell migration (Calabrò et al., 1998).

In the context of neuroregeneration, EGF is known to stimulate proliferation of neural stem cell (NSC) under both *in vitro* and *in vivo* settings (Reynolds et al., 1992, Gonzalez-Perez and Quiñones-Hinojosa, 2010). It is a neurotrophic factor found to be responsible for active neurogenesis in mammalian subventricular zone and survival of striatal dopaminergic neuron in PD model (O'Keeffe et al., 2009, Iwakura et al., 2005). Nonetheless, depending on the status of cell fate, EGFR signaling may have differential effector actions on the NSC and neural progenitor cell pools (Aguirre et al., 2010).

Not only that, EGF seems to promote generation of both neurons and astrocytes by acting on a multipotent progenitor cell in the striatum (Reynolds et al., 1992). EGF directs a migratory pattern of neural progenitor cells from the proliferating zone to the target site before the newly-differentiated neurons are integrated into neuronal circuits (Teramoto et al., 2003). EGF infusion has also shown to stimulate cell proliferation, the generation and migration of striatal-specific neurons (Ninomiya et al., 2006).

2.2.5.2.2 Melatonin

Best recognized as the regulatory hormone for circardian cycle, melatonin is a methoxyindole synthesized within the pineal gland. Maximum level of hormone secretion is achieved during the night and many of its biological actions are mediated through the activation of receptors that are localized in retina, brain, ovaries, cerebral and peripheral arteries, kidney, pancreas, adipocytes and immune cells (Dubocovich and Markowska, 2005).

Melatonin in blood can be secreted into the saliva and may be involved in the wound healing of the oropharyngeal epithelia by regulating cell proliferation and inflammatory processes (Gröschl, 2009, Permuy et al., 2017). Besides from being naturally secreted in animal, it is also found in plants and microbes.

Numerous clinical applications of melatonin include anaesthetic uses, sleep promotion in insomniac and patient with depression, management of jet lag and mood regulator. However, there are a lot more other potentials of melatonin in immuno-regulation, free radical scavenging, cancer prevention and protection against neurodegenerative diseases (Srinivasan et al., 2011, Kostoglou-Athanassiou, 2013).

Specifically, neuroprotective action of melatonin is largely due to its role as a potent antioxidant. As oxidative stress is implicated in neurodegenerative diseases including Alzheimer's disease and PD, melatonin may help to protect neuronal cells against programmed cell death and various toxic challenges. Melatonin is a terminal antioxidant, which is distinctive from other antioxidant in a way that once it is being oxidized after reaction with free radicals like toxic hydroxyl and hydroperoxides, the melatonin itself will be consumed up and converted into stable end-product. Also, due to the high antioxidant capacity of melatonin and its metabolites, they are capable of initiating a prolonged free radical scavenging cascade. In the case of N(1)-acetyl-N(2)-formyl-5-methoxykynuramine, it is the metabolite of melatonin

which is able to neutralize 10 times the amount of ROS and RNS per molecule (Tan et al., 2007).

In a review, Pandi-Perumal et al. summarized mechanisms through which melatonin confers protection to neuronal cells, which include up-regulation of antioxidant enzyme activity and attenuation of mitochondrial dysfunction (Pandi-Perumal et al., 2013). On the other hand, melatonin signaling is implicated in PD because reduced expression of melatonin MT(1) and MT(2) receptors was found in the substantia nigra of patients as compared to normal subjects (Adi et al., 2010). Studies involving neurotoxin-induced animal model of parkinsonism displayed efficacy of melatonin in reversing PD pathology. The neuroprotective effect of melatonin has been substantiated by studies which reported reduced lipid peroxidation in neurons, less nigral cell damage and death, as well as increased gluthathione, superoxide dismutase and catalase level upon administration of melatonin (Acuna-Castroviejo et al., 1997, Antolin et al., 2002, Saravanan et al., 2007).

Furthermore, melatonin may promote neurogenesis. Findings have shown proliferative and differentiative effect of melatonin on NSC from the fetal mouse brain as well as in rat midbrain. Hippocampal neurogenesis, an important process of brain development, was promoted in animal models with melatonin use (Gerardo et al., 2009, Ramirez-Rodriguez et al., 2012). Melatonin was also able to restore neurogenesis which was impaired as a result of cranial irradiation in cancer therapy (Manda et al., 2009). Study by Kong et al. has demonstrated that melatonin promoted survival and

dopaminergic neuronal differentiation of NSC derived from rat ventral midbrain, in addition to increasing secretion of neurotrophic factors such as glial cell-derived growth factor (GDNF) and brain-derived neurotrophic factor (BDNF) (Kong et al., 2008). Melatonin is therefore a potential bioactive compound for neuroregeneration in PD.

2.2.5.2.3 Vascular endothelial growth factor

VEGF is an angiogenic protein comes from a big family comprises VEGF-A, VEGF-B, VEGF-C, VEGF-D, and placenta growth factor. VEGF is highly expressed in acinar cells of the salivary glands and its protein is secreted into the saliva. It was suggested that VEGF participates in the homeostasis of mucous membrane as well as in the regulation of salivary secretion, which facilitates wound healing in the oral cavity through neoangiogenesis (Pammer et al., 1998a). The proteins bind with varied affinity to different types of VEGF receptor (Matsumoto and Claesson-Welsh, 2001). NSC expresses VEGF receptor hence it is a target cell of VEGF (Ara et al., 2010).

VEGF acts at various levels in maintaining a neuron's integrity (Gora-Kupilas and Josko, 2005). Notably, VEGF inhibited apoptosis in stress-challenged neuronal cells through a number of mechanisms including the activation of anti-apoptotic proteins and inhibition of pro-apoptotic signalling. In addition, a positive VEGF-heme oxygenase feedback loop protects neurons by attenuating oxidative stress. It also protects brain from glucose deprivation by increasing permeability of the blood brain barrier and glucose

uptake as a result of up-regulated expression of glucose transporter at the blood vessel.

Several PD studies have also been carried out to evaluate therapeutic capacity of VEGF. Yasuhara et al. discovered that 6-OHDA-induced cell death in primary mesencephalic neuron cultures was much reduced after VEGF treatment (Yasuhara et al., 2004). Also, the use of engineered cell encapsulated in hollow fibres capable of providing sustainable release of VEGF in rat's striatum was shown to decrease drug-induced rotational behaviour after *in vivo* implantation. The study also pointed out possible neuro-rescue effect on nigrostriatal dopaminergic neurons by VEGF administration as seen by greater preservation of tyrosine hydroxylase-positive cell on brain sections. Further studies by the same group of researchers revealed a better VEGF performance at low dose administration and early treatment on neurotoxin-challenged models of PD (Yasuhara et al., 2005a, Yasuhara et al., 2005b). Interestingly, it was recently reported that grafting of human umbilical cord mesenchymal stem cell modified by adenovirus-mediated VEGF gene transfer promoted dopaminergic neuronal differentiation and eventually improved the PD outcome in rotenone-lesioned rat model (Xiong et al., 2011).

VEGF is also postulated to confer neurotrophic effects. Earlier study by Jin et al. showed that VEGF administration increased the population of neuronal precursor cells in cortical cultures isolated from rats, identified by expression of several significant surface markers such as embryonic nerve cell adhesion

molecule and nestin (Jin et al., 2002). This *in vitro* cell-proliferative effect was further confirmed by *in vivo* intracerebroventricular injection of VEGF which also enhanced 5-bromo-2′-deoxyuridine (BrdU) incorporation into the subventricular zone and subgranular zone in animal's brain. In another study, Palmer et al. reported that neurogenesis is a process that strongly coupled to blood vascularization (Palmer et al., 2000). The fact that VEGF promotes sprouting of new blood vessel by acting on endothelial cell, as well as the expression of VEGF receptors on endothelial and neuronal cells, suggest that VEGF plays a fundamental role in neurogenesis. It also enhances neurite formation (Khaibullina et al., 2004). Studies of intraventricular VEGF gene transfer and knockout mice have emphasized the role of VEGF in guiding migration of neural progenitor cell (Li et al., 2009, Wittko et al., 2009).

2.3 Tandem mass spectrometry for proteomic study

2.3.1 Database search versus *de novo* sequencing

Protein is the functional entity of gene expressed in cells and is made up by amino acids lined in specific sequential order. In order to characterize an unknown protein, tandem mass spectrometry (MS/MS) of tryptic digests of the protein sample coupled with database searching of protein sequences may be an useful approach. Generally, protein is first digested with endoproteases such as trypsin to yield protein fragments or the peptides. Then, the peptides are subjected to ionization through mass analyser to obtain mass-to-charge ratio (m/z) of every single amino acid that construct the individual peptide. The output of this process is a mass spectrum, which can be compared and matched to the theoretical spectra derived from predicted peptides in the protein library for accurate identification of amino

acid, and hence peptide in the sample. Some commonly used database search engine include X!Tandem, Mascot, SEQUEST, MS-GFDB, MS-Fit, MaxQuant and OMSSA (Dallas et al., 2015). However, the application of database search-based proteomic is greatly limited when the protein library is not available, in cases where the protein is derived from an organism with unsequenced or incomplete genomic profile. Therefore the major drawback of this approach is that it hinders the discovery of novel protein or post-translational modifications (PTM) of a known protein. On top of that, protein identification using this method has been challenged with issues of low sensitivity and accuracy (Zhang et al., 2012).

Alternatively, *de novo* sequencing can be used in the absence of sequence library for peptide mass fingerprinting (Dallas et al., 2015). It is a shotgun method which utilizes computational approaches to deduce the sequence or partial sequence of peptides directly from the experimental MS/MS spectra. In other word, the 'database' of a candidate peptide consists of the entire universe of possible amino acid sequences. Peptide sequences are identified by calculating mass differences between fragments hence a reference protein library is not necessary. Nevertheless, most spectra do not contain sufficient information to uniquely identify the correct peptide. Consequently, *de novo* identification methods may fail to provide as many correct hits as database search methods (Noble and MacCoss, 2012). Yet, Hughes et al.argued that *de novo* peptide sequencing may still be superior to database search method even when the genomes are known since it is not affected by errors in the search database (Hughes et al., 2010). Also, *de novo* sequencing will come in handy for exploratory studies of novel protein isoforms or polymorphism, PTM and mutant variant of a known protein, which could be

applied to improve food processing technology and discovery of novel disease marker (Noble and MacCoss, 2012, Dallas et al., 2015, Hughes et al., 2010). *De novo* sequencing programs that are available include PEAKS, Lutefisk, UStags, PepNovo, Sherenga, DirecTag and MS-Tag (Zhang et al., 2012, Dallas et al., 2015).

PEAKS, particularly, is a software package that features its own database search engine with *de novo* sequencing function. It also provides additional function such as PTM identification, homology search and quantification. The benefit of PEAKS software is that its built-in automated decoy fusion algorithm enables quick validation of the vast amount of search results. By introducing decoy and target sequence of the same protein together as a single entry of the database, the chance of detecting a true protein by the algorithm can be normalized against the odds of detecting a false positive protein, hence maximizing the accuracy of protein identification (Zhang et al., 2012). On top of that, the software computes a confidence score for each amino acid in the whole stretch of *de novo* sequence that it generates, as well as an additional novel positional scoring scheme for portions of the sequence (Ma et al., 2003). Zhang et al. convinced that the unique scoring function in PEAKS software significantly improved sensitivity and accuracy of protein identification in comparison to existing database search software (Zhang et al., 2012).

In database search method, peptides are scored by the algorithm and generally filtered according to the scoring threshold that the user presets. Otherwise, it has been recommended that ≥2 unique peptides identified within a single protein may be used to validate positive results (Omenn et al., 2005). However, such result filter

has raised disputes, concerning that many proteins may be only identified based on single peptide match due to low peptide concentration or few tryptic cleavage site in the protein (Higdon and Kolker, 2007). Higdon et al. also suggested that it is inappropriate to exclude the possibility that a protein is present in the sample simply because of single peptide match result, which may be caused by low protein abundance. Furthermore, since most scoring system is dataset and search parameter-dependent, the cut-off score value for accurate identification of a protein, which is represented by -10lgP score in PEAKS DB, may not be applicable equally in all experiment (Required Manuscript Content and Publication Guidelines for Molecular & Cellular Proteomics [Online] [Accessed September 2018]). Instead, it should be defined by 1% of false discovery rate (FDR) when the dataset is large, or a minimum -10lgP score of 20 (which is equivalent to P value of 1%) when the dataset is small (False Discovery Rate Tutorial [Online] [Accessed September 2018]). Any protein or peptide with -10lgP score of greater than 20 indicates high confidence that it is a true positive because many targets but very few decoy matches above that threshold.

2.3.2 Proteomic studies of EBN

In recent years, there was an increasing effort in the investigation of EBN protein profile. Due to the limited protein information of *Aerodramus fuciphagus* swiftlet in UniProt, one of the major depositories for protein sequence and annotation data, many EBN studies have been using other closely-related species or genus for protein matching. This concern has been raised by Wong et al. in two of his recent studies (Wong et al., 2017, Wong et al., 2018). Intriguingly, there were highly variable methodologies used in the proteomic profiling of EBN between researchers in terms

of protein extraction, MS technology, database search engine and protein library. However, there is a common concensus among researchers that EBN may contain water-soluble and water-insoluble proteins. Hence, Zukefli et al. attempted both ultrasonification and detergent lysis while Wong et al. tried over-stewing to maximize protein hydrolysis of EBN (Zukefli et al., 2017, Wong et al., 2018). Kong et al., on the other hand, focused on elucidating the protein content of hot water insoluble fraction of EBN (Kong et al., 2016).

While Zukefli et al. and Kong et al. both ran their sample through time-of-flight mass analyzer, the ionization sources used were different; the former used turbo spray ionization while the latter used matrix-assisted laser desorption/ionization (MALDI). Concurrently, Kong et al. also ran the sample through Ion Trap mass analyzer, which Wong et al. did too, but the former used collision-induced-dissociation while the latter used electron-transfer dissociation to fragmentate protein molecules for tandem MS. Various database search approach was adopted by these researchers; Using Mascot Daemon (version 2.3.0) to search against the protein library of *Chaetura pelagica*, a bird species within the same family as *Aerodramus fuciphagus*, Wong et al. found acidic mammalian chitinase-like, lysyl oxidase homolog 3, mucin-5AC-like, ovoinhibitor-like, nucleobindin-2 and 45kDa calcium-binding protein in the water extract of EBN. Kong et al. performed *de novo* sequencing of the sample with Data Analysis v2.3 and Biotool v3.1, and searched for sequence homology with Aves using basic local alignment search tool (BLAST 2.2.9+). As a result, they discovered possible presence of NADH dehydrogenase, immunoglobulin, proline-rich protein, von Willebrand factor and epidermal growth factor domain-containing protein from the hot water insoluble fractions of EBN.

On the other hand, Zukefli et al. conducted proteomic analysis using both in-solution digest and in-gel digest with ProteinPilot™ Software 4.0 and *Gallus gallus* as the protein library, and unveiled a total of 29 proteins. Among the in-solution digests, some water-soluble proteins that were identified included acidic mammalian chitinase precursor and signal transducer and activator of transcription 6-like isoform X5, which play regulatory roles in the immune system against allergic inflammation and asthma, respectively. On top of that, a number of proteins with known health benefits have been discovered including coenzyme Q-binding protein homolog A, lysyl oxidase homolog 3, collagen alpha-1 type VII chain-like and collagen alpha-2 type I were detected. Coenzyme Q-binding protein homolog A is a mitochondrial protein which is required for the function of powerful antioxidant coenzyme Q; lysyl oxidase homolog 3 is a collagen-processing enzyme essential for the cross-linking of collagens and elastins; Meanwhile, type I collagen is a fibrillar collagen ubiquitous in most connective tissues whilst type VII collagen is synthesized by keratinocytes and dermal fibroblasts of the skin. Apart from the highly water-soluble protein, transferrin receptor protein 1 and 78-kDa glucose-regulated protein precursor, which are known for their roles in regulating cellular iron homeostasis and protein assembly in the endoplasmic reticulum, respectively. Moreover, Zukefli et al. detected a totally different array of proteins through the in-gel digestion technique. These proteins include trypsinogen, transmembrane protease serine 13-like isoform X2 and phospholipase A2-like protein. Trypsinogen is the inactive form of trypsin, while transmembrane protease serine 13-like isoform X2 functions in the development, homeostasis, infection, and tumorigenesis. Phospholipase A2-like protein plays roles in lipid signalling, inhibiting apoptosis and promoting cell proliferation. There is also

inter-alpha-trypsin inhibitor heavy chain H2 precursor which regulates the localization, synthesis, and degradation of hyaluronan, and tumor necrosis factor receptor superfamily member 5 precursor, which is the activator of immunoglobulin production. SH3 domain-containing RING finger protein 3 and zinc finger protein 830 are zinc-binding proteins which are important for cell division, cell growth and wound healing.

2.4 References

False Discovery Rate (FDR) Tutorial [Online]. Bioinformatics Solutions Inc. Available: http://www.bioinfor.com/fdr-tutorial/ [Accessed September 2018].

Required Manuscript Content and Publication Guidelines for Molecular & Cellular Proteomics [Online]. Molecular & Cellular Proteomics. Available: http://www.mcponline.org/page/content/mass-spec-guidelines [Accessed September 2018].

ABEYAWARDHANE, D. L., FERNANDEZ, R. D., MURGAS, C. J., HEITGER, D. R., FORNEY, A. K., CROZIER, M. K. & LUCAS, H. R. 2018. Iron Redox Chemistry Promotes Antiparallel Oligomerization of alpha-Synuclein. *J Am Chem Soc,* 140**,** 5028-5032.

ACUNA-CASTROVIEJO, D., COTO-MONTES, A., GAIA MONTI, M., ORTIZ, G. G. & REITER, R. J. 1997. Melatonin is protective against MPTP-induced striatal and hippocampal lesions. *Life Sci,* 60**,** PL23-9.

ADI, N., MASH, D. C., ALI, Y., SINGER, C., SHEHADEH, L. & PAPAPETROPOULOS, S. 2010. Melatonin MT1 and MT2 receptor expression in Parkinson's disease. *Med Sci Monit,* 16**,** BR61-7.

AGUIRRE, A., RUBIO, M. E. & GALLO, V. 2010. Notch and EGFR pathway interaction regulates neural stem cell number and self-renewal. *Nature,* 467**,** 323-7.

ALENZI, F. Q. 2004. Links between apoptosis, proliferation and the cell cycle. *Br J Biomed Sci,* 61**,** 99-102.

ALEXANDER, G. E., CRUTCHER, M. D. & DELONG, M. R. 1990. Basal ganglia-thalamocortical circuits: parallel substrates for motor, oculomotor, "prefrontal" and "limbic" functions. *Prog Brain Res,* 85**,** 119-46.

ALEXANDER, G. E., DELONG, M. R. & STRICK, P. L. 1986. Parallel organization of functionally segregated circuits linking basal ganglia and cortex. *Annu Rev Neurosci,* 9**,** 357-81.

ALMEIDA, Q. J. & HYSON, H. C. 2008. The evolution of pharmacological treatment for Parkinson's disease. *Recent Pat CNS Drug Discov,* 3**,** 50-4.

ANGELES, D. C., GAN, B. H., ONSTEAD, L., ZHAO, Y., LIM, K. L., DACHSEL, J., MELROSE, H., FARRER, M., WSZOLEK, Z. K., DICKSON, D. W. & TAN, E. K. 2011. Mutations in LRRK2 increase phosphorylation of peroxiredoxin 3 exacerbating oxidative stress-induced neuronal death. *Hum Mutat,* 32**,** 1390-7.

ANTOLIN, I., MAYO, J. C., SAINZ, R. M., DEL BRIO MDE, L., HERRERA, F., MARTIN, V. & RODRIGUEZ, C. 2002. Protective effect of melatonin in a chronic experimental model of Parkinson's disease. *Brain Res,* 943**,** 163-73.

ARA, J., FEKETE, S., ZHU, A. & FRANK, M. 2010. Characterization of neural stem/progenitor cells expressing VEGF and its receptors in the subventricular zone of newborn piglet brain. *Neurochem Res,* 35**,** 1455-70.

ASANUMA, M., MIYAZAKI, I. & OGAWA, N. 2003. Dopamine- or L-DOPA-induced neurotoxicity: The role of dopamine quinone formation and tyrosinase in a model of Parkinson’s disease. *Neurotoxicity Research,* 5**,** 165-176.

AYTON, S. & LEI, P. 2014. Nigral Iron Elevation Is an Invariable Feature of Parkinson's Disease and Is a Sufficient Cause of Neurodegeneration. *BioMed Research International,* 2014**,** 581256.

BANERJEE, R., STARKOV, A. A., BEAL, M. F. & THOMAS, B. 2009. Mitochondrial dysfunction in the limelight of Parkinson's disease pathogenesis. *Biochim Biophys Acta,* 1792**,** 651-63.

BEAL, M. F. 2002. Oxidatively modified proteins in aging and disease. *Free Radical Biology and Medicine,* 32**,** 797-803.

BENDER, A., KRISHNAN, K. J., MORRIS, C. M., TAYLOR, G. A., REEVE, A. K., PERRY, R. H., JAROS, E., HERSHESON, J. S., BETTS, J., KLOPSTOCK, T., TAYLOR, R. W. & TURNBULL, D. M. 2006. High levels of mitochondrial DNA deletions in substantia nigra neurons in aging and Parkinson disease. *Nat Genet,* 38**,** 515-517.

BERAUD, D. & MAGUIRE-ZEISS, K. A. 2012. Misfolded alpha-synuclein and Toll-like receptors: therapeutic targets for Parkinson's disease. *Parkinsonism Relat Disord,* 18 Suppl 1**,** S17-20.

BLESA, J., TRIGO-DAMAS, I., QUIROGA-VARELA, A. & JACKSON-LEWIS, V. R. 2015. Oxidative stress and Parkinson's disease. *Frontiers in Neuroanatomy,* 9.

BLUM-DEGENA, D., MÜLLER, T., KUHN, W., GERLACH, M., PRZUNTEK, H. & RIEDERER, P. 1995. Interleukin-1β and interleukin-6 are elevated in the cerebrospinal fluid of Alzheimer's and de novo Parkinson's disease patients. *Neuroscience Letters,* 202**,** 17-20.

BONIFATI, V., RIZZU, P., VAN BAREN, M. J., SCHAAP, O., BREEDVELD, G. J., KRIEGER, E., DEKKER, M. C., SQUITIERI, F., IBANEZ, P., JOOSSE, M., VAN DONGEN, J. W., VANACORE, N., VAN SWIETEN, J. C., BRICE, A., MECO, G.,

VAN DUIJN, C. M., OOSTRA, B. A. & HEUTINK, P. 2003. Mutations in the DJ-1 gene associated with autosomal recessive early-onset parkinsonism. *Science,* 299**,** 256-9.

BONNET, A.-M. 2000. Involvement of Non-Dopaminergic Pathways in Parkinson's Disease. *CNS Drugs,* 13**,** 351-364.

BOVÉ, J., PROU, D., PERIER, C. & PRZEDBORSKI, S. 2005. Toxin-induced models of Parkinson's disease. *NeuroRX,* 2**,** 484-494.

BRAAK, H., DEL TREDICI, K., RUB, U., DE VOS, R. A., JANSEN STEUR, E. N. & BRAAK, E. 2003. Staging of brain pathology related to sporadic Parkinson's disease. *Neurobiol Aging,* 24**,** 197-211.

BRAAK, H., GHEBREMEDHIN, E., RUB, U., BRATZKE, H. & DEL TREDICI, K. 2004. Stages in the development of Parkinson's disease-related pathology. *Cell Tissue Res,* 318**,** 121-34.

BRUNNGRABER, E. G., WITTING, L. A., HABERLAND, C. & BROWN, B. 1972. Glycoproteins in Tay-sachs disease: isolation and carbohydrate composition of glycopeptides. *Brain Res,* 38**,** 151-62.

CACABELOS, R. 2017. Parkinson's Disease: From Pathogenesis to Pharmacogenomics. *International Journal of Molecular Sciences,* 18**,** 551.

CALABRÒ, A., ORSINI, B., RENZI, D., PAPI, L., MILANI, S. & SURRENTI, C. 1998. *What is known about the distribution and expression of growth factors, such as EGF and TGFa and their receptors, in the defense of the esophageal mucosa, and in healing of reflux induced injury?* .

CHAN, D., CITRO, A., CORDY, J. M., SHEN, G. C. & WOLOZIN, B. 2011. Rac1 protein rescues neurite retraction caused by G2019S leucine-rich repeat kinase 2 (LRRK2). *J Biol Chem,* 286**,** 16140-9.

COHEN, S. 1962. Isolation of a mouse submaxillary gland protein accelerating incisor eruption and eyelid opening in the new-born animal. *J Biol Chem,* 237**,** 1555-62.

COOKSON, M. R. 2010. The role of leucine-rich repeat kinase 2 (LRRK2) in Parkinson's disease. *Nat Rev Neurosci,* 11**,** 791-7.

CRICHTON, R. R., WILMET, S., LEGSSYER, R. & WARD, R. J. 2002. Molecular and cellular mechanisms of iron homeostasis and toxicity in mammalian cells. *J Inorg Biochem,* 91**,** 9-18.

DALFÓ, E., PORTERO-OTÍN, M., AYALA, V., MARTÍNEZ, A., PAMPLONA, R. & FERRER, I. 2005. Evidence of oxidative stress in the neocortex in incidental Lewy body disease. *Journal of neuropathology and experimental neurology,* 64**,** 816-830.

DALLAS, D. C., GUERRERO, A., PARKER, E. A., ROBINSON, R. C., GAN, J., GERMAN, J. B., BARILE, D. & LEBRILLA, C. B. 2015. Current peptidomics: applications, purification, identification, quantification, and functional analysis. *Proteomics,* 15**,** 1026-38.

DAUER, W. & PRZEDBORSKI, S. 2003. Parkinson's Disease: Mechanisms and Models. *Neuron,* 39**,** 889-909.

DAVIE, C. A. 2008. A review of Parkinson's disease. *British Medical Bulletin,* 86**,** 109-127.

DEXTER, D. T., WELLS, F. R., LEES, A. J., AGID, F., AGID, Y., JENNER, P. & MARSDEN, C. D. 1989. Increased nigral iron content and alterations in other metal ions occurring in brain in Parkinson's disease. *J Neurochem,* 52**,** 1830-6.

DIAMOND, A. & JANKOVIC, J. 2005. The effect of deep brain stimulation on quality of life in movement disorders. *J Neurol Neurosurg Psychiatry,* 76**,** 1188-93.

DO VAN, B., GOUEL, F., JONNEAUX, A., TIMMERMAN, K., GELE, P., PETRAULT, M., BASTIDE, M., LALOUX, C., MOREAU, C., BORDET, R., DEVOS, D. &

DEVEDJIAN, J. C. 2016. Ferroptosis, a newly characterized form of cell death in Parkinson's disease that is regulated by PKC. *Neurobiol Dis,* 94**,** 169-78.

DOBBS, R. J., CHARLETT, A., PURKISS, A. G., DOBBS, S. M., WELLER, C. & PETERSON, D. W. 1999. Association of circulating TNF-α and IL-6 with ageing and parkinsonism. *Acta Neurologica Scandinavica,* 100**,** 34-41.

DOLL, S., PRONETH, B., TYURINA, Y. Y., PANZILIUS, E., KOBAYASHI, S., INGOLD, I., IRMLER, M., BECKERS, J., AICHLER, M., WALCH, A., PROKISCH, H., TRUMBACH, D., MAO, G., QU, F., BAYIR, H., FULLEKRUG, J., SCHEEL, C. H., WURST, W., SCHICK, J. A., KAGAN, V. E., ANGELI, J. P. & CONRAD, M. 2017. ACSL4 dictates ferroptosis sensitivity by shaping cellular lipid composition. *Nat Chem Biol,* 13**,** 91-98.

DUBOCOVICH, M. L. & MARKOWSKA, M. 2005. Functional MT1 and MT2 melatonin receptors in mammals. *Endocrine,* 27**,** 101-10.

EBADI, M., SHARMA, S., SHAVALI, S. & EL REFAEY, H. 2002. Neuroprotective actions of selegiline. *J Neurosci Res,* 67**,** 285-9.

EGGERS, A. E. 2009. Why do Alzheimer's disease and Parkinson's disease target the same neurons? *Med Hypotheses,* 72**,** 698-700.

ELMORE, S. 2007. Apoptosis: a review of programmed cell death. *Toxicol Pathol,* 35**,** 495-516.

ERIKSEN, J. L., DAWSON, T. M., DICKSON, D. W. & PETRUCELLI, L. 2003. Caught in the act: alpha-synuclein is the culprit in Parkinson's disease. *Neuron,* 40**,** 453-6.

ERIKSEN, J. L., WSZOLEK, Z. & PETRUCELLI, L. 2005. Molecular pathogenesis of parkinson disease. *Archives of Neurology,* 62**,** 353-357.

FAHN, S. 2000. The spectrum of levodopa-induced dyskinesias. *Ann Neurol,* 47**,** S2-9; discussion S9-11.

FAROOQUI, T. & FAROOQUI, A. A. 2011. Lipid-Mediated Oxidative Stress and Inflammation in the Pathogenesis of Parkinson's Disease. *Parkinson's Disease,* 2011.

FERRARI, C. C. & TARELLI, R. 2011. Parkinson's Disease and Systemic Inflammation. *Parkinson's Disease,* 2011.

GANDHI, S. & ABRAMOV, A. Y. 2012. Mechanism of Oxidative Stress in Neurodegeneration. *Oxidative Medicine and Cellular Longevity,* 2012**,** 11.

GANGULY, G., CHAKRABARTI, S., CHATTERJEE, U. & SASO, L. 2017. Proteinopathy, oxidative stress and mitochondrial dysfunction: cross talk in Alzheimer's disease and Parkinson's disease. *Drug Design, Development and Therapy,* 11**,** 797-810.

GERARDO, R.-R., FRIEDERIKE, K., HARISH, B., GLORIA, B.-K. & GERD, K. 2009. Melatonin Modulates Cell Survival of New Neurons in the Hippocampus of Adult Mice. *Neuropsychopharmacology,* 34**,** 2180-2191.

GIASSON, B. I., DUDA, J. E., MURRAY, I. V. J., CHEN, Q., SOUZA, J. M., HURTIG, H. I., ISCHIROPOULOS, H., TROJANOWSKI, J. Q. & -Y. LEE, V. M. 2000. Oxidative Damage Linked to Neurodegeneration by Selective α-Synuclein Nitration in Synucleinopathy Lesions. *Science,* 290**,** 985-989.

GILL, S. S. & TUTEJA, N. 2010. Reactive oxygen species and antioxidant machinery in abiotic stress tolerance in crop plants. *Plant Physiol Biochem,* 48**,** 909-30.

GOH, D. L., CHUA, K. Y., CHEW, F. T., LIANG, R. C., SEOW, T. K., OU, K. L., YI, F. C. & LEE, B. W. 2001. Immunochemical characterization of edible bird's nest allergens. *J Allergy Clin Immunol,* 107**,** 1082-7.

GONZALEZ-PEREZ, O. & QUIÑONES-HINOJOSA, A. 2010. Dose-dependent effect of EGF on migration and differentiation of adult subventricular zone astrocytes. *GLIA,* 58**,** 975-983.

GORA-KUPILAS, K. & JOSKO, J. 2005. The neuroprotective function of vascular endothelial growth factor (VEGF). *Folia Neuropathol,* 43**,** 31-9.

GRIFFITHS, P. D., DOBSON, B. R., JONES, G. R. & CLARKE, D. T. 1999. Iron in the basal ganglia in Parkinson's diseaseAn in vitro study using extended X-ray absorption fine structure and cryo-electron microscopy. *Brain,* 122**,** 667-673.

GRÖSCHL, M. 2009. The physiological role of hormones in saliva. *BioEssays,* 31**,** 843-852.

GUAY, D. R. 2006. Rasagiline (TVP-1012): a new selective monoamine oxidase inhibitor for Parkinson's disease. *Am J Geriatr Pharmacother,* 4**,** 330-46.

GUO, C. T., TAKAHASHI, T., BUKAWA, W., TAKAHASHI, N., YAGI, H., KATO, K., HIDARI, K. I., MIYAMOTO, D., SUZUKI, T. & SUZUKI, Y. 2006. Edible bird's nest extract inhibits influenza virus infection. *Antiviral Res,* 70**,** 140-6.

HALIMI, N. M., KASIM, Z. M. & BABJI, A. S. 2014. Nutritional composition and solubility of edible bird nest (Aerodramus fuchiphagus). *AIP Conference Proceedings,* 1614**,** 476-481.

HIGDON, R. & KOLKER, E. 2007. A predictive model for identifying proteins by a single peptide match. *Bioinformatics,* 23**,** 277-80.

HOU, J.-G. G. & LAI, E. C. 2007. Non-motor Symptoms of Parkinson's Disease. *International Journal of Gerontology,* 1**,** 53-64.

HOU, Z., IMAM, M. U., ISMAIL, M., OOI, D. J., IDERIS, A. & MAHMUD, R. 2015. Nutrigenomic effects of edible bird's nest on insulin signaling in ovariectomized rats. *Drug Des Devel Ther,* 9**,** 4115-25.

HUGHES, C., MA, B. & LAJOIE, G. A. 2010. De novo sequencing methods in proteomics. *Methods Mol Biol,* 604**,** 105-21.

HUNG, A. Y. & SCHWARZSCHILD, M. A. 2014. Treatment of Parkinson’s Disease: What’s in the Non-dopaminergic Pipeline? *Neurotherapeutics,* 11**,** 34-46.

IWAKURA, Y., PIAO, Y. S., MIZUNO, M., TAKEI, N., KAKITA, A., TAKAHASHI, H. & NAWA, H. 2005. Influences of dopaminergic lesion on epidermal growth factor-ErbB signals in Parkinson's disease and its model: neurotrophic implication in nigrostriatal neurons. *J Neurochem,* 93**,** 974-83.

JIN, K., ZHU, Y., SUN, Y., MAO, X. O., XIE, L. & GREENBERG, D. A. 2002. Vascular endothelial growth factor (VEGF) stimulates neurogenesis in vitro and in vivo. *Proceedings of the National Academy of Sciences,* 99**,** 11946-11950.

KEENEY, P. M., XIE, J., CAPALDI, R. A. & BENNETT, J. P., JR. 2006. Parkinson's disease brain mitochondrial complex I has oxidatively damaged subunits and is functionally impaired and misassembled. *J Neurosci,* 26**,** 5256-64.

KEMP, A., MELLOW, L. & SABBADINI, E. 1985. Suppression and enhancement of in vitro lymphocyte reactivity by factors in rat submandibular gland extracts. *Immunology,* 56**,** 261-7.

KHAIBULLINA, A. A., ROSENSTEIN, J. M. & KRUM, J. M. 2004. Vascular endothelial growth factor promotes neurite maturation in primary CNS neuronal cultures. *Brain Res Dev Brain Res,* 148**,** 59-68.

KIM, K., KANG, K., LIM, C., PARK, J., JUNG, K. & HYUN, J. 2012. Water extract of edible bird’s nest attenuated the oxidative stress-induced matrix metalloproteinase-1 by regulating the mitogen-activated protein kinase and activator protein-1 pathway in human keratinocytes. *Journal of the Korean Society for Applied Biological Chemistry,* 55**,** 347-354.

KITADA, T., ASAKAWA, S., HATTORI, N., MATSUMINE, H., YAMAMURA, Y., MINOSHIMA, S., YOKOCHI, M., MIZUNO, Y. & SHIMIZU, N. 1998. Mutations in the parkin gene cause autosomal recessive juvenile parkinsonism. *Nature,* 392**,** 605-8.

KLEIN, C. & WESTENBERGER, A. 2012. Genetics of Parkinson's disease. *Cold Spring Harb Perspect Med,* 2**,** a008888.

KONG, H.-K., WONG, K.-H. & LO, S. C.-L. 2016. Identification of peptides released from hot water insoluble fraction of edible bird's nest under simulated gastro-intestinal conditions. *Food Research International,* 85**,** 19-25.

KONG, X., LI, X., CAI, Z., YANG, N., LIU, Y., SHU, J., PAN, L. & ZUO, P. 2008. Melatonin regulates the viability and differentiation of rat midbrain neural stem cells. *Cell Mol Neurobiol,* 28**,** 569-79.

KONG, Y. C., KEUNG, W. M., YIP, T. T., KO, K. M., TSAO, S. W. & NG, M. H. 1987. Evidence that epidermal growth factor is present in swiftlet's (Collocalia) nest. *Comp Biochem Physiol B,* 87**,** 221-6.

KOSTOGLOU-ATHANASSIOU, I. 2013. Therapeutic applications of melatonin. *Ther Adv Endocrinol Metab,* 4**,** 13-24.

KRUGER, R., EBERHARDT, O., RIESS, O. & SCHULZ, J. B. 2002. Parkinson's disease: one biochemical pathway to fit all genes? *Trends Mol Med,* 8**,** 236-40.

KUPSCH, A., SAUTTER, J., GOTZ, M. E., BREITHAUPT, W., SCHWARZ, J., YOUDIM, M. B., RIEDERER, P., GERLACH, M. & OERTEL, W. H. 2001. Monoamine oxidase-inhibition and MPTP-induced neurotoxicity in the non-human primate: comparison of rasagiline (TVP 1012) with selegiline. *J Neural Transm (Vienna),* 108**,** 985-1009.

LEE, T. H., TAN, E. T. T., SARMIDI, M., AZIZ, R., CHUA, L. S. & LEE, C. T. 2009. Protein Extractability and Antioxidant Studies of Edible Bird's Nest Extracts. *International Scientific Conference on Nutraceuticals and Functional Foods (Food and Function 2009).* Holiday Inn Hotel, Zilina, Slovakia.

LI, S. F., SUN, Y. B., MENG, Q. H., LI, S. R., YAO, W. C., HU, G. J., LI, Z. J. & WANG, R. Z. 2009. Recombinant adeno-associated virus serotype 1-vascular endothelial growth factor promotes neurogenesis and neuromigration in the subventricular zone and rescues neuronal function in ischemic rats. *Neurosurgery,* 65**,** 771-9; discussion 779.

LI, X., ZHUANG, P. & LI, Y. 2015. Altered Neuronal Firing Pattern of the Basal Ganglia Nucleus Plays a Role in Levodopa-Induced Dyskinesia in Patients with Parkinson's Disease. *Frontiers in Human Neuroscience,* 9**,** 630.

LIM, C. K. & CRANBROOK, E. O. 2002. *Swiftlets of Borneo – Builders of edible nests* Sabah, Malaysia, Natural History Publication (Borneo) SDN., B.H.D. .

MA, B., ZHANG, K., HENDRIE, C., LIANG, C., LI, M., DOHERTY-KIRBY, A. & LAJOIE, G. 2003. PEAKS: powerful software for peptide de novo sequencing by tandem mass spectrometry. *Rapid Commun Mass Spectrom,* 17**,** 2337-42.

MA, F. & LIU, D. 2012. Sketch of the edible bird's nest and its important bioactivities. *Food Research International,* 48**,** 559-567.

MANDA, K., UENO, M. & ANZAI, K. 2009. Cranial irradiation-induced inhibition of neurogenesis in hippocampal dentate gyrus of adult mice: attenuation by melatonin pretreatment. *J Pineal Res,* 46**,** 71-8.

MARCONE, M. F. 2005. Characterization of the edible bird's nest the "Caviar of the East". *Food Research International,* 38**,** 1125-1134.

MARUKAWA, H., SHIMOMURA, T. & TAKAHASHI, K. 1996. Salivary substance P, 5-hydroxytryptamine, and gamma-aminobutyric acid levels in migraine and tension-type headache. *Headache,* 36**,** 100-04.

MASELLA, R., DI BENEDETTO, R., VARI, R., FILESI, C. & GIOVANNINI, C. 2005a. Novel mechanisms of natural antioxidant compounds in biological systems:

involvement of glutathione and glutathione-related enzymes. *J Nutr Biochem,* 16**,** 577-86.

MASELLA, R., DI BENEDETTO, R., VARÌ, R., FILESI, C. & GIOVANNINI, C. 2005b. Novel mechanisms of natural antioxidant compounds in biological systems: involvement of glutathione and glutathione-related enzymes. *The Journal of Nutritional Biochemistry,* 16**,** 577-586.

MATHISON, R. D., DAVISON, J. S., BEFUS, A. D. & GINGERICH, D. A. 2010. Salivary gland derived peptides as a new class of anti-inflammatory agents: review of preclinical pharmacology of C-terminal peptides of SMR1 protein. *J Inflamm (Lond),* 7**,** 49.

MATSUKAWA, N., MATSUMOTO, M., BUKAWA, W., CHIJI, H., NAKAYAMA, K., HARA, H. & TSUKAHARA, T. 2011. Improvement of bone strength and dermal thickness due to dietary edible bird's nest extract in ovariectomized rats. *Biosci Biotechnol Biochem,* 75**,** 590-2.

MATSUMOTO, T. & CLAESSON-WELSH, L. 2001. VEGF receptor signal transduction. *Sci STKE,* 2001**,** re21.

MATTSON, M. P. 2006. Neuronal life-and-death signaling, apoptosis, and neurodegenerative disorders. *Antioxid Redox Signal,* 8**,** 1997-2006.

MCJARROW, P., SCHNELL, N., JUMPSEN, J. & CLANDININ, T. 2009. Influence of dietary gangliosides on neonatal brain development. *Nutr Rev,* 67**,** 451-63.

MCNAUGHT, K. S., BELIZAIRE, R., ISACSON, O., JENNER, P. & OLANOW, C. W. 2003. Altered proteasomal function in sporadic Parkinson's disease. *Exp Neurol,* 179**,** 38-46.

MEDEIROS, M. S., SCHUMACHER-SCHUH, A., CARDOSO, A. M., BOCHI, G. V., BALDISSARELLI, J., KEGLER, A., SANTANA, D., CHAVES, C. M. M. B. S.,

SCHETINGER, M. R. C., MORESCO, R. N., RIEDER, C. R. M. & FIGHERA, M. R. 2016. Iron and Oxidative Stress in Parkinson's Disease: An Observational Study of Injury Biomarkers. *PLoS ONE,* 11**,** e0146129.

MELO, A., MONTEIRO, L., LIMA, R. M. F., DE OLIVEIRA, D. M., DE CERQUEIRA, M. D. & EL-BACHÁ, R. S. 2011. Oxidative Stress in Neurodegenerative Diseases: Mechanisms and Therapeutic Perspectives. *Oxidative Medicine and Cellular Longevity,* 2011**,** 467180.

MERELLO, M. & CAMMAROTA, A. 2000. [Functional anatomy of the basal ganglia]. *Rev Neurol,* 30**,** 1055-60.

MIOCINOVIC, S., SOMAYAJULA, S., CHITNIS, S. & VITEK, J. L. 2013. History, applications, and mechanisms of deep brain stimulation. *JAMA Neurology,* 70**,** 163-171.

MOGI, M., HARADA, M., KONDO, T., RIEDERER, P., INAGAKI, H., MINAMI, M. & NAGATSU, T. 1994. Interleukin-1β, interleukin-6, epidermal growth factor and transforming growth factor-α are elevated in the brain from parkinsonian patients. *Neuroscience Letters,* 180**,** 147-150.

MOON, J. K. & SHIBAMOTO, T. 2009. Antioxidant assays for plant and food components. *J Agric Food Chem,* 57**,** 1655-66.

NAKAGAWA, H., HAMA, Y., SUMI, T., LI, S. C., MASKOS, K., KALAYANAMITRA, K., MIZUMOTO, S., SUGAHARA, K. & LI, Y. T. 2007. Occurrence of a nonsulfated chondroitin proteoglycan in the dried saliva of Collocalia swiftlets (edible bird's-nest). *Glycobiology,* 17**,** 157-64.

NG, M. H., CHAN, K. H. & KONG, Y. C. 1986. Potentiation of mitogenic response by extracts of the swiftlet's (Collocalia) nest. *Biochem Int,* 13**,** 521-31.

NINOMIYA, M., YAMASHITA, T., ARAKI, N., OKANO, H. & SAWAMOTO, K. 2006. Enhanced neurogenesis in the ischemic striatum following EGF-induced expansion of transit-amplifying cells in the subventricular zone. *Neurosci Lett,* 403**,** 63-7.

NOBLE, W. S. & MACCOSS, M. J. 2012. Computational and statistical analysis of protein mass spectrometry data. *PLoS Comput Biol,* 8**,** e1002296.

NOHL, H., GILLE, L. & STANIEK, K. 2005. Intracellular generation of reactive oxygen species by mitochondria. *Biochem Pharmacol,* 69**,** 719-23.

NOMOTO, M., NAGAI, M., NAKATSUKA, A., NISHIKAWA, N., YABE, H., MORITOYO, H., MORITOYO, T. & NOMURA, T. 2006. Pharmacokinetic characteristics of agents applied in the treatment of Parkinson's disease. *Journal of Neurology,* 253**,** iii53-iii59.

O'KEEFFE, G. C., TYERS, P., AARSLAND, D., DALLEY, J. W., BARKER, R. A. & CALDWELL, M. A. 2009. Dopamine-induced proliferation of adult neural precursor cells in the mammalian subventricular zone is mediated through EGF. *Proc Natl Acad Sci U S A,* 106**,** 8754-9.

OBESO, J. A., RODRIGUEZ-OROZ, M. C., BENITEZ-TEMINO, B., BLESA, F. J., GURIDI, J., MARIN, C. & RODRIGUEZ, M. 2008. Functional organization of the basal ganglia: therapeutic implications for Parkinson's disease. *Mov Disord,* 23 Suppl 3**,** S548-59.

OFFEN, D., ELKON, H. & MELAMED, E. 2000. Apoptosis as a general cell death pathway in neurodegenerative diseases. *J Neural Transm Suppl***,** 153-66.

OKUN, M. S., TAGLIATI, M., POURFAR, M., FERNANDEZ, H. H., RODRIGUEZ, R. L., ALTERMAN, R. L. & FOOTE, K. D. 2005. Management of referred deep brain stimulation failures: a retrospective analysis from 2 movement disorders centers. *Arch Neurol,* 62**,** 1250-5.

OLANOW, C. W., HAUSER, R. A., GAUGER, L., MALAPIRA, T., KOLLER, W., HUBBLE, J., BUSHENBARK, K., LILIENFELD, D. & ESTERLITZ, J. 1995. The effect of deprenyl and levodopa on the progression of Parkinson's disease. *Ann Neurol,* 38**,** 771-7.

OMENN, G. S., STATES, D. J., ADAMSKI, M., BLACKWELL, T. W., MENON, R., HERMJAKOB, H., APWEILER, R., HAAB, B. B., SIMPSON, R. J., EDDES, J. S., KAPP, E. A., MORITZ, R. L., CHAN, D. W., RAI, A. J., ADMON, A., AEBERSOLD, R., ENG, J., HANCOCK, W. S., HEFTA, S. A., MEYER, H., PAIK, Y. K., YOO, J. S., PING, P., POUNDS, J., ADKINS, J., QIAN, X., WANG, R., WASINGER, V., WU, C. Y., ZHAO, X., ZENG, R., ARCHAKOV, A., TSUGITA, A., BEER, I., PANDEY, A., PISANO, M., ANDREWS, P., TAMMEN, H., SPEICHER, D. W. & HANASH, S. M. 2005. Overview of the HUPO Plasma Proteome Project: results from the pilot phase with 35 collaborating laboratories and multiple analytical groups, generating a core dataset of 3020 proteins and a publicly-available database. *Proteomics,* 5**,** 3226-45.

PALMER, T. D., WILLHOITE, A. R. & GAGE, F. H. 2000. Vascular niche for adult hippocampal neurogenesis. *The Journal of Comparative Neurology,* 425**,** 479-494.

PAMMER, J., WENINGER, W., MILDNER, M., BURIAN, M., WOJTA, J. & TSCHACHLER, E. 1998a. *Vascular endothelial growth factor is constitutively expressed in normal human salivary glands and is secreted in saliva of healthy individuals*.

PAMMER, J., WENINGER, W., MILDNER, M., BURIAN, M., WOJTA, J. & TSCHACHLER, E. 1998b. Vascular endothelial growth factor is constitutively expressed in normal human salivary glands and is secreted in the saliva of healthy individuals. *The Journal of Pathology,* 186**,** 186-191.

PANDEY, S. & SRIVANITCHAPOOM, P. 2017. Levodopa-induced Dyskinesia: Clinical Features, Pathophysiology, and Medical Management. *Ann Indian Acad Neurol,* 20**,** 190-198.

PANDI-PERUMAL, S. R., BAHAMMAM, A. S., BROWN, G. M., SPENCE, D. W., BHARTI, V. K., KAUR, C., HARDELAND, R. & CARDINALI, D. P. 2013. Melatonin antioxidative defense: therapeutical implications for aging and neurodegenerative processes. *Neurotox Res,* 23**,** 267-300.

PERMUY, M., LOPEZ-PENA, M., GONZALEZ-CANTALAPIEDRA, A. & MUNOZ, F. 2017. Melatonin: A Review of Its Potential Functions and Effects on Dental Diseases. *Int J Mol Sci,* 18.

PICILLO, M., LOZANO, A. M., KOU, N., PUPPI MUNHOZ, R. & FASANO, A. 2016. Programming Deep Brain Stimulation for Parkinson's Disease: The Toronto Western Hospital Algorithms. *Brain Stimul,* 9**,** 425-437.

POZSGAY, V., JENNINGS, H. & KASPER, D. L. 1987. 4,8-anhydro-N-acetylneuraminic acid. Isolation from edible bird's nest and structure determination. *Eur J Biochem,* 162**,** 445-50.

PRIDGEON, J. W., OLZMANN, J. A., CHIN, L. S. & LI, L. 2007. PINK1 protects against oxidative stress by phosphorylating mitochondrial chaperone TRAP1. *PLoS Biol,* 5**,** e172.

PROIA, R. L. 2004. Gangliosides help stabilize the brain. *Nat Genet,* 36**,** 1147-8.

PRZEDBORSKI, S. 2005. Pathogenesis of nigral cell death in Parkinson's disease. *Parkinsonism Relat Disord,* 11 Suppl 1**,** S3-7.

RAMIREZ-RODRIGUEZ, G., VEGA-RIVERA, N. M., BENITEZ-KING, G., CASTRO-GARCIA, M. & ORTIZ-LOPEZ, L. 2012. Melatonin supplementation delays the

decline of adult hippocampal neurogenesis during normal aging of mice. *Neurosci Lett,* 530**,** 53-8.

REDDY, M. B. & CLARK, L. 2004. Iron, oxidative stress, and disease risk. *Nutr Rev,* 62**,** 120-4.

REEVE, A., SIMCOX, E. & TURNBULL, D. 2014. Ageing and Parkinson's disease: Why is advancing age the biggest risk factor?(). *Ageing Research Reviews,* 14**,** 19-30.

REYNOLDS, B. A., TETZLAFF, W. & WEISS, S. 1992. A multipotent EGF-responsive striatal embryonic progenitor cell produces neurons and astrocytes. *Journal of Neuroscience,* 12**,** 4565-4574.

ROH, K.-B., LEE, J., KIM, Y.-S., PARK, J., KIM, J.-H., LEE, J. & PARK, D. 2012. Mechanisms of Edible Bird's Nest Extract-Induced Proliferation of Human Adipose-Derived Stem Cells. *Evidence-Based Complementary and Alternative Medicine,* 2012.

ROSS, C. A. & POIRIER, M. A. 2004. Protein aggregation and neurodegenerative disease. *Nat Med,* 10 Suppl**,** S10-7.

SAIKI, S., SATO, S. & HATTORI, N. 2012. Molecular pathogenesis of Parkinson's disease: update. *J Neurol Neurosurg Psychiatry,* 83**,** 430-6.

SARAVANAN, K. S., SINDHU, K. M. & MOHANAKUMAR, K. P. 2007. Melatonin protects against rotenone-induced oxidative stress in a hemiparkinsonian rat model. *J Pineal Res,* 42**,** 247-53.

SARKAR, S., RAYMICK, J. & IMAM, S. 2016. Neuroprotective and Therapeutic Strategies against Parkinson's Disease: Recent Perspectives. *International Journal of Molecular Sciences,* 17**,** 904.

SCALZO, P., KUMMER, A., CARDOSO, F. & TEIXEIRA, A. L. 2009. Increased serum levels of soluble tumor necrosis factor-alpha receptor-1 in patients with Parkinson's disease. *J Neuroimmunol,* 216**,** 122-5.

SCHAPIRA, A. H. 2010. Complex I: inhibitors, inhibition and neurodegeneration. *Exp Neurol,* 224**,** 331-5.

SEET, R. C. S., LEE, C.-Y. J., LIM, E. C. H., TAN, J. J. H., QUEK, A. M. L., CHONG, W.-L., LOOI, W.-F., HUANG, S.-H., WANG, H., CHAN, Y.-H. & HALLIWELL, B. 2010. Oxidative damage in Parkinson disease: Measurement using accurate biomarkers. *Free Radical Biology and Medicine,* 48**,** 560-566.

SEGLER-STAHL, K., WEBSTER, J. C. & BRUNNGRABER, E. G. 1983. Changes in the concentration and composition of human brain gangliosides with aging. *Gerontology,* 29**,** 161-8.

SIAN-HULSMANN, J., MANDEL, S., YOUDIM, M. B. & RIEDERER, P. 2011. The relevance of iron in the pathogenesis of Parkinson's disease. *J Neurochem,* 118**,** 939-57.

SNYDER, C. H. & ADLER, C. H. 2007. The patient with Parkinson's disease: part I-treating the motor symptoms; part II-treating the nonmotor symptoms. *J Am Acad Nurse Pract,* 19**,** 179-97.

SRINIVASAN, V., CARDINALI, D. P., SRINIVASAN, U. S., KAUR, C., BROWN, G. M., SPENCE, D. W., HARDELAND, R. & PANDI-PERUMAL, S. R. 2011. Therapeutic potential of melatonin and its analogs in Parkinson's disease: focus on sleep and neuroprotection. *Ther Adv Neurol Disord,* 4**,** 297-317.

SULLIVAN, A. M. & TOULOUSE, A. 2011. Neurotrophic factors for the treatment of Parkinson's disease. *Cytokine Growth Factor Rev,* 22**,** 157-65.

TAN, D. X., MANCHESTER, L. C., TERRON, M. P., FLORES, L. J. & REITER, R. J. 2007. One molecule, many derivatives: a never-ending interaction of melatonin with reactive oxygen and nitrogen species? *J Pineal Res,* 42**,** 28-42.

TAN, E. K. & SKIPPER, L. M. 2007. Pathogenic mutations in Parkinson disease. *Hum Mutat,* 28**,** 641-53.

TANSEY, M. G. & GOLDBERG, M. S. 2010. Neuroinflammation in Parkinson's disease: its role in neuronal death and implications for therapeutic intervention. *Neurobiol Dis,* 37**,** 510-8.

TATTON, W. G., CHALMERS-REDMAN, R., BROWN, D. & TATTON, N. 2003. Apoptosis in Parkinson's disease: Signals for neuronal degradation. *Annals of Neurology,* 53**,** S61-S72.

TENOVUO, J. 2002. Antimicrobial agents in saliva - protection for the whole body. *Journal of Dental Research,* 81**,** 807 - 809.

TERAMOTO, T., QIU, J., PLUMIER, J. C. & MOSKOWITZ, M. A. 2003. EGF amplifies the replacement of parvalbumin-expressing striatal interneurons after ischemia. *J Clin Invest,* 111**,** 1125-32.

TUITE, P. & RISS, J. 2003. Recent developments in the pharmacological treatment of Parkinson's disease. *Expert Opin Investig Drugs,* 12**,** 1335-52.

VALENTE, E. M., ABOU-SLEIMAN, P. M., CAPUTO, V., MUQIT, M. M., HARVEY, K., GISPERT, S., ALI, Z., DEL TURCO, D., BENTIVOGLIO, A. R., HEALY, D. G., ALBANESE, A., NUSSBAUM, R., GONZALEZ-MALDONADO, R., DELLER, T., SALVI, S., CORTELLI, P., GILKS, W. P., LATCHMAN, D. S., HARVEY, R. J., DALLAPICCOLA, B., AUBURGER, G. & WOOD, N. W. 2004. Hereditary early-onset Parkinson's disease caused by mutations in PINK1. *Science,* 304**,** 1158-60.

VENDA, L. L., CRAGG, S. J., BUCHMAN, V. L. & WADE-MARTINS, R. 2010. alpha-Synuclein and dopamine at the crossroads of Parkinson's disease. *Trends Neurosci,* 33**,** 559-68.

VOULTSIOS, A., KENNAWAY, D. J. & DAWSON, D. 1997. Salivary Melatonin as a Circadian Phase Marker: Validation and Comparison to Plasma Melatonin. *Journal of Biological Rhythms,* 12**,** 457-466.

WAGLE SHUKLA, A. & OKUN, M. S. 2014. Surgical Treatment of Parkinson's Disease: Patients, Targets, Devices, and Approaches. *Neurotherapeutics,* 11**,** 47-59.

WAGLE SHUKLA, A., ZEILMAN, P., FERNANDEZ, H., BAJWA, J. A. & MEHANNA, R. 2017. DBS Programming: An Evolving Approach for Patients with Parkinson's Disease. *Parkinson's Disease,* 2017**,** 8492619.

WANG, B. 2012. Molecular mechanism underlying sialic acid as an essential nutrient for brain development and cognition. *Adv Nutr,* 3**,** 465S-72S.

WANG, B. & BRAND-MILLER, J. 2003. The role and potential of sialic acid in human nutrition. *Eur J Clin Nutr,* 57**,** 1351-69.

WANG, B., MILLER, J. B., MCNEIL, Y. & MCVEAGH, P. 1998. Sialic acid concentration of brain gangliosides: variation among eight mammalian species. *Comp Biochem Physiol A Mol Integr Physiol,* 119**,** 435-9.

WANG, B., YU, B., KARIM, M., HU, H., SUN, Y., MCGREEVY, P., PETOCZ, P., HELD, S. & BRAND-MILLER, J. 2007. Dietary sialic acid supplementation improves learning and memory in piglets. *Am J Clin Nutr,* 85**,** 561-9.

WANG, C. & HAN, Z. 2015. Ginkgo Biloba Extract Enhances Differentiation and Performance of Neural Stem Cells in Mouse Cochlea. *Cellular and Molecular Neurobiology,* 35**,** 861-869.

WANG, C. C. 1921. THE COMPOSITION OF CHINESE EDIBLE BIRDS' NESTS AND THE NATURE OF THEIR PROTEINS. *Journal of Biological Chemistry,* 49**,** 429-439.

WIERUSZESKI, J. M., MICHALSKI, J. C., MONTREUIL, J., STRECKER, G., PETER-KATALINIC, J., EGGE, H., VAN HALBEEK, H., MUTSAERS, J. H. & VLIEGENTHART, J. F. 1987. Structure of the monosialyl oligosaccharides derived from salivary gland mucin glycoproteins of the Chinese swiftlet (genus Collocalia). Characterization of novel types of extended core structure, Gal beta(1----3)[GlcNAc beta(1----6)] GalNAc alpha(1----3)GalNAc(-ol), and of chain termination, [Gal alpha(1----4)]0-1[Gal beta(1----4)]2GlcNAc beta(1----.). *J Biol Chem,* 262**,** 6650-7.

WITTKO, I. M., SCHANZER, A., KUZMICHEV, A., SCHNEIDER, F. T., SHIBUYA, M., RAAB, S. & PLATE, K. H. 2009. VEGFR-1 regulates adult olfactory bulb neurogenesis and migration of neural progenitors in the rostral migratory stream in vivo. *J Neurosci,* 29**,** 8704-14.

WONG, C.-F., CHAN, G. K.-L., ZHANG, M.-L., YAO, P., LIN, H.-Q., DONG, T. T.-X., LI, G., LAI, X.-P. & TSIM, K. W.-K. 2017. Characterization of edible bird's nest by peptide fingerprinting with principal component analysis. *Food Quality and Safety,* 1**,** 83-92.

WONG, Z. C. F., CHAN, G. K. L., WU, L., LAM, H. H. N., YAO, P., DONG, T. T. X. & TSIM, K. W. K. 2018. A comprehensive proteomics study on edible bird's nest using new monoclonal antibody approach and application in quality control. *Journal of Food Composition and Analysis,* 66**,** 145-151.

WU, J. R., TUO, Q. Z. & LEI, P. 2018. Ferroptosis, a Recent Defined Form of Critical Cell Death in Neurological Disorders. *J Mol Neurosci*.

XIONG, N., ZHANG, Z., HUANG, J., CHEN, C., ZHANG, Z., JIA, M., XIONG, J., LIU, X., WANG, F., CAO, X., LIANG, Z., SUN, S., LIN, Z. & WANG, T. 2011. VEGF-expressing human umbilical cord mesenchymal stem cells, an improved therapy strategy for Parkinson's disease. *Gene Ther,* 18**,** 394-402.

YAGI, H., YASUKAWA, N., YU, S. Y., GUO, C. T., TAKAHASHI, N., TAKAHASHI, T., BUKAWA, W., SUZUKI, T., KHOO, K. H., SUZUKI, Y. & KATO, K. 2008. The expression of sialylated high-antennary N-glycans in edible bird's nest. *Carbohydr Res,* 343**,** 1373-7.

YANG, W. S., KIM, K. J., GASCHLER, M. M., PATEL, M., SHCHEPINOV, M. S. & STOCKWELL, B. R. 2016. Peroxidation of polyunsaturated fatty acids by lipoxygenases drives ferroptosis. *Proceedings of the National Academy of Sciences of the United States of America,* 113**,** E4966-E4975.

YASUHARA, T., SHINGO, T., KOBAYASHI, K., TAKEUCHI, A., YANO, A., MURAOKA, K., MATSUI, T., MIYOSHI, Y., HAMADA, H. & DATE, I. 2004. Neuroprotective effects of vascular endothelial growth factor (VEGF) upon dopaminergic neurons in a rat model of Parkinson's disease. *Eur J Neurosci,* 19**,** 1494-504.

YASUHARA, T., SHINGO, T., MURAOKA, K., KAMEDA, M., AGARI, T., WEN JI, Y., HAYASE, H., HAMADA, H., BORLONGAN, C. V. & DATE, I. 2005a. Neurorescue effects of VEGF on a rat model of Parkinson's disease. *Brain Res,* 1053**,** 10-8.

YASUHARA, T., SHINGO, T., MURAOKA, K., WEN JI, Y., KAMEDA, M., TAKEUCHI, A., YANO, A., NISHIO, S., MATSUI, T., MIYOSHI, Y., HAMADA, H. & DATE, I. 2005b. The differences between high and low-dose administration of VEGF to dopaminergic neurons of in vitro and in vivo Parkinson's disease model. *Brain Res,* 1038**,** 1-10.

YIDA, Z., IMAM, M. U., ISMAIL, M., ISMAIL, N. & HOU, Z. 2015. Edible bird's nest attenuates procoagulation effects of high-fat diet in rats. *Drug Des Devel Ther,* 9**,** 3951-9.

YOKOTA, T., SUGAWARA, K., ITO, K., TAKAHASHI, R., ARIGA, H. & MIZUSAWA, H. 2003. Down regulation of DJ-1 enhances cell death by oxidative stress, ER stress, and proteasome inhibition. *Biochem Biophys Res Commun,* 312**,** 1342-8.

ZAITONE, S. A., ABO-ELMATTY, D. M. & ELSHAZLY, S. M. 2012. Piracetam and vinpocetine ameliorate rotenone-induced Parkinsonism in rats. *Indian J Pharmacol,* 44**,** 774-9.

ZHANG, J., XIN, L., SHAN, B., CHEN, W., XIE, M., YUEN, D., ZHANG, W., ZHANG, Z., LAJOIE, G. A. & MA, B. 2012. PEAKS DB: De Novo Sequencing Assisted Database Search for Sensitive and Accurate Peptide Identification. *Molecular & Cellular Proteomics : MCP,* 11**,** M111.010587.

ZHIPING, H., IMAM, M. U., ISMAIL, M., ISMAIL, N., YIDA, Z., IDERIS, A., SAREGA, N. & MAHMUD, R. 2015. Effects of edible bird's nest on hippocampal and cortical neurodegeneration in ovariectomized rats. *Food Funct,* 6**,** 1701-11.

ZIEMSSEN, T. & REICHMANN, H. 2007. Non-motor dysfunction in Parkinson's disease. *Parkinsonism Relat Disord,* 13**,** 323-32.

ZUCCA, F. A., SEGURA-AGUILAR, J., FERRARI, E., MUÑOZ, P., PARIS, I., SULZER, D., SARNA, T., CASELLA, L. & ZECCA, L. 2017. INTERACTIONS OF IRON, DOPAMINE AND NEUROMELANIN PATHWAYS IN BRAIN AGING AND PARKINSON'S DISEASE. *Progress in neurobiology,* 155**,** 96-119.

ZUKEFLI, S. N., CHUA, L. S. & RAHMAT, Z. 2017. Protein Extraction and Identification by Gel Electrophoresis and Mass Spectrometry from Edible bird’s Nest Samples. *Food Analytical Methods,* 10**,** 387-398.

Chapter 3

Edible bird's nest ameliorates oxidative stress-induced apoptosis in SH-SY5Y human neuroblastoma cells

3.1 Summary of Chapter 3

PD is characterized by the degeneration of dopaminergic neurons in the substantia nigra of the midbrain region, as well as marked reduction of dopamine concentration in the striatum. The dopamine is a chemical messenger in the central nervous system which controls movement via signalling to the motor cortex in basal ganglia. Loss of dopamine results in lack of movement control, hence PD patient performs poorly in terms of motor function.

Neurodegeneration is largely attributed to the oxidative stress in the brain microenvironment. Evidence has demonstrated that oxidative adducts of biological matter such as DNA, protein and lipids are apparent in post-mortem brain sample of PD patients. Hence, an *in vitro* PD model is created by inducing oxidative stress in neuronal cell. In our study, we aimed to induce apoptosis, or programmed cell death, of neuroblastoma cell line SH-SY5Y to reproduce PD pathology with the use of neurotoxin 6-OHDA. The model has long been well-established for drug discovery purposes.

The objectives for the study in Chapter 3 were as follow:

1. To evaluate the effect of EBN on 6-OHDA-induced oxidative status, or ROS level, in neuronal cell.
2. To examine the effect of EBN on 6-OHDA-induced apoptosis of neuronal cell.
3. To understand the mechanism underlying the 6-OHDA-induced apoptosis of neuronal cell.

Results showed that EBN extracts protected SH-SY5Y cell against 6-OHDA-induced cell injury through attenuation of ROS level and salvation from caspase-3-mediated apoptosis. The mechanism of neuroprotection was found to be independent of the mitochondrial pathway.

3.2 Published paper

Yew et al. BMC Complementary and Alternative Medicine 2014, 14:391
http://www.biomedcentral.com/1472-6882/14/391

BMC Complementary & Alternative Medicine

RESEARCH ARTICLE Open Access

Edible bird's nest ameliorates oxidative stress-induced apoptosis in SH-SY5Y human neuroblastoma cells

Mei Yeng Yew[1], Rhun Yian Koh[2], Soi Moi Chye[2], Iekhsan Othman[1] and Khuen Yen Ng[1*]

Abstract

Background: Parkinson's disease (PD) is the second most common neurodegenerative disorder affecting the senile population with manifestation of motor disability and cognitive impairment. Reactive oxygen species (ROS) is implicated in the progression of oxidative stress-related apoptosis and cell death of the midbrain dopaminergic neurons. Its interplay with mitochondrial functionality constitutes an important aspect of neuronal survival in the perspective of PD. Edible bird's nest (EBN) is an animal-derived natural food product made of saliva secreted by swiftlets from the *Aerodamus* genus. It contains bioactive compounds which might confer neuroprotective effects to the neurons. Hence this study aims to investigate the neuroprotective effect of EBN extracts in the neurotoxin-induced *in vitro* PD model.

Methods: EBN was first prepared into pancreatin-digested crude extract and water extract. *In vitro* PD model was generated by exposing SH-SY5Y cells to neurotoxin 6-hydroxydopamine (6-OHDA). Cytotoxicity of the extracts on SH-SY5Y cells was tested using MTT assay. Then, microscopic morphological and nuclear examination, cell viability test and ROS assay were performed to assess the protective effect of EBN extracts against 6-OHDA-induced cellular injury. Apoptotic event was later analysed with Annexin V-propidium iodide flow cytometry. To understand whether the mechanism underlying the neuroprotective effect of EBN was mediated via mitochondrial or caspase-dependent pathway, mitochondrial membrane potential (MMP) measurement and caspase-3 quantification were carried out.

Results: Cytotoxicity results showed that crude EBN extract did not cause SH-SY5Y cell death at concentrations up to 75 μg/ml while the maximum non-toxic dose (MNTD) of water extract was double of that of crude extract. Morphological observation and nuclear staining suggested that EBN treatment reduced the level of 6-OHDA-induced apoptotic changes in SH-SY5Y cells. MTT study further confirmed that cell viability was better improved with crude EBN extract. However, water extract exhibited higher efficacy in ameliorating ROS build up, early apoptotic membrane phosphatidylserine externalization as well as inhibition of caspase-3 cleavage. None of the EBN treatment had any effect on MMP.

Conclusions: Current findings suggest that EBN extracts might confer neuroprotective effect against 6-OHDA-induced degeneration of dopaminergic neurons, particularly through inhibition of apoptosis. Thus EBN may be a viable nutraceutical option to protect against oxidative stress-related neurodegenerative disorders such as PD.

Keywords: Edible bird's nest, Apoptosis, SH-SY5Y, 6-OHDA, Neurodegenerative disorder, Parkinson's disease, Neuroprotection

* Correspondence: ng.khuen.yen@monash.edu
[1]Jeffrey Cheah School of Medicine & Health Sciences, Monash University Malaysia, Selangor, Malaysia
Full list of author information is available at the end of the article

BioMed Central

© 2014 Yew et al.; licensee BioMed Central Ltd. This is an Open Access article distributed under the terms of the Creative Commons Attribution License (http://creativecommons.org/licenses/by/4.0), which permits unrestricted use, distribution, and reproduction in any medium, provided the original work is properly credited. The Creative Commons Public Domain Dedication waiver (http://creativecommons.org/publicdomain/zero/1.0/) applies to the data made available in this article, unless otherwise stated.

Background

Parkinson's disease (PD) is an age-related progressive neurodegenerative disease with estimated worldwide prevalence approaching 9 million of people over the age of 50 by 2030 [1]. Pathologically, there is loss of dopaminergic neurons in the substantia nigra which subsequently causes dopamine depletion in the striatum [2]. Abnormal aggregation of α-synuclein known as Lewy bodies is also detected in surviving neurons [3]. Dopamine depletion ultimately leads to deterioration of motor functions whereby the patients are often manifested with clinical signs such as tremor, rigidity and slow responsiveness [4].

Several hypotheses including neuroinflammation, mitochondrial dysfunction, failure of ubiquitin-proteasome system and proteinopathy have been proposed to explain the neurodegeneration events in PD [5,6]. Amongst those, oxidative stress-related apoptosis has been implicated in the pathogenesis of neurodegenerative diseases. Oxidative stress is caused by the production and accumulation of excessive partially reduced reactive oxygen species (ROS) within the cell, which attacks electron-rich biological molecules such as DNA, protein and lipid to affect cellular functions [7]. ROS is generated as a part of normal cellular metabolism. In the cells with high oxygen-utilizing capacity such as the neurons, however, greater amount of highly reactive oxygen radical is being produced which renders these cells more vulnerable to oxidative damages [8]. In PD, substantial post-mortem studies noted that impaired mitochondrial function and ROS build up are two events linked to apoptotic episode in dopaminergic neurons [6,9]. Experimental models of PD which are generated through the use of mitochondrial complex I activity-inhibiting and ROS-inducing neurotoxins are able to recapitulate the pathological features in PD, further reinforces that ROS introduction is critically involved in the disease [10]. Therefore the brain requires an effective antioxidant system to counteract the impact of ROS, as well as an anti-apoptotic mechanism to maintain the neuronal integrity.

Edible bird nest (EBN) is natural food product made from saliva of the swiftlets of the genus *Aerodramus* (or *Collocalia).* Numerous *in vitro* and *in vivo* researches have shown that administration of EBN was able to boost immunity, promote cell division and proliferation, neutralize influenza activity as well as improve osteoporosis [11-14]. Studies have shown that EBN contains the bioactive compound sialic acid [15-17]. Furthermore, EBN may also contain epidermal growth factor (EGF) because EGF-like activity was detected in protein fractions partially purified from EBN extract. In fact, sialic acid and EGF are neurotrophic factors known to promote neuron and brain development [18-21]. On the other hand, animal saliva was previously found to contain vascular endothelial growth factor and melatonin [22,23]. These compounds are powered with anti-apoptotic and antioxidant properties [24,25]. As apoptosis and oxidative stress have been suggested as crucial events in neurodegeneration, EBN, the salivary secretion of swiftlets, may have neuroprotective relevance in the therapeutic context of PD. Nevertheless no scientific investigation has been conducted thus far to confirm this. Hence this study aimed to investigate the neuroprotective effect of EBN.

Methods

Preparation of EBN extracts

Raw EBN from the swiftlet of *Aerodamus* genus collected from bird's nest farm in Perak, Malaysia was kindly provided by a local EBN distributor Yew Kee Pte Ltd. Cleaning was carried out by first soaking the unprocessed EBN in ultrapure water until softened and protein strands became slightly loosened. Dirt and feathers were removed manually by forceps. Cleaned EBN was subsequently oven-dried at 50°C before being grounded into fine powder. A portion of cleaned EBN was kept for water extraction whereby the EBN was first soaked in cold distilled water for 48 hours followed by boiling at 100°C for 30 minutes. The solution mixture was filtered and the filtrate was freeze-dried with freeze dryer (EYELA Freeze Dryer FOU 2100) to obtain EBN water extract powder.

Traditionally, a bird's nest soup was prepared by double-boiling the cleaned EBN strands with water until softened, whereby sugar is often added to enrich the taste. In the current study, however, both raw EBN and its water extracts were prepared by enzymatic digestion using method adopted from Guo *et al.* [13]. Pancreatin digestion was performed as numerous studies have suggested that proteolytic breakdown of EBN produced greater bioactivities when compared to the undigested EBN [13,14]. This additional step of enzymatic hydrolysis is suggested to enhance solubilisation of bioactive compounds, which subsequently leading to cellular assimilation. Briefly, raw EBN and water extract powder dissolved in ultrapure water at 2.5% (w/v) were digested with pancreatin (final concentration 0.5 mg/ml) (Sigma Aldrich, USA) in a 45°C water bath for 4 hours at pH 8.5- 9.0. Pancreatin enzyme was then deactivated at 90°C for 5 minutes. The mixtures were then filtered and freeze-dried to obtain the final crude and water EBN extracts, which were denoted as S1 and S2 respectively. Finally, products were dissolved in dimethyl sulphoxide (DMSO) (Sigma Aldrich, USA) as a stock of 50 mg/ml and sonicated until the powder was fully solubilized. Then the EBN solutions were centrifuged at 3000 rpm for 10 minutes to precipitate the undissolved EBN particles. The supernatant was collected and stored at -20°C for future use.

Neuronal cell culture

Human neuroblastoma cells SH-SY5Y was purchased from the American Type Culture Collection (ATCC no.

CRL-2266) and cultured in complete medium prepared from Dulbecco's Modified Eagle's Medium (Gibco, UK) supplemented with 10% fetal bovine serum (Gibco, UK). The cells were maintained at 37°C humidified incubator with 5% CO_2 for 2-3 days until 70% confluent. Cell collection was carried out by rinsing the cells with phosphate-buffered saline (PBS) (Biobasic, Canada) followed by addition of trypsin-EDTA (Gibco, UK) to detach the cells. The action of trypsin was later neutralized with complete medium and cells were harvested by centrifugation at 1500 rpm for 5 minutes. The cells were then sub-cultured into new tissue culture flask or plated for assays.

Determination of maximum non-toxic dose (MNTD) and effect of the EBN extracts on 6-OHDA-induced cytotoxicity

Cytotoxic test was performed with tetrazolium reduction assay using 3-(4, 5-dimethylthiazol-2-yl)-2, 5-diphenyltetrazolium bromide (MTT) reagent (Sigma Aldrich, USA). Cells were first seeded onto 96-well plate at a density of 4×10^4 cells/well with complete medium, which then was replaced by serum-free medium for treatment in the next day. Cytotoxic effect of both crude and water EBN extracts on SH-SY5Y cells was tested across a wide range of concentrations from 0 to 500 μg/ml. DMSO, which was used to dissolve the extracts, was included as vehicle control. After 48 hours incubation, MTT solution was added into the culture to a final concentration of 0.5 mg/ml. After 4 hours incubation at 37°C, the medium was removed and replaced with equal volume of DMSO to dissolve the purple formazan crystal. Absorbance of the solution was measured spectrophotometrically with microplate reader (DynexOpsys MR 24100) at 570 nm and was compared to control to be presented in percentage of cell viability or toxicity. MNTD and ½ MNTD of EBN extracts were determined from graph plotted.

To determine the effect of EBN extracts on SH-SY5Y intoxicated with neurotoxin, cells were pre-treated with EBN extracts at MNTD and ½ MNTD for 24 hours followed by co-incubation with 100 μM 6-OHDA for another 24 hours. Upon completion of treatment, MTT assay was performed to determine the cell viability. All test assays followed the same treatment whereby DMSO alone (0.5% v/v) was used as vehicle control.

Morphological examination

Apoptotic cells experiencing damage in the nuclei are featured by cell shrinkage, membrane blebbing and presence of apoptotic bodies [26]. In order to perform morphological study, cells were first grown in 60 mm culture dish and treated accordingly whereby groups such as vehicle control, 6-OHDA, S1 MNTD + 6-OHDA and S2 MNTD + 6-OHDA were included. Then, cell morphology was examined under bright field inverted microscope (Nikon Eclipse T*i*, Japan). In addition to that, nuclear staining was performed with Hoechst staining. Treated cells were fixed with 4% paraformaldehyde for 15 minutes before stained with Hoechst 33258 (1 μg/ml) (Sigma Aldrich, USA) for 15-20 minutes. Nuclear changes were examined under fluorescence excitation using the same microscope for features such as chromatin condensation, DNA fragmentation and cell shrinkage. Photomicrographs were taken using attaching camera.

Intracellular reactive oxygen species (ROS) level measurement

Intracellular ROS production was assessed with 2′, 7′-dichlorofluorescein diacetate (DCFH-DA) fluorescent probe. Cells were seeded into 12-well plate at a density of 1.5×10^5 cells/well. Upon completion of treatment, cells were collected and washed before added with 40 μM DCFH-DA (Sigma Aldrich, USA) working solution in 96-well black plate. Fluorescence reading was taken at 0, 10, 20 and 30 minutes with fluorescence microplate reader using excitation and emission wavelengths of 485 nm and 535 nm (Tecan, Austria). The fluorescence readings were then normalized to the respective cell number to give relative value of DCF fluorescence unit. Fold change in ROS production of the treated groups was determined by comparing to the untreated control.

Apoptosis analysis

The procedure was performed with Annexin V-FITC Apoptosis Detection Kit (BD Pharmingen, USA) using a modified protocol by Rieger *et al.* [27]. Briefly, upon completion of treatments, cells were harvested and washed with binding buffer. Cells were counted to obtain a final concentration of 1×10^6 cells/ml. Then Annexin V and propidium iodide (PI) were added and incubated in dark for 15 minutes. After washing, cell suspension was fixed with 1% formaldehyde for 10 minutes on ice. Subsequently, washing was performed twice with binding buffer followed by addition of RNase (EMD Biosciences, USA) which then incubated for 15 minutes at 37°C. Finally, samples were washed and ready for analysis with FACSCalibur flow cytometer (BD Biosciences, USA) and the software Cell Quest Pro.

Mitochondrial membrane potential measurement

Mitochondrial membrane potential (MMP or $\Delta\Psi m$) is an important indicator of mitochondrial functionality. Apoptosis through mitochondrial-mediated pathway can be assessed by performing MMP assay using MitoScreen kit (BD Pharmingen, USA) according to the protocols provided. Briefly, cells were collected by trypsinization and centrifugation. Washing with PBS was carried out and cells were counted to obtain a final concentration of 1×10^6 cells/ml. Working staining solution was prepared

from the JC-1 powdered dye and assay buffer at a ratio of 1:99, which was then added to the cells. Incubation was carried out at 37°C in 5% CO_2 incubator for 15 minutes. Cells were washed twice in assay buffer before analyzed with flow cytometer. Mitochondrial depolarization is indicated by a decrease in the red JC aggregates/green JC monomer fluorescence intensity ratio.

Caspase-3 detection

Caspase-3 is a proteolytic enzyme activated during apoptosis. It was detected using FITC active caspase-3 apoptosis kit (BD Pharmingen, USA) according to the protocol provided. Cells were first collected by trypsinization and centrifugation. Then, cells were washed with PBS twice and resuspended in BD Cytofix/ Cytoperm™ fixation and permeabilization solution at 1×10^6 cells/0.5 ml. Subsequently cells were incubated on ice for 20 minutes. Fixation solution was discarded after centrifugation and cells were washed twice with 0.5 ml of BD Perm/Wash™ buffer. A hundred microliters of BD Perm/Wash™ buffer and 20 μl of FITC anti-active caspase-3 antibody were added to each sample and incubated for 30 minutes at room temperature. Then, cells were washed with 1 ml of BD Perm/Wash™ buffer. Finally cells were resuspended in 0.5 ml of the same buffer and transferred to FACS tube for flow cytometry analysis.

Statistical analysis

Data was collected as triplicate from at least 3 independent experiments. The results were expressed as mean ± standard deviation. Statistical significance was assessed with Student's t-test. P value <0.05 was considered significant.

Results & Discussion

Cytotoxic profile of EBN extracts (S1 and S2)

Toxicity study was first performed with addition of EBN extracts to SH-SY5Y cells to determine the concentration-wide effect as well as MNTDs of the extracts on neuronal culture. MNTD is the maximal dose just below the threshold for cell toxicity that demonstrates no cytotoxic effect. Half of the MNTD value was also determined in order to study the effect of EBN treatment at lower concentration.

In the graph of cytotoxicity percentage in SH-SY5Y cells against EBN extract concentration (Figure 1), it was found that there was an increasing trend of cytotoxicity along with the concentration. However, cell death was not evident at concentration below 100 μg/ml for S1 and 200 μg/ml for S2. MNTDs are the concentrations at which cytotoxicity starts to become evident (where line touches x-axis). As determined from the graph, MNTDs were 76.25 ± 16.52 μg/ml for S1 and 150 ± 36.06 μg/ml for S2. Meanwhile the ½ MNTDs were 38.13 μg/ml and 75 μg/ml for S1 and S2, respectively. Overall the cytotoxicity of S1 was double as much as the cytotoxicity of S2. Such discrepancy could be due to varying methods employed in preparing the two extracts. In fact, compound solubility and stability are major factors that contribute to varied activities in different extracts [28]. S2 was extracted with water thus one might expect the resulting sample to contain only water-soluble substances. Also, high temperature applied during the water extraction process might have affected the potency of proteins within the EBN, possibly through denaturation. Based on the observations, it is likely that the water-soluble substances possess less cytotoxic effect comparing to S1, the crude EBN extract.

EBN extracts prevent 6-OHDA-induced apoptotic changes in SH-SY5Y cells

A number of cellular morphological changes including cytoplasmic condensation resulting in reduced cell size, plasma membrane undulations or blebbing, condensation of chromatin at nuclear periphery, dilatation of endoplasmic reticulum and formation of apoptotic bodies represent the typical characteristics of apoptosis [29,30]. In the present study, changes in cellular morphology of SH-SY5Y upon different treatments were assessed by microscopic examination. Untreated SH-SY5Y cells had a distinctive neuronal shape with typical long neurite outgrowth. In addition, cell membrane was intact and there were minimal dead cells (Figure 2A). Nuclear staining with DNA-binding fluorescent dye Hoechst 33258 showed homogenously stained regular rounded nuclei in control cells (Figure 2E). However, when incubated with 100 μM 6-OHDA (an optimum concentration determined from our studies earlier; Data not shown), cell death was made evident by the presence of shiny, floating and round-shaped cells under bright field microscopy (Figure 2B). Shrinking cells which gradually lost their elongated neuronal shape and have shrunken in size were also detected (yellow arrow in Figure 2B). Meanwhile, increased number of bright fluorescent nuclei indicative of chromatin condensation (white arrow in Figure 2F), as well as nuclear fragmentation (red arrow in Figure 2F) were apparent after Hoechst staining. Smaller asymmetrical nuclei were also seen as a result of cell shrinkage (green arrow in Figure 2F). These features altogether suggest that 6-OHDA-induced SH-SY5Y cell death was likely to be mediated through apoptosis. This finding is supported by previous study which concluded that the selective catecholaminergic neurotoxin induces oxidative stress-associated cell death primarily through apoptosis [31].

Nonetheless, pre-treatment with S1 or S2 for 24 hours prior to the addition of 6-OHDA conferred protection to SH-SY5Y cells by reducing cell death in the culture (Figure 2C-D). In addition, the nuclear apoptotic changes induced by 6-OHDA were less noted in the cells after pre-treatment with S1 and S2 (Figure 2G-H), suggesting that

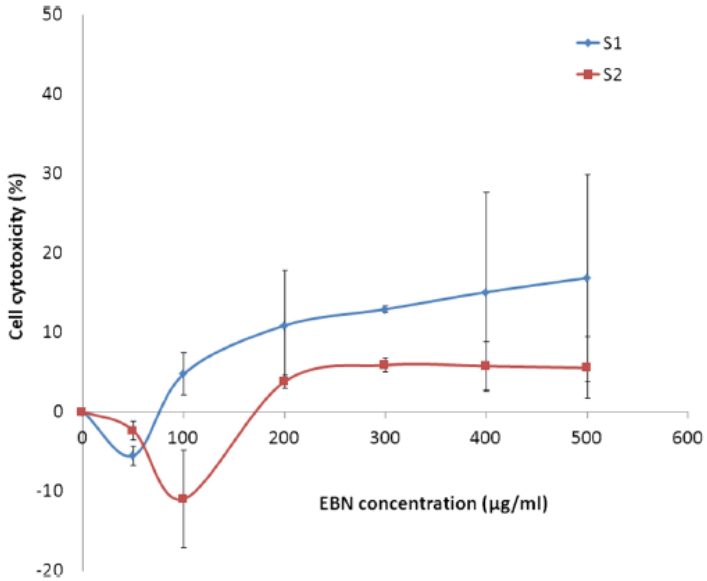

Figure 1 Cytotoxic effect of EBN extracts on SH-SY5Y cells. Cytotoxicity percentage of SH-SY5Y cells upon 48 hours treatment with either S1 or S2 was tested across a wide range of concentration from 0 to 500 µg/ml and MTT assay was carried out. Maximum non-toxic dose was then determined from the graph. The data shown are means ± S.D. of three independent experiments performed in triplicates.

EBN may be effective in reversing the cytotoxic effect of 6-OHDA.

S1 improves cell viability in 6-OHDA-challenged SH-SY5Y cells

To quantify the cell viability from those observed in the morphological study, MTT assay was performed. Upon challenge with 100 µM 6-OHDA for 24 hours, cell viability decreased significantly to about 40% of that of control (Figure 3). Pre-treatment with EBN extracts followed by co-incubation with 6-OHDA generally did not improve cell viability except in the cells treated with S1 at respective MNTD. About 20% increase in the cell viability was observed under that treatment as compared to the 6-OHDA group. This could be due to mitogenic property of S1 that promoted cell growth, as made evident by a study by Zainal Abidin *et al.* which shows that EBN promoted cell division in rabbit corneal keratocytes [32]. Moreover, acid hydrolysates of EBN have been shown to promote proliferation of human colonic adenocarcinoma (Caco-2) cells [33]. The same report also pointed out that sialic acid treatment alone induced significant Caco-2 proliferation. Taken together the finding by Yagi *et al.* which showed that sialic acid was present in EBN, it is suggested that sialic acid could be the bioactive compound that we are interested in [17].

On the contrary, S2 in overall did not prevent cell death, which may be explained by the lower activity associated with the water extract discussed earlier. Meanwhile, EBN treatment alone for 48 hours did not affect cell survival, indicating that EBN treatments at MNTDs were non-cytotoxic to SH-SY5Y cells.

S2 attenuates ROS build up in 6-OHDA-challenged SH-SY5Y cells

The overall oxidative status in SH-SY5Y cells was assessed with the DCFH-DA assay. Figure 4 showed that ROS was maintained at basal level when SH-SY5Y cells were treated with EBN extracts alone, indicating that EBN alone did not induce oxidative stress within the cell. Furthermore, S2 caused significant drop in ROS production suggesting the protective role of EBN as a free radical species scavenger.

Intracellular ROS production was augmented by 4 fold upon 6-OHDA exposure when compared to control group. Pre-treatment with S1 at high dose (MNTD) did not restore ROS to the basal level, but instead promoted intracellular ROS build up twice as much as the level of that in cell treated with 6-OHDA alone. This could be due to the presence of reactive compounds in S1 which prompted the generation of extra free radical in cells on top of the existing oxidative load, for example a 66 kDa major allergen protein in EBN [34]. As allergenic immune reaction is often linked to increased intracellular ROS production, this putative protein possesses homology to a domain of an ovoinhibitor precursor in chicken could possibly be the contributor of intracellular ROS load in S1-treated SH-SY5Y cells [35,36].

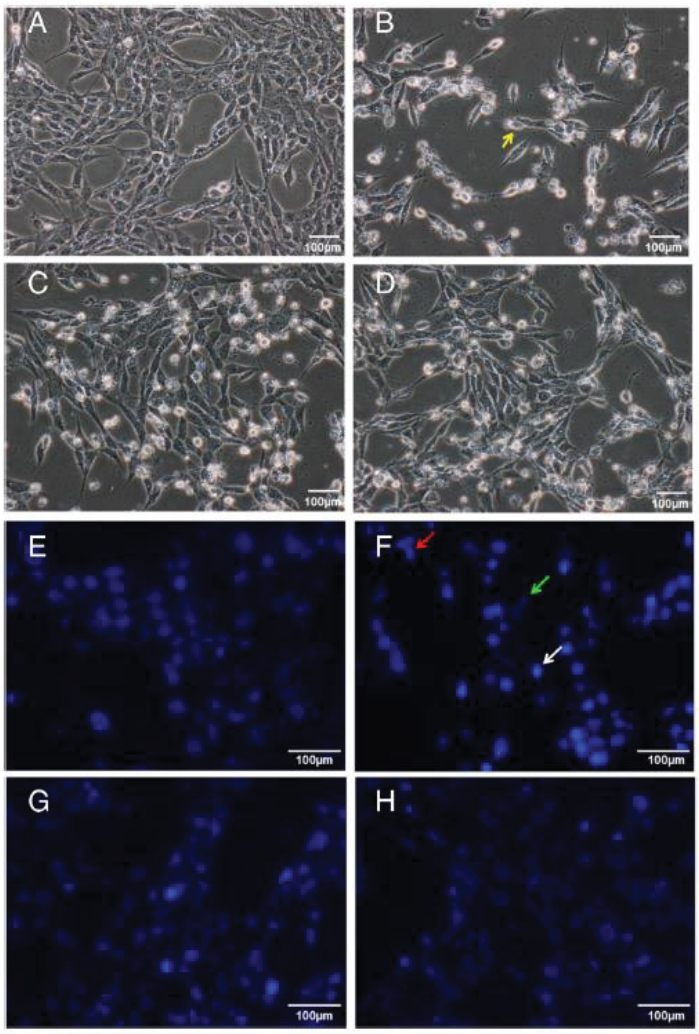

Figure 2 Effect of EBN extracts on morphological and nuclear changes of 6-OHDA-challenged SH-SY5Y cells. Microscopic images were taken after 48 hours of treatment. Figures **A-D** are bright field images while Figures **E-H** are fluorescent images taken after Hoechst 33258 staining. Figures **A** and **E**: control group; Figures **B** and **F**: 6-OHDA group; Figures **C** and **G**: S1 MNTD + 6-OHDA-treated group; Figures **D** and **H**: S2 MNTD + 6-OHDA-treated group. Cell shrinkage is indicated by cell losing its distinctive neuronal shape and has becomes smaller in size (yellow arrow in Figure 2B), DNA fragmentation is indicated by cluster of nuclei fragments (red arrow in Figure 2F), shrunken cell is indicated by smaller and distorted nuclei (green arrow in Figure 2F) while nuclear chromatin condensation is indicated by brightly fluorescent nuclei (white arrow in Figure 2F).

Meanwhile, ROS production was significantly attenuated to sub-control level by S2 treatment, in which high dose seemed to suppress ROS production better than low dose. These findings suggest that the water-soluble compounds in S2 could be more effective in scavenging intracellular ROS if present in high dose, whereas in crude extract high dose would do the opposite effect. The difference in activities of S1 and S2 can be inferred from the different methods used in extract preparation. Although both extracts derived from the same raw material, solubility and solvent accessibility of bioactive compounds in crude and water extracts may affect their chemical properties and hence, the bioactivities. In particular, water extraction method involves heat treatment at 100°C and therefore may modify tertiary conformational structure of the native EBN protein. This manipulation could possibly uncover the nucleophilic amino acid residues that present in the protein core, such as cysteine's sulfhydryl groups [37]. These amino acid residues are free radical scavenger because they are

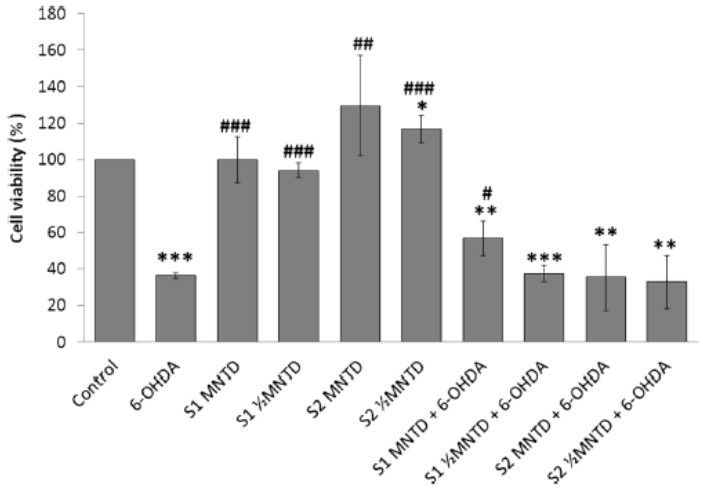

Figure 3 Effect of EBN extracts on 6-OHDA-challenged SH-SY5Y cell viability. Cell viability was assessed with MTT assay and data shown are means ± S.D. of three independent experiments performed in triplicates. *P < 0.05; **P < 0.01; ***P < 0.001 versus untreated control cells while #P < 0.05, ##P < 0.01; ###P < 0.001 versus 6-OHDA treated cells.

oxidized preferentially to the membrane phospholipids. S2 may therefore possess higher antioxidant potential than S1 because of greater solvent exposure of free radical scavenging amino acid residues as a result of heat-assisted protein denaturation.

Generally, reduction of ROS level would ameliorate oxidative stress-related cellular damage and cell death, but this was not observed in the present study. Results from ROS measurement when put together with MTT results raised an intriguing question because S1 had successfully improved cell viability although it triggered ROS generation. One explanation for this is that S1 could have initiated cytoprotective mechanism other than direct ROS-scavenging, such as the promotion of antioxidant defense system through nuclear erythroid 2-related factor 2 - antioxidant responsive element (Nrf2-ARE) signaling [38]. It has been suggested that exogenous protein can act through Nrf2-ARE signaling pathway to induce expression of endogenous antioxidant enzymes [39]. In fact, ARE activation have been demonstrated to be protective against *in vitro* cell death induced by dopamine and 6-OHDA, likely due to enhanced expression of the antioxidant proteins such as glutathione S-transferase A2, heme oxygenase-1 and NAD(P)H quinoneoxidoreductase 1 [40-42]. Interestingly, Nrf2-ARE activation is a redox-sensitive process thus this process can be triggered in response to intracellular oxidative changes, as seen in the action of apomorphine whereby ROS produced by the drug

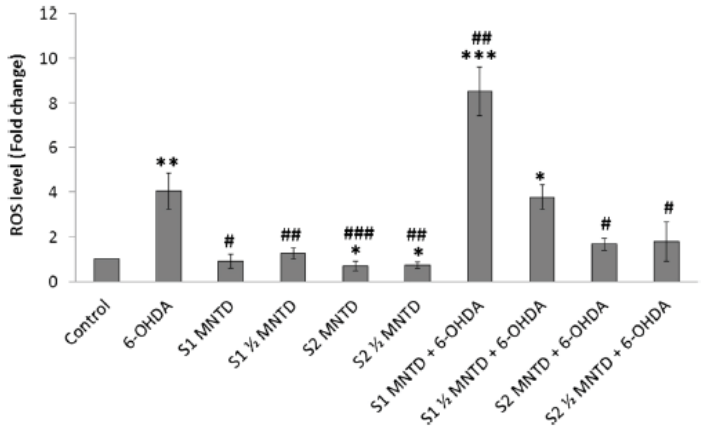

Figure 4 Effect of EBN extracts on intracellular reactive oxygen species (ROS) production in 6-OHDA-challenged SH-SY5Y cells. Intracellular ROS levels of treated groups were assessed with DCFH-DA assay and data shown are means ± S.D. of three independent experiments performed in triplicates. *P < 0.05; **P < 0.01; ***P < 0.001 versus untreated control cells while #P < 0.05, ##P < 0.01; ###P < 0.001 versus 6-OHDA treated cells.

itself acts as Nrf2-ARE pathway activator [43,44]. Therefore, it is possible that S1, in the presence of ROS, generates signals that initialize molecular changes to result in cytoprotection and hence improved cell viability. However, further works should be done to confirm the role of these members of the intracellular antioxidant response system in the neuroprotective mechanism of S1. Investigations on expression of the antioxidant genes or proteins, and nuclear translocation of Nrf2 protein could be performed in the future.

EBN extracts reduce early apoptotic event in 6-OHDA-challenged SH-SY5Y cells

Apoptotic event was investigated by Annexin V-PI double staining method to identify the mode of cell death. Several previous reports showed that apoptosis of dopaminergic neurons was found to increase with 6-OHDA-induced oxidative stress [45-48]. In this assay, cells residing at different stages of apoptosis upon exposure to 6-OHDA were identified by differential staining of membrane phosphatidylserine and DNA, whereby cells are grouped and represented in dot plot as healthy (lower left quadrant), early apoptotic (lower right quadrant), late apoptotic (upper right quadrant) and necrotic (upper left quadrant) ones. Early apoptosis, represented by cell stained positively with Annexin V due to phosphatidylserine translocation towards outer membrane surface followed by loss of membrane integrity, was found to be the major cell death mechanism in cell treated with 6-OHDA for 24 hours. It accounted for about 30% of the cell population (Figure 5B, lower right quadrant), which is in concordance with other reports [49,50].

Generally EBN treatment alone did not stimulate apoptotic event (Figure 5D-F), but it effectively reduced early apoptotic injury in cells challenged with 6-OHDA (Figure 5H-J). The results suggest that EBN is a potential neuroprotective agent which acts by inhibiting apoptosis. However, S1 treatment increased the percentage of apoptotic population in normal culture (Figure 5C) and did not reduced the early apoptosis induced by 6-OHDA (Figure 5G) when given at MNTD. Such findings imply that high dose of crude extract did not improve apoptosis and could have itself contributed to apoptosis in SH-SY5Y cells, despite the fact that MNTD used for S1 treatment had been pre-determined as non-toxic. The apoptosis-inducing nature of S1 at MNTD may be related to the elevated intracellular ROS produced as determined from the DCFH-DA assay previously.

EBN extracts did not improve mitochondrial dysfunction in 6-OHDA-challenged SH-SY5Y cells

Mitochondrial dysfunction as defined by collapse in MMP is an early and critical event in cellular apoptosis. In fact, the opening of mitochondrial transition pore

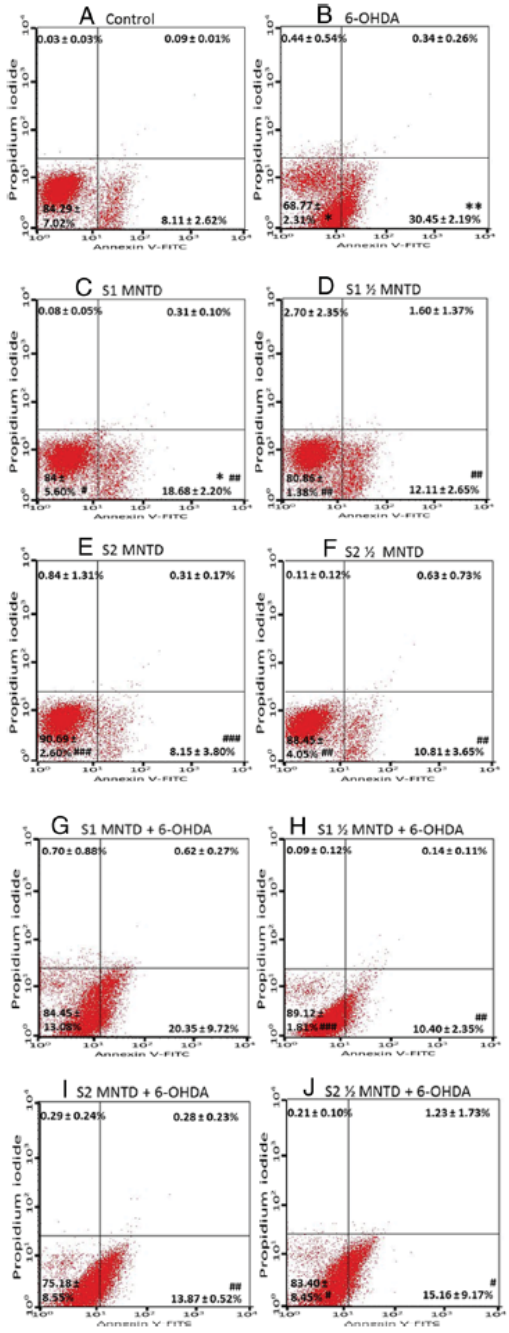

Figure 5 Effect of EBN extracts on 6-OHDA-induced apoptosis in SH-SY5Y cells. Cells treated with EBN extracts for 48 hours were analyzed by Annexin V-propidium iodide double staining. Representative plots of propidium iodide versus Annexin V-FITC fluorescence signals are shown **(A-J)**. Results shown are the mean ± S.D. of three independent experiments. *P < 0.05; **P < 0.01 versus untreated control cells while #P < 0.05, ##P < 0.01; ###P < 0.001 versus 6-OHDA treated cells.

upon different stimuli precedes the depolarization of mitochondrial potential, subsequently leading to increased mitochondrial permeability and thus the efflux of pro-apoptotic factors such as cytochrome c and procaspases [51]. The MMP in SH-SY5Y cells was measured in order to study the alteration in mitochondrial activity during apoptosis. In the present study, MMP of SH-SY5Y cells dropped drastically to 27% of that in control when the cell was exposed to 100 μM 6-OHDA for 24 hours (Figure 6). Although the action through which 6-OHDA induces cytotoxicity in neuronal cell lines such as SH-SY5Y and PC12 has been linked to ROS outburst, literature is available to show that failure of cellular respiratory complex may be the direct cause of apoptosis. Gomez- Lazaro *et al.* found that mitochondrial fragmentation constitutes early event in mitochondrial dysfunction and eventually cell death of SH-SY5Y. The author further revealed that 6-OHDA-induced SH-SY5Y cell death was reversible by blockage of the mitochondrial fission activity [51]. Taken together, the findings support the indispensable role of mitochondrial integrity in SH-SY5Y cells' survival. In fact, studies have successfully demonstrated neuroprotection against apoptosis via restoration of mitochondrial functionality by natural products, such as the herbal medicine Chunghyuldan, which ameliorated PD-like behavioral symptoms by preserving dopaminergic neurons in the nigrostriatal region of PD mice model [52].

Yet, mitochondrial functionality in the intoxicated cell was not improved with EBN treatment in the present study. There was no significant difference in MMPs between the EBN-co-treated and 6-OHDA groups. Therefore, the cell-promoting effect of S1 seen in MTT assay may be not related to resuscitation of MMP in 6-OHDA-challenged SH-SY5Y cells. Although 6-OHDA-induced cytotoxicity is mainly associated with mitochondrial respiratory dysfunction, an opposite mitochondrial-independent pathway is as well indicated in a number of studies [53,54]. As such, involvement of non-mitochondrial mechanism may be implicated in the neuroprotection conferred by the EBN crude extract.

Notably, EBN treatment alone was shown to bring down the level of MMP significantly, indicating that the addition of foreign compound to the SH-SY5Y culture could affect the mitochondrial status. Still, treatment with EBN extracts alone for 48 hours did not exhibit any detrimental effect on the SH-SY5Y's cell viability and oxidative status.

S2 inhibits cleavage of caspase-3 in 6-OHDA-challenged SH-SY5Y cells

Caspase-3 is the executioner protein of the apoptotic process and remains as inactive procaspase until it is being cleaved by activated initiator caspases such as caspase-8 or caspase-9. Its activation leads to downstream mechanisms which involve poly(ADP-ribose) polymerase-mediated DNA cleavage and breakdown of proteins essential for maintenance of cytoskeletal structure. Eventually, activation of caspase-3 results in DNA fragmentation and apoptosis [55].

Elevated active caspase-3 level was detected in SH-SY5Y cells treated with 6-OHDA, which was 7.8% as compared to 3.5% in control (Figure 7). However, S2 at ½ MNTD managed to attenuate caspase-3 activation in the cell. This explains the parallel reduction in early apoptotic population by S2 at ½ MNTD as seen from

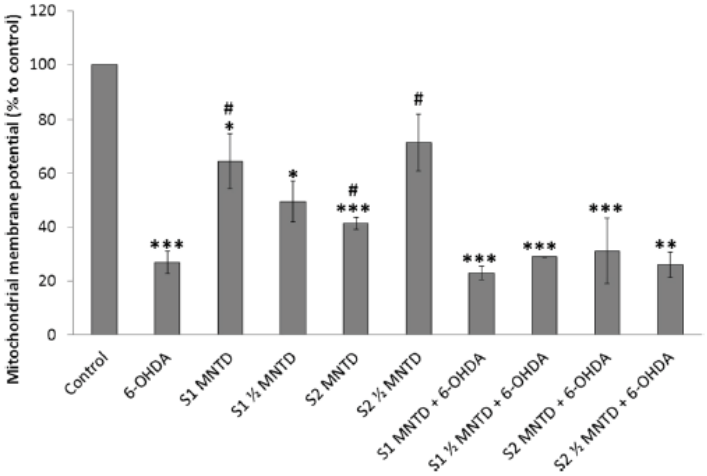

Figure 6 Effect of EBN extracts on mitochondrial membrane potential (MMP) in 6-OHDA-challenged SH-SY5Y cells. MMP was assessed with mitochondria-selective JC-1 dye and results shown are the mean ± S.D. for three independent experiments. *P < 0.05; **P < 0.01 versus untreated control cells while #P < 0.05 versus 6-OHDA treated cells.

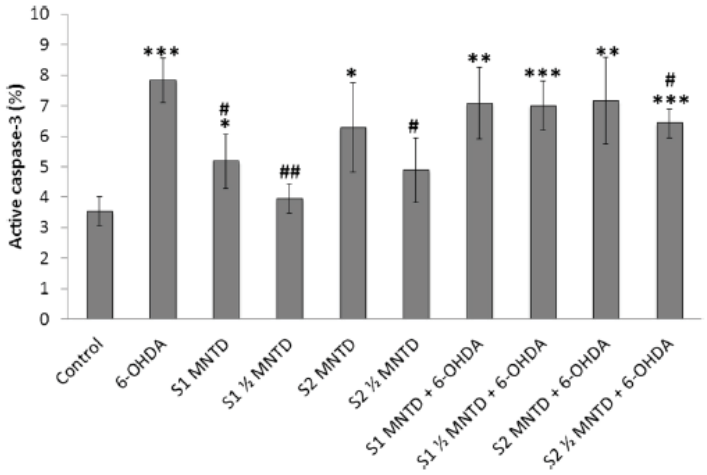

Figure 7 Effect of EBN extracts on cleavage of caspase-3 in SH-SY5Y cells challenged with 6-OHDA. The release of active caspase-3 into cytosol was assessed by immunostaining using FITC-conjugated antibody and results were generated from flow cytometry. Results shown are the mean ± S.D. of three independent experiments. **P < 0.05; **P < 0.01 versus untreated control cells while #P < 0.05, ##P < 0.01versus 6-OHDA treated cells.

Annexin V-PI analysis, thus consolidates the role of caspase-3 activation in the process of 6-OHDA-induced SH-SY5Y apoptosis [56].

Caspase-3 can be activated through two machineries, namely the mitochondria-related apoptosis protease-activating factor-1/caspase-9/caspase-3 cascade, and Fas-associated adapter protein/caspase-8/caspase-3 cascade which is the extrinsic apoptotic pathway [57]. Based on the observation from MMP assay in which S2 failed to resuscitate mitochondrial depolarization in SH-SY5Y cells challenged with 6-OHDA, it is likely that S2 inhibited caspase-3 through modulation of the extrinsic pathway which has little relation to the mitochondrial activity. However, future study is warranted to investigate the involvement of extrinsic pathway in S2-mediated neuroprotection. For EBN treatment only, both S1 and S2 when given at MNTD induced release of active caspase-3, signifying that high dose of the extracts may trigger early apoptosis event and hence lower concentrations should be used for the treatment.

Remarks on discordance between cytotoxicity and apoptotic parameters

Current finding showed that S1 treatment at MNTD improved SH-SY5Y cell viability despite being unable to prevent apoptosis and restore ROS and caspase-3 to basal level. On the contrary, S2 treatment has successfully attenuated ROS development and reduced apoptosis and caspase-3 release, yet it failed to reverse cytotoxic effect of 6-OHDA. This is intriguing as cytotoxicity is positively associated with apoptotic event, oxidative stress and caspase-3 activation. However, it is worth mentioning that cytotoxicity can be mediated by several different cell death mechanisms. Other than apoptosis, cell death can also be orchestrated by autophagy and necrosis [58]. Under such circumstances, cells are likely to either slowly sequestrated and then degraded by autolysomes through autophagy, or undergo necrosis upon activation of death domain receptors on cell surface. Cytotoxicity is thus attributed, but not exclusively, to apoptosis parameters such as externalization of phosphatidylserine on plasma membrane and activation of caspase signaling cascade. Meanwhile caspase-dependent cell death mechanism has often been described as cardinal to 6-OHDA-induced apoptosis in SH-SY5Y cells, it is proposed that another caspase-independent mechanism may also exist in a cell death scenario [59]. Such claim is supported by literatures, stating that in dying cells, caspase inhibition alone does not necessary grant full resuscitation from apoptosis but may switch cell death to alternative autophagic or necrotic modes instead [60,61]. In fact, dysregulation of autophagic response in the neurons has been linked to PD incidence [62] and autophagic changes in SH-SY5Y cells are inducible with 6-OHDA treatment [63]. On the other hand, oxidative burst from 6-OHDA could contribute to membrane rupture and therefore necrosis in neurons too [64]. Considering that autophagy or other cell death mechanisms could be activated and participated in regulating cell death in our PD cell model, hence it is indefinite that inhibition of apoptosis or caspase activation by S2 treatment would see corresponding decrease in cell death or cytotoxicity. This may partly explain the failure of S2 extract to counteract cytotoxicity due to 6-OHDA exposure regardless of its ability to attenuate apoptosis and caspase-3 cleavage.

Conclusions

It has been successfully demonstrated that EBN extracts confer neuroprotection in 6-OHDA-challenged SH-SY5Y cell model. Particularly, S1 demonstrated neuroprotective potential by improving cell viability while S2 inhibited oxidative stress and caspase-3 activation. Both the EBN extracts shown to inhibit apoptosis. Further investigation is needed to identify and elaborate the properties of the bioactive compounds in EBN that are responsible for the neuroprotective benefits. In summary, the present study suggests that EBN may be effective in the treatment of neurodegenerative diseases where oxidative stress plays a causal role.

Abbreviations

6-OHDA: 6-hydroxydopamine; ARE: Antioxidant responsive element; Caco-2: Human colonic adenocarcinoma; DCF-DA: 2′ 7′-dichlorofluorescein diacetate; DMSO: Dimethyl sulphoxide; EBN: Edible bird's nest; EGF: Epidermal growth factor; MMP: Mitochondrial membrane potential; MNTD: Maximum non-toxic dose; MTT: 3-(4 5-dimethylthiazol-2-yl)-2, 5-diphenyltetrazolium bromide; Nrf2: nuclear erythroid 2-related factor 2; PBS: Phosphate-buffered saline; PD: Parkinson's disease; PI: Propidium iodide; ROS: Reactive oxygen species; SH-SY5Y: Human neuroblastoma cell.

Competing interests

The authors declare that they have no competing interests.

Authors' contributions

MYY carried out the study, performed the statistical analysis and penned the manuscript. RYK, SMC and KYN were involved in the design of the study, coordination of the experiment and revision of the manuscript. IO was involved in the design of the study and revision of the manuscript. All authors read and approved the final manuscript.

Acknowledgements

This study was supported by Exploratory Research Grant Scheme fund 2011 ERGS/1/2011/SKK/MUSM/03/3 from Ministry of Higher Education of Malaysia. The authors would also like to thank Dr Lim Chooi Ling for her guidance in preparing the EBN water extract.

Author details

[1]Jeffrey Cheah School of Medicine & Health Sciences, Monash University Malaysia, Selangor, Malaysia. [2]Department of Human Biology, School of Medicine, International Medical University, Kuala Lumpur, Malaysia.

Received: 25 April 2014 Accepted: 1 October 2014
Published: 13 October 2014

References

1. Dorsey ER, Constantinescu R, Thompson JP, Biglan KM, Holloway RG, Kieburtz K, Marshall FJ, Ravina BM, Schifitto G, Siderowf A, Tanner CM: **Projected number of people with Parkinson disease in the most populous nations, 2005 through 2030.** *Neurology* 2007, **68**(5):384–386.
2. Dauer W, Przedborski S: **Parkinson's disease: mechanisms and models.** *Neuron* 2003, **39**(6):889–909.
3. Przedborski S: **Pathogenesis of nigral cell death in Parkinson's disease.** *Parkinsonism Relat Disord* 2005, **11**(Suppl 1):S3–S7.
4. Snyder CH, Adler CH: **The patient with Parkinson's disease: part I-treating the motor symptoms; part II-treating the nonmotor symptoms.** *J Am Acad Nurse Pract* 2007, **19**(4):179–197.
5. Schulz JB: **Mechanisms of neurodegeneration in idiopathic Parkinson's disease.** *Parkinsonism Relat Disord* 2007, **13**(Suppl 3):S306–S308.
6. Melo A, Monteiro L, Lima RM, Oliveira DM, Cerqueira MD, El-Bacha RS: **Oxidative stress in neurodegenerative diseases: mechanisms and therapeutic perspectives.** *Oxid Med Cell Longev* 2011, **2011**:467180.
7. Farooqui T, Farooqui AA: **Lipid-mediated oxidative stress and inflammation in the pathogenesis of Parkinson's disease.** *Parkinsons Dis* 2011, **2011**:247467.
8. Gandhi S, Abramov AY: **Mechanism of Oxidative Stress in Neurodegeneration.** *Oxid Med Cell Longev* 2012, **2012**:11.
9. Mounsey RB, Teismann P: **Mitochondrial dysfunction in Parkinson's disease: pathogenesis and neuroprotection.** *Parkinsons Dis* 2010, **2011**:617472.
10. Bové J, Prou D, Perier C, Przedborski S: **Toxin-induced models of Parkinson's disease.** *Neurotherapeutics* 2005, **2**(3):484–494.
11. Ng MH, Chan KH, Kong YC: **Potentiation of mitogenic response by extracts of the swiftlet's (Collocalia) nest.** *Biochem Int* 1986, **13**(3):521–531.
12. Kong YC, Keung WM, Yip TT, Ko KM, Tsao SW, Ng MH: **Evidence that epidermal growth factor is present in swiftlet's (Collocalia) nest.** *Comp Biochem Physiol B, Comparative biochemistry* 1987, **87**(2):221–226.
13. Guo CT, Takahashi T, Bukawa W, Takahashi N, Yagi H, Kato K, Hidari KI, Miyamoto D, Suzuki T, Suzuki Y: **Edible bird's nest extract inhibits influenza virus infection.** *Antiviral Res* 2006, **70**(3):140–146.
14. Matsukawa N, Matsumoto M, Bukawa W, Chiji H, Nakayama K, Hara H, Tsukahara T: **Improvement of bone strength and dermal thickness due to dietary edible bird's nest extract in ovariectomized rats.** *Biosci Biotechnol Biochem* 2011, **75**(3):590–592.
15. Pozsgay V, Jennings H, Kasper DL: **4,8-anhydro-N-acetylneuraminic acid. Isolation from edible bird's nest and structure determination.** *Eur J Biochem* 1987, **162**(2):445–450.
16. Wieruszeski JM, Michalski JC, Montreuil J, Strecker G, Peter-Katalinic J, Egge H, van Halbeek H, Mutsaers JH, Vliegenthart JF: **Structure of the monosialyl oligosaccharides derived from salivary gland mucin glycoproteins of the Chinese swiftlet (genus Collocalia). Characterization of novel types of extended core structure, Gal beta(1——3)[GlcNAc beta(1——6)] GalNAc alpha(1——3)GalNAc(-ol), and of chain termination, [Gal alpha(1——4)] 0-1[Gal beta(1——4)]2Gl.** *J Biol Chem* 1987, **262**(14):6650–6657.
17. Yagi H, Yasukawa N, Yu SY, Guo CT, Takahashi N, Takahashi T, Bukawa W, Suzuki T, Khoo KH, Suzuki Y, Kato K: **The expression of sialylated high-antennary N-glycans in edible bird's nest.** *Carbohydr Res* 2008, **343**(8):1373–1377.
18. Schneider JS, Sendek S, Daskalakis C, Cambi F: **GM1 ganglioside in Parkinson's disease: Results of a five year open study.** *J Neurol Sci* 2010, **292**(1–2):45–51.
19. Wang B: **Molecular mechanism underlying sialic acid as an essential nutrient for brain development and cognition.** *Adv Nutr (Bethesda, Md)* 2012, **3**(3):465S–472S.
20. O'Keeffe GC, Tyers P, Aarsland D, Dalley JW, Barker RA, Caldwell MA: **Dopamine-induced proliferation of adult neural precursor cells in the mammalian subventricular zone is mediated through EGF.** *Proc Natl Acad Sci U S A* 2009, **106**(21):8754–8759.
21. Ninomiya M, Yamashita T, Araki N, Okano H, Sawamoto K: **Enhanced neurogenesis in the ischemic striatum following EGF-induced expansion of transit-amplifying cells in the subventricular zone.** *Neurosci Lett* 2006, **403**(1–2):63–67.
22. Voultsios A, Kennaway DJ, Dawson D: **Salivary melatonin as a circadian phase marker: validation and comparison to plasma melatonin.** *J Biol Rhythms* 1997, **12**(5):457–466.
23. Pammer J, Weninger W, Mildner M, Burian M, Wojta J, Tschachler E: **Vascular endothelial growth factor is constitutively expressed in normal human salivary glands and is secreted in the saliva of healthy individuals.** *J Pathol* 1998, **186**(2):186–191.
24. Falk T, Yue X, Zhang S, McCourt AD, Yee BJ, Gonzalez RT, Sherman SJ: **Vascular endothelial growth factor-B is neuroprotective in an in vivo rat model of Parkinson's disease.** *Neurosci Lett* 2011, **496**(1):43–47.
25. Mehraein F, Talebi R, Jameie B, Joghataie MT, Madjd Z: **Neuroprotective effect of exogenous melatonin on dopaminergic neurons of the substantia nigra in ovariectomized rats.** *Iran Biomed J* 2011, **15**(1–2):44–50.
26. Ossola B, Kaarainen TM, Raasmaja A, Mannisto PT: **Time-dependent protective and harmful effects of quercetin on 6-OHDA-induced toxicity in neuronal SH-SY5Y cells.** *Toxicology* 2008, **250**(1):1–8.
27. Rieger AM, Nelson KL, Konowalchuk JD, Barreda DR: **Modified Annexin V/Propidium Iodide Apoptosis Assay For Accurate Assessment of Cell Death.** *JoVE* 2011, **50**:e2597.
28. Lopes AP, Bagatela BS, Rosa PC, Nanayakkara DN, Carlos Tavares Carvalho J, Maistro EL, Bastos JK, Perazzo FF: **Antioxidant and cytotoxic effects of**

crude extract, fractions and 4-nerolidylcathecol from aerial parts of Pothomorphe umbellata L. (Piperaceae). *BioMed research international* 2013, **2013**:206581.
29. Hacker G: **The morphology of apoptosis.** *Cell Tissue Res* 2000, **301**(1):5–17.
30. Ziegler U, Groscurth P: **Morphological features of cell death.** *Physiology* 2004, **19**(3):124–128.
31. Tobón-Velasco JC, Limón-Pacheco JH, Orozco-Ibarra M, Macías-Silva M, Vázquez-Victorio G, Cuevas E, Ali SF, Cuadrado A, Pedraza-Chaverrí J, Santamaría A: **6-OHDA-induced apoptosis and mitochondrial dysfunction are mediated by early modulation of intracellular signals and interaction of Nrf2 and NF-κB factors.** *Toxicology* 2013, **304**:109–119.
32. Zainal Abidin F, Hui CK, Luan NS, Mohd Ramli ES, Hun LT, Abd Ghafar N: **Effects of edible bird's nest (EBN) on cultured rabbit corneal keratocytes.** *BMC Complement Altern Med* 2011, **11**:94.
33. A AR, WN WM: **Effect of edible bird's nest on cell proliferation and tumor necrosis factor-alpha (TNF-α) release in vitro.** *Int Food Res J* 2011, **18**:1123–1127.
34. Goh DLM, Chua KY, Chew FT, Liang RCMY, Seow TK, Ou KL, Yi FC, Lee BW: **Immunochemical characterization of edible bird's nest allergens.** *J Allergy Clin Immunol* 2001, **107**(6):1082–1088.
35. Zuo L, Otenbaker NP, Rose BA, Salisbury KS: **Molecular mechanisms of reactive oxygen species-related pulmonary inflammation and asthma.** *Mol Immunol* 2013, **56**(1–2):57–63.
36. Boldogh I, Bacsi A, Choudhury BK, Dharajiya N, Alam R, Hazra TK, Mitra S, Goldblum RM, Sur S: **ROS generated by pollen NADPH oxidase provide a signal that augments antigen-induced allergic airway inflammation.** *J Clin Invest* 2005, **115**(8):2169–2179.
37. Elias RJ, Kellerby SS, Decker EA: **Antioxidant activity of proteins and peptides.** *Crit Rev Food Sci Nutr* 2008, **48**(5):430–441.
38. Johnson JA, Johnson DA, Kraft AD, Calkins MJ, Jakel RJ, Vargas MR, Chen PC: **The Nrf2-ARE pathway: an indicator and modulator of oxidative stress in neurodegeneration.** *Ann N Y Acad Sci* 2008, **1147**:61–69.
39. Erdmann K, Grosser N, Schipporeit K, Schröder H: **The ACE Inhibitory Dipeptide Met-Tyr Diminishes Free Radical Formation in Human Endothelial Cells via Induction of Heme Oxygenase-1 and Ferritin.** *J Nutr* 2006, **136**(8):2148–2152.
40. Jakel RJ, Kern JT, Johnson DA, Johnson JA: **Induction of the protective antioxidant response element pathway by 6-hydroxydopamine in vivo and in vitro.** *Toxicol Sci* 2005, **87**(1):176–186.
41. Hara H, Ohta M, Ohta K, Kuno S, Adachi T: **Increase of antioxidative potential by tert-butylhydroquinone protects against cell death associated with 6-hydroxydopamine-induced oxidative stress in neuroblastoma SH-SY5Y cells.** *Brain Res Mol Brain Res* 2003, **119**(2):125–131.
42. Nguyen T, Nioi P, Pickett CB: **The Nrf2-Antioxidant response element signaling pathway and its activation by oxidative stress.** *J Biol Chem* 2009, **284**(20):13291–13295.
43. Singh S, Vrishni S, Singh BK, Rahman I, Kakkar P: **Nrf2-ARE stress response mechanism: a control point in oxidative stress-mediated dysfunctions and chronic inflammatory diseases.** *Free Radic Res* 2010, **44**(11):1267–1288.
44. Hara H, Ohta M, Adachi T: **Apomorphine protects against 6-hydroxydopamine-induced neuronal cell death through activation of the Nrf2-ARE pathway.** *J Neurosci Res* 2006, **84**(4):860–866.
45. Lotharius J, Dugan LL, O'Malley KL: **Distinct mechanisms underlie neurotoxin-mediated cell death in cultured dopaminergic neurons.** *J Neurosci* 1999, **19**(4):1284–1293.
46. Choi WS, Yoon SY, Oh TH, Choi EJ, O'Malley KL, Oh YJ: **Two distinct mechanisms are involved in 6-hydroxydopamine- and MPP + -induced dopaminergic neuronal cell death: role of caspases, ROS, and JNK.** *J Neurosci Res* 1999, **57**(1):86–94.
47. Holtz WA, Turetzky JM, Jong YJ, O'Malley KL: **Oxidative stress-triggered unfolded protein response is upstream of intrinsic cell death evoked by parkinsonian mimetics.** *J Neurochem* 2006, **99**(1):54–69.
48. Bernstein AI, Garrison SP, Zambetti GP, O'Malley KL: **6-OHDA generated ROS induces DNA damage and p53- and PUMA-dependent cell death.** *J Biol Chem* 2011, **6**(1):2.
49. Wei L, Sun C, Lei M, Li G, Yi L, Luo F, Li Y, Ding L, Liu Z, Li S, Xu P: **Activation of Wnt/beta-catenin pathway by exogenous Wnt1 protects SH-SY5Y cells against 6-hydroxydopamine toxicity.** *J Mol Neurosci* 2013, **49**(1):105–115.
50. Ikeda Y, Tsuji S, Satoh A, Ishikura M, Shirasawa T, Shimizu T: **Protective effects of astaxanthin on 6-hydroxydopamine-induced apoptosis in human neuroblastoma SH-SY5Y cells.** *J Neurochem* 2008, **107**(6):1730–1740.
51. Gomez-Lazaro M, Bonekamp NA, Galindo MF, Jordan J, Schrader M: **6-Hydroxydopamine (6-OHDA) induces Drp1-dependent mitochondrial fragmentation in SH-SY5Y cells.** *Free Radic Biol Med* 2008, **44**(11):1960–1969.
52. Kim HG, Ju MS, Kim DH, Hong J, Cho SH, Cho KH, Park W, Lee EH, Kim SY, Oh MS: **Protective effects of Chunghyuldan against ROS-mediated neuronal cell death in models of Parkinson's disease.** *Basic Clin Pharmacol Toxicol* 2010, **107**(6):958–964.
53. Storch A, Kaftan A, Burkhardt K, Schwarz J: **6-Hydroxydopamine toxicity towards human SH-SY5Y dopaminergic neuroblastoma cells: independent of mitochondrial energy metabolism.** *J Neural Transm* 2000, **107**(3):281–293.
54. Giordano S, Lee J, Darley-Usmar VM, Zhang J: **Distinct Effects of Rotenone, 1-methyl-4-phenylpyridinium and 6-hydroxydopamine on Cellular Bioenergetics and Cell Death.** *PLoS One* 2012, **7**(9):e44610.
55. Chang HY, Yang X: **Proteases for cell suicide: functions and regulation of caspases.** *Microbiol Mol Biol Rev* 2000, **64**(4):821–846.
56. Ossola B, Lantto TA, Puttonen KA, Tuominen RK, Raasmaja A, Männistö PT: **Minocycline protects SH-SY5Y cells from 6-hydroxydopamine by inhibiting both caspase-dependent and -independent programmed cell death.** *J Neurosci Res* 2012, **90**(3):682–690.
57. MacKenzie SH, Clark AC: **Death by caspase dimerization.** *Adv Exp Med Biol* 2012, **747**:55–73.
58. Nikoletopoulou V, Markaki M, Palikaras K, Tavernarakis N: **Crosstalk between apoptosis, necrosis and autophagy.** *Biochim Biophys Acta (BBA) - Molecular Cell Research* 2013, **1833**(12):3448–3459.
59. Kroemer G, Galluzzi L, Vandenabeele P, Abrams J, Alnemri ES, Baehrecke EH, Blagosklonny MV, El-Deiry WS, Golstein P, Green DR, Hengartner M, Knight RA, Kumar S, Lipton SA, Malomi W, Nuñez G, Peter ME, Tschopp J, Yuan J, Piacentini M, Zhivotovsky B, Melino G: **Classification of cell death: recommendations of the Nomenclature Committee on Cell Death 2009.** *Cell Death Differ* 2009, **16**(1):3–11.
60. Chipuk JE, Green DR: **Do inducers of apoptosis trigger caspase-independent cell death?** *Nat Rev Mol Cell Biol* 2005, **6**(3):268–275.
61. Golstein P, Kroemer G: **Redundant cell death mechanisms as relics and backups.** *Cell Death Differ* 2005, **12**(Suppl 2):1490–1496.
62. Cheung ZH, Ip NY: **The emerging role of autophagy in Parkinson's disease.** *Mol Brain* 2009, **2**:29.
63. Solesio ME, Saez-Atienzar S, Jordan J, Galindo MF: **Characterization of mitophagy in the 6-hydoxydopamine Parkinson's disease model.** *Toxicol Sci* 2012, **129**(2):411–420.
64. Chao J, Li H, Cheng K-W, Yu M-S, Chang RC-C, Wang M: **Protective effects of pinostilbene, a resveratrol methylated derivative, against 6-hydroxydopamine-induced neurotoxicity in SH-SY5Y cells.** *J Nutr Biochem* 2010, **21**(6):482–489.

doi:10.1186/1472-6882-14-391
Cite this article as: Yew *et al.*: Edible bird's nest ameliorates oxidative stress-induced apoptosis in SH-SY5Y human neuroblastoma cells. *BMC Complementary and Alternative Medicine* 2014 **14**:391.

Submit your next manuscript to BioMed Central and take full advantage of:

- **Convenient online submission**
- **Thorough peer review**
- **No space constraints or color figure charges**
- **Immediate publication on acceptance**
- **Inclusion in PubMed, CAS, Scopus and Google Scholar**
- **Research which is freely available for redistribution**

Submit your manuscript at
www.biomedcentral.com/submit

BioMed Central

Chapter 4

Edible bird's nest extracts confer neurotrophic effects by enhancing proliferation, migration and neurogenesis of neural stem cell *in vitro*

4.1 Summary of Chapter 4

Trophic factors were previously demonstrated to enhance growth of pluripotent stem cells and support the maturation of these cells into lineage-specific, terminally differentiated and functional cells. Stem cells in the brain resides at specific region are responsive to neurotrophic factors, some of which were well-known to directly affect neurogenesis, such as brain-derived neurotrophic factor, nerve growth factor and transforming growth factor. Stem cells in the neurogenic region of the brain can be guided to proliferate, mobilize and differentiate, therefore they have the potential to be manipulated with various cocktails of neurotrophic factors for desired purposes, which makes stem cell therapy possible for the treatment of CNS-related injury or neurodegenerative diseases.

The objectives for the study in Chapter 4 were as follow:

1. To determine the effect of EBN on proliferation of neural stem cells.
2. To study the effect of EBN on migration of neural stem cells.
3. To examine the effect of EBN on neuronal differentiation of neural stem cells.

We discovered that EBN increased proliferation of neural stem cells in both BrdU assay and cell cycle analysis, promoted migration in scratch assay and enhanced retinoic-acid-induced neuronal differentiation. These findings concluded that EBN exerted neurotrophic effects on the proliferation, cell motility and neurogenesis of neural stem cells *in vitro*.

4.2 Manuscript

Edible bird's nest extracts confer neurotrophic effects by enhancing proliferation, migration and neurogenesis of neural stem cell *in vitro*

MeiYeng Yew[1], RhunYian Koh[2], SoiMoi Chye[2], Iekhsan Othman[1], KhuenYen Ng[1,3]*

[1] Jeffrey Cheah School of Medicine & Health Sciences, Monash University Malaysia, Selangor, Malaysia

[2] Department of Human Biology, School of Medicine, International Medical University, Kuala Lumpur, Malaysia

3 Brain Research Institute Monash Sunway, Monash University Malaysia, Selangor, Malaysia

Corresponding author:

Dr. Khuen Yen Ng

Brain Research Institute Monash Sunway, Monash University Malaysia.

[redacted]

Number: +6012-4500575

ORCID: 0000-0002-9453-4999

Acknowledgement:

We would like to thank Yew Kee Pte Ltd for providing raw EBN material to this study.

Abstract

Edible bird's nest (EBN) is a food product made of saliva of swiftlets from the *Aerodramus* genus and may contain potent neurotrophic compounds. Neural stem cells (NSC) are multipotent precursor cells residing in neurogenic regions of the brain that are responsive to trophic factors. Neurotrophic factors released by NSC transplantation have been shown to contribute to enrichment of brain microenvironment for functional recovery of amyotrophic lateral sclerosis, Parkinson's disease and Huntington's disease, indicating potential of compounds with neurotrophic properties as therapeutic agents in neurodegenerative diseases. This study aimed to assess the neurotrophic effect of EBN extracts on NSC. By using embryonic mouse neuroectodermal cell, NE-4C, maximum non-toxic dose (MNTD) of crude and water extracts of EBN was determined for subsequent treatment. Bromodeoxyuridine (BrdU) incorporation and S-phase population in NE-4C were increased after EBN extract treatments at ½MNTDs, indicating higher cell proliferation. EBN extracts also enhanced cell migration rate in scratch assay and selective differentiation of retinoic acid-primed NE-4C into mature neurons. These results described the regulatory effects of EBN extracts on proliferation, migration and differentiation of NSC, which allowed better understanding of stem cell behaviours in respond to neurotrophic compounds, hence leading to potential application of such finding into development of stem cell therapy for the treatment of neurodegenerative diseases. Our study supports the idea of using EBN as a potential neuroregenerative strategy against neurodegenerative diseases.

Keywords

Edible bird's nest; Neural stem cell; Neurotrophic effect; Neuronal differentiation; Neurodegenerative diseases

Contribution of authors

MYY, SMC, RYK and KYN conceived the study design. MYY conducted the experiment. MYY and RYK contributed in the data analysis and interpretation. MYY, RYK and KYN helped to draft and revise the manuscript. All authors read and approved the final manuscript.

Introduction

Neurogenesis is the formation of functional neuron from precursor stem cell residing in the neurogenic regions in the brain, which includes subventricular zone of the lateral ventricle and subgranular zone of the dentate gyrus in hippocampus (Gage, 2000). Stem cell is pluripotent in itself that it can self-renew continuously and is inducible to form different cell types of any specific lineages if appropriate signals were given. Due to the indispensable role of neural stem cells (NSC) in brain development, which is a life-long process that continues throughout the adulthood (Ming and Song, 2011), NSC represents a valuable tool for the study of developing brains and neurologic disorders. In fact stem cell research has always been a key research area for the treatment of neurodegenerative diseases including Alzheimer's disease, Parkinson's disease and Huntington's disease (Lo Furno et al., 2017). Pathologically, the hallmarks of neurodegenerative diseases include but not limited to degeneration of the axon, neuronal body, dendrites and synapses of a neuron, hence the breach of an intact brain circuitry (Luo and O'Leary, 2005). Studies have shown that restoration of impaired or degenerated neurons using endogenous resident stem cell are promising with exogenous neurotrophic support. Notably, several natural neurotrophic compounds have demonstrated functional recovery such as Huperzine A for the treatment of cognitive deficiencies in Alzheimer's disease (Ha et al., 2011) and Puerarin for the treatment of motor dysfunction in Parkinson's disease (Li et al., 2013). These findings conclude that

endogenous NSC is responsive to a variety of exogenous factors and can be induced into desired cell phenotype if appropriate signals were given (Xu et al., 2014).

Edible bird nest (EBN) is a natural food product made from saliva of the swiftlets, particularly by the genus *Aerodramus.* Chinese being the largest consumer community of EBN usually prepared it in soup and regard it as delicacy with substantial medicinal value. Traditionally, EBN has been used for its tonic effect towards complications in the respiratory airways and gastrointestinal system. In addition to that, EBN is also well-sought after for claims such as ability to enhance skin complexion, immunity, growth, metabolism and blood circulation (Lim and Cranbrook, 2002, Chye et al., 2017). Increasing public interest on the benefits of EBN has prompted the study of its bioactivities. Notably, *in vitro* and *in vivo* studies have proved that EBN extract was able to promote cell division and proliferation (Ng et al., 1986), inhibit influenza activity (Guo et al., 2006), protect neurons against oxidative stress (Yew et al., 2014) and prevent osteoporosis (Matsukawa et al., 2011). These literatures suggest that EBN may be a rich source of animal-derived natural compound that may offer a range of health advantage.

More than a decade ago, epidermal growth factor (EGF)-like compound was identified in EBN extract (Kong et al., 1987). It is known that EGF modulates the proliferative, migration and neurogenesis pattern of NSC *in vivo* (Reynolds et al., 1992, Gonzalez-Perez and Quiñones-Hinojosa, 2010). Therefore it is presumed that EBN extracts might also possess EGF-like activity that would confer similar effects on NSC. Later, high-antennary sialic acid was also been discovered and studied in EBN extract (Yagi et al., 2008). Sialic acid-bound glyocoproteins such as gangliosides and neural cell adhesion molecule were known to play a big role in the development of brain network and connectivity (Wang, 2012). In spite of the

fact that EBN extract contains high amount of sialic acids and possess EGF-like activity, the exact neurotrophic effects of EBN extract has never been evaluated. The current investigation explored the neurotrophic properties of EBN extracts and its potential application as a therapeutic agent for the treatment of neurodegenerative diseases. For that purpose, we used embryonic neuroectodermal stem cells, NE-4C, in this study to study the effect of EBN treatment on the proliferation, migration and neuronal differentiation of NSC.

Materials and methods

Materials

Embryonic mouse neuroectodermal cell NE-4C was purchased from American Type Culture Collection (Manassas, VA, USA). Pancreatin powder, dimethyl sulphoxide (DMSO), poly-L-lysine (PLL), formaldehyde, 3-(4,5-dimethylthiazol-2-yl)-2,5-diphenyltetrazolium bromide (MTT) powder, bovine serum albumin, Hoechst 33258, propidium iodide and retinoic acid were obtained from Sigma-Aldrich (Sigma, St. Louis, MO, USA). All cell culture reagents including Modified Eagle's medium, L-glutamine and fetal bovine serum were purchased from Gibco (Grand Island, NY, USA). Alexa Fluor 488-conjugated rabbit anti-β-III tubulin and Cy3-conjugated mouse anti-glial fibrilary acidic protein (GFAP), RNase A, bromodeoxyuridine (BrdU) cell proliferation assay kit as well as the remaining chemicals and solvents of analytical grade were purchased from Merck (Darmstadt, Germany).

Preparation of EBN extracts

EBN were prepared into pancreatin-digested extracts denoted as S1 (crude extract) and S2 (water extract) according to our previously established protocol (Yew et al., 2014). Briefly, raw EBN collected from a local bird's nest farm in Perak, Malaysia was cleaned in ultrapure water and oven-dried at 50°C before being grounded into fine powder. Some of the cleaned

EBN was extracted in water, whereby EBN was first soaked in cold distilled water for 48 hours followed by boiling at 100°C for 30 minutes. The solution mixture was filtered and the filtrate was freeze-dried with freeze dryer (EYELA Freeze Dryer FOU 2100) to obtain water extract powder.

Subsequently, raw EBN powder and its water extract powder were digested using enzymatic method adopted from Guo et al. (Guo et al., 2006). The powders were digested with pancreatin (final concentration 0.5 mg/ml) in ultrapure water at 2.5% (w/v) over a 45°C water bath for 4 hours at pH 8.5- 9.0. The solutions were heated at 90°C for 5 minutes to halt the action of the enzyme. After filtration, the solutions were freeze-dried to obtain the final sample S1 and S2. The powders were solubilized in DMSO for subsequent *in vitro* treatment.

Neural stem cells culture

Neural stem cell, NE-4C was cultured in Modified Eagle's medium with non-essential amino acids and 4 mM L-glutamine supplemented with 10% fetal bovine serum, and maintained in incubator at 37°C with 5% CO_2. PLL was used to coat all culture consumables to ensure monolayer cell growth.

Cell viability test

For dose optimization, NE-4C was incubated with 0 to 500 µg/ml EBN extracts for 48 hours under serum free condition in 96-well plate. Cell viability of NE-4C was then tested using MTT assay to determine the maximum non-toxic dose (MNTD) and ½ MNTD. Briefly, MTT solution was added to cells and incubated for 4 hours. After that, the solution was removed and DMSO was added to lyse the formed formazan. Finally, the absorbance of the solution which is indicative of cell viability was read at 570 nm using a microplate reader

(DynexOpsys MR 24100, VA, USA) and the result was expressed as percentage of cytotoxicity in comparison to untreated control. MNTD and ½ MNTD of EBN extracts were determined from the cytotoxicity graph.

Treatment with EBN extracts

The cell was treated under serum free condition according to the following grouping in subsequent experiments: (1) Untreated control; (2) S1 treatment at MNTD; (3) S1 treatment at ½ MNTD; (4) S2 treatment at MNTD; (5) S2 treatment at ½ MNTD.

Cell cycle profiling

NE-4C was cultured and treated on PLL-coated 60mm dish until 80% confluent. Cell cycle progression was studied in NE-4C using the flow cytometry method. Cell was washed and fixed overnight at 4°C in ice cold 70% ethanol. Fixed cell was washed and stained with 20 µg/ml propidium iodide dye and 15 µg/ml RNase A, after which analyzed with FACSCalibur flow cytometer (BD Biosciences, USA). The distribution of cell population in all stages of cell cycle was noted.

BrdU cell proliferation assay

NE-4C was cultured and treated on PLL-coated 96-well plate. Using BrdU cell proliferation assay kit, BrdU reagent was added to the cell 2 hours before the treatment period ended. Then, the cell was fixed, washed and added with detector anti-BrdU antibody. Secondary goat anti-mouse IgG peroxidase-conjugated antibody (1:2000) was added and incubated for 30 minutes at room temperature. After washing, 3,3',5,5'-Tetramethylbenzidine (TMB) Peroxidase Substrate was added and incubated for 30 minutes at room temperature in dark before added with Stop Solution. The fluorescence absorbance was read spectrophotometrically at 450/

550nm using a SpectraMax M5 microplate reader (Molecular Devices, Sunnyvale, California).

Scratch assay for cell migration analysis

NE-4C was cultured in PLL-coated 12-well plate and a single cell scratch was introduced in each well using a yellow micropipette tip on monolayer cell. Cell debris was removed with washing, and then fresh medium containing treatment was added. Cell culture image was taken at 0, 6, 12 and 18 hours with a camera on bright field inverted microscope (Nikon Eclipse Ti-U, Japan) at 200X magnification. Gap width of the scratched line was then measured using ImageJ Software. The migration rate of cell was calculated as a result of distance moved over time.

Immunocytochemistry for quantification of neuronal differentiation

Differentiation of NE-4C was determined by immunostaining with neuronal class β-III tubulin and GFAP, which are the markers for neurons and astrocytes, respectively. After treatment, the cell in PLL-coated 24-well plate was first fixed with 4% paraformaldehyde. Blocking was performed by adding bovine serum albumin for 1 hour, followed by incubation with fluorophore-conjugated antibodies including rabbit anti-β-III tubulin (AlexaFluor 488-tagged, 1:500) and mouse anti-GFAP (Cy3-tagged, 1:500), for 1 hour at room temperature. Lastly, cells were counterstained with nuclear stain Hoechst 33258 (1µg/ ml) for 5 minutes before visualized at 200X magnification under fluorescence microscope (Nikon Eclipse Ti-U, Japan). Cell treated with EBN extracts was observed for duration of 14 days to study the time-course of spontaneous neuronal and astrocytic differentiation.

Neuronal differentiation using retinoic acid

Dose of differentiation agent retinoic acid was tested across 10^{-8} M to 10^{-5} M over 5 to 7 days to optimize the existing protocol for the induction of neuronal differentiation in NE-4C (Schlett and Madarasz, 1997). It was determined that the cell to be induced with 10^{-6} M retinoic acid for 48 hours and maintained in fresh medium containing treatment afterwards for up to 7 days to allow for neuronal differentiation. Immunocytochemical studies were then performed by staining the cells with neuronal and astrocytes markers. Image was taken with fluorescence microscope (Nikon Eclipse Ti-U, Japan) at 200X magnification using respective fluorescence filter. Cell stained positively for β-III tubulin and total cell number (stained with Hoechst 33258) were counted manually. The percentage of differentiated neuron was determined using the following equation:

$$\frac{\text{Cell stained positively for } \beta - \text{III tubulin}}{\text{Total cell number}} \times 100$$

Statistical analysis

Data was presented as mean ± standard deviation from at least two to three independent experiments. Statistical analysis is performed with Student's *t*-test and a value of $P< 0.05$ is considered significant.

Results and discussion

Dose optimization for EBN treatment

Toxicity study was performed on neural stem cell NE-4C treated with EBN extracts to determine the concentration-wide effect as well as MNTD. No cytotoxicity was demonstrated at the lowest dose tested (100 µg/ml), but cell death was seen at 200 µg/ml for S1 and 300 µg/ml for S2 (Fig.1). As determined from the graph of cytotoxicity against concentration of

EBN (Fig.1), the MNTDs on NE-4C were 130 µg/ml for S1 and 290 µg/ml for EBN water extract S2. Meanwhile, ½ MNTDs were 65 µg/ml and 145 µg/ml for S1 and S2, respectively. These concentrations were then used for treatment in further studies with NE-4C as they were close to the highest possible amount of extract with expectedly minimal toxic side effect.

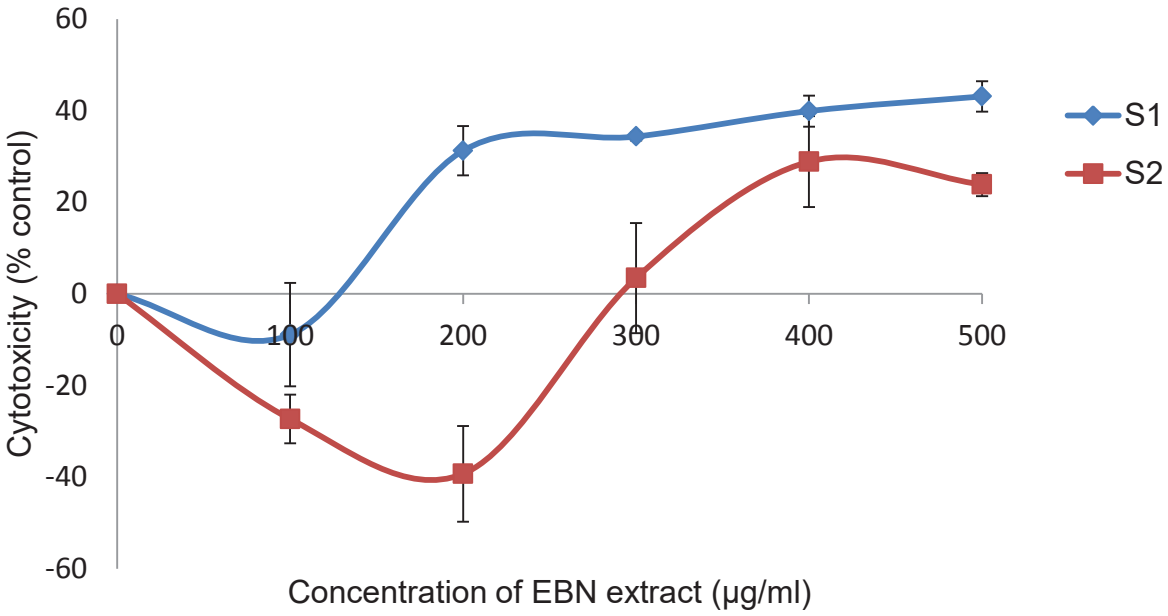

Fig.1 Cytotoxic effect of EBN extracts on NE-4C. Cytotoxicity percentage of NE-4C upon 48 hours treatment with S1 and S2 was tested across a wide range of concentration from 0 to 500 µg/ml using MTT assay. Maximum non-toxic dose was then determined from the graph. The data shown are means ± standard deviation of three independent experiments.

The cytotoxicity of S1 was nearly double as much as the cytotoxicity of S2, possibly due to the different extraction methods that affected their bioactivities. This finding is consistent with our previous work on human neuroblastoma cell line in which we noticed varied bioactivities between the extracts (Yew et al., 2014). Although traditionally EBN is boiled in water for consumption, Wong et al. suggested that only about 5% of EBN protein can be extracted after 1-2 hours of stewing in water (Wong et al., 2017). Hence, in order to look into

the complete profile of EBN protein, the present study prepared both S1 and S2 extract. S1 was prepared via direct enzymatic digestion of the raw EBN powder. Direct enzymatic digestion of the raw EBN powder will be expected to breakdown the water-holding or hydrophilic glycoprotein matrix in EBN and improve solubility of hydrophilic compounds (Segu et al., 2010). S2 was extracted with cold water for 48 hours followed by 30 minutes of boiling thus it is anticipated that highly water-soluble compounds were extracted in this sample. S1 is therefore believed to be a better representation of the original content in the raw EBN than S2.

On top of that, boiling of the sample up to 100˚C during water extraction process may have affected the potency of compounds in the S2 or EBN water extract. It has been previously described that thermal processing tends to alter the characteristics of proteins in peanuts, milk, eggs and soy, resulting in deviations in, for instance, their allergenic potentials (Verhoeckx et al., 2015). Whether the application of heat will promote or demote the bioactivities of food nutrients, however, was not clearly defined because while sterilization reduced allergenicity of whey protein in milk, allergenicity of roasted peanut proteins can be exaggerated due to glycation process (Taheri-Kafrani et al., 2009, Chung and Champagne, 2001). Based on the observed effect of EBN extract treatment on NE-4C cell viability, it is likely that S2 sample, the water extract, is less potent comparing to S1, the crude EBN extract. The exact neurotrophic potential of EBN extracts was tested in subsequent studies on proliferation, migration and neuronal differentiation.

Cell cycle analysis

Cell cycle profiling by flow cytometry enables detailed analysis of a cell's progression through different stages of cell growth. The proportion of cell residing at the sub G1, G0/G1,

S or G2/M phase in cell cycle describes the process of which a cell is active in, for instance, protein synthesis, DNA synthesis, or cell division. In the current study (Fig.2), EBN treatment was shown to induce NE-4C cell proliferation, but the effect is time-dependent. The distribution of EBN-treated NE-4C throughout the cell cycle did not change much from the control group as early as 6 hours post-treatment (Fig.2a), but there was a significant increase in S-phase population in cell treated for 12 hours with ½ MNTDs of S1 and S2 under serum-free condition (Fig.2b), indicating that it is the time point at which genetic duplication is at peak. However, cell proliferation subsequently decreased with longer incubation duration. Cell arrest at G0/G1 was seen in S1-treated cell at 18th hour (Fig.2c) followed by cell arrest at G2/M at 24th hour in S2-treated cell (Fig. 2d), which is likely an effect caused by serum starvation (Brooks, 1976, Chen et al., 2012).

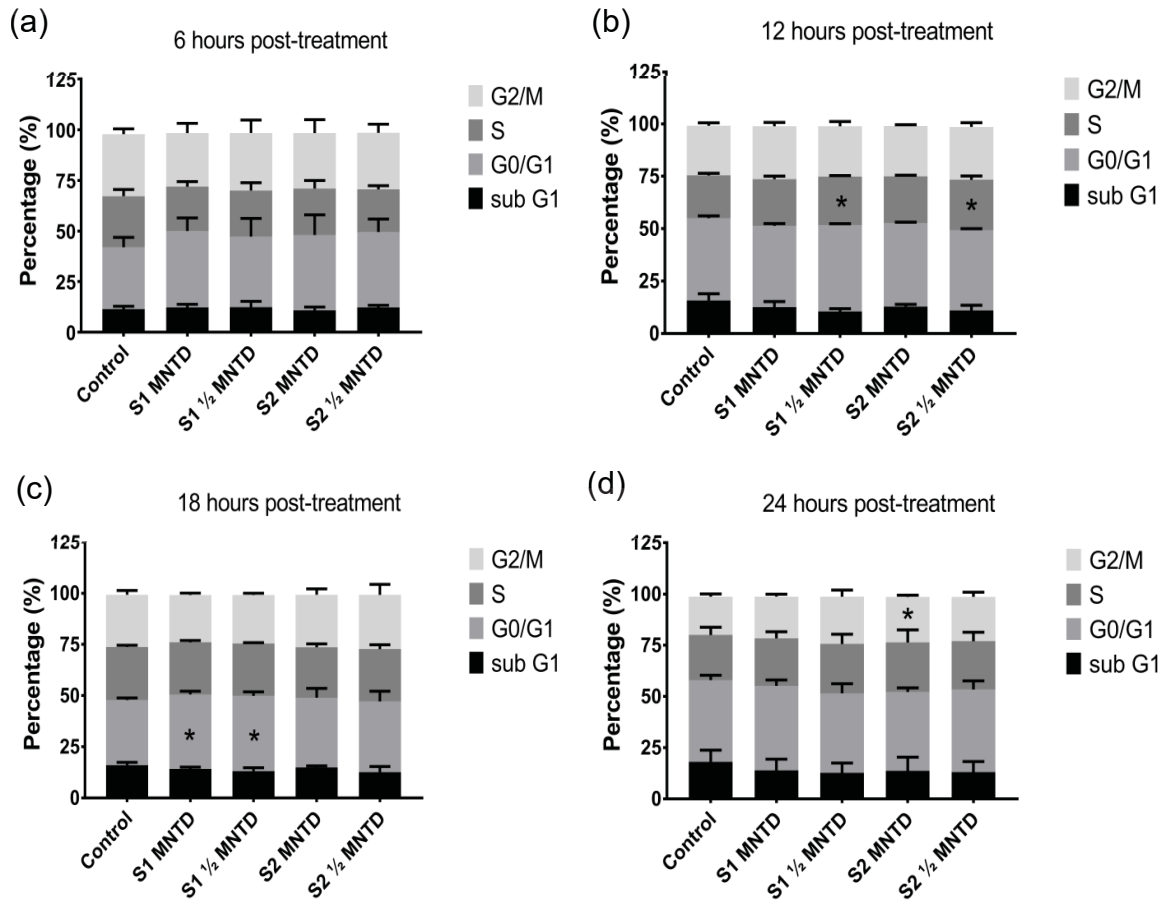

Fig.2 Cell cycle profiling of EBN-treated NE-4C. After EBN extract treatments at various time points, cell cycle pattern was studied in NE-4C. The percentage of cell distribution at sub G_1, G0/G1, S or G2/M phase after (a) 6 hours, (b) 12 hours, (c) 18 hours and (d) 24 hours of treatment was expressed in stacked charts. The data shown are means ± standard deviation of two to three independent experiments. **P*<0.05 versus untreated control cells.

EBN extracts increase BrdU incorporation in NE-4C

BrdU is a synthetic nucleoside analogy of thymidine and can be incorporated into the newly synthesized DNA of replicating cells. By measuring the level of BrdU incorporated, the proliferation activity of a cell can be studied. In accordance to the results from cell cycle profiling, increased BrdU optical density values in Fig. 3 showed that proliferation of NE-4C was greatly promoted at 12th hour after treated with ½ MNTDs of S1 and S2 under serum-free condition when compared to the control. Taken together, results from cell cycle and BrdU studies agreed that EBN extracts increased cell proliferation in NE-4C as soon as 12 hours after treatment. Although it has been demonstrated previously that EBN extract had mitogenic effect on human adipose-derived stem cells, the compound responsible for such effect is not determined (Roh et al., 2012). Nevertheless, Roh et al. found that interleukin-6 and vascular endothelial growth factor (VEGF) genes was up-regulated in human adipose-derived stem cells. Such information will warrant future studies to investigate the bioactive compounds in EBN extract that might be responsible for the proliferative effect seen on stem cells.

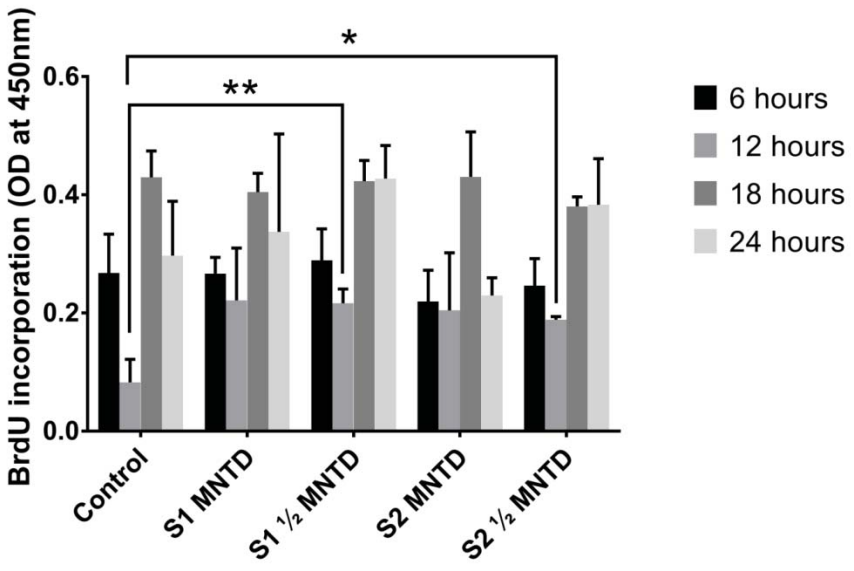

Fig.3 BrdU incorporation in EBN-treated NE-4C. BrdU reagent was added 2 hours prior to the end of treatment and its uptake into newly-synthesised DNA was reflected in optical density (OD) values after being quantified by detector antibodies. The data shown are means ± standard deviation of three independent experiments. **P*<0.05 versus untreated control cells; ***P*<0.01 versus untreated control cells.

Cell migration studies with scratch assay

The migratory pattern of NE-4C was investigated with cell imaging. NE-4C needs to be grown on a confluent monolayer prior to the introduction of a scratched line. This ensures that the cells are non-proliferating and therefore wound closure will be achieved by cell migrating from the scratched edge (Oudin et al., 2011). The gap width of the 'wound' was measured immediately (time 0) and constantly monitored over various time points. After 18 hours of treatment, wound closure was improved in all EBN extract-treated cells (Fig. 4a). Quantitative analysis of the width of scratched area showed that cell migration rate was higher when compared to control after being treated with ½ MNTDs of S1 and S2 for 18 hours (Fig. 4b).

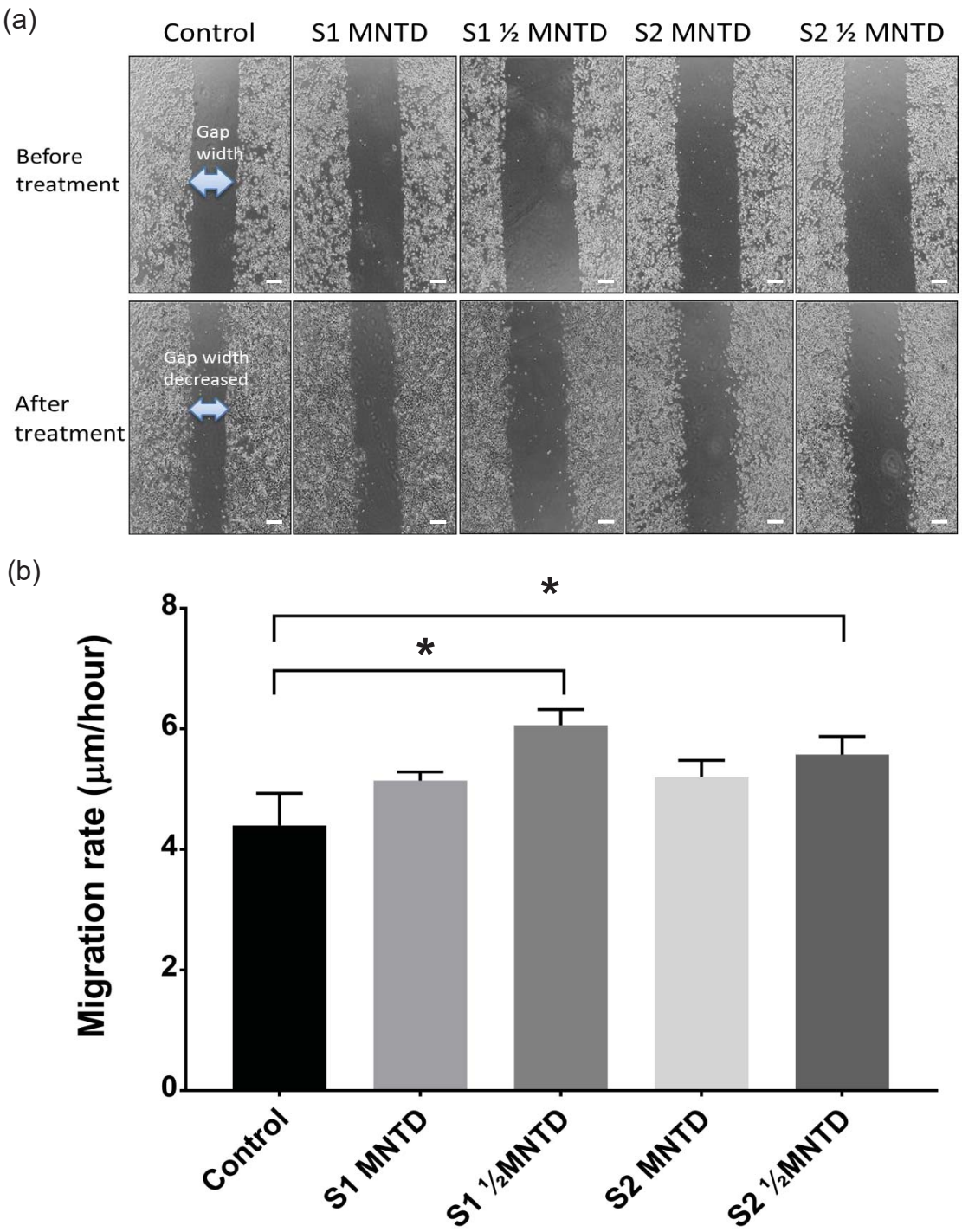

Fig.4 Cell migration studies in EBN-treated NE-4C. Monolayer cell was obtained and a scratch wound was introduced to allow migration of cell from the scratched end to the area devoid of cell. (a) Image was taken with microscope camera and analyzed with software to measure the gap width before and after 18hours of treatment. Images were viewed at 40X magnification. (b) Migration rate was averaged from the cell after 18 hours of incubation. The data shown are means ± standard deviation of three independent experiments. *P<0.05 versus untreated control cells. Scale bar = 100 μm.

Modulation of cellular structures related to actin and microtubule dynamics was found to be related to migratory character in the adherent NE-4C (Williams et al., 2013). Hereby we postulated that EBN extracts might indirectly regulate the remodelling of these structures to enable cell motility across the scratched area in the cell migration study. Previous studies are especially helpful in elucidating the basis of this observation. Kong et al. reported in 1987 that partially-purified protein elution from chromatographic separation of EBN exhibited similar activity and physical properties to that of murine EGF (Kong et al., 1987). In fact, EGF has been shown to determine migratory pattern of neural precursors in the fetal telencephalon (Caric et al., 2001, Ciccolini et al., 2005), confers motile phenotype to NSC *in vitro* (Boockvar et al., 2003) and induces migration of subventricular zone-derived cells (Aguirre et al., 2005). Presence of EGF-like compound in EBN may promote cell migration in EBN-treated NE-4C, perhaps through extracellular-signal-regulated kinase (ERK) signalling-mediated focal adhesion dissociation during cell spreading (Flinder et al., 2011). However more investigations are required to identify the presence of EGF-like compound as well as to confirm the underlying mechanism and its association with ERK signalling pathway.

EBN extracts do not induce spontaneous neuronal and astrocytic differentiation in NE-4C

The potential of EBN to induce differentiation of multi-potent NSC into mature cell with well-defined function such as neuron and astrocyte was investigated with immunocytochemistry techniques. There was no formation of neuron and astrocytes when NE-4C was treated with EBN alone, even after prolonged incubation up to 7 (Fig.5a) and 14 days (Fig.5b).

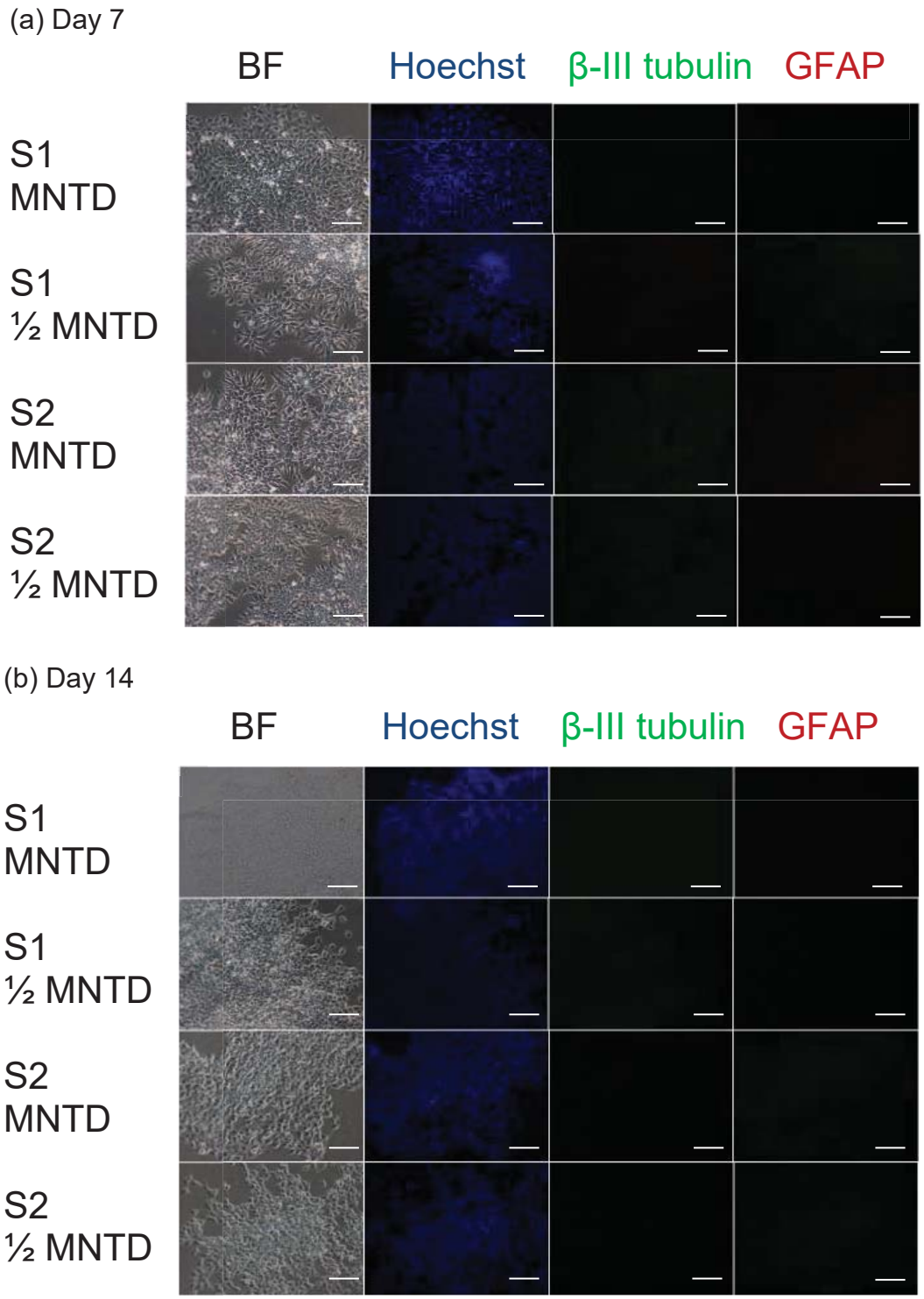

Fig.5 Cell differentiation studies in NE-4C. Immunocytochemistry studies with neuronal marker β-III tubulin and glial marker GFAP revealed that EBN extract treatments alone, although incubated for up to 14 days, did not induce neuronal differentiation and astrocyte formation in NE-4C. Images shown are (a) Day 7 and (b) Day 14 of EBN extract treatments alone. Hoechst dye was used to stain cell nuclei and the images were viewed at 200X magnification. BF: Bright-field. Scale bar = 100 µm.

EBN extracts promote neuronal differentiation in retinoic acid-primed NE-4C model

In an alternative approach, NE-4C was tested with different concentrations of differentiation agent retinoic acid. It was found that 2-day priming with 10^{-6} M of retinoic acid produced prominent neuronal differentiation on Day 7 (Fig.6). Using this retinoic acid-primed model, NE-4C was co-incubated with EBN to observe if the presence of EBN would enhance the neuronal differentiation process. Our results show that, co-incubation with EBN effectively promoted neuronal differentiation in these cells (Fig.7a). After seven days of incubation, only 40% of the cell was stained positive for the neuronal marker β-III tubulin in control, whereas S1 treatment enhanced the differentiation rate to 60% and S2 treatment to 55% (Fig.7b).

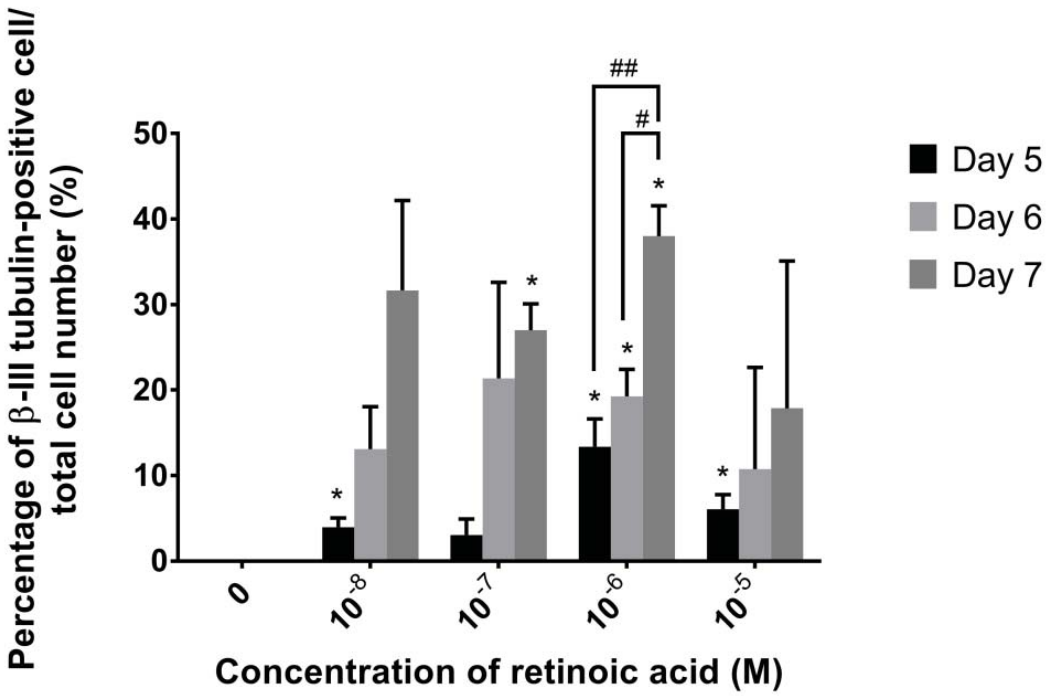

Fig.6 Neuronal differentiation in retinoic acid-primed NE-4C. Concentration of differentiation agent retinoic acid was tested across 10^{-8} M – 10^{-5} M. Cell was primed 2 days with retinoic acid and further cultured up to Day 5, 6 and 7 to achieve maximum neuronal differentiation. Percentage of neuronal differentiation was presented as percentage of cell stained positively for β-III tubulin over total cell number. The data shown are means ± standard deviation of two independent experiments. **P*<0.05 versus untreated control cells; #*P*<0.05 versus treated cell on Day 5; ##*P*<0.01 versus treated cell on Day 5.

(a)

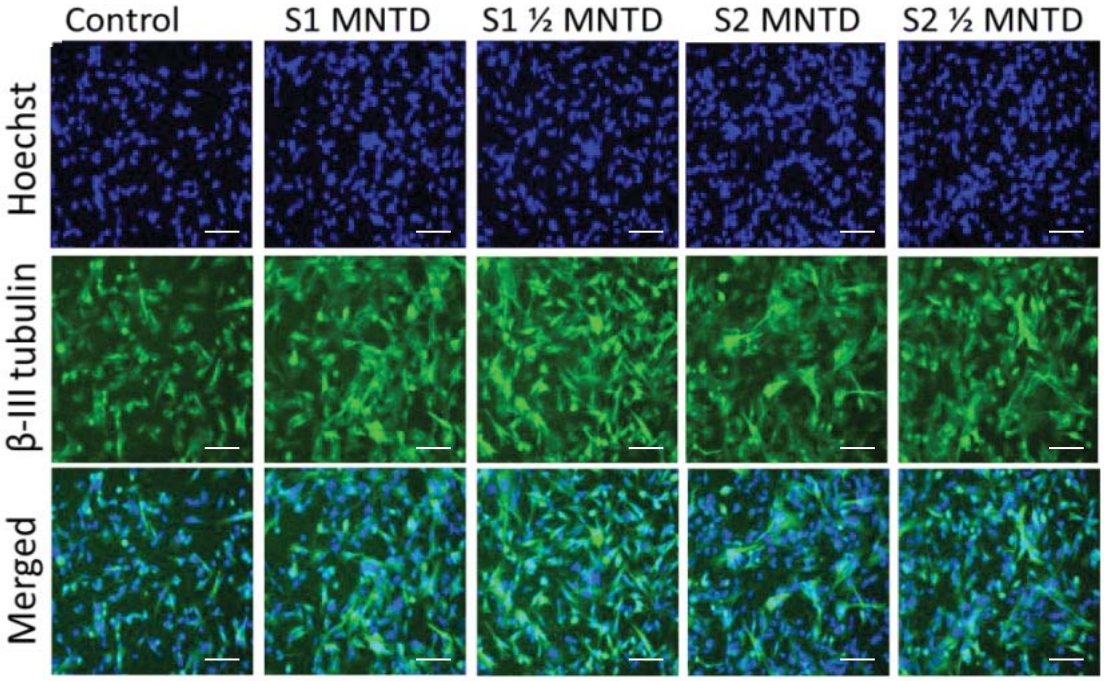

(b)

Treatment Group	Percentage of β-III tubulin-positive cell (%)
Control	38.01 ± 3.56
S1 MNTD	50.42 ± 0.64 *
S1 ½ MNTD	58.98 ± 0.85 *
S2 MNTD	55.29 ± 1.52 *
S2 ½ MNTD	55.36 ± 3.24 *

Fig.7 Neuronal differentiation after EBN extract treatments in retinoic acid-primed NE-4C. EBN extracts promoted neuronal differentiation (β-III tubulin-positive cell) in retinoic acid-primed NE-4C significantly after 7 days of co-incubation, as shown in (a) fluorescence imaging and (b) quantitative data from cell counting. Hoechst dye was used to stain cell nuclei and the images were viewed at 200X magnification. The data shown are means ± standard deviation of two independent experiments. *P<0.05 versus untreated control cells. Scale bar = 100 μm.

The multipotency nature of a NSC enables cell differentiation into neuron, oligodendrocytes and astrocytes under desirable culture conditions. Apparently EBN extract treatments did not prompt differentiation of NE-4C into neuron and astrocyte even after 7 days and 14 days of culture, which are the indicative periods needed for neurogenesis and gliogenesis of NE-4C under the effect of differentiation agent retinoic acid, respectively (Hadinger et al., 2009). Then, an alternative approach was used by adopting the retinoic acid-primed NE-4C. Neuronal differentiation in this cell model was detectable from Day 5 onwards, with the fluorescence signal getting stronger over time. This happened as cells were progressing towards maturation, as Temple et al. has pointed out that neurogenic phase usually takes 5 days (Temple, 2001). It was found that 2 days priming with 10^{-6} M retinoic acid resulted in considerable (38%) neuronal formation at Day 7, which is consistent with the study by Schlett et al. (Schlett and Madarasz, 1997). About 10-20% increase in the proportion of cell positively stained with neuronal marker β-III tubulin were seen in EBN-treated groups compared to the retinoic acid -treated only control cell (Fig.7b).

ERK1 and ERK2 belong to an important group of signal transduction mediators for neuron-targeted differentiation cues in the process of cell maturation (Ina et al., 2007). The ability of natural compounds such as pheophytin from brown algae and nardosinone from *Nardostachys* root to induce neurite outgrowth were associated with increased ERK1/2 activity (Li et al., 2014, Ina et al., 2007). As mentioned earlier, EGF-like compound in EBN might activate ERK signalling mechanism to facilitate cell migration, therefore it is hypothesized that the same mechanism might also be functional in promoting neuronal differentiation in EBN-treated NE-4C.

N-acetylneuraminic acid, or known as sialic acid, in EBN was discovered by Guo et al. (Guo et al., 2006). On a side note, it was reported that dietary consumption of sialic acid is essential to brain development and cognition because it represents building units of gangliosides which are important components of the brain's neuronal network (Wang, 2009). Indeed, at the cellular level sialic acid was found to initiate neurite outgrowth, axon elongation, synaptic formation, the migration and differentiation of NSC (Angata and Fukuda, 2010). Intake of exogenous source of sialic acid was linked to increased biosynthesis of gangliosides in infant fed with human milk compared to those fed with cow milk-based infant formula, which contains less sialic acid content (Wang, 2012). Therefore, the presence of sialic acid will add value to the neurotrophic potential of EBN as a functional food.

Conventional treatments for neurodegenerative diseases are mostly limited to symptomatic relief, which means they tend to fail against progressive neurodegeneration in chronic neurodegenerative diseases caused by hostile pathological events such as oxidative stress, inflammation and protein aggregation (Carletti et al., 2011). Stem cell therapy in several neurodegenerative diseases has achieved successful neuroprotective results and it is likely to be mediated through neurotrophic factors enrichment of the brain microenvironment. For example, glial cell-derived growth factor (GDNF), brain-derived neurotrophic factor (BDNF), neurotrophin-3 (NT-3) and transforming growth factor alpha (TGF-α) secreted from intrathecal or intravenous injection of human induced pluripotent stem cells-derived NSC has greatly improved neuromuscular function in amyotrophic lateral sclerosis mouse model (Nizzardo et al., 2014). Increased level of BDNF, NT-3, and GDNF were also correlated to improvement of motor behaviours in Parkinson's disease mouse model intrastriatally transplanted with human NSC (Zuo et al., 2015). The authors agreed that the release of neurotrophic factors following the transplantation may establish a favourable niche for

effective neurogenesis, enhance neurite plasticity of stem cell, and ultimately lead to functional recovery of Parkinson's disease. BDNF was also involved in neuroprotection of NSC-transplanted rat model of Huntington disease (Al-Gharaibeh et al., 2017). In short, neurotrophic factors are able to overturn neurodegeneration by fostering the survival, growth, differentiation and maintenance of neurons (Tang et al., 2017). In our present study, we found that EBN extracts greatly enhanced proliferation, migration and percentage of NE-4C committed to neuronal-lineage following retinoic acid-induced differentiation, suggesting that the neurotrophic attribute of EBN extracts may be applied *in vivo* for therapeutic purposes.

As such, neurotrophic properties of EBN extracts seen in this study were solely concluded based on *in vitro* setting. Pharmacologically, effect of a drug in actual biological environment or in a whole living organism is highly dependent on the concentration time course of drug exposure and can be very different from effect observed in cell culture system due to complexity of pharmacokinetics (Yoon et al., 2012). Also, since EBN is commonly consumed orally, the biological effect, if any, will be subjected to digestion in the gastrointestinal tract and first pass effect, which may result in reduced bioavailability of the active compound at the target site (El-Kattan A. and M., 2012). On top of that, blood-brain-barrier lined by tight junctions remains one of the major hurdles for food nutrient to be effectively delivered to the brain after ingestion (Serlin et al., 2015). It is not known yet if oral intake of EBN will harness similar benefit in the human brain. The fact that EBN has a long history of human consumption reminds us that further study has to be considered to confirm the health-promoting value of EBN in neuroprotection and neurotrophism. Our findings confirmed that EBN extracts possessed potent neurotrophic effect *in vitro* but the *in vivo* application and identification of neurotrophic compounds in EBN extracts that may be

employed to supplement cell replacement therapy in neurodegenerative diseases may be studied in the future.

Conclusion

This study has demonstrated that EBN extracts confer neurotrophic effect in NE-4C neural stem cell model. EBN extracts significantly enhanced proliferation, migration and neuronal differentiation of NE-4C. This study is the first to report on the neurotrophic effect of EBN extracts. The findings of this study will provide foundation to the understanding of medicinal effects of EBN and its potential application as therapeutic agent in the treatment of neurodegenerative diseases. Despite so, the underlying mechanism of these biological activities of EBN extracts requires further investigations. There is also a compelling need to identify the potent neurotrophic component in EBN extracts for future clinical translations.

Funding

This work was supported by Ministry of Higher Education of Malaysia (grant number: ERGS/1/2011/SKK/MUSM/03/3).

Conflict of Interest

The authors declare that they have no conflict of interest.

4.3 References

AGUIRRE, A., RIZVI, T. A., RATNER, N. & GALLO, V. 2005. Overexpression of the epidermal growth factor receptor confers migratory properties to nonmigratory postnatal neural progenitors. *J Neurosci,* 25**,** 11092-106.

AL-GHARAIBEH, A., CULVER, R., STEWART, A. N., SRINAGESHWAR, B., SPELDE, K., FROLLO, L., KOLLI, N., STORY, D., PALADUGU, L., ANWAR, S., CRANE, A., WYSE, R., MAITI, P., DUNBAR, G. L. & ROSSIGNOL, J. 2017. Induced Pluripotent Stem Cell-Derived Neural Stem Cell Transplantations Reduced Behavioral Deficits and Ameliorated Neuropathological Changes in YAC128 Mouse Model of Huntington's Disease. *Frontiers in Neuroscience,* 11**,** 628.

ANGATA, K. & FUKUDA, M. 2010. Roles of polysialic acid in migration and differentiation of neural stem cells. *Methods Enzymol,* 479**,** 25-36.

BOOCKVAR, J. A., KAPITONOV, D., KAPOOR, G., SCHOUTEN, J., COUNELIS, G. J., BOGLER, O., SNYDER, E. Y., MCINTOSH, T. K. & O'ROURKE, D. M. 2003. Constitutive EGFR signaling confers a motile phenotype to neural stem cells. *Mol Cell Neurosci,* 24**,** 1116-30.

BROOKS, R. F. 1976. Regulation of the fibroblast cell cycle by serum. *Nature,* 260**,** 248-250.

CARIC, D., RAPHAEL, H., VITI, J., FEATHERS, A., WANCIO, D. & LILLIEN, L. 2001. EGFRs mediate chemotactic migration in the developing telencephalon. *Development,* 128**,** 4203-16.

CARLETTI, B., PIEMONTE, F. & ROSSI, F. 2011. Neuroprotection: The Emerging Concept of Restorative Neural Stem Cell Biology for the Treatment of Neurodegenerative Diseases. *Current Neuropharmacology,* 9**,** 313-317.

CHEN, M., HUANG, J., YANG, X., LIU, B., ZHANG, W., HUANG, L., DENG, F., MA, J., BAI, Y., LU, R., HUANG, B., GAO, Q., ZHUO, Y. & GE, J. 2012. Serum Starvation

Induced Cell Cycle Synchronization Facilitates Human Somatic Cells Reprogramming. *PLoS ONE,* 7**,** e28203.

CHUNG, S. Y. & CHAMPAGNE, E. T. 2001. Association of end-product adducts with increased IgE binding of roasted peanuts. *J Agric Food Chem,* 49**,** 3911-6.

CHYE, S. M., TAI, S. K., KOH, R. Y. & NG, K. Y. 2017. A Mini Review on Medicinal Effects of Edible Bird's Nest. *Letters In Health And Biological Sciences*.

CICCOLINI, F., MANDL, C., HOLZL-WENIG, G., KEHLENBACH, A. & HELLWIG, A. 2005. Prospective isolation of late development multipotent precursors whose migration is promoted by EGFR. *Dev Biol,* 284**,** 112-25.

EL-KATTAN A. & M., V. 2012. Oral Absorption, Intestinal Metabolism and Human Oral Bioavailability. *Topics on Drug Metabolism.*

FARRER, M. J. 2006. Genetics of Parkinson disease: paradigm shifts and future prospects. *Nat Rev Genet,* 7**,** 306-18.

FLINDER, L. I., TIMOFEEVA, O. A., ROSSELAND, C. M., WIEROD, L., HUITFELDT, H. S. & SKARPEN, E. 2011. EGF-induced ERK-activation downstream of FAK requires rac1-NADPH oxidase. *J Cell Physiol,* 226**,** 2267-78.

GAGE, F. H. 2000. Mammalian neural stem cells. *Science,* 287**,** 1433-8.

GONZALEZ-PEREZ, O. & QUIÑONES-HINOJOSA, A. 2010. Dose-dependent effect of EGF on migration and differentiation of adult subventricular zone astrocytes. *GLIA,* 58**,** 975-983.

GUO, C. T., TAKAHASHI, T., BUKAWA, W., TAKAHASHI, N., YAGI, H., KATO, K., HIDARI, K. I., MIYAMOTO, D., SUZUKI, T. & SUZUKI, Y. 2006. Edible bird's nest extract inhibits influenza virus infection. *Antiviral Res,* 70**,** 140-6.

HA, G. T., WONG, R. K. & ZHANG, Y. 2011. Huperzine A as Potential Treatment of Alzheimer's Disease: An Assessment on Chemistry, Pharmacology, and Clinical Studies. *Chemistry & Biodiversity,* 8**,** 1189-1204.

HADINGER, N., VARGA, B. V., BERZSENYI, S., KORNYEI, Z., MADARASZ, E. & HERBERTH, B. 2009. Astroglia genesis in vitro: distinct effects of retinoic acid in different phases of neural stem cell differentiation. *Int J Dev Neurosci,* 27**,** 365-75.

INA, A., HAYASHI, K., NOZAKI, H. & KAMEI, Y. 2007. Pheophytin a, a low molecular weight compound found in the marine brown alga Sargassum fulvellum, promotes the differentiation of PC12 cells. *Int J Dev Neurosci,* 25**,** 63-8.

KONG, Y. C., KEUNG, W. M., YIP, T. T., KO, K. M., TSAO, S. W. & NG, M. H. 1987. Evidence that epidermal growth factor is present in swiftlet's (Collocalia) nest. *Comp Biochem Physiol B,* 87**,** 221-6.

LI, R., LIANG, T., XU, L., ZHENG, N., ZHANG, K. & DUAN, X. 2013. Puerarin attenuates neuronal degeneration in the substantia nigra of 6-OHDA-lesioned rats through regulating BDNF expression and activating the Nrf2/ARE signaling pathway. *Brain Res,* 1523**,** 1-9.

LI, Z. H., LI, W., SHI, J. L. & TANG, M. K. 2014. Nardosinone improves the proliferation, migration and selective differentiation of mouse embryonic neural stem cells. *PLoS One,* 9**,** e91260.

LIM, C. K. & CRANBROOK, E. O. 2002. *Swiftlets of Borneo – Builders of edible nests* Sabah, Malaysia, Natural History Publication (Borneo) SDN., B.H.D. .

LO FURNO, D., MANNINO, G. & GIUFFRIDA, R. 2017. Functional role of mesenchymal stem cells in the treatment of chronic neurodegenerative diseases. *J Cell Physiol*.

LUO, L. & O'LEARY, D. D. 2005. Axon retraction and degeneration in development and disease. *Annu Rev Neurosci,* 28**,** 127-56.

MATSUKAWA, N., MATSUMOTO, M., BUKAWA, W., CHIJI, H., NAKAYAMA, K., HARA, H. & TSUKAHARA, T. 2011. Improvement of bone strength and dermal thickness due to dietary edible bird's nest extract in ovariectomized rats. *Biosci Biotechnol Biochem,* 75**,** 590-2.

MING, G.-L. & SONG, H. 2011. Adult Neurogenesis in the Mammalian Brain: Significant Answers and Significant Questions. *Neuron,* 70**,** 687-702.

NG, M. H., CHAN, K. H. & KONG, Y. C. 1986. Potentiation of mitogenic response by extracts of the swiftlet's (Collocalia) nest. *Biochem Int,* 13**,** 521-31.

NIZZARDO, M., SIMONE, C., RIZZO, F., RUGGIERI, M., SALANI, S., RIBOLDI, G., FARAVELLI, I., ZANETTA, C., BRESOLIN, N., COMI, G. P. & CORTI, S. 2014. Minimally invasive transplantation of iPSC-derived ALDHhiSSCloVLA4+ neural stem cells effectively improves the phenotype of an amyotrophic lateral sclerosis model. *Human Molecular Genetics,* 23**,** 342-354.

OUDIN, M. J., GAJENDRA, S., WILLIAMS, G., HOBBS, C., LALLI, G. & DOHERTY, P. 2011. Endocannabinoids regulate the migration of subventricular zone-derived neuroblasts in the postnatal brain. *J Neurosci,* 31**,** 4000-11.

PRZEDBORSKI, S. 2005. Pathogenesis of nigral cell death in Parkinson's disease. *Parkinsonism Relat Disord,* 11 Suppl 1**,** S3-7.

REYNOLDS, B. A., TETZLAFF, W. & WEISS, S. 1992. A multipotent EGF-responsive striatal embryonic progenitor cell produces neurons and astrocytes. *Journal of Neuroscience,* 12**,** 4565-4574.

ROH, K.-B., LEE, J., KIM, Y.-S., PARK, J., KIM, J.-H., LEE, J. & PARK, D. 2012. Mechanisms of Edible Bird's Nest Extract-Induced Proliferation of Human Adipose-Derived Stem Cells. *Evidence-Based Complementary and Alternative Medicine,* 2012.

SCHLETT, K. & MADARASZ, E. 1997. Retinoic acid induced neural differentiation in a neuroectodermal cell line immortalized by p53 deficiency. *J Neurosci Res,* 47**,** 405-15.

SEGU, Z. M., HAMMAD, L. A. & MECHREF, Y. 2010. Rapid and efficient glycoprotein identification through microwave-assisted enzymatic digestion. *Rapid Commun Mass Spectrom,* 24**,** 3461-8.

SERLIN, Y., SHELEF, I., KNYAZER, B. & FRIEDMAN, A. 2015. Anatomy and Physiology of the Blood-Brain Barrier. *Seminars in cell & developmental biology,* 38**,** 2-6.

TAHERI-KAFRANI, A., GAUDIN, J. C., RABESONA, H., NIOI, C., AGARWAL, D., DROUET, M., CHOBERT, J. M., BORDBAR, A. K. & HAERTLE, T. 2009. Effects of heating and glycation of beta-lactoglobulin on its recognition by IgE of sera from cow milk allergy patients. *J Agric Food Chem,* 57**,** 4974-82.

TANG, Y., YU, P. & CHENG, L. 2017. Current progress in the derivation and therapeutic application of neural stem cells. *Cell Death & Disease,* 8**,** e3108.

TEMPLE, S. 2001. The development of neural stem cells. *Nature,* 414**,** 112-7.

VERHOECKX, K. C. M., VISSERS, Y. M., BAUMERT, J. L., FALUDI, R., FEYS, M., FLANAGAN, S., HEROUET-GUICHENEY, C., HOLZHAUSER, T., SHIMOJO, R., VAN DER BOLT, N., WICHERS, H. & KIMBER, I. 2015. Food processing and allergenicity. *Food and Chemical Toxicology,* 80**,** 223-240.

WANG, B. 2009. Sialic acid is an essential nutrient for brain development and cognition. *Annu Rev Nutr,* 29**,** 177-222.

WANG, B. 2012. Molecular mechanism underlying sialic acid as an essential nutrient for brain development and cognition. *Adv Nutr,* 3**,** 465S-72S.

WILLIAMS, G., ZENTAR, M. P., GAJENDRA, S., SONEGO, M., DOHERTY, P. & LALLI, G. 2013. Transcriptional Basis for the Inhibition of Neural Stem Cell

Proliferation and Migration by the TGFβ-Family Member GDF11. *PLoS ONE,* 8**,** e78478.

WONG, C.-F., CHAN, G. K.-L., ZHANG, M.-L., YAO, P., LIN, H.-Q., DONG, T. T.-X., LI, G., LAI, X.-P. & TSIM, K. W.-K. 2017. Characterization of edible bird's nest by peptide fingerprinting with principal component analysis. *Food Quality and Safety,* 1**,** 83-92.

XU, J., LACOSKE, M. H. & THEODORAKIS, E. A. 2014. Neurotrophic Natural Products: Chemistry and Biology. *Angewandte Chemie International Edition,* 53**,** 956-987.

YAGI, H., YASUKAWA, N., YU, S. Y., GUO, C. T., TAKAHASHI, N., TAKAHASHI, T., BUKAWA, W., SUZUKI, T., KHOO, K. H., SUZUKI, Y. & KATO, K. 2008. The expression of sialylated high-antennary N-glycans in edible bird's nest. *Carbohydr Res,* 343**,** 1373-7.

YEW, M. Y., KOH, R. Y., CHYE, S. M., OTHMAN, I. & NG, K. Y. 2014. Edible bird's nest ameliorates oxidative stress-induced apoptosis in SH-SY5Y human neuroblastoma cells. *BMC Complementary and Alternative Medicine,* 14**,** 391.

YOON, M., CAMPBELL, J. L., ANDERSEN, M. E. & CLEWELL, H. J. 2012. Quantitative in vitro to in vivo extrapolation of cell-based toxicity assay results. *Critical Reviews in Toxicology,* 42**,** 633-652.

ZUO, F.-X., BAO, X.-J., SUN, X.-C., WU, J., BAI, Q.-R., CHEN, G., LI, X.-Y., ZHOU, Q.-Y., YANG, Y.-F., SHEN, Q. & WANG, R.-Z. 2015. Transplantation of Human Neural Stem Cells in a Parkinsonian Model Exerts Neuroprotection via Regulation of the Host Microenvironment. *International Journal of Molecular Sciences,* 16**,** 26473-26492.

Chapter 5

Edible bird's nest improves motor behavior and protects dopaminergic neuron against oxidative and nitrosative stress in Parkinson's disease mouse model

5.1 Summary of Chapter 5

One of the manifestations of PD is the physical disability to execute motor function. This is caused by the degeneration of dopaminergic neurons of the substantia nigra in the midbrain, which subsequently leads to depletion of the neurotransmitter known as dopamine along the innervated nigrostriatal pathway to the basal ganglia. Reduced dopamine signalling in the motor circuitry results in movement impairments which include slow movement, tremor and muscle rigidity in the patient. In both familial and sporadic forms of PD, oxidative stress is highly implicated in the pathogenesis of this neurodegenerative disease. On the other hand, nitrosative stress-associated inflammatory response from the activated microglia is also pivotal to the death of neurons in PD.

Hence, the objectives for the study in Chapter 5 were as follow:

1. To examine the effect of EBN on the motor functions of PD mouse model.
2. To evaluate the effect of EBN on the dopaminergic neuron in PD mouse model.
3. To study the effect of EBN on the antioxidant enzyme in PD mouse model.
4. To study the effect of EBN on the microglial activation in PD mouse model.
5. To examine the effect of EBN on the nitric oxide release and lipid peroxidation in PD neuronal cell model.

Sub-chronic oral supplementation with EBN was shown to be protective against 6-OHDA-induced degeneration of the dopaminergic neuron and microglial activation in the PD mouse model. Motor function of the PD mouse model including locomotion, gait and balance, as well as expression of antioxidant enzyme, glutathione peroxidase 1 were improved by

EBN. Lastly, it was further shown that oxidative stress and nitrosative stress can be counteracted by EBN as nitric oxide production and lipid peroxidation in PD neuronal cell model was reduced after being treated with EBN. These data showed that EBN possesses neuroprotective effect by modulating the oxidative and nitrosative status in both *in vitro* and *in vivo* models.

5.2 Manuscript

Edible bird's nest improves motor behavior and protects dopaminergic neuron in Parkinson's disease mouse model against oxidative and nitrosative stress

Mei Yeng Yew[1], Rhun Yian Koh[2], Soi Moi Chye[2], Iekhsan Othman[1], Tomoko Soga[3], Ishwar Parhar[3], Khuen Yen Ng[1,3]*

[1] Jeffrey Cheah School of Medicine & Health Sciences, Monash University Malaysia, Selangor, Malaysia

[2] Department of Human Biology, School of Medicine, International Medical University, Kuala Lumpur, Malaysia

[3] Brain Research Institute Monash Sunway, Monash University Malaysia, Selangor, Malaysia.

Declaration of interest:

None.

Corresponding author:

Dr. Khuen Yen Ng

Brain Research Institute Monash Sunway, Monash University Malaysia. Jalan Lagoon

[redacted]

Number: +612-4500575

ORCID: 0000-0002-9453-4999

Funding

This work was supported by Ministry of Higher Education of Malaysia (grant number: ERGS/1/2011/SKK/MUSM/03/3).

Keywords

Edible bird's nest; Parkinson's disease; Neurodegenerative disease; Neuroprotection; Oxidative stress; Nitrosative stress

Abstract

Parkinson's disease (PD) is a debilitating disease which greatly affects motor function of the elderly patients due to the death of dopaminergic neurons in the midbrain. Evidences showed that in PD, antioxidant activity was diminished in the substantia nigra region of the midbrain, leading to the formation of reactive oxygen species and oxidative adducts of proteins, lipids and DNA. Microglia activation and formation of reactive nitrogen species are also prevalent in the case of PD. Oxidative and nitrosative stresses are detrimental to the brain as they contribute to apoptosis and neurotoxicity in PD. We have reported previously that edible bird's nest (EBN) confers protection against toxin-induced neurotoxicity in *in vitro* PD cell model. In this study, we examine the neuroprotective effects of EBN (20 mg/kg and 100 mg/kg) in 6-hydroxydopamine (6-OHDA)-treated C57BL/6J mice. We found that 28 days oral administration of EBN greatly improved locomotor activity of PD mouse model in terms of travel distance, gait and balancing. In addition to that, EBN also protected dopaminergic neuron against 6-OHDA in the substantia nigra. Reduction in the expression of antioxidant enzyme glutathione peroxidase 1 and the increased microglia activation in PD mice were

reversed by EBN. Our results also showed that EBN effectively reduced nitric oxide formation and lipid peroxidation in human neuroblastoma cell SH-SY5Y induced by 6-OHDA. The data altogether indicates that EBN exerted neuroprotection through enhancement of antioxidant enzyme activity, inhibition of microglia activation, nitric oxide formation and lipid peroxidation, hence may have therapeutic potential for PD.

1. Introduction

Parkinson's disease is a progressive neurodegenerative disease affecting more than 1% of the population over 60 years of age [1]. Pathologically, there is loss of dopaminergic neurons in the substantia nigra which subsequently causes dopamine depletion in the striatum [2]. Dopamine depletion ultimately leads to deterioration of motor function, as seen in most PD patients [3]. Patients of this disorder are manifested with clinical signs such as tremor, rigidity and slow responsiveness. In addition, abnormal α-synuclein protein aggregation known as Lewy bodies is also detected in surviving neurons [4]. The disease is not fatal, but it imposes a huge economic burden to the country due to the huge cost in medical care and morbidity associated with the disease.

Substantial number of evidences has proved that interplay of oxidative stress and apoptosis is a critical determinant in the pathogenesis of PD. To name a few, accumulation of protein aggregates and the loss of dopaminergic neurons in the midbrain region are two hallmarks of PD that are known to be associated to increased level of reactive oxygen species (ROS) and reactive nitrogen species (RNS) in the midbrain [5]. The neurotransmitter dopamine in nigral neuronal cells can auto-oxidize and release toxic dopamine-quinone species, superoxide radicals and hydrogen peroxide [6]. Glutathione peroxidase (GPX) is a member of the intracellular antioxidant defence system that

catalyzes the reduction of hydrogen peroxide and lipid hydroperoxides, hence eradicates these highly reactive biomolecules [7]. Under the circumstances of PD, GPX level in substantia nigra becomes lower than in healthy individual [8]. In addition, microglial activation in neurodegenerative diseases was linked to up-regulation of the enzyme inducible nitric oxide synthase (iNOS) [9] and hence the production of nitric oxide (NO), which reacts with ROS to form the aberrant RNS including peroxynitrite and eventually give rise to hydroxyl radicals [10]. RNS is as unfavourable as ROS in the brain because it is believed to participate in the adverse events involved in neurodegeneration. Both high oxidative stress and nitrosative stress within the biological system would render cells and tissues more prone to the free radicals attack. Since cells consist mostly of proteins and lipids, they belong to the labile target of these chemically-reactive electron-rich molecules. This is supported by evidence of elevated levels of oxidative adducts of lipids, proteins and DNA in substantia nigra of PD patients [11-13]. Also, higher levels of NOS expression and peroxynitrite were found in PD patients [14, 15]. In fact, it was recognized that pathological protein aggregation in PD was mediated by peroxynitrite, hence further emphasizes the role of RNS in the development of PD as an inflammatory mediator [16].

On a side note, lipid peroxidation is a process whereby lipid-rich components in cell are oxidized by free radicals to results in a number of highly reactive electrophilic aldehydes including malondialdehyde, 4-hydroxy-2-nonenal (HNE) and acrolein [17]. Malondialdehyde adducts and HNE have been found in Lewy bodies in PD [18, 19]. HNE modified alpha-synuclein protein by potentiating its oligomerization and led to toxicity in neuronal cultures [20]. It was also demonstrated that dopamine uptake by the rat striatal synaptosomes was disrupted by HNE [21]. Inefficient dopamine transport and protein

aggregation due to lipid peroxidation may be pivotal to neurodegeneration and progression of PD.

Edible bird nest (EBN) is the hardened salivary product of the *Aerodramus* swiftlets and is commonly prepared in sugary water before consumption. It is a highly regarded natural food popular among Asians due to traditional use in enhancing skin complexion, appetite immunity, growth, metabolism and blood circulation [22, 23]. EBN has been scientifically implicated for influenza-inhibiting [24], osteoporosis-improving [25], neuroprotection [26, 27] and prevention of cardiometabolic disease [28]. Although the specific bioactive compounds accounted for the effects observed were yet to be identified in these studies, complex compositional makeup of EBN may suggest a plethora of therapeutic potentials [29]. In our previous study, we have found that EBN treatment ameliorated neurotoxicity of 6-hydroxydopamine (6-OHDA) in PD cell model [27]. The mechanism behind the neuroprotective effect of EBN was associated with apoptosis-inhibiting and ROS-reducing effects of the treatment. There was, however, lack of study to confirm the neuroprotective effects of EBN in *in vivo* system. Application of EBN to mitigate PD-related motor dysfunction, degeneration of midbrain dopaminergic neuron and neuroinflammation in whole living organisms were never investigated, hence such investigation is a potential venue to explore.

In this study, we first establish the animal toxicology profile in our animal model with the EBN doses used in previous publication, followed by investigation into the neuroprotective effects of EBN with respect to motor function and dopaminergic neuron in substantia nigra of PD mouse model. The expression of antioxidant marker GPX1 was evaluated to indicate changes in intraneuronal antioxidant state. Microglial marker,

cluster of differentiation molecule 11B (CD11b), was also studied to assess the inflammatory process in the midbrain. We complemented these studies by measuring NO release and lipid hydroperoxides formation in neuronal model SH-SY5Y to better understand if EBN suppresses nitrosative and oxidative stresses. This study further explores the application of EBN in the treatment of neurodegenerative diseases especially PD.

2. Materials and methods

2.1 Materials

Antibodies used in immunostaining including anti-tyrosine hydroxylase (TH), anti-GPX1, anti-CD11b were purchased from Novus Biologicals. Alexa Fluor 488-conjugated secondary antibody and Alexa Fluor 647-conjugated secondary antibody were obtained from Abcam. Biotinylated horseradish peroxidase-conjugated secondary antibody and 3,3′-diaminobenzidine (DAB) kit were purchased from Vector Laboratories.

Bovine serum albumin (BSA), phosphate buffered saline (PBS), 6-OHDA, Triton-X, paraformaldehyde, sucrose and Griess reagent were obtained from Sigma-Aldrich.

Human neuroblastoma cells SH-SY5Y was obtained from the American Type Culture Collection (ATCC no. CRL-2266). All cell culture reagents including Dulbecco's Modified Eagle's Medium and fetal bovine serum were purchased from Gibco.

2.2 Preparation of EBN

Raw EBN collected from a local bird's nest farm in Perak, Malaysia. EBN were prepared into pancreatin-digested extracts denoted as S1 (crude extract) and S2 (water extract) according to our previously established protocol [27].

2.3 Animal

Male C57BL/6J mice were housed at 3 to 4 per cage. Standard laboratory chow and drinking water were available *ad libitum*. The animals were kept under controlled conditions of 12-h/12-h light/dark schedule and temperature at 23±2˚C. Animal experimentation has obtained ethics approval from the Monash Animal Research Platform-1 Animal Ethics Committee of Monash University (AEC number MARP/2014/081).

2.4 Toxicology screening

Prior to the commencement of the experiment, animals were screened for the toxicology profile of EBN administration according to the Organisation for Economic Co-operation and Development guidelines [30]. Sub-chronic oral exposure to EBN (20 mg/kg and 100 mg/kg daily) for 28 days was selected as criteria to test the effect of EBN on the animal's overall health and well-being. The dosages selected were adopted from the study by Matsukawa et al. using rats [25]. Therefore in this study safety profile was reassessed using C57BL/6J mice. The animals were taken good care throughout the 28 days. Water and food intake, as well as the signs of toxic effects and/or mortality were monitored daily. Body weight was recorded weekly. At the end of 4-week feeding period, the mice were euthanized by cardiac puncture on the 29th day. Maximal volume of blood was extracted from the heart and collected into plain blood tube. The blood was transported on ice to Faculty of Veterinary at University Putra Malaysia for biochemistry tests. The test included assessment of biomarkers for toxicity in the liver (eg. alanine transaminase (ALT), aspartate aminotransferase (AST), alkaline phosphatase (ALP), total protein and albumin levels), heart (eg. creatine kinase level), kidney (eg. urea and creatinine levels) and pancreas (eg. glucose level), and for lipid metabolism (eg. triglyceride and

cholesterol levels). Vital organs such as lung, heart, liver, kidney and spleen were excised from the animals and examined macroscopically. The weights of the organs were recorded. Afterwards, the organs were fixed in formalin and sent for histopathological processing in Faculty of Veterinary at University Putra Malaysia. Tissue from the organs was made into slides, stained with Haematoxylin & Eosin. Images were taken under the light microscope for further histopathological analysis. All values and findings were compared between treated and control groups.

2.5 Oral gavage

EBN (S1 and S2) were prepared according to a previously established protocol [27], dissolved in distilled water and fed to the animals via oral gavage daily for 28 days at 20 mg/kg & 100 mg/kg. The total volume of solution administered each day was 100 µl. Animals of the sham group were fed with same volume of distilled water as vehicle. The treatment groups were as follows (8 animals/ group):

i. Sham
ii. Neurotoxin 6-OHDA-injected
iii. 20 mg/kg of S1 + 6-OHDA-injected
iv. 100 mg/kg of S1 + 6-OHDA-injected
v. 20 mg/kg of S2 + 6-OHDA-injected
vi. 100 mg/kg of S2 + 6-OHDA-injected

2.6 Surgical procedure for establishment of *in vivo* PD model

The surgical procedure was established following the protocol by da Conceição et al. [31]. At Day 29 after oral treatment with EBN, the mice were anesthetized and 4 µg of 6-OHDA (in 2 µl of ice cold saline) or saline alone was injected into the midbrain at the

desired coordinates: anterior-posterior (AP: +0.04 cm), lateral (L: -0.18 cm, left) and dorsal-ventral (DV: -0.35 cm) measured from bregma. Injection was made at the rate of 0.5 μL/min with a further 3 min allowed for the toxin to diffuse before slow withdrawal of the needle, followed by wound closure. Animals were allowed to recover for 2 weeks after lesioning before behavioral evaluation.

2.7 Behavioral studies

2.7.1 Open field test

The test was conducted for 5 minutes. Mice were placed in a 50 cm x 50 cm x 20 cm cage subdivided to 25 zones with the field of illumination set to 15 lux. The mice were individually placed into the periphery of the open field, and their behaviors were video recorded and analyzed using a Limelight system (Actimetrics). The 5 minutes test durations allowed measurement of the overall distance travelled and grid crossings, which are the indicators of locomotor activity and exploratory behavior in terms of frequency of rearing and traveling pattern.

2.7.2 Beam test

A 2 cm-wide and 50 cm-long beam was set up in a bright laboratory. The animals were placed onto a hanging terminal, and the time required for the mice to traverse through the beam to a platform terminal was recorded.

2.8 Histological preparation

Two weeks after lesioning, the animals were anesthetized and perfused transcardially with heparinized saline, followed by ice-cold 4% paraformaldehyde. The brains were removed and post-fixed for 4 hours in 4% paraformaldehyde solution. After post-fixation,

the brains were equilibrated in 30% sucrose until sunk, and sectioned (35 μm thick, coronal) on a freezing microtome. Sections were collected in series and stored at -20°C in an anti-freeze solution until free-floating immunohistochemistry is performed.

2.9 Immunohistochemistry

Free-floating sections were incubated in blocking buffer (PBS containing 0.3% Triton X-100 and 5% BSA for 30 minutes, followed by 48 hours incubation with anti-TH (dopaminergic marker) antibody at 4°C. Biotinylated horseradish peroxidase-conjugated secondary antibody was added and stained for 1 hour. Immunolabeling was then visualized using DAB revelation. The sections were washed with PBS in between incubations. Finally, sections were mounted on gelatin-coated slides, dehydrated, and coverslipped. TH-positive staining was observed in substantia nigra under bright-field microscope. Images taken via the MIRAX MIDI slide scanner (Carl Zeiss AG, Germany) were uploaded to ImageJ Software for quantification of staining intensity. The staining intensity of the injected side (left) was compared to the intact side (right) to obtain percentage of staining intensity.

2.10 Immunofluorescence

Free-floating sections were incubated in blocking buffer (PBS containing 0.3% Triton X-100 and 5% BSA) for 1 hour, followed by overnight incubation with anti-glutathione peroxidase 1 (GPX1, antioxidant marker; 1:500 dilution) and anti-CD11b (microglial marker; 1:200 dilution) antibodies at 4°C. Secondary antibodies with Alexa 488 and Cy3 fluorescence tag (1:200 dilution) were added for 1 hour incubation at room temperature. The sections were washed before being mounted onto glass slide and cover-slipped with fluorescence mounting medium. Image acquisition was done with the *Eclipse*

90i fluorescence microscope (Nikon Instruments Inc., USA) and MIRAX MIDI slide scanner (Carl Zeiss AG, Germany).

2.11 Development of PD cell model

SH-SY5Y was maintained in Dulbecco's Modified Eagle's Medium supplemented with 10% fetal bovine serum and kept in 37°C humidified incubator with 5% CO_2. PD cell model was created with 6-OHDA and treated with EBN according to the method previously published [27].

2.12 NO measurement

NO production was determined from level of nitrites in the culture medium using Griess method following manufacturer's instructions (Sigma Aldrich, USA). Equal volume of culture medium and Griess reagent were incubated at room temperature for 15 minutes. The absorbance was then read at 540 nm (Tecan Trading AG, Switzerland). A standard curve using sodium nitrite was constructed to extrapolate the nitrite level in the sample.

2.13 Quantification of lipid peroxidation

Lipid hydroperoxides were quantified using Lipid Hydroperoxide Assay Kit following manufacturer's instructions (Cayman Chemical Company, USA). Briefly, treated cells were extracted with chloroform and mixed with chloroform-methanol solvent. Chromogen was added and mixed well. Absorbance was taken at 500 nm (Tecan Trading AG, Switzerland) and a standard curve was constructed to extrapolate the level of lipid hydroperoxides in the sample.

2.14 Statistical analysis

Data was presented as mean ± standard deviation. Statistical analysis was performed using one-way analysis of variance (ANOVA) followed by *post-hoc* Fisher's Least Significant Difference test and a value of $P < 0.05$ was considered significant.

3. Results

3.1 Sub-chronic treatment with 20 mg/kg and 100 mg/kg of EBN has no toxic effect on body weight, blood biochemistry, organ weight and histology of the mice

There were no abnormalities and signs of toxicity exhibited by the animal subjects, particularly in terms of skin condition, activity, breathing, movement, diet and mood of the mice in experiment. Observation on the mice also noted that food and water intake were normal. There was no mortality reported hence EBN at 20 mg/kg and 100 mg/kg were within safe dosage.

Body weight was monitored weekly in all mice (Fig. 1). All treated and untreated mice showed slight increase in the body weight at the end of the first week of oral treatment, followed by a small drop in the body weight at the end of 2nd week. However, the body weight of the mice started to gain steadily in 3rd and 4th week. Changes in animal's body weight throughout the 4 weeks were not statistically significant between treated and control groups.

Table 1 summarizes the blood biochemistry profile in EBN-treated and control mice. Among the liver test panel, only ALT and total protein levels were significantly increased whereas AST and ALP levels were not affected by the treatment with EBN. However, elevated ALT and total protein levels were still within normal range for C57BL/6J mice [32]. Notably, blood glucose and triglyceride levels in the mice were also significantly

raised following treatment of EBN for 28 days. Despite so, the levels fell within the normal range. No significant difference was observed in the biochemical parameters of the heart and kidney such as creatinine kinase, urea and creatinine levels between the treated and control mice. Cholesterol in EBN-treated mice was also maintained at a comparable level with the control mice.

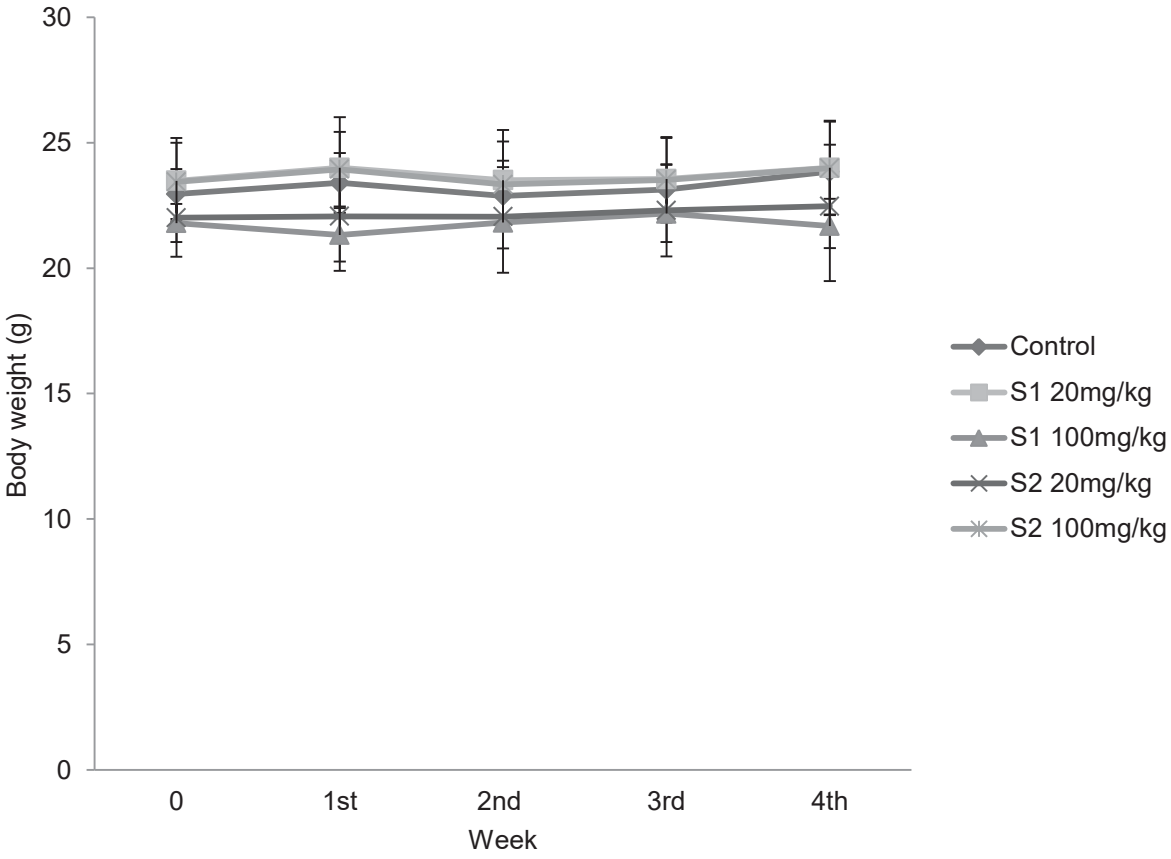

Fig. 1. Body weight of animal subjects across 4 weeks of oral treatment with EBN. The weight remained fairly constant and there was no statistical significant changes between the EBN treated and control groups.

Parameters		Control	S1 20mg/kg	S1 100mg/kg	S2 20mg/kg	S2 100mg/kg
Liver	**AST (U/L)**	647.33 ± 135.63	929.33 ± 214.01	889.00 ± 159.57	740.00 ± 241.09	632.20 ± 417.42
	ALT (U/L)	53.80 ± 12.62	137.50 ± 3.54 [a]	75.33 ± 11.37	87.20 ± 20.56 [a]	67.00 ± 30.24
	ALP (U/L)	113.57 ± 12.20	104.25 ± 17.27	112.50 ± 7.78	175.60 ± 104.18	104.00 ± 11.31
	Total Protein (g/L)	51.25 ± 3.70	52.20 ± 0.71	59.96 ± 8.05	52.15 ± 0.49	55.48 ± 0.64 [a]
	Albumin (g/L)	27.70 ± 3.07	26.20 ± 0.85	29.50 ± 2.99	26.20 ± 0.14	28.44 ± 1.43
Heart	**Creatinine Kinase (U/L)**	6548.00 ± 3142.52	6430.67 ± 3760.86	6031.00 ± 2480.70	5882.33 ± 4309.15	3248.40 ± 3015.71
Pancreas	**Glucose (mmol/L)**	15.60 ± 4.93	23.20 ± 6.22	24.36 ± 6.28 [a]	27.95 ± 0.07 [a]	26.02 ± 2.95 [a]
Kidney	**Urea (mmol/L)**	12.28 ± 3.29	12.93 ± 6.48	11.56 ± 4.10	20.50 ± 13.49	9.78 ± 3.88
	Creatinine (µmol/L)	36.20 ±	32.33 ±	34.60 ±	30.00 ±	39.20 ±

		12.97	3.21	22.00	3.00	14.96
Lipid metabolism	**Triglyceride (mmol/L)**	0.47 ± 0.10	1.08 ± 0.09 [a]	1.07 ± 0.08 [a]	1.01 ± 0.25 [a]	0.83 ± 0.45
	Cholesterol (mmol/L)	1.56 ± 0.67	1.83 ± 0.18	2.60 ± 0.23	2.18 ± 0.35	1.96 ± 0.52

Table 1. Blood biochemistry of animal subjects after 28 days of treatment with EBN crude and water extracts. The data shown are means ± standard deviation. Significant values of $P < 0.05$ versus control group are indicated as a.

Vital organs such as lung, heart, liver, kidney and spleen were obtained from the animal subjects during necropsy and the weights were presented in Table 2. The weight of lung, heart, liver, kidney and spleen of the mice were not affected by EBN treatment after comparing to the organ weight in control mice. No visible lesion was found on vital organs during gross pathology observation. The organs were further prepared into thin sections for microscopic examination at the cellular level from which overall tissue architecture and cellular morphology were studied under the light microscope (Fig. 2). Lung sections revealed normal rounded alveolar space with a thin layer of cell between alveoli, and presence of bronchioles lined by ciliated columnar epithelium and cuboidal epithelium in both control and treated subjects. Heart histology in both control and treated mice showed normal muscle fibres with centrally located nuclei stained in blue colour as well as acidophilic cytoplasm that stained in red colour. Meanwhile, histology from the livers of control and EBN-treated animals showed normal hepatic parenchyma with granulated cytoplasm. In kidney histology, control and treated mice had normal size of glomeruli and tubules. Spleen sections from both control and treated mice showed normal organization of white pulp and red pulp marginal zone. No signs of hyperemia, cellular distortion and inflammatory cell infiltration were noted in all the tissues studied. Preservation of tissue morphology in lung, heart, liver, kidney and spleen sections in EBN-treated mice further confirms that there was no pathology as a consequence of repeated EBN treatment over 28 days.

Table 2. Organ weight of animal subjects.

	Control	S1 20mg/kg	S1 100mg/kg	S2 20mg/kg	S2 100mg/kg
Lung	0.14 ± 0.03	0.17 ± 0.04	0.14 ± 0.04	0.12 ± 0.02	0.17 ± 0.04
Heart	0.11 ± 0.01	0.11 ± 0.01	0.10 ± 0.01	0.12 ± 0.01	0.11 ± 0.02
Liver	0.97 ± 0.10	0.89 ± 0.15	0.90 ± 0.15	0.94 ± 0.11	0.98 ± 0.07
Kidney	0.32 ± 0.04	0.33 ± 0.04	0.30 ± 0.01	0.30 ± 0.01	0.33 ± 0.04
Spleen	0.05 ± 0.02	0.05 ± 0.01	0.05 ± 0.02	0.05 ± 0.01	0.05 ± 0.01

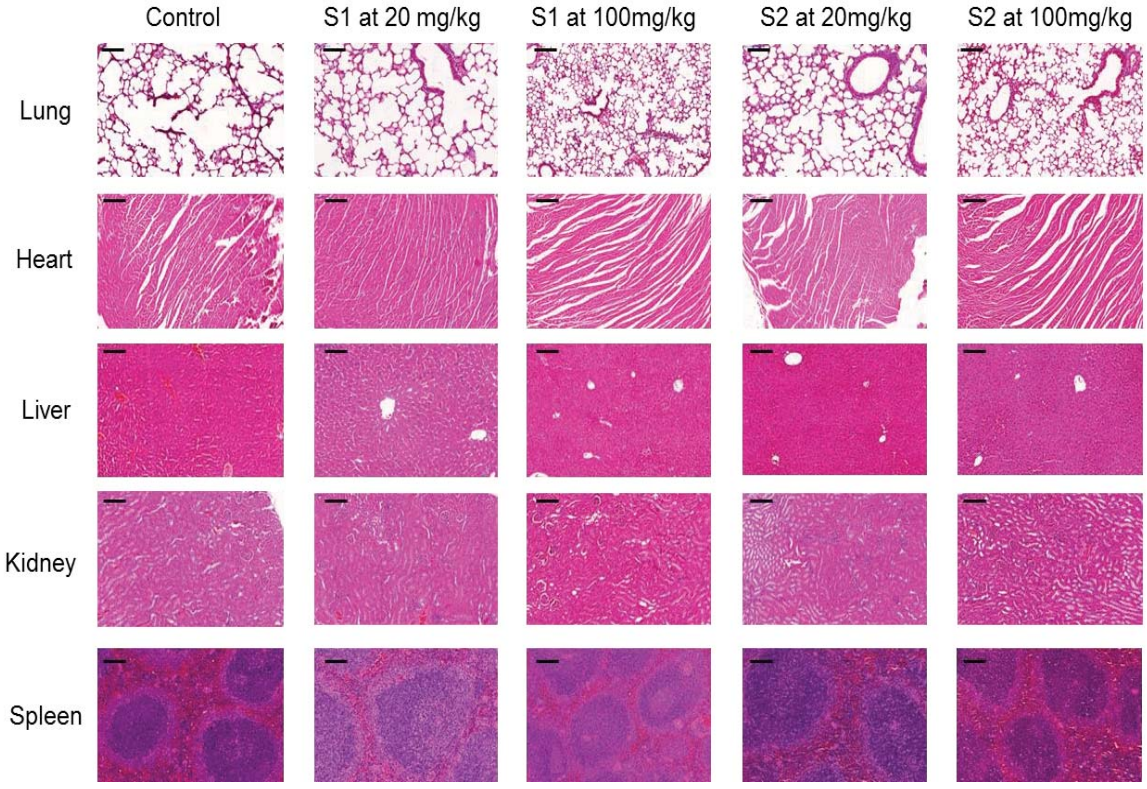

Fig. 2. H&E staining of lung, heart, liver, kidney and spleen sections from control mice, mice fed with S1 at 20 mg/kg, S1 at 100 mg/kg, S2 at 20 mg/kg and S2 at 100 mg/kg. Scale bar = 50 μm.

3.2 EBN improves motor function and balancing in PD mice

Open field test was performed twice throughout the experiment. The first test was performed after the completion of 28-day oral treatment with EBN but before any brain microinjection to assess the behavioral pattern. Results (Fig. 3A) showed that there was no notable difference in the distance travelled by animal among the treatment groups. Second test was carried out 2 weeks after the brain microinjection. Mice injected with 6-OHDA, as a model of PD, exhibited significant reduction in the total distance travelled as compared to the sham-operated mice, which received injection with PBS as vehicle only. 6-OHDA-injected mice that received 28 days of oral pre-treatment with EBN, regardless of whether they were fed with crude or water extract, travelled longer distance than the PD model alone. Nevertheless, 6-OHDA-injected mice that were fed with 20 mg/kg of S2 did not show significant improvement in locomotor activity.

On the other hand, track plot from the open field test was analyzed for locomotor activity and exploratory behavior of the animal. It was shown that the traveling pattern of sham-operated mice was smooth, straightforward and focused primarily at the periphery of the field, with occasional crossing to the centre (Fig.3B). In contrast, 6-OHDA-injected mice travelled with no specific pattern but all over the field. Noticeably, the mice manifested abnormal locomotor activity as characterized by the jerky lines in the plot. It is also apparent that there was frequent turnaround of the body resulting in change of motion direction. PD mouse model that received pre-treatment with EBN prior to brain injection with 6-OHDA, however, displayed more coordinated travelling pattern as seen by less turnaround of the body, as well as less jerky plot.

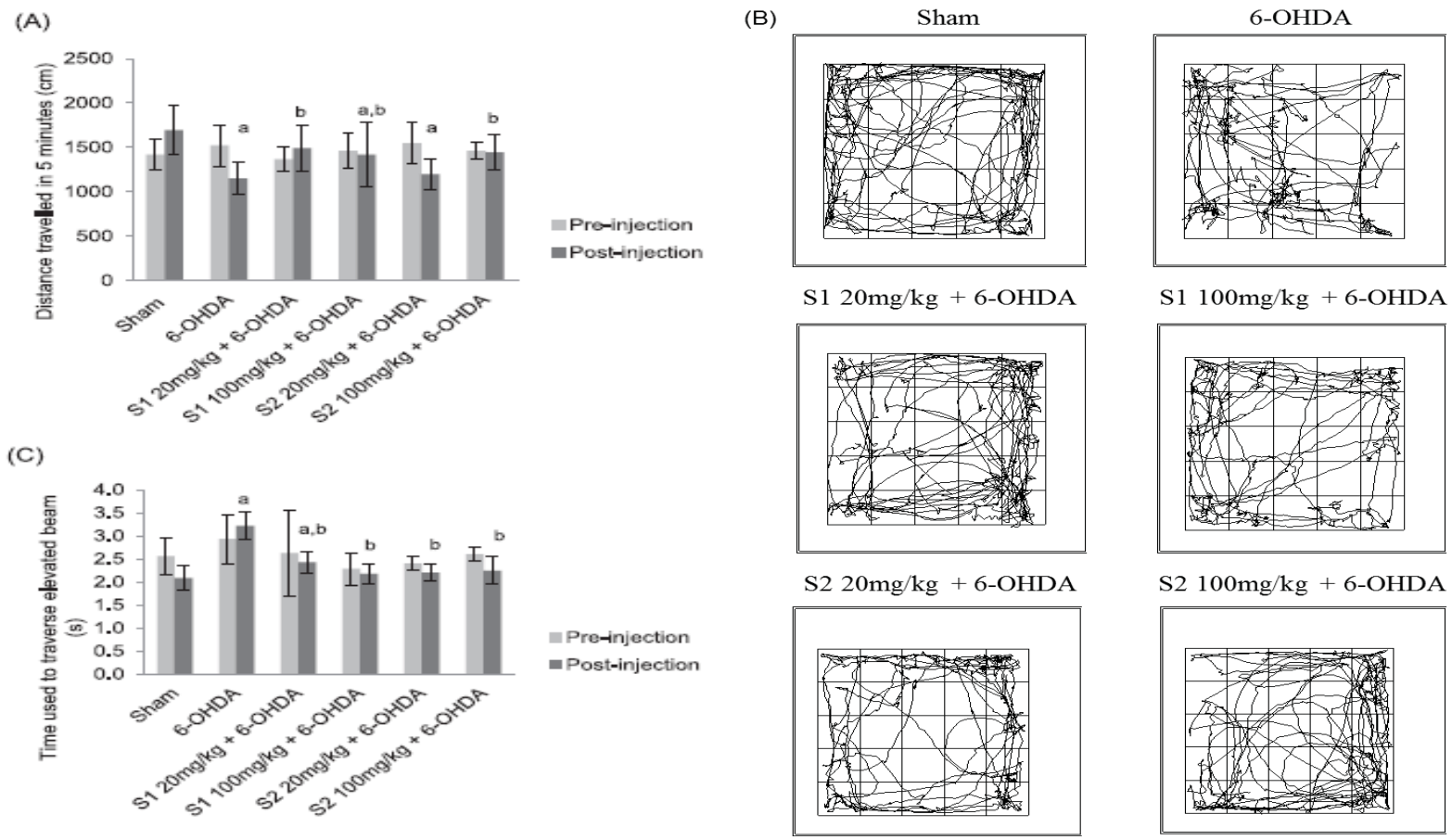

Fig. 3. Behavioral tests were applied to examine the locomotor activity of treated mice. Open field test revealed locomotor activity of the animals in terms of (A) distance travelled in 5 minutes and (B) track plot. Beam walking test enabled the study of (C) time used to traverse elevated beam. The data shown are means ± standard deviation and representative track plot from each treatment group was presented. Significant values of $P < 0.05$ are indicated as: a, versus sham group; b, versus 6-OHDA group.

Beam walking test was also performed as part of the locomotor activity assessment. Prior to brain microinjection, there was no significant difference in the time taken for mice to traverse a 50 cm-long elevated beam among the treatment groups tested (Fig. 3C). However, after brain microinjection, 6-OHDA-injected mice took longer time to complete the walking task as compared to the sham-operated mice. Interestingly, all mice which underwent oral pre-treatment with EBN utilized shorter time to traverse the elevated narrow beam.

Number of grid crossings and rear bouts of the animal in open field test were also determined in this study as an additional parameter to assess locomotor activity (Table 3). Grid crossing is when all 4 paws of the mouse moved from one grid to another. Results showed that the number of grid crossings for all the treatment groups were not statistically different. Frequency of animal standing on the hind leg is known as rearing bouts and may reflect the exploratory behavior of an animal. It was found that sham-operated mice stood on their hind leg on an average of 7 times throughout the 5 minutes test duration whereas 6-OHDA-injected mice only did so twice in average. However, neither of these values nor the data from the mice that received oral supplementation of EBN prior to 6-OHDA injection was significantly different to each other.

Table 3. Number of grid crossing and number of rear bouts of mice in open field test.

Group	Number of grid crossing	Number of rear bouts
Sham	196 ± 39	7 ± 11
6-OHDA	199 ± 42	2 ± 5
S1 20 mg/kg + 6-OHDA	188 ± 49	7 ± 11
S1 100 mg/kg + 6-OHDA	206 ± 47	1 ± 3
S2 20 mg/kg + 6-OHDA	194 ± 22	2 ± 4
S2 100 mg/kg + 6-OHDA	190 ± 63	2 ± 5

The data shown are means ± standard deviation.

3.3 EBN prevents 6-OHDA-induced loss of dopaminergic neuron in substantia nigra of PD mice

Presence of dopaminergic neurons were identified with anti-TH antibody labelling to determine the extent of neurodegeneration induced by intrastriatal injection of 6-OHDA. Brain sections (Fig. 4A) showed that TH-positive cells were well preserved in the substantia nigra of vehicle-injected mice. Quantification of staining intensity showed that in sham-operated mice, substantia nigra on left and right hemispheres displayed as much as 97% similarity (Fig. 4B). On the contrary, depletion of TH staining was seen in the left side of brain sections of 6-OHDA-injected animal. TH staining intensity of substantia nigra on the lesioned side plummeted to about 66% of that in the unlesioned side. This confirmed the loss of dopaminergic neurons in the substantia nigra at the same side of injection site. However, pre-treatment with EBN was found to attenuate the loss of TH-positive neurons in substantia nigra induced by 6-OHDA injection and the effect was not dose-dependent. Both S1 and S2 extracts given at dose as low as 20 mg/kg on a daily

basis for 28 days increased TH staining intensity in the lesioned substantia nigra in 6-OHDA-injected mice by 10%. On the other hand, there was no significant difference in the TH staining intensity of substantia nigra in mice supplemented with EBN at higher dose (100 mg/kg) when compared to the 6-OHDA-injected mice.

3.4 Antioxidant and microglia markers are regulated by EBN in substantia nigra of PD mice

The protein marker GPX1 was used to evaluate the antioxidant level in the substantia nigra region of mouse model. GPX1 staining intensity of the substantia nigra in control mice was almost similar on both hemispheres (about 96%) whereas the staining in substantia nigra of the lesioned side in 6-OHDA-injected mice was markedly reduced to 89% in relative to the unlesioned side (Fig. 5A & 5B). Treatment with 20mg/kg of either S1 or S2 extracts generally improved the staining intensity of GPX1 in substantia nigra at the lesioned side. Meanwhile, staining intensity of microglia marker CD11b in the substantia nigra at the lesioned side was 103% of that in the unlesioned side in sham mice (Figure 5C). The staining intensity at the lesioned side was elevated to 110% in the 6-OHDA-injected mice. The expression of CD11b at the lesioned side was restored to sub-control level in all EBN-treated mice, except the one fed with S2 at 100mg/kg.

3.5 NO production and lipid peroxidation are attenuated by EBN in PD cell model

Measurement of nitrite level in cell culture medium via Griess method is reflective of NO production of the cell. 6-OHDA-treated cell had almost double the amount of nitrite level of the control cell (Fig. 6A). Treatments with EBN extracts at MNTDs were able to attenuate NO production. Lipid hydroperoxides extracted from 6-OHDA-treated cell were

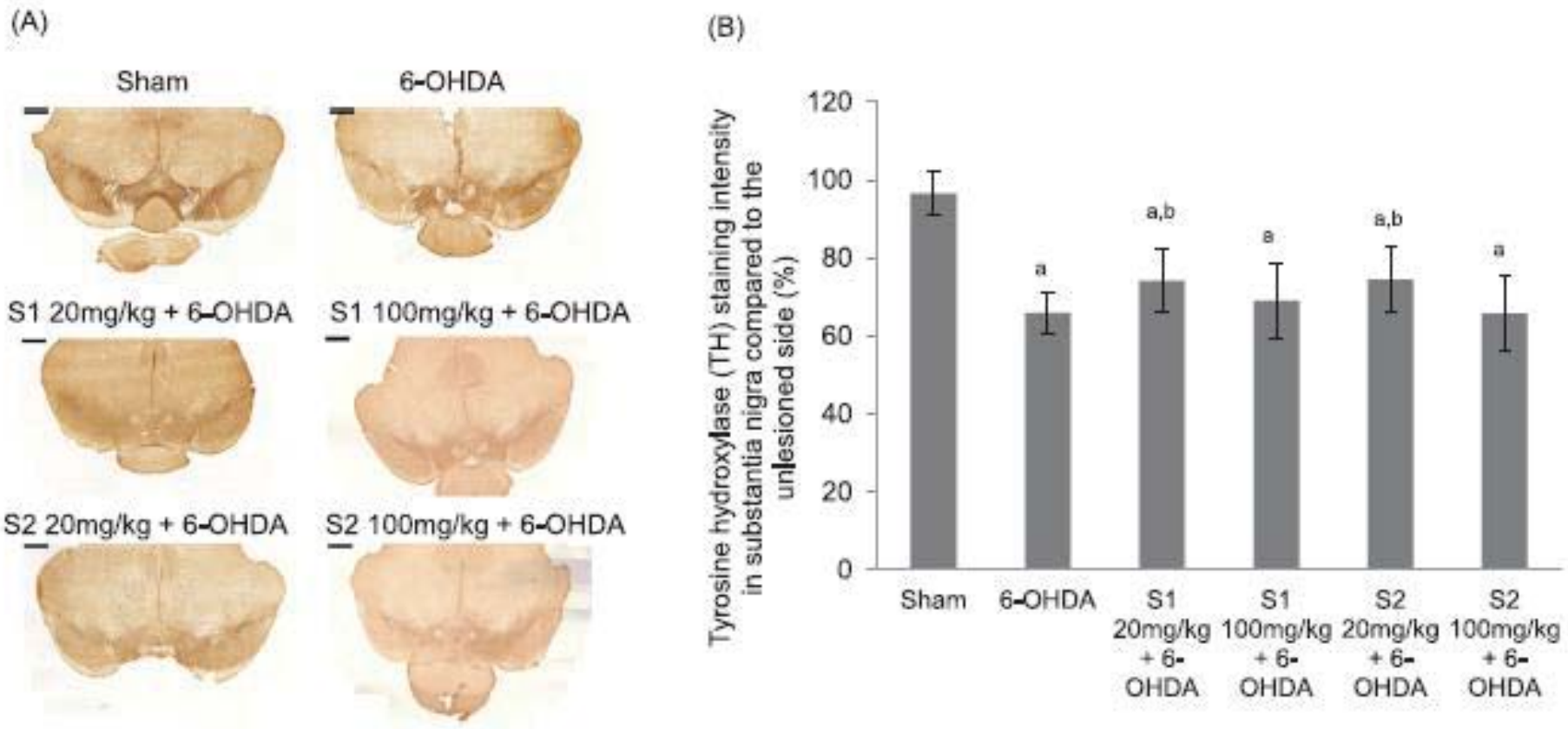

Fig. 4. Immunohistological studies of dopaminergic neurons in substantia nigra. Unilateral injection was performed with saline or 6-OHDA on the left striatum. (A) Immunohistochemistry study was performed using anti-TH antibody to stain for dopaminergic neuron in the substantia nigra region. Brown-coloured area indicates positive staining. Side that received injection was the 'lesioned side', which was on the left while the intact or 'unlesioned' side was on the right. Scale bar = 500 μm. (B) Quantitative analysis of staining intensity of the lesioned side as a percentage of the unlesioned side was performed with ImageJ software. The data shown are means ± standard deviation. Significant values of $P < 0.05$ are indicated as: a, versus sham group; b, versus 6-OHDA group.

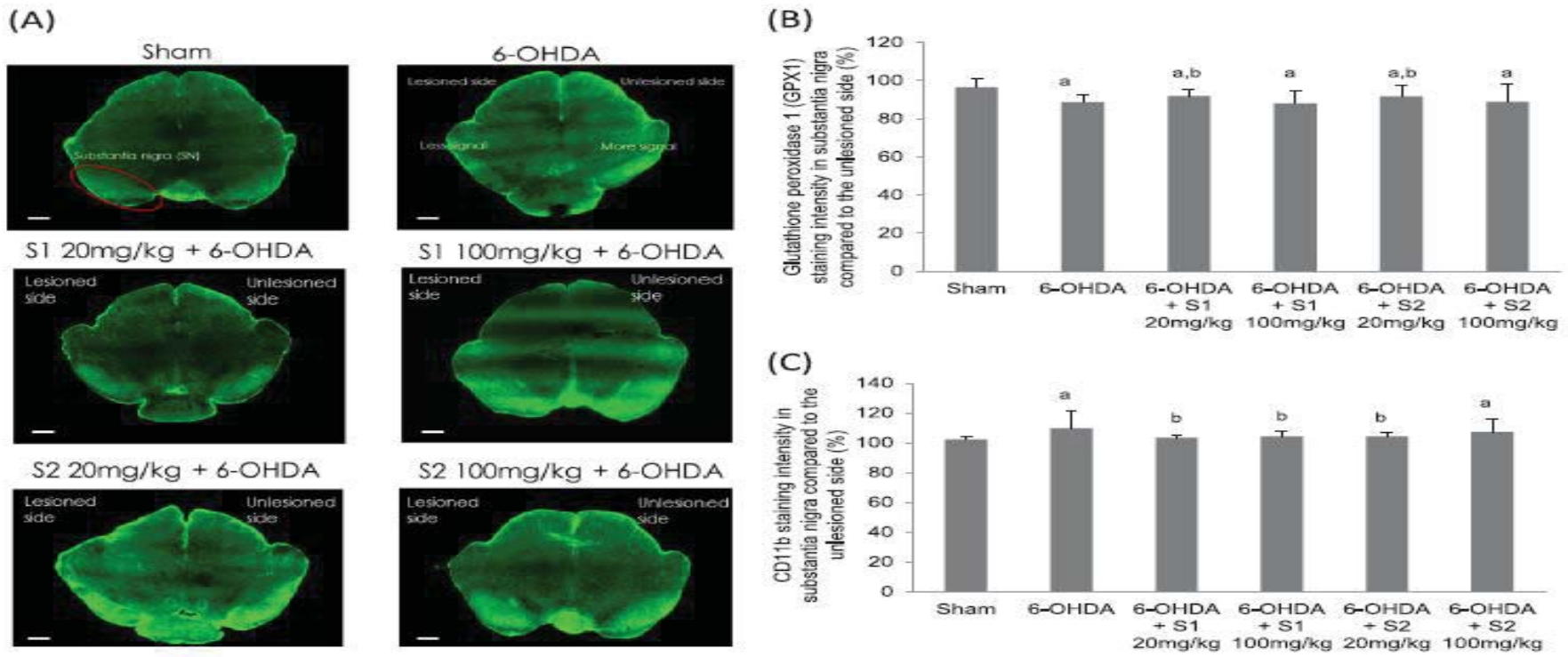

Fig. 5. Immunohistological studies of GPX1-positive and CD11b-positive neurons in substantia nigra of PD mice. Unilateral injection was performed with saline or 6-OHDA on the left striatum. Immunohistochemistry study was performed using anti-GPX1 and anti-CD11b antibodies to stain for glutathione peroxidase 1, an antioxidant enzyme and microglia, respectively. (A) Green fluorescence signal at the substantia nigra (red circle) sections indicates positive staining for GPX1 as a result of Alexa 488 fluorescence tag. Side that received injection was the 'lesioned side', which was on the left while the intact or 'unlesioned' side was on the right. Scale bar = 500 µm. (B) Staining intensity of the GPX1 on the lesioned side was quantified against the unlesioned side. (C) Staining intensity of the CD11b on the lesioned side was quantified against the unlesioned side. The data shown are means ± standard deviation. Significant values of $P < 0.05$ are indicated as: a, versus sham group; b, versus 6-OHDA group.

13% higher than control cell (Fig. 6B). However, treatment with S1 extract at both ½ MNTD and MNTD was able to restore lipid peroxidation to the level similar to control.

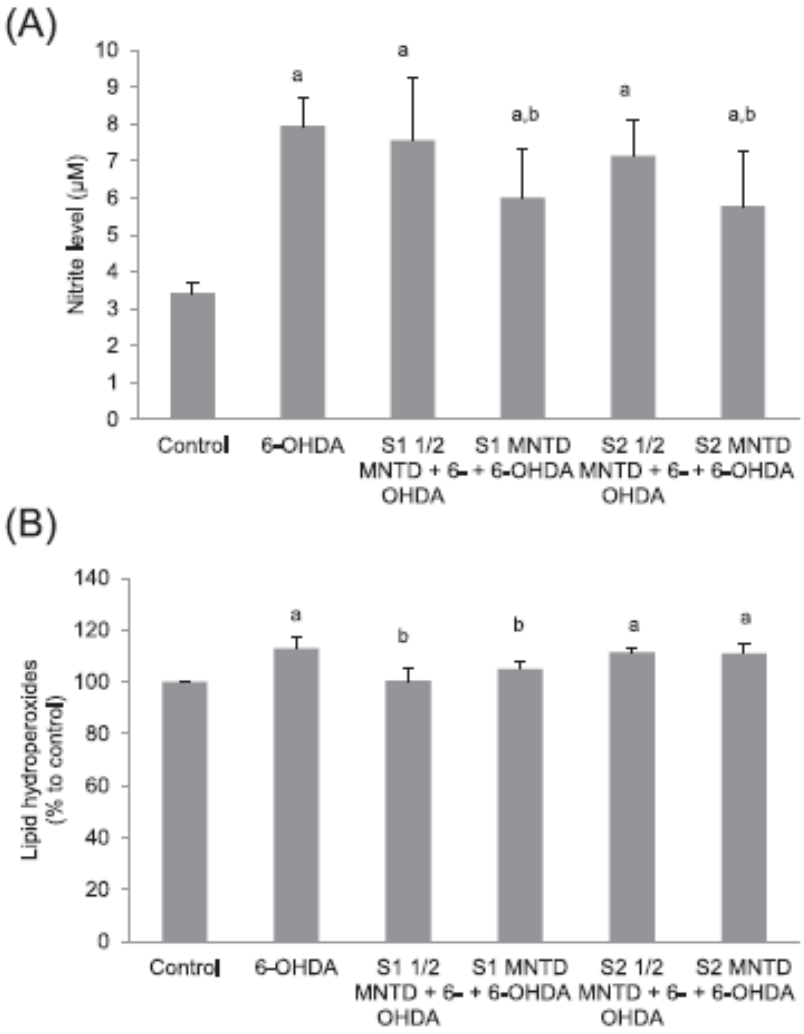

Fig. 6. NO production and lipid peroxidation assessment in PD cell model. *In vitro* PD cell model was created by treating SH-SY5Y with 6-OHDA intoxication. (A) Nitrite level and (B) lipid hydroperoxides were measured using Griess method and commercial kit, respectively. The data shown are means ± standard deviation. Significant values of $P < 0.05$ are indicated as: a, versus sham group; b, versus 6-OHDA group.

4. Discussion

Our previous *in vitro* study has found that administration of EBN conferred protective effect on neuronal cell model against 6-OHDA-induced apoptosis [27]. In order to further explore the neuroprotective effect of EBN *in vivo*, we used 6-OHDA-toxicated animal as a valid PD model, whereby investigation of PD-like behavioral manifestation and neurodegeneration of dopaminergic neuron in brain were carried out.

Before the commencement of EBN treatment in PD mouse model, we conducted toxicology studies to evaluate the safety profile of EBN at 20 mg/kg (low dose) and 100 mg/kg (high dose) in normal mice. These dosages were used in Matsukawa's study [25] previously but have yet to be tested in C57BL/6J mice, which we have proposed to be the animal model for PD in the present study. There was no study that used mice to study the effect of EBN that we can refer to. Hence, we evaluated the effect of EBN after sub-chronic treatment, which, according to OECD guidelines for drug testing, the animal shall be treated across a 28-day (4 weeks) period. With this duration, the study could describe possible health hazards likely to appear from repeated exposure over a considerably short period of time. The method is also preliminary to any long term study [30]. Throughout the 4-week treatment period, water and food consumption of the mice were not affected despite daily oral intervention with EBN treatment. Body weight can be an indicator of toxicity if there is more than 10% of weight loss from initial weight when drugs are administered in laboratory animal [33]. Similarly, physiological and pathological status of animal will reflect in the weight of vital organs as these are the metabolic centres of the entire body [34]. The body weight of control and EBN-treated mice changed in a similar trend: there was a slight decrease in body weight on 2nd week of experiment, followed by weight gain which continued to the 4th week. This phenomenon was not surprising, as the

same effect was seen across both treated and untreated group hence it is likely that the initial drop in body weight was due to psychological disturbance in animal as a result of daily oral gavage.

On a side note, the circulatory blood system runs through the entire body and carries protein marker released from organs as a consequence of toxin-induced cell damage and macrophages infiltration. Therefore blood biochemistry is highly predictive of toxicity in the body. In liver, transaminases such as ALT and AST, as well as ALP, albumin and total protein levels are indicator of protein synthesis function. The liver is also functional in lipid metabolism, in which triglyceride and cholesterol will be processed in this organ. Hence changes in the level of these markers will indicate the functionality of the liver. EBN treatment was not toxic to the liver because, although ALT, total protein and triglyceride levels were elevated in treated group as compared to untreated group, all the liver function tests had values that fell within the normal range. On the other hand, glucose level in the mice was significantly increased by EBN treatment, but it could be rationalized by the fact that EBN is rich in carbohydrates that can easily spike blood glucose level when consumed [35]. Similarly, this can explain the increase in triglyceride level too, since liver converts excess glucose into triglyceride. However, as blood glucose, triglyceride and cholesterol levels were maintained within normal range, it can be deduced that EBN did not exert adverse effect on the metabolism of carbohydrate and lipid. There was no observable difference in the biochemical parameters of heart and kidney in EBN-treated mice when compared to control, confirming that sub-chronic treatment with EBN did not impact the organ health of the mice.

Safety profile of EBN treatment at 20 mg/kg and 100 mg/kg was further confirmed based on the observation on the internal organs (eg. liver, heart, lungs, kidneys and spleen). The weight of these organs was not altered in treated group as compared to the control group. The organs were also checked for external abnormalities and no special remark was noted in terms of drug-induced and spontaneous lesions, changes in size, shape, texture and colour. Subsequent histopathological examination showed that tissue morphology in lung, heart, liver, kidney and spleen sections in EBN-treated mice was well-preserved, hence confirms that there was no pathological changes at the microscopic level as a consequence of repeated EBN treatment over 28 days.

In the brains of PD patients, dopaminergic neuronal loss is observed in the substantia nigra and causes motor dysfunctions such as bradykinesia, rigidity, postural instability, gait impairment, and resting tremor. Physiologically, these symptoms stem from the depletion of the neurotransmitter known as dopamine. Therefore to create an *in vivo* model of PD, the neurotoxin 6-OHDA is used to induce death of dopamine-generating cells in midbrain. The 6-OHDA is structurally similar to the endogenous neurotransmitter dopamine, thus it can enter dopaminergic neurons via the dopamine transporter. Once in the neuron, 6-OHDA accumulates in the cytosol and undergoes auto-oxidation, promoting a high rate of hydrogen peroxide formation. 6-OHDA also inhibits complex I activity, subsequently leading to cell death. The lesion obtained with 6-OHDA is highly reproducible. However, local administration of 6-OHDA is needed as the neurotoxin does not cross the blood-brain-barrier. By direct injection into the striatum unilaterally, 6-OHDA is shown to induce damage to the striatal fibres, followed by delayed but progressive loss of neuron in the substantia nigra. It has been shown that intrastriatal injection of 6-OHDAin mouse model resulted in detrimental changes in midbrain

dopaminergic neuronal until a compensatory change (recovery) in animal's behavior is seen at 56th day post-injection [36]. It is expected that this chemical intervention causes injury to 60-70% of the neuronal network (decreased density of dopaminergic neuron in striatum and substantia nigra) and motor impairment of limbs contralateral to the injected hemisphere (loss of balance and motor coordination). Such modality therefore provides a progressive model of nigrostriatal degeneration similar to the course of disease in human patients.

The open field test is a versatile experiment in animal behavioral studies due to the extensive type of information one can obtain from each single test. Locomotor activity of the animal can be assessed from the total distance travelled and number of grid crossings. The longer the total distance travelled, the more agile the animal is in terms of motor coordination. Meanwhile, although frequency of grid crossings is an assessment similar to the total distance measurement, the pitfall of this parameter is that higher number of grid crossings does not necessarily mean greater distance travelled. Findings from the current study showed that 6-OHDA-injected mice travelled significantly shorter distance as compared to the sham-operated mice, apparently due to poorer motor performance as a result of neurotoxin injection, but there was no noteworthy difference in terms of the number of grid crossings between the two groups of mice. Such gap in our hypothesis and the test results is largely attributed to the nature of the parameters mentioned above. In fact, total distance travelled is a direct measurement of motor function while number of grid crossings is an indirect one. This is because different motion pattern of the animal in an open field, for instance, whether the mouse travels in a straight line, constantly changing direction, or travels into adjacent grid or to the diagonal grid, will determine how relevant grid crossings count is to the travelling ability by the animal. Eventually

these criteria will affect the reliability of the parameter as a measurement of motor function especially when the method is used to compare subtle difference between treatment groups. Study by Vila et al. [37] have also pointed out that size of the animal will affect the outcome of the test. Hence, it is inappropriate to relate grid crossings directly to the animal's motor skills but the results should always be evaluated with precaution.

On the other hand, rearing behavior could be an indicator for anxiety and exploratory behavior of the animal. In the present study, 6-OHDA-injected mice were found to have averagely less rearing bouts as compared to sham-operated mice, which could be associated to heightened anxiety level and reduced exploration in response to novel environment. Such alteration in the emotion of the subject is a resemblance of non-motor complications, such as anxiety and depression, experienced by PD patient [38]. However, the difference in rear bouts was not significant between the groups. Indeed, rearing behavior should not be entirely translated into the sole effect of fear and anxiety state of the animal because studies have shown that rearing activity was never easily countered by anxiolytics nor exacerbated by anxiogenics in various models of anxiety [39]. Moreover, we have overlooked the effect of social isolation on anxiety-like behaviors in this study [40]. The fact that the mice in this study were not housed in a fixed number of animal per cage, whereby some mice was housed together with 2-3 other animals while some was housed individually, might already altered social interaction and stress tolerance threshold, hence the poor statistical outcome of this parameter. When a mouse is physically separated from cage mates during the test, the stress level will be higher than the stress experienced by a socially isolated mouse which was housed independently of others.

Therefore we would like to highlight the importance of social isolation in animal behavioral study as such.

Last but not least, the track plot is an image that allows insight into the entire movement pattern of the animal in an open field. The tracker system of the LimeLight 2 software detects moving object in the open field and tracks the motion via the video camera, which is then reflected in the track plot. The fact that sham-operated mice travelled in a straightforward manner with occasional crossing to the centre of the field refer to smooth motor coordination, exploratory behavior and low anxiety level in the animals. In comparison, 6-OHDA-injected mice had jerky movement, disoriented travel direction and turned around their body more frequently. Such observation could be due to the difficulty of the animal to execute motor function in one side of the body after unilateral 6-OHDA injection into the brain and therefore failure to control movement. The mice were, however, not affected in terms of their exploratory activity and anxiety level because of the frequent crossing to the centre of the field.

Neurochemistry in the midbrain of PD alters when there is severe depletion of dopamine-releasing neurons due to the death of these cells. As the disease progresses, initial site of cell death extends from striatum and propagate along the nigrostriatal bundle to the substantia nigra. As a result, dopamine pool in the two regions begins to drop gradually and eventually leading to motor deficit. Unilateral injection of neurotoxin 6-OHDA into striatum has been established for successfully inducing functional impairment, and long-lasting reduction in residual dopamine content in striatum and TH-positive neuron in substantia nigra in mice [31]. In this study, 6-OHDA-injected mice demonstrated hampered motor skills as well as degeneration of dopaminergic neuron in both striatum

and substantia nigra. However EBN oral supplementation prior to brain injection with neurotoxin was able to attenuate the extent of neuronal death induced by 6-OHDA. Interestingly, such effect was not dose-dependent. Only mice that received 20 mg/kg/day EBN were protected from neurodegeneration by 10% whereas mice that received 100 mg/kg/day EBN were not showing any improvement. Although we have yet to identify the biologically-important compounds present in EBN, we postulate that the brain could be more sensitive and responsive to certain biological stimulus at submicromolar amount, be it growth factors, hormones or small molecules. This is known as non-monotonicity in dose-response studies, which explains the non-linear relationship between dose and effect, and that the effect of low dose cannot be predicted by the effect observed at high dose [41].

Further immunostaining against the GPX1, an antioxidant marker was carried out on the brain sections obtained from PD mouse model. GPX1 is a member of the glutathione peroxidase protein family which plays an important role in the detoxification of hydrogen peroxide, hence functional in protecting cells from oxidative damage. It is one of the most abundant selenium-containing antioxidant enzymes which are expressed in nearly all types of mammalian tissue. In control human brain section, expression of GPX1 enzyme is concentrated around the doparminergic neurons in substantia nigra. Therefore under immunofluorescence study, positive staining could be seen across the entire midbrain section but higher staining intensity was noted in the substantia nigra region. In the current study, 6-OHDA-induced loss of dopaminergic neurons was accompanied by the reduced expression of glutathione peroxidase in the substantia nigra. This finding echoed with the observation from post mortem studies whereby marked decrease in peroxidase

activity and amount of reduced glutathione were associated to the neurodegeneration in PD patient [8, 42].

The mechanism behind neurodegeneration following glutathione depletion may be attributed to the insufficiency of neuromelanin production to maintain redox balance in cells [43, 44]. A decrease in peroxidase activity would directly hamper the capacity of the neurons to detoxify hydrogen peroxide and accelerate free radical generation and lipid peroxidation. However, in this study we found that EBN treatment increased expression of GPX1 in substantia nigra of 6-OHDA-induced PD mouse model. As documented by Hashimoto et al., elevated GPX1 activity would confer neuroprotective effect to the dopaminergic neuron [45]. We therefore postulate that EBN protects dopaminergic neuron against 6-OHDA-induced cell death by increasing the activity of antioxidant enzyme GPX for counteracting damaging effect of free radicals. Microglia is one of the resident macrophages in the brain, which once activated upon exposure to noxious stimuli, can release inflammatory cytotoxic factors such as NO, interleukin-6 and tumor necrosis factor-alpha [46]. Our results show that EBN treatment effectively dampens the neuroinflammation by reducing the expression of microglia marker CD11b. Study on SH-SY5Y also shows that EBN treatment effectively ameliorates RNS and nitrosative stress, suggesting that it could be one of neuroprotective mechanisms exerted by EBN. Furthermore, lipid peroxidation in 6-OHDA-treated SH-SY5Y was also diminished after EBN treatment, which otherwise could have negative impacts on the integrity of cellular membrane, membrane-bound receptors and transport proteins [17].

In summary, oral supplementation of EBN was demonstrated to be beneficial to PD mouse model by restoring motor function and preserving dopaminergic neuron. Increased

expression of antioxidant glutathione peroxidase 1 and reduced microglial activation in PD mice after EBN treatment further complement the findings of reduced NO production and lipid peroxidation to provide basis to the neuroprotective mechanism of EBN. These extensive data point out that EBN may protect neuron against oxidative stress and nitrosative stress and could be a potential therapeutic agent for counteracting neurodegeneration in PD.

Acknowledgement

We would like to thank Yew Kee Pte Ltd for providing raw EBN material to this study.

Funding

This work was supported by Ministry of Higher Education of Malaysia (grant number: ERGS/1/2011/SKK/MUSM/03/3).

5.3 References

[1] Farrer MJ. Genetics of Parkinson disease: paradigm shifts and future prospects. Nature reviews Genetics. 2006;7:306-18.

[2] Dauer W, Przedborski S. Parkinson's Disease: Mechanisms and Models. Neuron. 2003;39:889-909.

[3] Snyder CH, Adler CH. The patient with Parkinson's disease: part I-treating the motor symptoms; part II-treating the nonmotor symptoms. Journal of the American Academy of Nurse Practitioners. 2007;19:179-97.

[4] Przedborski S. Pathogenesis of nigral cell death in Parkinson's disease. Parkinsonism & related disorders. 2005;11 Suppl 1:S3-7.

[5] Bernstein AI, Garrison SP, Zambetti GP, O'Malley KL. 6-OHDA generated ROS induces DNA damage and p53- and PUMA-dependent cell death. Molecular neurodegeneration. 2011;6:2.

[6] Fernández-Espejo E. Pathogenesis of Oxidative Stress and the Destructive Cycle in the Substantia Nigra in Parkinson's Disease. In: Tseng K-Y, editor. Cortico-Subcortical Dynamics in Parkinson's Disease. Totowa, NJ: Humana Press; 2009. p. 261-71.

[7] Lei XG, Cheng WH, McClung JP. Metabolic regulation and function of glutathione peroxidase-1. Annual review of nutrition. 2007;27:41-61.

[8] Kish SJ, Morito C, Hornykiewicz O. Glutathione peroxidase activity in Parkinson's disease brain. Neuroscience letters. 1985;58:343-6.

[9] Liberatore GT, Jackson-Lewis V, Vukosavic S, Mandir AS, Vila M, McAuliffe WG, et al. Inducible nitric oxide synthase stimulates dopaminergic neurodegeneration in the MPTP model of Parkinson disease. Nature medicine. 1999;5:1403-9.

[10] Yokoyama H, Kuroiwa H, Yano R, Araki T. Targeting reactive oxygen species, reactive nitrogen species and inflammation in MPTP neurotoxicity and Parkinson's disease.

Neurological sciences : official journal of the Italian Neurological Society and of the Italian Society of Clinical Neurophysiology. 2008;29:293-301.

[11] Dexter DT, Carter CJ, Wells FR, Javoy-Agid F, Agid Y, Lees A, et al. Basal lipid peroxidation in substantia nigra is increased in Parkinson's disease. Journal of neurochemistry. 1989;52:381-9.

[12] Alam ZI, Jenner A, Daniel SE, Lees AJ, Cairns N, Marsden CD, et al. Oxidative DNA damage in the parkinsonian brain: an apparent selective increase in 8-hydroxyguanine levels in substantia nigra. Journal of neurochemistry. 1997;69:1196-203.

[13] Floor E, Wetzel MG. Increased protein oxidation in human substantia nigra pars compacta in comparison with basal ganglia and prefrontal cortex measured with an improved dinitrophenylhydrazine assay. Journal of neurochemistry. 1998;70:268-75.

[14] Huerta C, Sanchez-Ferrero E, Coto E, Blazquez M, Ribacoba R, Guisasola LM, et al. No association between Parkinson's disease and three polymorphisms in the eNOS, nNOS, and iNOS genes. Neuroscience letters. 2007;413:202-5.

[15] Kouti L, Noroozian M, Akhondzadeh S, Abdollahi M, Javadi MR, Faramarzi MA, et al. Nitric oxide and peroxynitrite serum levels in Parkinson's disease: correlation of oxidative stress and the severity of the disease. European review for medical and pharmacological sciences. 2013;17:964-70.

[16] Good PF, Hsu A, Werner P, Perl DP, Olanow CW. Protein nitration in Parkinson's disease. Journal of neuropathology and experimental neurology. 1998;57:338-42.

[17] Sultana R, Perluigi M, Butterfield DA. Lipid Peroxidation Triggers Neurodegeneration: A Redox Proteomics View into the Alzheimer Disease Brain. Free radical biology & medicine. 2013;62:157-69.

[18] Dalfó E, Ferrer I. Early α-synuclein lipoxidation in neocortex in Lewy body diseases. Neurobiology of aging. 2008;29:408-17.

[19] Castellani RJ, Perry G, Siedlak SL, Nunomura A, Shimohama S, Zhang J, et al. Hydroxynonenal adducts indicate a role for lipid peroxidation in neocortical and brainstem Lewy bodies in humans. Neuroscience letters. 2002;319:25-8.

[20] Qin Z, Hu D, Han S, Reaney SH, Di Monte DA, Fink AL. Effect of 4-hydroxy-2-nonenal modification on alpha-synuclein aggregation. The Journal of biological chemistry. 2007;282:5862-70.

[21] Morel P, Tallineau C, Pontcharraud R, Piriou A, Huguet F. Effects of 4-hydroxynonenal, a lipid peroxidation product, on dopamine transport and Na+/K+ ATPase in rat striatal synaptosomes. Neurochemistry international. 1998;33:531-40.

[22] Lim CK, Cranbrook Eo. Swiftlets of Borneo – Builders of edible nests Sabah, Malaysia: Natural History Publication (Borneo) SDN., B.H.D. ; 2002.

[23] Chye SM, Tai SK, Koh RY, Ng KY. A Mini Review on Medicinal Effects of Edible Bird's Nest. Letters In Health And Biological Sciences. 2017;2.

[24] Guo CT, Takahashi T, Bukawa W, Takahashi N, Yagi H, Kato K, et al. Edible bird's nest extract inhibits influenza virus infection. Antiviral research. 2006;70:140-6.

[25] Matsukawa N, Matsumoto M, Bukawa W, Chiji H, Nakayama K, Hara H, et al. Improvement of bone strength and dermal thickness due to dietary edible bird's nest extract in ovariectomized rats. Bioscience, biotechnology, and biochemistry. 2011;75:590-2.

[26] Hou Z, He P, Imam MU, Qi J, Tang S, Song C, et al. Edible Bird's Nest Prevents Menopause-Related Memory and Cognitive Decline in Rats via Increased Hippocampal Sirtuin-1 Expression. Oxidative Medicine and Cellular Longevity. 2017;2017:8.

[27] Yew MY, Koh RY, Chye SM, Othman I, Ng KY. Edible bird's nest ameliorates oxidative stress-induced apoptosis in SH-SY5Y human neuroblastoma cells. BMC complementary and alternative medicine. 2014;14:391.

[28] Hou Z, Imam MU, Ismail M, Ooi DJ, Ideris A, Mahmud R. Nutrigenomic effects of edible bird's nest on insulin signaling in ovariectomized rats. Drug design, development and therapy. 2015;9:4115-25.

[29] Marcone MF. Characterization of the edible bird's nest the "Caviar of the East". Food Research International. 2005;38:1125-34.

[30] OECD OfEC-oaD. Test No. 407: Repeated Dose 28-day Oral Toxicity Study in Rodents. Section 4: Health Effects2008.

[31] da Conceição FSL, Ngo-Abdalla S, Houzel J-C, Rehen SK. Murine Model for Parkinson's Disease: from 6-OH Dopamine Lesion to Behavioral Test. 2010:e1376.

[32] Zhou X, Hansson GK. Effect of sex and age on serum biochemical reference ranges in C57BL/6J mice. Comparative medicine. 2004;54:176-8.

[33] Vaghasiya YK, Shukla VJ, Chanda SV. Acute Oral Toxicity Study of Pluchea arguta Boiss Extract in Mice. Journal of Pharmacology and Toxicology. 2011;6:113-23.

[34] Dybing E, Doe J, Groten J, Kleiner J, O'Brien J, Renwick AG, et al. Hazard characterisation of chemicals in food and diet. dose response, mechanisms and extrapolation issues. Food and chemical toxicology : an international journal published for the British Industrial Biological Research Association. 2002;40:237-82.

[35] Yida Z, Imam MU, Ismail M, Ooi D-J, Sarega N, Azmi NH, et al. Edible Bird's Nest Prevents High Fat Diet-Induced Insulin Resistance in Rats. Journal of Diabetes Research. 2015;2015:11.

[36] Alvarez-Fischer D, Henze C, Strenzke C, Westrich J, Ferger B, Hoglinger GU, et al. Characterization of the striatal 6-OHDA model of Parkinson's disease in wild type and alpha-synuclein-deleted mice. Experimental neurology. 2008;210:182-93.

[37] Vila JL, Philpot RM, Kirstein CL. Grid Crossing: Inability to Compare Activity Levels between Adolescent and Adult Rats. Annals of the New York Academy of Sciences. 2004;1021:418-21.

[38] Menza MA, Robertson-Hoffman DE, Bonapace AS. Parkinson's disease and anxiety: comorbidity with depression. Biological psychiatry. 1993;34:465-70.

[39] Lever C, Burton S, O'Keefe J. Rearing on Hind Legs, Environmental Novelty, and the Hippocampal Formation. Reviews in the Neurosciences. 2006;17:111–34.

[40] File SE. The use of social interaction as a method for detecting anxiolytic activity of chlordiazepoxide-like drugs. Journal of Neuroscience Methods. 1980;2:219-38.

[41] Rhomberg LR, Goodman JE. Low-dose effects and nonmonotonic dose–responses of endocrine disrupting chemicals: Has the case been made? Regulatory Toxicology and Pharmacology. 2012;64:130-3.

[42] Pearce RKB, Owen A, Daniel S, Jenner P, Marsden CD. Alterations in the distribution of glutathione in the substantia nigra in Parkinson's disease. Journal of Neural Transmission. 1997;104:661-77.

[43] Ambani LM, Van Woert MH, Murphy S. Brain peroxidase and catalase in Parkinson disease. Archives of neurology. 1975;32:114-8.

[44] Sofic E, Lange KW, Jellinger K, Riederer P. Reduced and oxidized glutathione in the substantia nigra of patients with Parkinson's disease. Neuroscience letters. 1992;142:128-30.

[45] Hashimoto K, Ueda S, Ehara A, Sakakibara S, Yoshimoto K, Hirata K. Neuroprotective effects of melatonin on the nigrostriatal dopamine system in the zitter rat. Neuroscience letters. 2012;506:79-83.

[46] Wilms H, Rosenstiel P, Sievers J, Deuschl G, Zecca L, Lucius R. Activation of microglia by human neuromelanin is NF-kappaB dependent and involves p38 mitogen-activated protein kinase: implications for Parkinson's disease. FASEB journal : official

publication of the Federation of American Societies for Experimental Biology. 2003;17:500-2.

Chapter 6

De novo sequencing-assisted peptide profiling and antioxidant study of edible bird's nest extracts

6.1 Summary of Chapter 6

Proteomic profiling is a technique which allows detailed identification of the protein components of a sample. Based on our findings in previous chapters, EBN is a natural food product contains a library of potentially bioactive compounds. It demonstrated promising neuroprotective and neurotrophic effects in cell and animal model of PD, yet the exact compound that brought about such effects is still unknown. It has been frequently reported that protein is the most abundant compound in the EBN, which amounts to as high as 60% of its dry weight. However, there is limited study to identify the diversity of proteins that may be variably present in raw powder and water extracts of EBN.

Hence, the objectives for the study in Chapter 6 were as follow:

1. To characterize the protein profile of raw powder and water extracts of EBN.
2. To evaluate the antioxidant activity of pancreatin-digested raw powder and water extracts of EBN in terms of free radical scavenging, reductive ability and metal chelation.

Following protein digestion, liquid chromatography and tandem mass spectrometry analysis of our EBN samples, we employed Agilent MassHunter and PEAKS Studio software to perform *de novo* peptide sequencing and identify the proteins based on the curated protein database, Swiss-Prot. The results differed between the raw powder and water extracts of EBN in which 17 proteins were identified in raw EBN and 22 proteins were discovered in water extract of EBN. Out of these, 20 of them are reported for the first time in EBN. We have also identified the major mechanisms through which pancreatin-digested raw powder and water extract of EBN exert their antioxidant effect and the various level of antioxidant activity that they possessed.

6.2 Manuscript

De novo sequencing-assisted peptide profiling and antioxidant study of edible bird's nest extracts

Mei Yeng Yew[1], Rhun Yian Koh[2], Iekhsan Othman[1], Syafiq Asnawi Zainal Abidin[1], Soi Moi Chye[2], Khuen Yen Ng[1,3]*

[1] Jeffrey Cheah School of Medicine & Health Sciences, Monash University Malaysia, Selangor, Malaysia

[2] Department of Human Biology, School of Medicine, International Medical University, Kuala Lumpur, Malaysia

[3] Brain Research Institute Monash Sunway, Monash University Malaysia, Selangor, Malaysia.

Corresponding author:

Dr. Khuen Yen Ng

Brain Research Institute Monash Sunway, Monash University Malaysia.

[redacted]

Number: +6012-4500575

ORCID: 0000-0002-9453-4999

Abstract

Edible bird's nest (EBN), a natural food product made of the saliva of the *Aerodramus* swiftlets, is appraised for its traditional nutritional claims. Reports on the proteomic analysis of EBN are limited thus validation of nutraceutical benefits of EBN protein has yet to be established. EBN is commonly boiled and consumed in water. In this study, raw powder and water extracts of EBN were analyzed by *de novo* peptide sequencing-assisted database search, which presents greater search efficiency than database search alone, and 17 proteins and 22 proteins were detected respectively. These proteins might play roles in immunity, extracellular matrix formation, neurodevelopment, cell survival and apoptosis, cell proliferation and migration, antioxidation, and common cellular processes. Among which, 20 proteins are reported for the first time in EBN. Subsequently, we found potential antioxidant activities in both EBN samples. The raw powder exhibited higher radical scavenging and reducing power than the water extract, which demonstrated higher metal-chelating activities, the difference of which may be attributed to the different amino acid composition. The findings of this study will provide clues to the nutritional and medicinal effects of EBN presented in previous literatures, and support EBN as a potential functional food.

Keywords

Antioxidant; De novo peptide sequencing; Edible bird's nest; Functional food; Mass spectrometry; Proteomic analysis

1. Introduction

In the long history of Chinese Traditional Medicine, edible bird's nest (EBN) is a prestigious food item in which the access to it is only granted for the privileged. EBN is the hardened salivary secretion of swiftlets from the *Aerodramus* genus widely found in the south-east Asia. Particularly, white bird's nest produced by the swiftlet *Aerodramus fuciphagus* is the most popular among consumer. EBN is traditionally consumed after hours of stewing with sugar and water, and is known to be beneficial to the maintenance of general well-being of the body as well as treatment of ailments such as cough, tuberculosis and gastric ulcers [1]. Folklore has it that EBN also helps patient to regain vitality after illness or surgery. These claims are not by chance, as science has reported that EBN contains 60% protein, with the rest consists of carbohydrates, lipids and trace minerals, all of which are believed to contribute to the nutritional value of EBN [2,3]. The market of EBN among Asian is exceptionally huge, which is currently estimated to exceed 210 tonnes per annum, fetching as much as US$1.6 billion worth of trade internationally [4]. Despite so, scientific evidence to its medicinal benefit is scarce.

Despite continuous effort in proteomic profiling of EBN protein, there are varying reports on EBN proteome mainly attributed to the variety of protein extraction and separation method, as well as the algorithm used in peptide mass fingerprinting [5-8]. Up to date, only a handful of biomolecules has been reported in EBN, among which includes sialic acid [9] and ovoinhibitor [10]. These biomolecules were probably responsible for several bioactivities including influenza-inhibiting activity [11] and allergenicity of the EBN [12], respectively. Unfortunately, bioactive compounds responsible for many newly-discovered bioactivities of EBN such as neuroprotection [13], mitogenic effect [14] and anti-osteoporosis [15] are yet to

be identified, therefore this study aims to establish the extensive protein profile of EBN, which would help in the identification of these bioactive compounds.

Oxidative stress is caused by production and accumulation of excessive reactive oxygen species (ROS) within the cell, which damages DNA, protein and lipid to affect cellular functions [16]. It has been proven that oxidative stress activates apoptotic cascade to cause neurodegenerative diseases, metabolic diseases, autoimmune diseases and cancers [17]. Therefore, anti-oxidation is a subject commonly studied in search of therapeutic strategy. Dietary antioxidant is believed to reduce the risk or retard the progression of chronic diseases particularly via inhibition of lipid peroxidation. Many natural antioxidants with potential for nutraceutical application have since been discovered [18]. Our previous study has shown that EBN possessed neuroprotective effect by counteracting oxidative stress induced by neurotoxin in neuronal cell line SH-SY5Y [13]. It was found later that EBN increased expression of antioxidant-related genes and enzyme activities to attenuate cell death of H_2O_2-treated SH-SY5Y cell [19] and increase survivability of *Drosophila Melanogaster* in heat-stress test [20]. However, the underlying working principle of antioxidant properties exhibited by EBN is undefined.

Nutritional study of EBN should be carefully evaluated given the fact that consumption practice of EBN among individual can be different. Due to its high glycoprotein content, when boiled in water EBN forms water-insoluble fraction which some may find unappealing and selectively opt them out during consumption. It is imperative that any nutritional claims for EBN shall take both raw powder and water extracts into consideration. Hence the current study aimed to look into the difference of protein profile between raw powder and water extracts of EBN as well as their antioxidant activities. In the current study, we characterized

the protein profile in white EBN sourced from a local swiftlet farm in Malaysia using liquid chromatography and mass spectrometry system, with the aid of emerging bioinformatics tools for *de novo* peptide sequencing. This study employed an innovative approach in protein identification that will improve our understanding of the protein make-up of the EBN extracts. Lastly, assays that determine the different antioxidant mechanisms in terms of free radical scavenging, reductive ability and metal chelation were used to examine the antioxidant capacities of the EBN extracts [21]. A comprehensive evaluation of the protein profile and antioxidant power of both crude and water extracts of EBN further elaborated the potential nutritional value of this food product.

2. Materials and method

2.1Materials

Ammonium bicarbonate, dimethyl sulphoxide (DMSO), 2,2-diphenyl-1-picrylhydrazyl (DPPH), dithiothreitol (DTT), ethylene diaminetetracetic acid (EDTA), ferric chloride ($FeCl_3$), ferrous chloride ($FeCl_2$), ferrozine, iodoacetamide (IAM), pancreatin, trifluoroethanol, trypsin, vitamin C and 2,4,6-Tris(2-pyridyl)-*s*-triazine (TPTZ) were obtained from Sigma-Aldrich (St. Louis, MO, USA). Acetic acid, acetonitrile, formic acid, hydrochloric acid (HCl), methanol were purchased from Merck (Darmstadt, Germany).White EBN collected from a swiftlet farm in Perak, a state in the northern region of Malaysia, was kindly provided by Yew Kee Ptd. Ltd.

2.2 Proteomic profiling

2.2.1 Sample preparation

Raw EBN powder and EBN water extract powder were prepared using a part of the procedures from our previous study [13]. Briefly, raw EBN was cleaned and grounded

into fine powder. For the preparation of water extract powder, raw EBN was soaked in cold distilled water for 48 hours followed by boiling at 100°C for 30 minutes. The solution mixture was filtered and freeze-dried to obtain the powder.

2.2.2 In-solution tryptic digestion

One milligram of powder from raw and water extract of EBN was re-suspended with 25 µL of 100 mM ammonium bicarbonate, 25 µL of trifluoroethanol and 1 µL of 200 mM DTT. The mixture was heated at 60˚C for 1 hour. Then, alkylation of sample was achieved by adding 4 µL of IAM to the mixture and incubated in dark for 1 hour at room temperature. Excess IAM was quenched by addition of 1 µL of DTT and further incubated in dark for 1 hour at room temperature. Later, 300 µL of water and 100 µL of ammonium bicarbonate were added, whereby the pH was adjusted to between 7 and 9. About 1 µg of trypsin was subsequently added to the solution for digestion to occur overnight at 37˚C. Finally, 1 µL of formic acid was added to reduce the pH to below 4 in order to halt the digestion process. Samples were vacuum-dried to remove excess solvent in the solution and kept at -20˚C prior to analysis.

2.2.3 Nanoflow liquid chromatography-electrospray ionization-tandem mass spectrometry (Nanoflow LC-ESI-MS/MS)

Digested peptides were loaded into Agilent C18 300 Å Large Capacity Chip (Agilent, Santa Clara, CA, USA) column for liquid chromatography. Sample elution was performed by running a binary gradient system consists of solution A (0.1% formic acid in water) and solution B (0.1% formic acid in 90% acetonitrile). The column was firstly equilibrated in solution A, then the following gradient was used to run the

entire system: 5%–75% solution B for 30 minutes, 75% solution B for 9 minutes, and 75%–5% solution B for 8 minutes. Coupled with the liquid chromatography system was Quadrupole-time of flight (Q-TOF) (Agilent QTOF 6550B iFunnel Accurate Mass) mass spectrometer with ESI nanospray ionization source (Agilent ChipCube). The sample was analyzed in positive ionization mode. Capillary voltage was set to 2050 V while fragmentor voltage was set at 500 V. Auto MS mode was applied to scan peptide spectrum from 110–3000 *m*/*z* for MS scan and 50–3000 *m*/*z* for MS/MS scan.

2.2.4 Protein identification by de novo sequencing software PEAKS Studio 7.0

The spectra were then analyzed with Agilent MassHunter (Agilent Technologies, Santa Clara, CA, USA) and PEAKS Studio 7.0 software (Bioinformatics Slutions Inc., Waterloo, ON, Canada) for *de novo* sequencing. Homology search was conducted by comparing *de novo* sequence tag against Swiss-Prot protein database (Taxonomy: Aves, accessed in March 2017). Trypsin was specified as the digestion enzyme with maximum missed cleavages at 3. Error tolerance for both parent mass and fragment mass was 0.1 Da whereas precursor mass search type was set to monoisotopic. Inaccurate proteins were filtered out from the results by setting the false discovery rate (FDR) at 1%, number of unique peptide ≥1 and -10lgP score ≥20.

2.2.5 Basic Local Alignment Search Tool (BLAST)

BLAST is a bioinformatics tool used to compare a primary biological sequence data to a library of sequences with known identity in order to name the query sequence. Sequence of unidentified protein obtained from PEAKS Studio 7.0 software was

submitted to BLAST whereby the algorithm generated a list of possible match together with statistical information. The match with highest score was selected and the unidentified protein (query sequence) was named.

2.3 Antioxidant studies

2.3.1 Sample preparation

Following the protocol in our previous study, pancreatin-digested raw powder and water extract of EBN were prepared and denoted as S1 and S2, respectively [13].

2.3.2 DPPH radical scavenging activity

The DPPH radical scavenging activities of S1 and S2 were measured using the method described by Zhang et al. with slight modifications [22]. One hundred microliters of the EBN extracts was added to 100µl of DPPH (0.3 mM) methanolic solution in a 96-well plate. The plate was incubated in dark for 30 min at room temperature and absorbance reading was then taken at 490 nm using a microplate reader (DynexOpsys MR 24100, USA). DMSO added with DPPH solution was used as control while vitamin C was used as positive control. DPPH radical scavenging activity was calculated using the following formula:

$$\text{DPPH radical scavenging activity (\%)} = \frac{\text{Absorbance of control} - \text{Absorbance of sample}}{\text{Absorbance of control}} \times 100$$

2.3.3 Ferric ion reducing antioxidant power (FRAP) assay

Reducing activities of S1 and S2 were assessed according to the FRAP method of Benzie and Strain with some modifications [23]. Working FRAP reagent was

prepared with 300 mM acetate buffer (at pH 3.6), 10 mM TPTZ solution in 40 mM HCl and 20 mM $FeCl_3$ solution, all mixed in a proportion of 10 : 1 : 1 (v/v/v). Ten microliters of the extracts was mixed with 190µl of freshly prepared FRAP reagent. The mixture was incubated at 37°C for 30 minutes after which the absorbance was read with a microplate reader (Tecan, Austria) at 595nm against blank. Vitamin C was used as positive control. The percentage of FRAP activity was calculated using the following equation:

$$\text{FRAP activity (\%)} = \frac{\text{Absorbance of sample} - \text{Absorbance of control}}{\text{Absorbance of control}} \times 100$$

2.3.4 *Metal chelating activity*

The ferrous ion chelating activity was performed by the method of Decker and Welch (24). A mixture of sample solution (0.1 ml), distilled water (0.1 ml) and 0.5 mM $FeCl_2$ (0.025 ml) was prepared. Then, 2.5 mM ferrozine (0.025 ml) was added into the mixture and incubated for 20 min at room temperature. The absorbance was measured with microplate reader (Tecan, Austria). EDTA was used as the positive control. The metal chelating activity was calculated using the following formula:

$$\text{Ferrous ion chelating activity (\%)} = \frac{\text{Absorbance of control} - \text{Absorbance of sample}}{\text{Absorbance of control}} \times 100$$

2.3.5 *Statistical analysis*

Data was presented as mean ± standard deviation of three independent experiments. Statistical analysis is performed with Student's *t*-test and a value of $P<0.05$ is considered significant.

3. *Results and discussion*

3.1 Proteomic analysis of EBN extracts

Proteomes of raw powder and water extract of EBN were identified using BLAST and PEAKS *de novo* sequencing software. Comparing to other database search tools available in the market such as Mascot and SEQUEST, PEAKS software offers faster peptide identification by *de novo* sequencing-assisted database search and generates results with higher sensitivity and higher accuracy. Results can be robustly validated via novel decoy fusion method using this technology hence provides greater confidence for proteomic analysis [22]. Proteins detected in the in-solution digests of raw powder and water extract of EBN were enlisted in Table 1 and Table 2, respectively. The complete list of peptide sequences and *m/z* values of these proteins were included in Supplementary File 1 and 2.

Generally, there were 17 different proteins identified in raw EBN powder and 22 different proteins found in water extract of EBN. However, both samples shared a total of 10 proteins in common. Our analysis denotes that there were 7 proteins remained distinctive to raw powder of EBN and 12 proteins unique to water extract of EBN. The proteins identified from both samples were illustrated in Fig.1.

Table 1. List of proteins detected in the in-solution digests of raw EBN.

Accession	-10lgP	Coverage (%)	No. of peptides	No. of unique peptides	Species	Average Mass	Description
tr|H0ZGY9|H0ZGY9_TAEGU	261	15	22	5	*Taeniopygia guttata*	189702	Mucin-5AC
tr|R7VT28|R7VT28_COLLI	232.41	15	21	3	*Columba livia*	181804	Mucin-5AC
tr|A0A0Q3U2A7|A0A0Q3U2A7_AMAAE	219.72	16	21	5	*Amazona aestiva*	152296	Hypothetical protein AAES_08852
tr|R0LBT0|R0LBT0_ANAPL	206.23	12	13	1	*Anas platyrhynchos*	163068	Mucin-5AC
tr|U3IV20|U3IV20_ANAPL	206.23	10	13	1	*Anas platyrhynchos*	199376	Mucin-5AC
tr|A0A1D5NVH7|A0A1D5NVH7_CHICK	202.37	11	17	2	*Gallus gallus*	231689	Mucin-5AC
tr|A0A093BIT2|A0A093BIT2_CHAPE	195.15	26	11	2	*Chaetura pelagica*	58700	Lysyl oxidase 3

tr|H0ZGZ6|H0ZGZ6_TAEGU	189.68	13	11	1	*Taeniopygia guttata*	90992	Mucin-5AC
tr|A0A093GK45|A0A093GK45_PICPB	175.02	14	7	2	*Picoides pubescens*	71711	Lysyl oxidase 3
tr|A0A093GFU4|A0A093GFU4_PICPB	147.23	24	6	1	*Picoides pubescens*	36488	Mucin-5AC
tr|A0A0Q3SEH9|A0A0Q3SEH9_AMAAE	116.95	3	5	2	*Amazona aestiva*	179462	Hypothetical protein AAES_28655
tr|U3KBI8|U3KBI8_FICAL	112.44	12	9	4	*Ficedula albicollis*	98051	Mucin-5AC isoform X2
tr|A0A091TEI1|A0A091TEI1_NESNO	103.76	7	4	3	*Nestor notabilis*	49822	Acidic mammalian chitinase
tr|A0A093BFV9|A0A093BFV9_CHAPE	101.15	12	4	2	*Chaetura pelagica*	39104	Acidic mammalian chitinase
tr|A0A091NM19|A0A091NM19_APAVI	100.84	4	3	3	*Apaloderma vittatum*	42841	Ovoinhibitor
tr|A0A093PIM5|A0A093PIM5_9PASS	98.74	10	5	1	*Manacus*	51174	Acidic mammalian chitinase

					vitellinus		
tr|A0A093JL69|A0A093JL69_STRCA	96.3	14	2	2	*Struthio camelus australis*	39259	45 kDa calcium-binding protein
tr|A0A093GZT0|A0A093GZT0_PICPB	96.3	14	2	2	*Picoides pubescens*	39088	45 kDa calcium-binding protein
tr|A0A091JRH3|A0A091JRH3_9AVES	96.3	14	2	2	*Egretta garzetta*	39054	45 kDa calcium-binding protein
tr|A0A093Q7F3|A0A093Q7F3_9PASS	96.3	14	2	2	*Manacus vitellinus*	39143	45 kDa calcium-binding protein
tr|A0A091I517|A0A091I517_CALAN	91.5	10	6	1	*Calypte anna*	78127	Hypothetical protein N300_06305
tr|A0A1D5PU28|A0A1D5PU28_CHICK	89	6	6	1	*Gallus gallus*	116475	Mucin-5AC
tr|A0A093F6E7|A0A093F6E7_TYTAL	87.43	15	4	1	*Tyto alba*	50789	Acidic mammalian chitinase
tr|A0A0Q3XB34|A0A0Q3XB34_AMAAE	82.59	5	2	1	*Amazona aestiva*	59745	Lysyl oxidase 3
tr|H0ZGX3|H0ZGX3_TAEGU	81.97	8	5	1	*Taeniopygia guttata*	79286	Mucin-5AC

tr|H0ZGW8|H0ZGW8_TAEGU	81.97	7	5	1	*Taeniopygia guttata*	80117	Mucin-5AC
tr|A0A091T9Y4|A0A091T9Y4_PHALP	81.49	11	5	1	*Phaethon lepturus*	78470	Mucin-5AC
tr|G1N931|G1N931_MELGA	80.93	4	7	2	*Meleagris gallopavo*	109955	Mucin-5AC
tr|A0A091T2D6|A0A091T2D6_9AVES	75.43	10	5	1	*Pelecanus crispus*	79070	Hypothetical protein N334_09374
tr|A0A093IYD2|A0A093IYD2_PICPB	61.4	6	2	1	*Picoides pubescens*	42067	Acidic mammalian chitinase
tr|H0ZM61|H0ZM61_TAEGU	53.88	7	4	4	*Taeniopygia guttata*	44824	Deleted in malignant brain tumors 1 protein
tr|A0A094MEI7|A0A094MEI7_ANTCR	46.99	9	1	1	*Antrostomus carolinensis*	43161	Ovoinhibitor
tr|A0A091M1K5|A0A091M1K5_CARIC	44.09	4	1	1	*Cariama cristata*	31834	Neuropilin and tolloid-like 1
tr|A0A1D5PQM2|A0A1D5PQM2_CHICK	44.09	4	1	1	*Gallus gallus*	36683	Neuropilin and tolloid-like protein 1 isoform X2

tr|A0A093FGT3|A0A093FGT3_TYTAL	44.09	3	1	1	*Tyto alba*	50062	Neuropilin and tolloid-like 1
tr|A0A087QND6|A0A087QND6_APTFO	44.09	3	1	1	*Aptenodytes forsteri*	52244	Neuropilin and tolloid-like 1
tr|R0LMR2|R0LMR2_ANAPL	44.09	2	1	1	*Anas platyrhynchos*	55432	Neuropilin and tolloid-like protein 1
tr|A0A091JZC9|A0A091JZC9_COLST	44.09	2	1	1	*Colius striatus*	57640	Neuropilin and tolloid-like 1
tr|A0A093FW41|A0A093FW41_GAVST	44.09	2	1	1	*Gavia stellata*	59478	Neuropilin and tolloid-like 1
tr|A0A091SKD1|A0A091SKD1_9GRUI	44.09	2	1	1	*Mesitornis unicolor*	59464	Neuropilin and tolloid-like 1
tr|A0A099Z9Q6|A0A099Z9Q6_TINGU	44.09	2	1	1	*Tinamus guttatus*	59478	Neuropilin and tolloid-like 1
tr|A0A091ICA8|A0A091ICA8_CALAN	44.09	2	1	1	*Calypte anna*	59492	Neuropilin and tolloid-like 1
tr|A0A091JE74|A0A091JE74_9AVES	44.09	2	1	1	*Egretta garzetta*	59431	Neuropilin and tolloid-like 1
tr|A0A0A0ARN5|A0A0A0ARN5_CHAVO	44.09	2	1	1	*Charadrius vociferus*	59438	Neuropilin and tolloid-like 1

tr|A0A093GYX1|A0A093GYX1_PICPB	44.09	2	1	1	*Picoides pubescens*	59384	Neuropilin and tolloid-like 1
tr|A0A093IPZ4|A0A093IPZ4_EURHL	44.09	2	1	1	*Eurypyga helias*	59428	Neuropilin and tolloid-like 1
tr|A0A091F3F2|A0A091F3F2_CORBR	44.09	2	1	1	*Corvus brachyrhynchos*	59520	Neuropilin and tolloid-like 1
tr|A0A093QEM7|A0A093QEM7_9PASS	44.09	2	1	1	*Manacus vitellinus*	59502	Neuropilin and tolloid-like 1
tr|H0ZFW8|H0ZFW8_TAEGU	44.09	2	1	1	*Taeniopygia guttata*	59619	Neuropilin and tolloid-like 1
tr|A0A093BGU1|A0A093BGU1_CHAPE	44.09	2	1	1	*Chaetura pelagica*	59483	Neuropilin and tolloid-like 1
tr|A0A091WRF1|A0A091WRF1_NIPNI	44.09	2	1	1	*Nipponia nippon*	59454	Neuropilin and tolloid-like 1
tr|A0A091WHV3|A0A091WHV3_OPIHO	44.09	2	1	1	*Opisthocomus hoazin*	59532	Neuropilin and tolloid-like 1
tr|A0A093HHJ2|A0A093HHJ2_STRCA	44.09	2	1	1	*Struthio camelus*	59432	Neuropilin and tolloid-like 1

					australis		
tr|A0A093NAE4|A0A093NAE4_PYGAD	44.09	2	1	1	*Pygoscelis adeliae*	59470	Neuropilin and tolloid-like 1
tr|A0A091TLD0|A0A091TLD0_9AVES	44.09	2	1	1	*Pelecanus crispus*	59326	Neuropilin and tolloid-like 1
tr|A0A091Q239|A0A091Q239_LEPDC	44.09	2	1	1	*Leptosomus discolor*	59355	Neuropilin and tolloid-like 1
tr|A0A091G4C9|A0A091G4C9_9AVES	44.09	2	1	1	*Cuculus canorus*	59396	Neuropilin and tolloid-like 1
tr|U3IQM0|U3IQM0_ANAPL	44.09	2	1	1	*Anas platyrhynchos*	60721	Neuropilin and tolloid-like protein 1 isoform X1
tr|G1N880|G1N880_MELGA	44.09	2	1	1	*Meleagris gallopavo*	60497	Neuropilin and tolloid-like 1
tr|A0A0Q3TPW3|A0A0Q3TPW3_AMAAE	44.09	2	1	1	*Amazona aestiva*	60357	Neuropilin and tolloid-like protein 1
tr|A0A091V887|A0A091V887_NIPNI	38.89	3	1	1	*Nipponia nippon*	43299	Ovoinhibitor
tr|A0A093BE17|A0A093BE17_CHAPE	37.4	19	1	1	*Chaetura pelagica*	13232	Deleted in malignant brain tumors 1 protein

tr|U3JHL5|U3JHL5_FICAL	33.66	3	1	1	*Ficedula albicollis*	72151	78 kDa glucose-regulated protein
tr|H0ZAB3|H0ZAB3_TAEGU	33.66	3	1	1	*Taeniopygia guttata*	72050	78 kDa glucose-regulated protein
tr|A0PA15|A0PA15_COTJA	33.66	3	1	1	*Coturnix coturnix japonica*	72019	Heat shock protein 70kDa
tr|A0ZT13|A0ZT13_COTJA	33.66	3	1	1	*Coturnix coturnix japonica*	71991	Heat shock protein 70kDa
tr|A0A091F8D2|A0A091F8D2_CORBR	33.66	3	1	1	*Corvus brachyrhynchos*	71909	78 kDa glucose-regulated protein
tr|A0A091KV08|A0A091KV08_9GRUI	33.66	3	1	1	*Chlamydotis macqueenii*	68613	78 kDa glucose-regulated protein
tr|A0A093QLZ7|A0A093QLZ7_9PASS	33.66	3	1	1	*Manacus vitellinus*	67732	78 kDa glucose-regulated protein
tr|U3I640|U3I640_ANAPL	33.66	3	1	1	*Anas*	67780	78 kDa glucose-regulated protein

					platyrhynchos		
tr|A0A091V9R8|A0A091V9R8_OPIHO	33.66	3	1	1	*Opisthocomus hoazin*	67776	78 kDa glucose-regulated protein
tr|A0A091VTR8|A0A091VTR8_NIPNI	33.66	3	1	1	*Nipponia nippon*	67746	78 kDa glucose-regulated protein
tr|A0A091HVD4|A0A091HVD4_CALAN	33.66	3	1	1	*Calypte anna*	67718	78 kDa glucose-regulated protein
tr|A0A087R4J8|A0A087R4J8_APTFO	33.66	3	1	1	*Aptenodytes forsteri*	67774	78 kDa glucose-regulated protein
tr|A0A093J3B2|A0A093J3B2_PICPB	33.66	3	1	1	*Picoides pubescens*	67732	78 kDa glucose-regulated protein
tr|A0A093EHT4|A0A093EHT4_TYTAL	33.66	3	1	1	*Tyto alba*	67746	78 kDa glucose-regulated protein
tr|A0A091LT36|A0A091LT36_CARIC	33.66	3	1	1	*Cariama cristata*	67774	78 kDa glucose-regulated protein
tr|A0A091H8K7|A0A091H8K7_9AVES	33.66	3	1	1	*Cuculus canorus*	67732	78 kDa glucose-regulated protein
tr|A0A093CJ49|A0A093CJ49_9AVES	33.66	3	1	1	*Pterocles gutturalis*	67788	78 kDa glucose-regulated protein

tr|A0A093HUL5|A0A093HUL5_STRCA	33.66	3	1	1	*Struthio camelus australis*	67746	78 kDa glucose-regulated protein
tr|A0A091MLL1|A0A091MLL1_9PASS	33.66	3	1	1	*Acanthisitta chloris*	67716	78 kDa glucose-regulated protein
tr|A0A091U752|A0A091U752_PHORB	33.66	3	1	1	*Phoenicopterus ruber ruber*	66560	78 kDa glucose-regulated protein
tr|A0A093J4G2|A0A093J4G2_EURHL	33.66	3	1	1	*Eurypyga helias*	66264	78 kDa glucose-regulated protein
tr|G1N8R5|G1N8R5_MELGA	33.66	4	1	1	*Meleagris gallopavo*	47391	78 kDa glucose-regulated protein
tr|A0A091N6E4|A0A091N6E4_9PASS	33.65	4	1	1	*Acanthisitta chloris*	42887	Ovoinhibitor
tr|A0A093TKC6|A0A093TKC6_PHACA	27.89	2	1	1	*Phalacrocorax carbo*	53236	Nucleobindin-2
tr|U3ISH1|U3ISH1_ANAPL	27.89	2	1	1	*Anas platyrhynchos*	47808	Nucleobindin-2

tr|A0A093GVR1|A0A093GVR1_PICPB	27.89	2	1	1	*Picoides pubescens*	51832	Nucleobindin-2
tr|A0A093IF41|A0A093IF41_FULGA	27.89	2	1	1	*Fulmarus glacialis*	52658	Nucleobindin-2
tr|A0A091TQN7|A0A091TQN7_PHALP	27.89	2	1	1	*Phaethon lepturus*	52676	Nucleobindin-2
tr|A0A091SAC3|A0A091SAC3_NESNO	27.89	2	1	1	*Nestor notabilis*	52864	Nucleobindin-2
tr|A0A091HNJ7|A0A091HNJ7_CALAN	27.89	2	1	1	*Calypte anna*	53387	Nucleobindin-2
tr|A0A091PFA1|A0A091PFA1_LEPDC	27.89	2	1	1	*Leptosomus discolor*	53645	Nucleobindin-2
tr|A0A0A0AZD6|A0A0A0AZD6_CHAVO	27.89	2	1	1	*Charadrius vociferus*	53503	Nucleobindin-2
tr|A0A091HJ71|A0A091HJ71_BUCRH	27.89	2	1	1	*Buceros rhinoceros silvestris*	53606	Nucleobindin-2
tr|F1NGB1|F1NGB1_CHICK	27.89	2	1	1	*Gallus gallus*	53838	Nucleobindin-2 isoform X1

tr|A0A091VMW6|A0A091VMW6_NIPNI	27.89	2	1	1	*Nipponia nippon*	53521	Nucleobindin-2
tr|A0A094KJ55|A0A094KJ55_ANTCR	27.89	2	1	1	*Antrostomus carolinensis*	53475	Nucleobindin-2
tr|A0A094L6H8|A0A094L6H8_9AVES	27.89	2	1	1	*Podiceps cristatus*	53577	Nucleobindin-2
tr|A0A093PSK0|A0A093PSK0_9PASS	27.89	2	1	1	*Manacus vitellinus*	53604	Nucleobindin-2
tr|H0ZEB8|H0ZEB8_TAEGU	27.89	2	1	1	*Taeniopygia guttata*	53497	Nucleobindin-2
tr|A0A091ED95|A0A091ED95_CORBR	27.89	2	1	1	*Corvus brachyrhynchos*	53595	Nucleobindin-2
tr|Q5ZHR1|Q5ZHR1_CHICK	27.89	2	1	1	*Gallus gallus*	53766	Nucleobindin-2 precursor
tr|A0A091L2T7|A0A091L2T7_9GRUI	27.89	2	1	1	*Chlamydotis macqueenii*	53765	Nucleobindin-2
tr|A0A093CUP2|A0A093CUP2_9AVES	27.89	2	1	1	*Pterocles gutturalis*	53634	Nucleobindin-2

tr|A0A091GCH4|A0A091GCH4_9AVES	27.89	2	1	1	*Cuculus canorus*	53605	Nucleobindin-2
tr|A0A093JDZ9|A0A093JDZ9_EURHL	27.89	2	1	1	*Eurypyga helias*	53591	Nucleobindin-2
tr|A0A087RK71|A0A087RK71_APTFO	27.89	2	1	1	*Aptenodytes forsteri*	53598	Nucleobindin-2
tr|R0LG94|R0LG94_ANAPL	27.89	2	1	1	*Anas platyrhynchos*	53663	Nucleobindin-2
tr|A0A091U6D8|A0A091U6D8_PHORB	27.89	2	1	1	*Phoenicopterus ruber ruber*	53912	Nucleobindin-2
tr|A0A093HG29|A0A093HG29_STRCA	27.89	2	1	1	*Struthio camelus australis*	53808	Nucleobindin-2
tr|A0A091IWJ1|A0A091IWJ1_9AVES	27.89	2	1	1	*Egretta garzetta*	53809	Nucleobindin-2
tr|G1N538|G1N538_MELGA	27.89	2	1	1	*Meleagris gallopavo*	54331	Nucleobindin-2
tr|U3JDE6|U3JDE6_FICAL	27.89	2	1	1	*Ficedula albicollis*	55246	Nucleobindin-2

tr|A0A0Q3X4D7|A0A0Q3X4D7_AMAAE	27.89	2	1	1	*Amazona aestiva*	58323	Nucleobindin-2
tr|A0A093QEZ4|A0A093QEZ4_9PASS	27.48	2	1	1	*Manacus vitellinus*	43373	Ovoinhibitor
tr|A0A0A0AR29|A0A0A0AR29_CHAVO	25.33	2	1	1	*Charadrius vociferus*	43584	RGM domain family member B
tr|A0A091U916|A0A091U916_PHORB	24.95	5	1	1	*Phoenicopterus ruber ruber*	33229	Calcineurin-like phosphoesterase domain-containing protein 1
tr|A0A091XAE4|A0A091XAE4_OPIHO	23.28	1	1	1	*Opisthocomus hoazin*	76026	Zona pellucida sperm-binding protein 2
tr|F1NNU1|F1NNU1_CHICK	23.28	1	1	1	*Gallus gallus*	77034	Zona pellucida sperm-binding protein 2
tr|Q2PGY2|Q2PGY2_CHICK	23.28	1	1	1	*Gallus gallus*	76971	Zona pellucida A
tr|Q5CZI6|Q5CZI6_CHICK	23.28	1	1	1	*Gallus gallus*	81004	Zona pellucida protein
tr|A0A091P1K5|A0A091P1K5_HALAL	23.04	0	1	1	*Haliaeetus albicilla*	305533	Lysosomal-trafficking regulator

tr|U3KGE0|U3KGE0_FICAL	23.04	0	1	1	*Ficedula albicollis*	426102	Lysosomal-trafficking regulator
tr|A0A1D5NWU9|A0A1D5NWU9_CHICK	23.04	0	1	1	*Gallus gallus*	209640	Lysosomal-trafficking regulator
tr|A0A093FWF9|A0A093FWF9_PICPB	23.04	0	1	1	*Picoides pubescens*	302584	Lysosomal-trafficking regulator
tr|A0A091LIV9|A0A091LIV9_CATAU	23.04	0	1	1	*Cathartes aura*	305521	Lysosomal-trafficking regulator
tr|A0A093F2B5|A0A093F2B5_TYTAL	23.04	0	1	1	*Tyto alba*	305446	Lysosomal-trafficking regulator
tr|A0A091W1W3|A0A091W1W3_OPIHO	23.04	0	1	1	*Opisthocomus hoazin*	305922	Lysosomal-trafficking regulator
tr|A0A087R6Y7|A0A087R6Y7_APTFO	23.04	0	1	1	*Aptenodytes forsteri*	305665	Lysosomal-trafficking regulator
tr|A0A091PAF4|A0A091PAF4_LEPDC	23.04	0	1	1	*Leptosomus discolor*	305166	Lysosomal-trafficking regulator
tr|A0A093LET3|A0A093LET3_FULGA	23.04	0	1	1	*Fulmarus glacialis*	305370	Lysosomal-trafficking regulator

tr|A0A0A0AJN3|A0A0A0AJN3_CHAVO	23.04	0	1	1	*Charadrius vociferus*	305535	Lysosomal-trafficking regulator
tr|A0A091T8Q1|A0A091T8Q1_PHALP	23.04	0	1	1	*Phaethon lepturus*	305667	Lysosomal-trafficking regulator
tr|A0A091VSX4|A0A091VSX4_NIPNI	23.04	0	1	1	*Nipponia nippon*	305563	Lysosomal-trafficking regulator
tr|A0A091SJ61|A0A091SJ61_9AVES	23.04	0	1	1	*Pelecanus crispus*	305929	Lysosomal-trafficking regulator
tr|A0A093P913|A0A093P913_PYGAD	23.04	0	1	1	*Pygoscelis adeliae*	305782	Lysosomal-trafficking regulator
tr|A0A091MNM3|A0A091MNM3_9PASS	23.04	0	1	1	*Acanthisitta chloris*	305942	Lysosomal-trafficking regulator
tr|A0A091RFP2|A0A091RFP2_MERNU	23.04	0	1	1	*Merops nubicus*	306438	Lysosomal-trafficking regulator
tr|A0A0Q3PLA9|A0A0Q3PLA9_AMAAE	23.04	0	1	1	*Amazona aestiva*	421546	Lysosomal-trafficking regulator
tr|A0A1D5PA68|A0A1D5PA68_CHICK	23.04	0	1	1	*Gallus gallus*	427282	Lysosomal-trafficking regulator
tr|R0JM22|R0JM22_ANAPL	23.04	0	1	1	*Anas platyrhynchos*	427406	Lysosomal-trafficking regulator

Table 2. List of proteins detected in the in-solution digests of water extract of EBN.

Accession	-10lgP	Coverage (%)	No. of peptides	No. of unique peptides	Species	Average Mass	Description
tr|H0ZGY9|H0ZGY9_TAEGU	194.5	11	16	6	*Taeniopygia guttata*	189702	Mucin-5AC
tr|R7VT28|R7VT28_COLLI	185.6	11	13	2	*Columba livia*	181804	Mucin-5AC
tr|A0A0A0B371|A0A0A0B371_CHAVO	171.18	16	7	4	*Charadrius vociferus*	54003	Lysyl oxidase 3
tr|A0A0Q3U2A7|A0A0Q3U2A7_AMAAE	157.91	9	10	1	*Amazona aestiva*	152296	Mucin-5AC
tr|A0A093F6E7|A0A093F6E7_TYTAL	145.12	25	11	1	*Tyto alba*	50789	Acidic mammalian chitinase
tr|H0ZGZ6|H0ZGZ6_TAEGU	135.48	10	7	2	*Taeniopygia guttata*	90992	Mucin-5AC
tr|A0A0A0AQX5|A0A0A0AQX5_CHAVO	126.09	13	8	1	*Charadrius vociferus*	50549	Acidic mammalian chitinase
tr|A0A093BIT2|A0A093BIT2_CHAPE	123.98	14	5	2	*Chaetura pelagica*	58700	Lysyl oxidase 3

tr|A0A093BFV9|A0A093BFV9_CHAPE	122.89	23	9	2	*Chaetura pelagica*	39104	Acidic mammalian chitinase
tr|A0A091TEI1|A0A091TEI1_NESNO	114.56	9	5	2	*Nestor notabilis*	49822	Acidic mammalian chitinase
tr|A0A091NM19|A0A091NM19_APAVI	103.89	10	4	4	*Apaloderma vittatum*	42841	Ovoinhibitor
tr|A0A093GK45|A0A093GK45_PICPB	86.46	6	3	1	*Picoides pubescens*	71711	Lysyl oxidase 3
tr|A0A1D5PU28|A0A1D5PU28_CHICK	82.16	6	5	1	*Gallus gallus*	116475	Mucin-5AC
tr|H0ZGX3|H0ZGX3_TAEGU	77.91	8	4	2	*Taeniopygia guttata*	79286	Mucin-5AC
tr|H0ZGW8|H0ZGW8_TAEGU	77.91	7	4	2	*Taeniopygia guttata*	80117	Mucin-5AC
tr|A0A091I517|A0A091I517_CALAN	75.37	6	3	1	*Calypte anna*	78127	Hypothetical protein N300_06305
tr|A0A091JRH3|A0A091JRH3_9AVES	71.1	8	1	1	*Egretta garzetta*	39054	45 kDa calcium-binding protein
tr|A0A091TMS0|A0A091TMS0_PHALP	71.1	8	1	1	*Phaethon lepturus*	39171	45 kDa calcium-binding protein
tr|A0A091NEX0|A0A091NEX0_APAVI	71.1	8	1	1	*Apaloderma vittatum*	39148	45 kDa calcium-binding protein
tr|A0A091PAL6|A0A091PAL6_LEPDC	71.1	8	1	1	*Leptosomus*	39171	45 kDa calcium-binding protein

					discolor		
tr|A0A093C625|A0A093C625_9AVES	71.1	8	1	1	*Pterocles gutturalis*	39129	45 kDa calcium-binding protein
tr|A0A091H4Q9|A0A091H4Q9_BUCRH	71.1	8	1	1	*Buceros rhinoceros silvestris*	39102	45 kDa calcium-binding protein
tr|A0A099Z957|A0A099Z957_TINGU	71.1	8	1	1	*Tinamus guttatus*	39169	45 kDa calcium-binding protein
tr|A0A0A0AQY4|A0A0A0AQY4_CHAVO	71.1	8	1	1	*Charadrius vociferus*	39173	45 kDa calcium-binding protein
tr|A0A091J9Q7|A0A091J9Q7_CALAN	71.1	8	1	1	*Calypte anna*	39519	45 kDa calcium-binding protein
tr|A0A093IV46|A0A093IV46_EURHL	71.1	8	1	1	*Eurypyga helias*	39129	45 kDa calcium-binding protein
tr|A0A091L3N9|A0A091L3N9_CATAU	71.1	8	1	1	*Cathartes aura*	39157	45 kDa calcium-binding protein
tr|A0A091M3R6|A0A091M3R6_CARIC	71.1	8	1	1	*Cariama cristata*	39197	45 kDa calcium-binding protein
tr|A0A091WMT3|A0A091WMT3_OPIHO	71.1	8	1	1	*Opisthocomus hoazin*	39171	45 kDa calcium-binding protein
tr|A0A091UV24|A0A091UV24_NIPNI	71.1	8	1	1	*Nipponia nippon*	39171	45 kDa calcium-binding protein

tr|A0A087VP14|A0A087VP14_BALRE	71.1	8	1	1	*Balearica regulorum gibbericeps*	39171	45 kDa calcium-binding protein
tr|A0A087QSB0|A0A087QSB0_APTFO	71.1	8	1	1	*Aptenodytes forsteri*	39171	45 kDa calcium-binding protein
tr|A0A091N2G3|A0A091N2G3_9PASS	71.1	8	1	1	*Acanthisitta chloris*	39103	45 kDa calcium-binding protein
tr|A0A093P6L7|A0A093P6L7_PYGAD	71.1	8	1	1	*Pygoscelis adeliae*	39171	45 kDa calcium-binding protein
tr|A0A091S825|A0A091S825_MERNU	71.1	8	1	1	*Merops nubicus*	39157	45 kDa calcium-binding protein
tr|A0A091FU09|A0A091FU09_9AVES	71.1	8	1	1	*Cuculus canorus*	39173	45 kDa calcium-binding protein
tr|A0A093D128|A0A093D128_TAUER	71.1	8	1	1	*Tauraco erythrolophus*	39143	45 kDa calcium-binding protein
tr|A0A091R7C3|A0A091R7C3_9GRUI	71.1	8	1	1	*Mesitornis unicolor*	39143	45 kDa calcium-binding protein
tr|A0A091KSZ2|A0A091KSZ2_9GRUI	71.1	10	1	1	*Chlamydotis macqueenii*	31583	45 kDa calcium-binding protein
tr|A0A091PRV2|A0A091PRV2_HALAL	71.1	10	1	1	*Haliaeetus albicilla*	31592	45 kDa calcium-binding protein

tr|A0A091UH75|A0A091UH75_PHORB	71.1	11	1	1	*Phoenicopterus ruber ruber*	31038	45 kDa calcium-binding protein
tr|A0A094KP97|A0A094KP97_9AVES	71.1	11	1	1	*Podiceps cristatus*	30812	45 kDa calcium-binding protein
tr|A0A094KKK3|A0A094KKK3_ANTCR	71.1	17	1	1	*Antrostomus carolinensis*	20008	45 kDa calcium-binding protein
tr|A0A093JL69|A0A093JL69_STRCA	71.1	8	1	1	*Struthio camelus australis*	39259	45 kDa calcium-binding protein
tr|A0A093GZT0|A0A093GZT0_PICPB	71.1	8	1	1	*Picoides pubescens*	39088	45 kDa calcium-binding protein
tr|A0A093Q7F3|A0A093Q7F3_9PASS	71.1	8	1	1	*Manacus vitellinus*	39143	45 kDa calcium-binding protein
tr|A0A093IF41|A0A093IF41_FULGA	50.3	6	1	1	*Fulmarus glacialis*	52658	Nucleobindin-2
tr|A0A091FRV3|A0A091FRV3_9AVES	42.29	4	2	1	*Cuculus canorus*	79887	Hypothetical protein N303_00190
tr|H0ZM61|H0ZM61_TAEGU	40.41	8	3	3	*Taeniopygia guttata*	44824	Deleted in malignant brain tumors 1 protein
tr|A0A0Q3XB34|A0A0Q3XB34_AMAAE	39.63	3	1	1	*Amazona aestiva*	59745	Lysyl oxidase 3

tr|A0A091M1K5|A0A091M1K5_CARIC	39.08	4	1	1	*Cariama cristata*	31834	Neuropilin and tolloid-like 1
tr|A0A1D5PQM2|A0A1D5PQM2_CHICK	39.08	4	1	1	*Gallus gallus*	36683	Neuropilin and tolloid-like protein 1 isoform X2
tr|A0A093FGT3|A0A093FGT3_TYTAL	39.08	3	1	1	*Tyto alba*	50062	Neuropilin and tolloid-like 1
tr|A0A087QND6|A0A087QND6_APTFO	39.08	3	1	1	*Aptenodytes forsteri*	52244	Neuropilin and tolloid-like 1
tr|R0LMR2|R0LMR2_ANAPL	39.08	2	1	1	*Anas platyrhynchos*	55432	Neuropilin and tolloid-like 1
tr|A0A091JZC9|A0A091JZC9_COLST	39.08	2	1	1	*Colius striatus*	57640	Neuropilin and tolloid-like 1
tr|A0A091TLD0|A0A091TLD0_9AVES	39.08	2	1	1	*Pelecanus crispus*	59326	Neuropilin and tolloid-like 1
tr|A0A091Q239|A0A091Q239_LEPDC	39.08	2	1	1	*Leptosomus discolor*	59355	Neuropilin and tolloid-like 1
tr|A0A091G4C9|A0A091G4C9_9AVES	39.08	2	1	1	*Cuculus canorus*	59396	Neuropilin and tolloid-like 1
tr|A0A093FW41|A0A093FW41_GAVST	39.08	2	1	1	*Gavia stellata*	59478	Neuropilin and tolloid-like 1
tr|A0A091SKD1|A0A091SKD1_9GRUI	39.08	2	1	1	*Mesitornis unicolor*	59464	Neuropilin and tolloid-like 1
tr|A0A099Z9Q6|A0A099Z9Q6_TINGU	39.08	2	1	1	*Tinamus guttatus*	59478	Neuropilin and tolloid-like 1

tr|A0A091ICA8|A0A091ICA8_CALAN	39.08	2	1	1	*Calypte anna*	59492	Neuropilin and tolloid-like 1
tr|A0A091JE74|A0A091JE74_9AVES	39.08	2	1	1	*Egretta garzetta*	59431	Neuropilin and tolloid-like 1
tr|A0A0A0ARN5|A0A0A0ARN5_CHAVO	39.08	2	1	1	*Charadrius vociferus*	59438	Neuropilin and tolloid-like 1
tr|A0A093GYX1|A0A093GYX1_PICPB	39.08	2	1	1	*Picoides pubescens*	59384	Neuropilin and tolloid-like 1
tr|A0A093IPZ4|A0A093IPZ4_EURHL	39.08	2	1	1	*Eurypyga helias*	59428	Neuropilin and tolloid-like 1
tr|A0A091F3F2|A0A091F3F2_CORBR	39.08	2	1	1	*Corvus brachyrhynchos*	59520	Neuropilin and tolloid-like 1
tr|A0A093QEM7|A0A093QEM7_9PASS	39.08	2	1	1	*Manacus vitellinus*	59502	Neuropilin and tolloid-like 1
tr|H0ZFW8|H0ZFW8_TAEGU	39.08	2	1	1	*Taeniopygia guttata*	59619	Neuropilin and tolloid-like 1
tr|A0A093BGU1|A0A093BGU1_CHAPE	39.08	2	1	1	*Chaetura pelagica*	59483	Neuropilin and tolloid-like 1
tr|A0A091WRF1|A0A091WRF1_NIPNI	39.08	2	1	1	*Nipponia nippon*	59454	Neuropilin and tolloid-like 1
tr|A0A091WHV3|A0A091WHV3_OPIHO	39.08	2	1	1	*Opisthocomus hoazin*	59532	Neuropilin and tolloid-like 1

tr|A0A093HHJ2|A0A093HHJ2_STRCA	39.08	2	1	1	*Struthio camelus australis*	59432	Neuropilin and tolloid-like 1
tr|A0A093NAE4|A0A093NAE4_PYGAD	39.08	2	1	1	*Pygoscelis adeliae*	59470	Neuropilin and tolloid-like 1
tr|U3IQM0|U3IQM0_ANAPL	39.08	2	1	1	*Anas platyrhynchos*	60721	Neuropilin and tolloid-like 1
tr|G1N880|G1N880_MELGA	39.08	2	1	1	*Meleagris gallopavo*	60497	Neuropilin and tolloid-like 1
tr|A0A0Q3TPW3|A0A0Q3TPW3_AMAAE	39.08	2	1	1	*Amazona aestiva*	60357	Neuropilin and tolloid-like 1
tr|A0A091T9Y4|A0A091T9Y4_PHALP	37.52	4	2	1	*Phaethon lepturus*	78470	Hypothetical protein N335_00594
tr|A0A093BE17|A0A093BE17_CHAPE	35.18	7	2	2	*Chaetura pelagica*	13232	Deleted in malignant brain tumors 1 protein
tr|A0A099ZAP5|A0A099ZAP5_TINGU	29.09	3	1	1	*Tinamus guttatus*	67762	78 kDa glucose-regulated protein
tr|H0ZAB3|H0ZAB3_TAEGU	29.09	3	1	1	*Taeniopygia guttata*	72050	78 kDa glucose-regulated protein
tr|A0PA15|A0PA15_COTJA	29.09	3	1	1	*Coturnix coturnix japonica*	72019	Heat shock protein 70kDa

tr|A0ZT13|A0ZT13_COTJA	29.09	3	1	1	*Coturnix coturnix japonica*	71991	Heat shock protein 70kDa
tr|A0A091F8D2|A0A091F8D2_CORBR	29.09	3	1	1	*Corvus brachyrhynchos*	71909	78 kDa glucose-regulated protein
tr|A0A091KV08|A0A091KV08_9GRUI	29.09	3	1	1	*Chlamydotis macqueenii*	68613	78 kDa glucose-regulated protein
tr|A0A093QLZ7|A0A093QLZ7_9PASS	29.09	3	1	1	*Manacus vitellinus*	67732	78 kDa glucose-regulated protein
tr|U3I640|U3I640_ANAPL	29.09	3	1	1	*Anas platyrhynchos*	67780	78 kDa glucose-regulated protein
tr|A0A091V9R8|A0A091V9R8_OPIHO	29.09	3	1	1	*Opisthocomus hoazin*	67776	78 kDa glucose-regulated protein
tr|A0A091VTR8|A0A091VTR8_NIPNI	29.09	3	1	1	*Nipponia nippon*	67746	78 kDa glucose-regulated protein
tr|A0A091HVD4|A0A091HVD4_CALAN	29.09	3	1	1	*Calypte anna*	67718	78 kDa glucose-regulated protein
tr|A0A087R4J8|A0A087R4J8_APTFO	29.09	3	1	1	*Aptenodytes forsteri*	67774	78 kDa glucose-regulated protein
tr|A0A093J3B2|A0A093J3B2_PICPB	29.09	3	1	1	*Picoides pubescens*	67732	78 kDa glucose-regulated protein

tr|A0A093EHT4|A0A093EHT4_TYTAL	29.09	3	1	1	*Tyto alba*	67746	78 kDa glucose-regulated protein
tr|A0A091LT36|A0A091LT36_CARIC	29.09	3	1	1	*Cariama cristata*	67774	78 kDa glucose-regulated protein
tr|A0A091H8K7|A0A091H8K7_9AVES	29.09	3	1	1	*Cuculus canorus*	67732	78 kDa glucose-regulated protein
tr|A0A093HUL5|A0A093HUL5_STRCA	29.09	3	1	1	*Struthio camelus australis*	67746	78 kDa glucose-regulated protein
tr|A0A091U752|A0A091U752_PHORB	29.09	3	1	1	*Phoenicopterus ruber ruber*	66560	78 kDa glucose-regulated protein
tr|A0A093J4G2|A0A093J4G2_EURHL	29.09	3	1	1	*Eurypyga helias*	66264	78 kDa glucose-regulated protein
tr|G1N8R5|G1N8R5_MELGA	29.09	4	1	1	*Meleagris gallopavo*	47391	78 kDa glucose-regulated protein
tr|U3JPD6|U3JPD6_FICAL	28.15	1	1	1	*Ficedula albicollis*	124301	Collagen alpha-2(V) chain
tr|H0ZL50|H0ZL50_TAEGU	28.15	1	1	1	*Taeniopygia guttata*	140668	Collagen alpha-2(V) chain
tr|G3UP25|G3UP25_MELGA	28.15	3	1	1	*Meleagris gallopavo*	39074	Collagen alpha-2(V) chain

tr|G3URW1|G3URW1_MELGA	28.15	3	1	1	*Meleagris gallopavo*	44832	Collagen alpha-2(V) chain
tr|R7VT76|R7VT76_COLLI	28.15	1	1	1	*Columba livia*	140544	Collagen alpha-2(V) chain
tr|R0LNH9|R0LNH9_ANAPL	28.15	1	1	1	*Anas platyrhynchos*	141375	Collagen alpha-2(V) chain
tr|U3IL67|U3IL67_ANAPL	28.15	1	1	1	*Anas platyrhynchos*	144299	Collagen alpha-2(V) chain
tr|A0A1D5P6W1|A0A1D5P6W1_CHICK	28.15	1	1	1	*Gallus gallus*	144811	Collagen alpha-2(V) chain isoform X3
tr|G1N2W3|G1N2W3_MELGA	28.15	1	1	1	*Meleagris gallopavo*	144727	Collagen alpha-2(V) chain isoform X3
tr|U3IA51|U3IA51_ANAPL	25.63	3	1	1	*Anas platyrhynchos*	48876	Keratin type II cytoskeletal 75
tr|R0J8L6|R0J8L6_ANAPL	25.63	3	1	1	*Anas platyrhynchos*	48905	Keratin type II cytoskeletal 75
tr|H9H0B7|H9H0B7_MELGA	25.63	6	1	1	*Meleagris gallopavo*	24943	Keratin, type II cytoskeletal 4-like
tr|H9H0B6|H9H0B6_MELGA	25.63	4	1	1	*Meleagris gallopavo*	34485	Keratin, type II cytoskeletal 4-like

tr|A0A093GRA7|A0A093GRA7_PICPB	25.63	3	1	1	*Picoides pubescens*	42321	Keratin type II cytoskeletal 75
tr|A0A091MSU7|A0A091MSU7_9PASS	25.63	3	1	1	*Acanthisitta chloris*	48349	Keratin type II cytoskeletal 75
tr|U3JP96|U3JP96_FICAL	25.63	2	1	1	*Ficedula albicollis*	55372	Keratin, type II cytoskeletal 4-like
tr|H0Z0C5|H0Z0C5_TAEGU	25.63	2	1	1	*Taeniopygia guttata*	55346	Keratin, type II cytoskeletal 4-like
tr|U3JP95|U3JP95_FICAL	25.63	2	1	1	*Ficedula albicollis*	57555	Keratin, type II cytoskeletal 4-like
tr|U3IFQ5|U3IFQ5_ANAPL	25.63	2	1	1	*Anas platyrhynchos*	63982	Keratin, type II cytoskeletal 4-like
tr|U3JPW5|U3JPW5_FICAL	25.63	2	1	1	*Ficedula albicollis*	59822	Keratin, type II cytoskeletal cochleal-like
tr|A0A1D5PXD0|A0A1D5PXD0_CHICK	23.68	1	1	1	*Gallus gallus*	63148	Selenocysteine-specific elongation factor isoform X1
tr|A0A091SIR2|A0A091SIR2_9GRUI	21.99	3	1	1	*Mesitornis unicolor*	71034	Hyaluronan mediated motility receptor
tr|A0A093GEW7|A0A093GEW7_PICPB	21.98	1	1	1	*Picoides pubescens*	132444	Fibronectin type III domain-containing protein 3B

tr|A0A091VQQ8|A0A091VQQ8_NIPNI	21.98	1	1	1	*Nipponia nippon*	134669	Fibronectin type III domain-containing protein 3B
tr|A0A091UL69|A0A091UL69_PHALP	21.65	5	1	1	*Phaethon lepturus*	77811	Putative threonine--tRNA ligase 2 cytoplasmic
tr|U3K2X6|U3K2X6_FICAL	21.58	0	1	1	*Ficedula albicollis*	409861	Protein bassoon
tr|A0A091HMJ8|A0A091HMJ8_BUCRH	20.92	0	1	1	*Buceros rhinoceros silvestris*	238446	Integrator complex subunit 1
tr|U3J1Y3|U3J1Y3_ANAPL	20.6	3	1	1	*Anas platyrhynchos*	61955	Protein lin-9 homolog isoform X1
tr|A0A091F4A8|A0A091F4A8_CORBR	20.6	3	1	1	*Corvus brachyrhynchos*	60595	Protein lin-9 (Fragment)
tr|A0A091IE25|A0A091IE25_CALAN	20.6	3	1	1	*Calypte anna*	60626	Protein lin-9 (Fragment)
tr|A0A091MQ05|A0A091MQ05_9PASS	20.6	3	1	1	*Acanthisitta chloris*	60656	Protein lin-9 (Fragment)
tr|H0Z1D7|H0Z1D7_TAEGU	20.6	3	1	1	*Taeniopygia guttata*	60643	Protein lin-9
tr|A0A093EQ52|A0A093EQ52_TYTAL	20.6	3	1	1	*Tyto alba*	60651	Protein lin-9

tr|A0A091H8T7|A0A091H8T7_9AVES	20.6	3	1	1	*Cuculus canorus*	60637	Protein lin-9
tr|A0A091VS37|A0A091VS37_NIPNI	20.6	3	1	1	*Nipponia nippon*	60644	Protein lin-9
tr|A0A093PYF4|A0A093PYF4_9PASS	20.6	3	1	1	*Manacus vitellinus*	60685	Protein lin-9
tr|R0K4G2|R0K4G2_ANAPL	20.6	3	1	1	*Anas platyrhynchos*	59713	Lin-9-like protein
tr|U3KAS0|U3KAS0_FICAL	20.6	3	1	1	*Ficedula albicollis*	56280	Protein lin-9 homolog isoform X2
tr|R7VWM6|R7VWM6_COLLI	20.6	4	1	1	*Columba livia*	51310	Lin-9 like protein
tr|A0A093IZM7|A0A093IZM7_FULGA	20.6	5	1	1	*Fulmarus glacialis*	38692	Protein lin-9
tr|L1J368|L1J368_GUITH	20.37	13	1	1	*Guillardia theta*	14476	Hypothetical protein GUITHDRAFT_110997

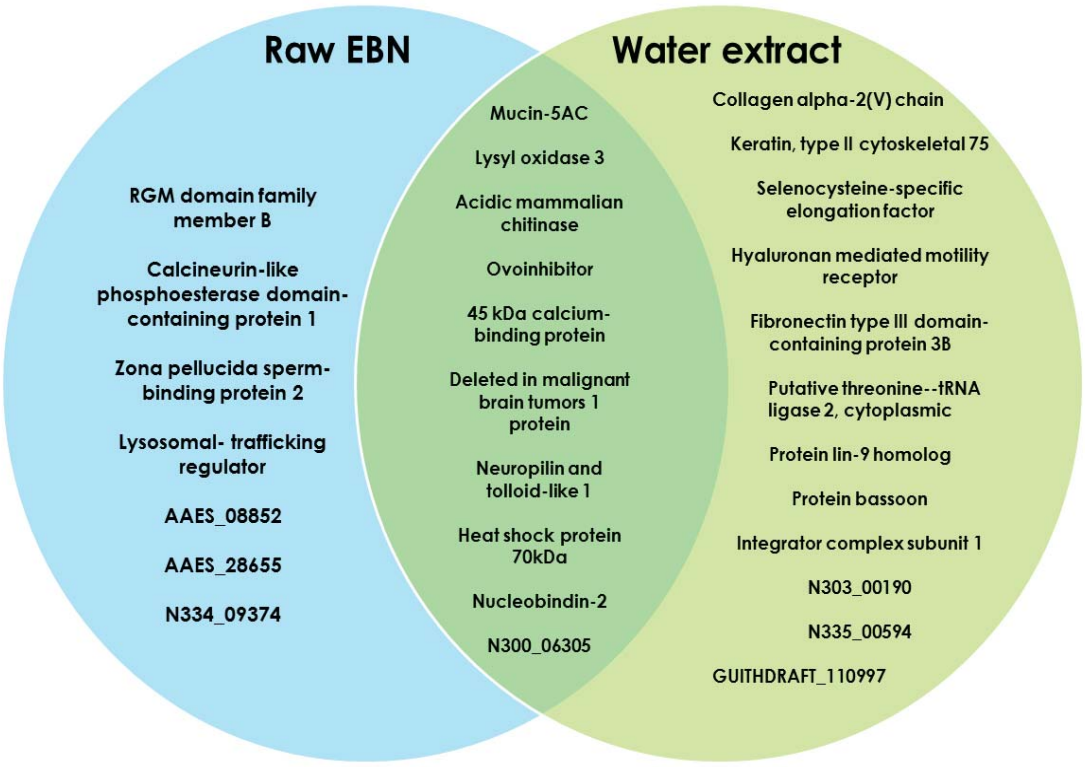

Fig.1. Venn diagram of proteins identified from raw EBN powder and water extract of EBN.

Proteome of EBN was previously studied using ultrasonic and detergent-assisted protein extraction method [6]. In that study, a total of 22 proteins were identified from the peptide mass spectra fingerprint matched against Swiss-Prot protein database, five of which were also recovered in our study, which includes lysyl oxidase 3, acidic mammalian chitinase, 78kDa glucose-regulated protein (or heat shock protein), repulsive guidance molecule (RGM) domain family member B and collagen alpha-2(V) chain. Later, Wong et al. had discovered 6 proteins in EBN, namely acidic mammalian chitinase-like, lysyl oxidase homolog 3, mucin-5AC-like, ovoinhibitor-like, nucleobindin-2 and 45kDa calcium-binding protein, which were also found in our current study [7, 8]. On the other hand, Kong et al. further described the possible presence of NADH dehydrogenase,

immunoglobulin, proline-rich protein, von Willebrand factor and epidermal growth factor domain-containing protein from the insoluble fractions of EBN [25]. The findings in these studies differ from our study probably due to the difference in the analytical methods, plus these proteins were not distinguished based on the extraction method, yet our analyses could complement each other and together give a better picture about the full proteome of EBN.

The full proteome of *Aerodramus fuciphagus* as well as its salivary secretion which forms the EBN are yet to be established. Due to limited protein entries in the database of *Aerodramus fuciphagus* (only 106 proteins, from 2 enzyme classes that are involved in energy metabolism), any study which aims to investigate the complete proteomic profile of EBN remains a challenge. Hence, the current study selected the class of *Aves* (the bird) as the choice of taxonomy filter in Swiss-Prot to enable screening of larger protein database (755,169 entries up to March 2017) for higher protein-peptide match possibility. A reasonable set of result filtration criteria was applied to manage result reliability and practicality, which includes FDR of 1% false discovery rate, number of unique peptide ≥1 and -10lgP score ≥20 [22].

EBN is commonly boiled in water thus is consumed by drinking the water and sometimes together with the softened EBN that appears as glutinous jelly-like strands. We took reference from this practice to carry out a comprehensive protein profiling of EBN by subjecting raw powder and water extract of EBN to direct digestion with trypsin. This "gel-free" approach minimizes sample processing, therefore prevents the issue of poor protein resolution commonly encountered in gel-based protein detection method and recovers proteins that have low abundance and low molecular weight [26]. This approach

has also been credited by Abhyankar et al. to enhance protein detection in insoluble sample, hence is suitable for the analysis of the hardly water-soluble glutinous EBN strand. A total of 20 proteins identified in our study were reported for the very first time in EBN.

Notably, a few proteins in EBN were found to be involved in immunomodulation. Acidic mammalian chitinase is a glycosidase that degrades chitin component on the skin of parasites and insects. It is highly inducible under asthmatic attack via a T helper-2 (Th2)–specific interleukin-13 (IL-13)–mediated pathway [27]. Acidic mammalian chitinase could be highly expressed in salivary gland of swiftlets and secreted into the saliva for digestion of insects. According to Zukefli et al., it possibly contributes to the previously reported virus-binding property of EBN against influenza virus due to its immunomodulatory effect [6]. On the other hand, cases of anaphylaxis after ingestion of EBN have been reported in children. Immunoglobulin E-mediated allergy was later found to be initiated by a putative 66 kDa allergen in EBN with homology to a domain of an ovoinhibitor precursor in chicken, which was also discovered in EBN proteome in the current study [12]. Besides that, the current study also revealed the presence of deleted in malignant brain tumors 1 protein (DMBT1), which belongs to the group of secreted scavenger receptor proteins and serves as part of the mucosal defense system. DMBT1 participates in immune response by binding to pathogen upon stimulation by local inflammatory reaction [28]. Broad bacteria binding spectrum previously reported in salivary variant of DMBT1, is likely to be linked to the effect of EBN in preventing growth of foodborne bacteria [29, 30].

We have also discovered lysyl oxidase 3 homolog and collagen alpha-2(V) chain, which are frequently detected in EBN sample [6, 7]. Lysyl oxidase 3 is a copper-dependent enzyme helps in the formation of cross-links which is essential for stabilization of collagen fibrils and elasticity of elastin [31]. Collagen alpha-2(V) chain is a member of group I collagen and forms the connective tissue in bone and skin. The co-availability of these proteins in EBN supports the claims of improving skin complexion with the consumption of EBN, as well as provides evidence to increased bone strength and dermal thickness seen in EBN-supplemented ovariectomized rats [15].

Proteins involved in neurodevelopment such as RGM domain family member B, neuropilin and tolloid-like 1 and Bassoon were also found in EBN. RGM domain family member B is a co-receptor of bone morphogenetic protein (BMP) with diverse biological roles including bone formation and development of nervous system [32]. It promotes neurite extension and axonal growth through BMP signalling [33]. Neuropilin and tolloid-like 1 found in both raw EBN and water extract of EBN is a transmembrane component of the excitatory ion channel N-methyl-D-aspartate (NMDA) receptor complex in the central nervous system. It is critical for maintaining NMDA receptor-dependent synaptic plasticity hence required for spatial learning and memory consolidation [34]. Meanwhile, Bassoon is a 420 kDa protein highly enriched at presynaptic neurotransmitter release sites and is involved in the organization of synaptic vesicles [35]. The role of Bassoon in glutamate neurotransmission may also be implicated in the study of cognition in Parkinson's disease patient [36, 37]. It was demonstrated previously that EBN effectively inhibited menopause-related cognition decline [38]. The question of whether neuropilin and tolloid-like 1 and protein Bassoon are indeed the proteins in EBN implicated in the

improvement of cognitive function in the study of Hou et al. may be worth exploring in the future.

We also found a few proteins responsible for regulating cell survival and apoptosis from EBN. Heat shock protein (or 78 kDa glucose-regulated protein) found in both raw EBN and its water extracts could be responsible for neuroprotective effect in 6-OHDA-treated neuroblastoma cell model SH-SY5Y in our previous study [13], due to their chaperone role in degradation of misfolded proteins and regulation of apoptotic activity [39-41]. Integrator complex subunit 1 (INTS1) belongs to a multiunit protein called integrator complex which regulates transcription process at the RNA polymerase. The role of INTS1 in sustaining cell growth was consolidated when mutant mouse embryo failed to grow past blastocyst stage and there was induction of caspase 3-mediated apoptosis [42]. INTS1 protein, discovered only in the water extract of EBN, is hypothesized to hinder caspase-3 activation and hence could be cell-protective. This assumption coincides with the observation in our previous study whereby reduced activated-caspase-3 level was seen in 6-OHDA-challenged neuronal cell treated with EBN water extract, suggesting that the mechanism behind neuroprotective effect of EBN water extract is likely INTS1-induced inhibition of caspase-3 activation [13]. In addition to that, latest finding also suggested that INTS1 plays a role in directing neuronal migration because knock-down of integrator complex subunit 1 *in vivo* has been shown to affect cortical neuronal patterning in mouse embryonic brain [43].

EBN was found to contain proteins with known function in cell proliferation and migration including protein lin-9 and hyaluronan mediated motility receptor. Protein lin-9 regulates cell proliferation by activating genes with important functions in mitosis and

cytokinesis [44, 45], which might explain the proliferative feature of EBN-treated human adipose-derived stem cells in a study by Roh et al. [46]. Hyaluronan mediated motility receptor is a protein bound to hyaluronan to coordinate cell migration as well as neurite extension in neuron, hence this suggests EBN might possess neurotrophic effect [47].

The current proteomic analysis also revealed the exclusive presence of selenocysteine-specific elongation factor in water extract of EBN. Selenocysteine-specific elongation factor is an essential mediator in biosynthesis of selenoproteins, one of which includes the antioxidant family known as glutathione peroxidase [48]. It is not surprising that, ROS-reducing effect of EBN water extract in our previous study [13] may be attributed to the presence of selenocysteine-specific elongation factor in EBN, which could have in one way or another strengthened the antioxidant system in the cellular model via effective sequestration of cell-damaging peroxides and other ROS, and prevention of lipid peroxidation to eventually led to neuroprotection [49]. Overall, proteins in EBN may be functional in immunity, extracellular matrix, neurodevelopment, cell survival and apoptosis, cell proliferation and migration, antioxidant and other cellular processes. Critical biological roles of these proteins and possible implication in EBN studies were summarized in Table 3. Seven hypothetical proteins were predicted by the PEAKS Studio 8.0 algorithm in EBN extracts and the sequences were matched with current entries in Swiss-Prot which were yet to be characterized (Table 4). These proteins may be studied in details in the future.

Table 3. Proteins identified in EBN, their biological function and (possible) implication in other EBN studies.

Protein	**Biological function (Annotated in UniProt/SwissProt)**	**(Possible) implication in other EBN studies**
A. Immunity		
Acidic mammalian chitinase	Chitin degradation, Inflammatory response against pathogen	Virus-binding effect against influenza virus by EBN (Zukefli et al., 2017)
Ovoinhibitor	Antiviral	IgE-mediated allergic reaction in children after EBN consumption (Goh et al., 2001b)
Deleted in malignant brain tumors 1 protein	Antiviral, Antibacterial	Growth inhibition by EBN against foodborne bacteria (Saengkrajang and Matan, 2011)
B. Extracellular matrix		
Mucin-5AC	Gel-forming glycoprotein of gastric and respiratory tract epithelia	N/A

Lysyl oxidase 3	Stabilization of collagen fibrils, Elasticity of mature elastin	Increased bone strength and dermal thickness in EBN-supplemented ovariectomized rats (Matsukawa et al., 2011)
Collagen alpha-2(V) chain	Collagen fibril organization, Tissue growth	
Zona pellucida sperm-binding protein 2	Fertilization of oocyte	N/A
Keratin, type II cytoskeletal 75	Hair and nail formation	N/A
Fibronectin type III domain-containing protein 3B	Cytoskeletal support, Cell adhesion, Cell motility, Wound healing	N/A
C. Neurodevelopment		
RGM domain family member B	BMP signaling pathway, Neuronal adhesion	N/A
Neuropilin and tolloid-like 1	Cognition, Neuronal synaptic plasticity	EBN was shown to improve menopause-related cognition decline in rats (Hou et al., 2017)
Protein bassoon	Synaptic neurotransmission	
D. Cell survival and apoptosis		
Heat shock 70 kDa/ 78 kDa	Stress response	N/A

glucose-regulated protein		
Integrator complex subunit 1	Regulates transcription, Prevents apoptosis	N/A
E. Cell proliferation and migration		
Protein lin-9 homolog	Cell cycle, DNA synthesis	N/A
Hyaluronan mediated motility receptor	Cell motility	N/A
F. Antioxidant		
Selenocysteine-specific elongation factor	Selenocysteine incorporation	N/A
G. Cellular process		
45 kDa calcium-binding protein	Exocytosis	N/A
Nucleobindin-2	Calcium homeostasis	N/A
Putative threonine--tRNA ligase 2, cytoplasmic	Nucleotide binding and ligase activity	N/A
Calcineurin-like phosphoesterase domain containing protein 1	Neutrophil degranulation	N/A
Lysosomal-trafficking	Lysosome organization	N/A

regulator		
H. Uncharacterized protein		
AAES_08852	N334_09374	N303_00190
AAES_28655	N300_06305	N335_00594
GUITHDRAFT_110997		

N/A: Not applicable

Table 4. Matched information from Swiss-Prot for uncharacterized EBN proteins predicted by *de novo* sequencing

Protein	**Accesion number**	**Organism**	**Domains**
AAES_08852	A0A0Q3U2A7	*Amazona aestiva*	von Willebrand factor type D (VWFD)
AAES_28655	A0A0Q3SEH9	*Amazona aestiva*	VWFD, von Willebrand factor type C (VWFC)
N334_09374	A0A091T2D6	*Pelecanus crispus*	VWFD, VWFC, C-terminal cystine knot-like domain (CTCK)
N300_06305	A0A091I517	*Calypte anna*	VWFD, VWFC, CTCK
N303_00190	A0A091FRV3	*Cuculus canorus*	VWFD, VWFC, CTCK
N335_00594	A0A091T9Y4	*Phaethon lepturus*	VWFD, VWFC, CTCK
GUITHDRAFT_110997	L1J368	Guillardia theta CCMP2712	N/A

N/A: Not applicable

3.2 Antioxidant activity studies of EBN

3.2.1 Radical scavenging activity

DPPH assay was performed to examine antioxidant capacity of EBN extracts especially in terms of free radical scavenging property. DPPH radical scavenging activity of both EBN extracts S1 and S2 were fluctuating and did not display a dose-dependent trend (Fig.2A). However, it is note-worthy that between the two EBN extracts, S1 displayed higher overall DPPH radical scavenging activity than S2. Particularly, S1 recorded highest activity of 16.70% at 0.0625 mg/ml whilst S2 only achieved comparable results (12.21%) at 4 mg/ml. Positive control vitamin C exhibited strong DPPH antioxidant activity which is concentration-dependent and was much higher than that of the EBN extracts. Although EBN was not a potent radical scavenger, it might still exert antioxidant effect which is likely to act on different mechanism.

3.2.2 Reducing power

Antioxidant capacity of EBN extracts in terms of reducing power was evaluated by FRAP assay. Reducing power of a compound reflects its ability to transfer electron to reduce metal ions, carbonyls and radicals. It has been shown that pro-oxidants such as peroxynitrite and hypochlorite can be reduced to harmless species by antioxidants [50]. We found that reductive ability of both EBN extracts increased in dose-dependent manner despite the noticeable fluctuating values at lower concentrations (Fig.2B). At highest concentration tested, S1 showed reducing power of 32.93% whereas S2 showed slightly lower activity of 26.25%. Meanwhile, the positive control vitamin C exhibited strong reductive activity, reaching saturation at 1 mg/ml. Antioxidant activities of EBN extracts in terms of reducing power were not as potent as

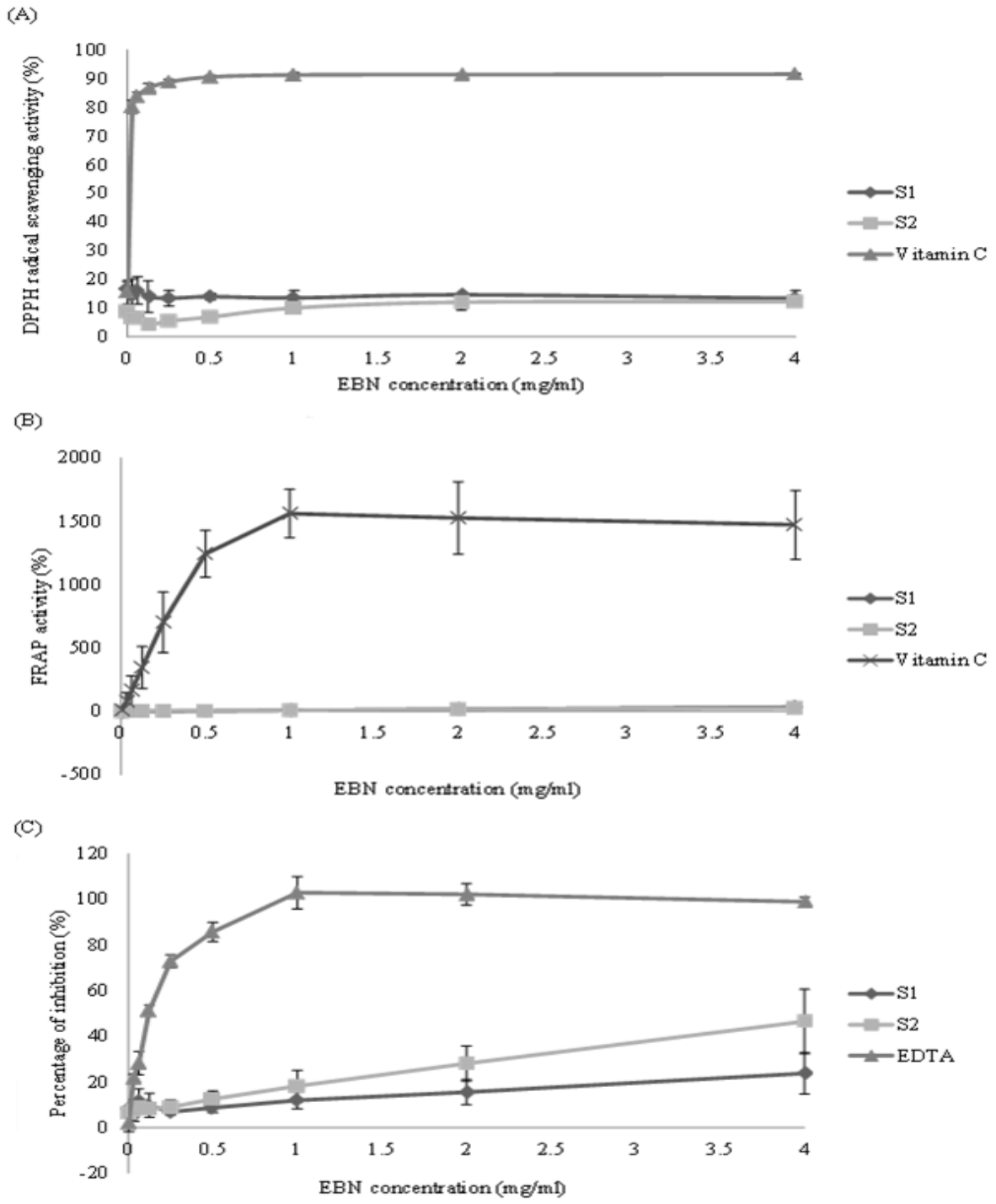

Fig.2. Antioxidant capacity of EBN and standard as evaluated by (A) DPPH radical scavenging assay, (B) FRAP assay and (C) metal chelating assay. Either vitamin C or EDTA was included as standard control. Data shown are means ± standard deviation of three independent experiments.

vitamin C, but generally, S1 displayed higher reducing power than S2. This is in coherence to the DPPH antioxidant assay that crude EBN extract seemed to offer more anti-oxidative advantage comparing to the water extract.

3.2.3 Metal chelating activity

Antioxidation can also be achieved through metal-chelating, which leads to the inhibition of metal-catalyzed oxidation reaction. Activities of EBN extracts in chelating ferrous ion (Fe^{2+}) were shown in Fig.2C. It was noted that metal-chelation effect increased steadily alongside the extract concentration, especially when approaching higher dose. At highest concentration tested, S2 displayed nearly 50% metal-chelating action, and that was twice as much than that in S1. The positive control EDTA exhibited potent chelating activity and recorded an IC_{50} value (the inhibitory concentration at which the ferrous ions were chelated by 50%) of 0.125 mg/ml. Thus the EBN extracts were weaker metal chelators compared to EDTA.

We observed that EBN possessed antioxidant activities and the effects might be contributed by the presence of active compounds in the samples. While EBN contains all type of essential amino acids, there are abundant amino acids like serine threonine, aspartic acid, glutamic acid, proline and valine [2]. Indeed, Sarmadi et al. had presented a comprehensive review on the antioxidant property associated with various amino acids [21]. Aromatic amino acids possess a ring structure that could stabilize free radical, whilst carboxyl and amino group in the side chains of acidic and basic amino acid such as tyrosine and phenylalanine are potent metal chelators to inhibit metal-catalyzed oxidation [50]. Meanwhile, hydrophobic amino acids are lipid soluble and permit an energy-independent diffusion across cell phospholipid hence it

promotes assimilation and leads to higher bioavailability within the cell. Hydrophobic amino acids which comprise valine, proline, isoleucine, leucine, tyrosine, phenylalanine, tryptophan, methionine and cysteine were found in EBN [2]. These amino acids enhance antioxidant property of proteins or peptides as they facilitate access to hydrophobic radical species especially within the phospholipids bilayer, thus inhibiting oxidation reaction at the cellular membrane [21]. Furthermore, sulphur-containing amino acid such as cysteine was suggested to have potent reducing power, which explains FRAP activity of raw powder and water extract of EBN in the current study [52]. Overall, studies have shown high correlation between total hydrophobic amino acids and antioxidant effect in terms of radical scavenging and reducing power [53]. Interestingly, S1 seemed to possess greater antioxidant activity than S2 in the DPPH and FRAP assays. Thus we believe that antioxidant effect displayed by EBN samples in the current study, especially for raw powder, could be contributed by hydrophobic amino acids.

We then inferred from here that S2 has less antioxidant activity likely because it contains less hydrophobic amino acids in the extract as a result of water extraction. However, it was demonstrated in our previous study that S2 had better ROS-lowering effect in cellular model of oxidative stress [13]. We attributed this finding to the metal-chelating property of S2, which was superior to S1. Therefore, although it has been a common practice to assess and compare antioxidant potential of a compound using any of the non-cell-based *in vitro* methods such as DPPH, FRAP and others, it should be noted that evaluation of antioxidant capacity must include various mechanisms for better interpretation into the effect at the cellular and *in vivo* level.

4. Conclusion

This study described the proteome of EBN. Particularly, protein analysis of raw powder and water extract of EBN has detected 29 bioactive proteins with potential roles in immunity, extracellular matrix formation, neurodevelopment, cell survival and apoptosis, cell proliferation and migration, antioxidation and common cellular processes. Among which, 20 proteins are reported for the first time in EBN, including uncharacterized proteins. In addition to that, raw powder and water extract of EBN were found to possess radical scavenging, reducing power and metal-chelating activities as part of the antioxidant mechanisms. The distinctive protein profile and antioxidant activities between raw powder and water extract of EBN may be due to the differences in the extraction methods. The findings of this study have provided insights to the understanding of nutritional and medicinal effects of EBN presented in previous literatures, and support EBN as a potential functional food due to the profound antioxidant activities of both raw powder and water extracts of EBN.

Funding

This study was supported by Ministry of Higher Education of Malaysia (Exploratory Research Grant Scheme 2011 ERGS/1/2011/SKK/MUSM/03/3).

6.3 References

[1] Ma F, Liu D. Sketch of the edible bird's nest and its important bioactivities Food Res Int 2012;48:559-67.

[2] Marcone MF. Characterization of the edible bird's nest the "Caviar of the East". Food Res Int 2005;38:1125-34.

[3] Chye SM, Tai SK, Koh RY, Ng KY. A Mini Review on Medicinal Effects of Edible Bird's Nest. Lett Health Biol Sci 2017;2(2). doi:10.15436/2475-6245.17.016

[4] Thorburn CC. The Edible Nest Swiftlet Industry in Southeast Asia: Capitalism Meets Commensalism. Hum Ecol 2015;43:179-84.

[5] Liu X, Lai X, Zhang S, Huang X, Lan Q, Li Y, Li B, Chen W, Zhang Q, Hong D, Yang G. Proteomic profile of edible bird's nest proteins. J Agric Food Chem. 2012 Dec 26;60(51):12477-81. doi: 10.1021/jf303533p. Epub 2012 Dec 14.

[6] Zukefli SN, Chua LS, Rahmat Z. Protein Extraction and Identification by Gel Electrophoresis and Mass Spectrometry from Edible bird's Nest Samples. Food Anal Methods 2017;10:387-98.

[7] Wong C-F, Chan GK-L, Zhang M-L, Yao P, Lin H-Q, Dong TT-X, Li G, Lai X-P, Tsim KW-K. Characterization of edible bird's nest by peptide fingerprinting with principal component analysis. Food Qual Saf 2017;1:83-92.

[8] Wong ZCF, Chan GKL, Wu L, Lam HHN, Yao P, Dong TTX, Tsim KWK. A comprehensive proteomics study on edible bird's nest using new monoclonal antibody approach and application in quality control. J Food Compost Anal 2018;66:145-51.

[9] Pozsgay V, Jennings H, Kasper DL. 4,8-anhydro-N-acetylneuraminic acid. Isolation from edible bird's nest and structure determination. Eur J Biochem. 1987 Jan 15;162(2):445-50.

[10] Goh DL, Chua KY, Chew FT, Liang RC, Seow TK, Ou KL, Yi FC, Lee BW. Immunochemical characterization of edible bird's nest allergens. J Allergy Clin Immunol. 2001 Jun;107(6):1082-7.

[11] Guo CT, Takahashi T, Bukawa W, Takahashi N, Yagi H, Kato K, Hidari KI, Miyamoto D, Suzuki T, Suzuki Y. Edible bird's nest extract inhibits influenza virus infection. Antiviral Res. 2006 Jul;70(3):140-6. Epub 2006 Mar 3.

[12] Goh DLM, Chua KY, Chew FT, Liang RCMY, Seow TK, Ou KL, Yi FC, Lee BW. Immunochemical characterization of edible bird’s nest allergens. J Allergy Clin Immunol. 2001 Jun;107(6):1082-7.

[13] Yew MY, Koh RY, Chye SM, Othman I, Ng KY. Edible bird's nest ameliorates oxidative stress-induced apoptosis in SH-SY5Y human neuroblastoma cells. BMC Complement Altern Med. 2014 Oct 13;14:391. doi: 10.1186/1472-6882-14-391.

[14] Ng MH, Chan KH, Kong YC. Potentiation of mitogenic response by extracts of the swiftlet's (Collocalia) nest. Biochem Int. 1986 Sep;13(3):521-31.

[15] Matsukawa N, Matsumoto M, Bukawa W, Chiji H, Nakayama K, Hara H, Tsukahara T. Improvement of bone strength and dermal thickness due to dietary edible bird's nest extract in ovariectomized rats. Biosci Biotechnol Biochem. 2011;75(3):590-2. Epub 2011 Mar 7.

[16] Farooqui T, Farooqui AA. Lipid-Mediated Oxidative Stress and Inflammation in the Pathogenesis of Parkinson's Disease. Parkinsons Dis. 2011 Feb 15;2011:247467. doi: 10.4061/2011/247467.

[17] Dalleau S, Baradat M, Guéraud F, Huc L. Cell death and diseases related to oxidative stress:4-hydroxynonenal (HNE) in the balance. Cell Death Differ. 2013 Dec;20(12):1615-30. doi: 10.1038/cdd.2013.138. Epub 2013 Oct 4.

[18] Masella R, Di Benedetto R, Vari R, Filesi C, Giovannini C. Novel mechanisms of natural antioxidant compounds in biological systems: involvement of glutathione and glutathione-related enzymes. J Nutr Biochem. 2005 Oct;16(10):577-86.

[19] Hou Z, Imam MU, Ismail M, Azmi NH, Ismail N, Ideris A, Mahmud R. Lactoferrin and ovotransferrin contribute toward antioxidative effects of Edible Bird's Nest against hydrogen peroxide-induced oxidative stress in human SH-SY5Y cells. Cell Mol Biol (Noisy-le-grand). 2016 Apr 30;62(4):116-22.

[20] Hu Q, Li G, Yao H, He S, Li H, Liu S, Wu Y, Lai X. Edible bird's nest enhances antioxidant capacity and increases lifespan in Drosophila Melanogaster. Cellular and molecular biology (Noisy-le-Grand, France) 2016;62:116-22.

[21] Sarmadi BH, Ismail A. Antioxidative peptides from food proteins: A review. Peptides. 2010 Oct;31(10):1949-56. doi: 10.1016/j.peptides.2010.06.020. Epub 2010 Jun 30.

[22] Zhang J, Xin L, Shan B, Chen W, Xie M, Yuen D, Zhang W, Zhang Z, Lajoie GA, Ma B. PEAKS DB: De Novo Sequencing Assisted Database Search for Sensitive and Accurate Peptide Identification. Mol Cell Proteomics. 2012 Apr;11(4):M111.010587. doi: 10.1074/mcp.M111.010587. Epub 2011 Dec 20.

[23] Benzie IF, Strain JJ. The ferric reducing ability of plasma (FRAP) as a measure of "antioxidant power": the FRAP assay. Anal Biochem. 1996 Jul 15;239(1):70-6.

[24] Decker E.A. and Welch B. Role of ferritin as a lipid oxidation catalyst in muscle food. J Agric Food Chem 1990; 38: 674–677

[25] Kong H-k, Wong K-H, Lo SC-l. Identification of peptides released from hot water insoluble fraction of edible bird's nest under simulated gastro-intestinal conditions. Food Res Int. 2016 Jul;85:19-25. doi: 10.1016/j.foodres.2016.04.002. Epub 2016 Apr 16.

[26] Abhyankar W, Beek AT, Dekker H, Kort R, Brul S, de Koster CG. Gel-free proteomic identification of the Bacillus subtilis insoluble spore coat protein fraction. Proteomics. 2011 Dec;11(23):4541-50. doi: 10.1002/pmic.201100003. Epub 2011 Oct 28.

[27] Zhu Z, Zheng T, Homer RJ, Kim Y-K, Chen NY, Cohn L, Hamid Q, Elias JA. Acidic Mammalian Chitinase in Asthmatic Th2 Inflammation and IL-13 Pathway Activation. Science. 2004 Jun 11;304(5677):1678-82.

[28] Rosenstiel P, Sina C, End C, Renner M, Lyer S, Till A, Hellmig S, Nikolaus S, Fölsch UR, Helmke B, Autschbach F, Schirmacher P, Kioschis P, Hafner M, Poustka A, Mollenhauer J, Schreiber S. Regulation of DMBT1 via NOD2 and TLR4 in Intestinal Epithelial Cells Modulates Bacterial Recognition and Invasion. J Immunol. 2007 Jun 15;178(12):8203-11.

[29] Bikker FJ, Ligtenberg AJM, End C, Renner M, Blaich S, Lyer S, Wittig R, van't Hof W, Veerman ECI, Nazmi K, de Blieck-Hogervorst JMA, Kioschis P, Amerongen AVN, Poustka A, Mollenhauer J. Bacteria Binding by DMBT1/SAG/gp-340 Is Confined to the VEVLXXXXW Motif in Its Scavenger Receptor Cysteine-rich Domains. J Biol Chem. 2004 Nov 12;279(46):47699-703. Epub 2004 Sep 7.

[30] Saengkrajang W, Matan N. Antimicrobial Activities of the Edible Bird's Nest Extracts Against Food-borne Pathogens. Thai J Agric Sci 2011;44:326-30.

[31] Eyre DR, Paz MA, Gallop PM. Cross-Linking in Collagen and Elastin. Annu Rev Biochem 1984;53:717-48.

[32] Liu A, Niswander LA. Bone morphogenetic protein signalling and vertebrate nervous system development. Nat Rev Neurosci. 2005 Dec;6(12):945-54.

[33] Ma CH, Brenner GJ, Omura T, Samad OA, Costigan M, Inquimbert P, Niederkofler V, Salie R, Sun CC, Lin HY, Arber S, Coppola G, Woolf CJ, Samad TA. The BMP co-receptor RGMb promotes while the endogenous BMP antagonist Noggin reduces neurite outgrowth

and peripheral nerve regeneration by modulating BMP signaling. J Neurosci 2011;31:18391-400.

[34] Ng D, Pitcher GM, Szilard RK, Sertie A, Kanisek M, Clapcote SJ, Lipina T, Kalia LV, Joo D, McKerlie C, Cortez M, Roder JC, Salter MW, McInnes RR. Neto1 is a novel CUB-domain NMDA receptor-interacting protein required for synaptic plasticity and learning. PLoS Biol. 2009 Feb 24;7(2):e41. doi: 10.1371/journal.pbio.1000041.

[35] tom Dieck S, Sanmarti-Vila L, Langnaese K, Richter K, Kindler S, Soyke A, Wex H, Smalla KH, Kampf U, Franzer JT, Stumm M, Garner CC, Gundelfinger ED. Bassoon, a novel zinc-finger CAG/glutamine-repeat protein selectively localized at the active zone of presynaptic nerve terminals. J Cell Biol. 1998 Jul 27;142(2):499-509.

[36] Richter K, Langnaese K, Kreutz MR, Olias G, Zhai R, Scheich H, Garner CC, Gundelfinger ED. Presynaptic cytomatrix protein bassoon is localized at both excitatory and inhibitory synapses of rat brain. J Comp Neurol. 1999 Jun 7;408(3):437-48.

[37] Yang Y, Tang B-s, Guo J-f. Parkinson's Disease and Cognitive Impairment. Parkinsons Dis 2016;2016:8.

[38] Hou Z, He P, Imam MU, Qi J, Tang S, Song C, Ismail M. Edible Bird's Nest Prevents Menopause-Related Memory and Cognitive Decline in Rats via Increased Hippocampal Sirtuin-1 Expression. Oxid Med Cell Longev. 2017;2017:7205082. doi: 10.1155/2017/7205082. Epub 2017 Sep 20.

[39] Leak RK. Heat shock proteins in neurodegenerative disorders and aging. J Cell Commun Signal. 2014 Dec;8(4):293-310. doi: 10.1007/s12079-014-0243-9. Epub 2014 Sep 11.

[40] Aridon P, Geraci F, Turturici G, D'Amelio M, Savettieri G, Sconzo G. Protective role of heat shock proteins in Parkinson's disease. Neurodegener Dis. 2011;8(4):155-68. doi: 10.1159/000321548. Epub 2011 Jan 5.

[41] Wang M, Ye R, Barron E, Baumeister P, Mao C, Luo S, Fu Y, Luo B, Dubeau L, Hinton DR, Lee AS. Essential role of the unfolded protein response regulator GRP78/BiP in protection from neuronal apoptosis. Cell Death Differ. 2010 Mar;17(3):488-98. doi: 10.1038/cdd.2009.144. Epub 2009 Oct 9.

[42] Hata T, Nakayama M. Targeted disruption of the murine large nuclear KIAA1440/Ints1 protein causes growth arrest in early blastocyst stage embryos and eventual apoptotic cell death. Biochim Biophys Acta. 2007 Jul;1773(7):1039-51. Epub 2007 Apr 29.

[43] van den Berg DLC, Azzarelli R, Oishi K, Martynoga B, Urbán N, Dekkers DHW, Demmers JA, Guillemot F. Nipbl Interacts with Zfp609 and the Integrator Complex to Regulate Cortical Neuron Migration. Neuron. 2017 Jan 18;93(2):348-361. doi: 10.1016/j.neuron.2016.11.047. Epub 2016 Dec 29.

[44] Esterlechner J, Reichert N, Iltzsche F, Krause M, Finkernagel F, Gaubatz S. LIN9, a Subunit of the DREAM Complex, Regulates Mitotic Gene Expression and Proliferation of Embryonic Stem Cells. PLoS One. 2013 May 7;8(5):e62882. doi: 10.1371/journal.pone.0062882. Print 2013.

[45] Osterloh L, von Eyss B, Schmit F, Rein L, Hübner D, Samans B, Hauser S, Gaubatz S. The human synMuv-like protein LIN-9 is required for transcription of G2/M genes and for entry into mitosis. EMBO J. 2007 Jan 10;26(1):144-57. Epub 2006 Dec 7.

[46] Roh K-B, Lee J, Kim Y-S, Park J, Kim J-H, Lee J, Park D. Mechanisms of Edible Bird's Nest Extract-Induced Proliferation of Human Adipose-Derived Stem Cells. Evid Based Complement Alternat Med. 2012;2012:797520. doi: 10.1155/2012/797520. Epub 2011 Nov 1.

[47] Nagy JI, Hacking J, Frankenstein UN, Turley EA. Requirement of the hyaluronan receptor RHAMM in neurite extension and motility as demonstrated in primary neurons and neuronal cell lines. J Neurosci. 1995 Jan;15(1 Pt 1):241-52.

[48] Dubey A, Copeland PR. The Selenocysteine-Specific Elongation Factor Contains Unique Sequences That Are Required for Both Nuclear Export and Selenocysteine Incorporation. PLoS One. 2016 Nov 1;11(11):e0165642. doi: 10.1371/journal.pone.0165642. eCollection 2016.

[49] Pillai R, Uyehara-Lock JH, Bellinger FP. Selenium and selenoprotein function in brain disorders. IUBMB Life. 2014 Apr;66(4):229-39. doi: 10.1002/iub.1262. Epub 2014 Mar 25.

[50] Huang D, Ou B, Prior RL. The chemistry behind antioxidant capacity assays. J Agric Food Chem. 2005 Mar 23;53(6):1841-56.

[51] Saiga A, Tanabe S, Nishimura T. Antioxidant activity of peptides obtained from porcine myofibrillar proteins by protease treatment. J Agric Food Chem. 2003 Jun 4;51(12):3661-7.

[52] Udenigwe CC, Aluko RE. Chemometric Analysis of the Amino Acid Requirements of Antioxidant Food Protein Hydrolysates. Int J Mol Sci. 2011;12(5):3148-61. doi: 10.3390/ijms12053148. Epub 2011 May 13.

[53] Ajibola CF, Fashakin JB, Fagbemi TN, Aluko RE. Effect of Peptide Size on Antioxidant Properties of African Yam Bean Seed (Sphenostylis stenocarpa) Protein Hydrolysate Fractions. Int J Mol Sci. 2011;12(10):6685-702. doi: 10.3390/ijms12106685. Epub 2011 Oct 11.

Supplementary File 1

Protein Group	Protein ID	Protein Accession	Protein Name	Peptide	Unique	-10lgP	Mass	Length	ppm	m/z	z	RT	Scan	#Spec	Start	End	PTM
1	4026	tr|H0ZGY9|H0ZGY9_TAEGU	Mucin-5AC	R.EC(+57.02)HC(+57.02)TYEGETYAPGASFSSKC(+57.02)R.S	N	90.74	2596.042	22	0	650.0177	4	6.29	940	2	393	414	Carbamidomethylation
1	4026	tr|H0ZGY9|H0ZGY9_TAEGU	Mucin-5AC	R.EC(+57.02)HC(+57.02)TYEGETYAPGASFSSK.C	N	86.05	2279.91	20	0.9	760.9779	3	6.5	987	2	393	412	Carbamidomethylation
1	4026	tr|H0ZGY9|H0ZGY9_TAEGU	Mucin-5AC	K.SLKYTYNVDSC(+57.02)QPTC(+57.02)R.S	N	77.4	1990.888	16	0.3	664.6367	3	6.29	938	4	707	722	Carbamidomethylation
1	4026	tr|H0ZGY9|H0ZGY9_TAEGU	Mucin-5AC	R.Q(-17.03)C(+57.02)AHAGGQPLNWR.T	N	69	1476.668	13	-1.3	739.3403	2	6.77	1053	2	317	329	Pyro-glu from Q; Carbamidomethylation
1	4026	tr|H0ZGY9|H0ZGY9_TAEGU	Mucin-5AC	K.YTYNVDSC(+57.02)QPTC(+57.02)R.S	N	64.29	1662.677	13	0.4	832.3459	2	5.9	864	2	710	722	Carbamidomethylation
1	4026	tr|H0ZGY9|H0ZGY9_TAEGU	Mucin-5AC	K.QC(+57.02)SIITSEVFAK.C	N	62.07	1381.691	12	11.6	691.8608	2	8.25	1407	2	1093	1104	Carbamidomethylation
1	4026	tr|H0ZGY9|H0ZGY9_TAEGU	Mucin-5AC	K.AWAQKQC(+57.02)SIITSEVFAK.C	N	61.8	1965.998	17	2.7	656.3418	3	8.51	1475	2	1088	1104	Carbamidomethylation
1	4026	tr|H0ZGY9|H0ZGY9_TAEGU	Mucin-5AC	R.VITENIPC(+57.02)GTTGTTC(+57.02)SK.S	N	61.05	1837.855	17	1.6	919.9363	2	6.38	958	4	945	961	Carbamidomethylation
1	4026	tr|H0ZGY9|H0ZGY9_TAEGU	Mucin-5AC	K.SC(+57.02)QTLDMEC(+57.02)YK.T	N	55.62	1433.563	11	0.7	717.7891	2	6.52	992	2	825	835	Carbamidomethylation
1	4026	tr|H0ZGY9|H0ZGY9_TAEGU	Mucin-5AC	K.LC(+57.02)DSNEFTVLGDIHK.C	N	55.26	1746.825	15	4	583.2845	3	8.37	1438	4	463	477	Carbamidomethylation
1	4026	tr|H0ZGY9|H0ZGY9_TAEGU	Mucin-5AC	S.GPNQGDFETYQHIR.A	Y	54.59	1660.759	14	5	554.5965	3	6.4	962	4	1618	1631	
1	4026	tr|H0ZGY9|H0ZGY9_TAEGU	Mucin-5AC	K.TTSGVIEGTSAAFGNTWK.T	N	51.15	1825.885	18	11.4	913.96	2	8.73	1522	2	584	601	
1	4026	tr|H0ZGY9|H0ZGY9_TAEGU	Mucin-5AC	R.VC(+57.02)STWGNFHFK.T	N	44.23	1381.624	11	-0.9	461.5481	3	7.89	1322	4	78	88	Carbamidomethylation
1	4026	tr|H0ZGY9|H0ZGY9_TAEGU	Mucin-5AC	S.GPN(+.98)QGDFETYQHIR.A	Y	43.22	1661.743	14	4	554.924	3	6.53	994	2	1618	1631	Deamidation (NQ)
1	4026	tr|H0ZGY9|H0ZGY9_TAEGU	Mucin-5AC	K.Q(+41.03)IEC(+57.02)QAEDYPDVAIQQVGQVVQC(+57.02)DVHFGLVC(+57.02)K.N	Y	43.08	3772.765	32	10.2	1258.608	3	13.25	2485	2	1643	1674	Amidination of lysines or N-terminal amines with methyl acetimidate; Carbamidomethylation

1	4026	tr|H0ZGY9|H0ZGY9_TAEGU	Mucin-5AC	R.TPSIC(+57.02)PLFC(+57.02)DYYNPQGEC(+57.02)EWHYKPC(+57.02)GAPC(+57.02)MK.T	N	42.5	3864.596	31	-61.6	967.0968	4	10.84	1972	2	1156	1186	Carbamidomethylation
1	4026	tr|H0ZGY9|H0ZGY9_TAEGU	Mucin-5AC	R.TPGGKMPFQIR.S	N	41.7	1230.654	11	-2.2	411.2245	3	7.39	1198	2	985	995	
1	4026	tr|H0ZGY9|H0ZGY9_TAEGU	Mucin-5AC	R.E(+57.02)(+14.02)C(+57.02)H(+57.02)C(+57.02)TYEGETYAPGASFSSK.C	N	38.03	2407.969	20	15.7	603.0089	4	6.25	929	4	393	412	Carbamidomethylation (DHKE X@N-term); Methyl ester; Carbamidomethylation
1	4026	tr|H0ZGY9|H0ZGY9_TAEGU	Mucin-5AC	K.FKMC(+57.02)LNYK(+27.99).I	Y	37.35	1130.525	8	11.7	377.8534	3	7.18	1148	3	1682	1689	Carbamidomethylation; Formylation
1	4026	tr|H0ZGY9|H0ZGY9_TAEGU	Mucin-5AC	K.Q(-17.03)C(+57.02)SIITSEVFAK.C	N	36.96	1364.665	12	49.7	683.3735	2	10.15	1834	2	1093	1104	Pyro-glu from Q; Carbamidomethylation
1	4026	tr|H0ZGY9|H0ZGY9_TAEGU	Mucin-5AC	R.SLSEPDVTC(+57.02)ST(sub I)K.F	N	36.18	1322.602	12	0.9	662.3091	2	5.71	830	1	723	734	Carbamidomethylation; Mutation
1	4026	tr|H0ZGY9|H0ZGY9_TAEGU	Mucin-5AC	E.DQTGKFKMC(+57.02)LNYK(+27.99).I	Y	34.44	1659.775	13	8.1	554.2701	3	7	1107	3	1677	1689	Carbamidomethylation; Formylation
1	4026	tr|H0ZGY9|H0ZGY9_TAEGU	Mucin-5AC	R.QPM(+15.99)(sub K)QIEC(+57.02)QAEDYPDVAIQQVGQVVQC(+57.02)DVHFGLVC(+57.02)K.N	Y	34.19	4103.885	35	27.5	1027.007	4	13.42	2520	4	1640	1674	Oxidation (M); Carbamidomethylation; Mutation
1	4026	tr|H0ZGY9|H0ZGY9_TAEGU	Mucin-5AC	R.E(+57.02)(+14.02)C(+57.02)H(+57.02)C(+57.02)TYEGETYAPGASFSSKC(+57.02)R.S	N	26.11	2724.1	22	13.1	682.0413	4	6.09	899	1	393	414	Carbamidomethylation (DHKE X@N-term); Methyl ester; Carbamidomethylation
1	4026	tr|H0ZGY9|H0ZGY9_TAEGU	Mucin-5AC	K.MPFQIR.S	N	24.55	790.416	6	-0.9	396.2149	2	7.59	1250	2	990	995	
1	4026	tr|H0ZGY9|H0ZGY9_TAEGU	Mucin-5AC	K.A(sub S)EYVSPSLLQR.Q	N	24.5	1261.667	11	33.7	631.8619	2	7.47	1218	1	36	46	Mutation
2	4025	tr|A0A0Q3U2A7|A0A0Q3U2A7_AMAAE	Hypothetical protein AAES_08852	R.SQSVVGNVLEFANSWK.V	N	68.76	1763.884	16	1.4	882.9506	2	13.65	2567	5	854	869	
2	4025	tr|A0A0Q3U2A7|A0A0Q3U2A7_AMAAE	Hypothetical protein AAES_08852	R.AEKFPNIPLKDLGQK.V	Y	67.17	1696.951	15	4.1	425.2468	4	8	1349	4	1195	1209	
2	4025	tr|A0A0Q3U2A7|A0A0Q3U2A7_AMAAE	Hypothetical protein AAES_08852	E.YTYNVDSC(+57.02)QPTC(+57.02)R.S	N	64.29	1662.677	13	0.4	832.3459	2	5.9	864	2	514	526	Carbamidomethylation
2	4025	tr|A0A0Q3U2A7|A0A0Q3U2A7_AMAAE	Hypothetical protein AAES_08852	K.QC(+57.02)SIITSEVFAK.C	N	62.07	1381.691	12	11.6	691.8608	2	8.25	1407	2	897	908	Carbamidomethylation
2	4025	tr|A0A0Q3U2A7|A0A0Q3U2A7_AMAAE	Hypothetical protein AAES_08852	K.AWAQKQC(+57.02)SIITSEVFAK.C	N	61.8	1965.998	17	2.7	656.3418	3	8.51	1475	2	892	908	Carbamidomethylation
2	4025	tr|A0A0Q3U2A7|A0A0Q	Hypothetical protein	R.VITENIPC(+57.02)GTTGTTC(+57.02)SK.S	N	61.05	1837.855	17	1.6	919.9363	2	6.38	958	4	749	765	Carbamidomethylation

		3U2A7_AMAAE	AAES_08852														
2	4025	tr|A0A0Q3U2A7|A0A0Q3U2A7_AMAAE	Hypothetical protein AAES_08852	K.VEC(+57.02)STTAGLIC(+57.02)YNKDQISTMC(+57.02)D(sub E)NYEIR.I	Y	60.88	3240.42	27	-1.8	1081.145	3	9.27	1635	2	1210	1236	Carbamidomethylation; Mutation
2	4025	tr|A0A0Q3U2A7|A0A0Q3U2A7_AMAAE	Hypothetical protein AAES_08852	K.THC(+57.02)VSGC(+57.02)VC(+57.02)PHNQVLDGK.G	N	60.38	2066.908	18	0.8	689.9773	3	5.7	827	3	640	657	Carbamidomethylation
2	4025	tr|A0A0Q3U2A7|A0A0Q3U2A7_AMAAE	Hypothetical protein AAES_08852	K.SC(+57.02)QTLDMEC(+57.02)YK.T	N	55.62	1433.563	11	0.7	717.7891	2	6.52	992	2	629	639	Carbamidomethylation
2	4025	tr|A0A0Q3U2A7|A0A0Q3U2A7_AMAAE	Hypothetical protein AAES_08852	K.SPYEDFNIQIR.R	N	53.73	1380.667	11	2.4	691.3426	2	8.66	1509	4	115	125	
2	4025	tr|A0A0Q3U2A7|A0A0Q3U2A7_AMAAE	Hypothetical protein AAES_08852	K.SPYEDFNIQIRR.A	N	46.04	1536.768	12	-0.1	513.2634	3	7.79	1298	2	115	126	
2	4025	tr|A0A0Q3U2A7|A0A0Q3U2A7_AMAAE	Hypothetical protein AAES_08852	R.GLEGC(+57.02)YPHC(+57.02)PK.N	N	44.9	1316.564	11	-2.6	659.2877	2	5.44	787	4	1005	1015	Carbamidomethylation
2	4025	tr|A0A0Q3U2A7|A0A0Q3U2A7_AMAAE	Hypothetical protein AAES_08852	K.SVQMPYSHMGVLIER(-.98).S	Y	44.75	1744.875	15	3.8	582.6346	3	8.55	1482	2	160	174	Amidation
2	4025	tr|A0A0Q3U2A7|A0A0Q3U2A7_AMAAE	Hypothetical protein AAES_08852	K.FPNIPLKDLGQK.V	Y	44.44	1368.777	12	3.5	457.2677	3	8.56	1485	2	1198	1209	
2	4025	tr|A0A0Q3U2A7|A0A0Q3U2A7_AMAAE	Hypothetical protein AAES_08852	R.VC(+57.02)STWGNFHFK.T	N	44.23	1381.624	11	-0.9	461.5481	3	7.89	1322	4	82	92	Carbamidomethylation
2	4025	tr|A0A0Q3U2A7|A0A0Q3U2A7_AMAAE	Hypothetical protein AAES_08852	R.TPGGKMPFQIR.S	N	41.7	1230.654	11	-2.2	411.2245	3	7.39	1198	2	789	799	
2	4025	tr|A0A0Q3U2A7|A0A0Q3U2A7_AMAAE	Hypothetical protein AAES_08852	K.TC(+57.02)NNPSGNC(+57.02)V(sub L)HELRGLEGC(+57.02)YPHC(+57.02)PK.N	N	37.62	2955.263	25	2	592.0611	5	6.69	1032	3	991	1015	Carbamidomethylation; Mutation
2	4025	tr|A0A0Q3U2A7|A0A0Q3U2A7_AMAAE	Hypothetical protein AAES_08852	K.Q(-17.03)C(+57.02)SIITSEVFAK.C	N	36.96	1364.665	12	49.7	683.3735	2	10.15	1834	2	897	908	Pyro-glu from Q; Carbamidomethylation
2	4025	tr|A0A0Q3U2A7|A0A0Q3U2A7_AMAAE	Hypothetical protein AAES_08852	K.GVLLTGWR.S	N	32.58	900.5181	8	5.8	451.269	2	8.29	1418	2	490	497	
2	4025	tr|A0A0Q3U2A7|A0A0Q3U2A7_AMAAE	Hypothetical protein AAES_08852	K.LEGAVIELTR.G	Y	30.14	1099.624	10	0.3	550.8193	2	7.88	1320	1	142	151	
2	4025	tr|A0A0Q3U2A7|A0A0Q3U2A7_AMAAE	Hypothetical protein AAES_08852	K.TC(+57.02)NNPSGNC(+57.02)V(sub L)HELR.G	N	28.54	1656.71	14	2.2	553.2451	3	4.59	663	2	991	1004	Carbamidomethylation; Mutation
2	4025	tr|A0A0Q3U2A7|A0A0Q3U2A7_AMAAE	Hypothetical protein AAES_08852	K.MPFQIR.S	N	24.55	790.416	6	-0.9	396.2149	2	7.59	1250	2	794	799	

3	4024	tr|R7VT28|R7VT28_COLLI	Mucin-5AC	K.TFDGDIFYFPGIC(+57.02)NYIFASNC(+57.02)K.S	Y	81.57	2648.172	22	2.1	1325.096	2	15.38	2899	4	93	114	Carbamidomethylation
3	4024	tr|R7VT28|R7VT28_COLLI	Mucin-5AC	R.Q(-17.03)C(+57.02)AHAGGQPLNWR.T	N	69	1476.668	13	-1.3	739.3403	2	6.77	1053	2	321	333	Pyro-glu from Q; Carbamidomethylation
3	4024	tr|R7VT28|R7VT28_COLLI	Mucin-5AC	R.SQSVVGNVLEFANSWK.V	N	68.76	1763.884	16	1.4	882.9506	2	13.65	2567	5	1064	1079	
3	4024	tr|R7VT28|R7VT28_COLLI	Mucin-5AC	K.QC(+57.02)SIITSEVFAK.C	N	62.07	1381.691	12	11.6	691.8608	2	8.25	1407	2	1107	1118	Carbamidomethylation
3	4024	tr|R7VT28|R7VT28_COLLI	Mucin-5AC	K.AWAQKQC(+57.02)SIITSEVFAK.C	N	61.8	1965.998	17	2.7	656.3418	3	8.51	1475	2	1102	1118	Carbamidomethylation
3	4024	tr|R7VT28|R7VT28_COLLI	Mucin-5AC	R.VITENIPC(+57.02)GTTGTTC(+57.02)SK.S	N	61.05	1837.855	17	1.6	919.9363	2	6.38	958	4	959	975	Carbamidomethylation
3	4024	tr|R7VT28|R7VT28_COLLI	Mucin-5AC	R.THC(+57.02)VSGC(+57.02)VC(+57.02)PHNQVLDGK.G	N	60.38	2066.908	18	0.8	689.9773	3	5.7	827	3	850	867	Carbamidomethylation
3	4024	tr|R7VT28|R7VT28_COLLI	Mucin-5AC	K.SPYEDFNIQIR.R	N	53.73	1380.667	11	2.4	691.3426	2	8.66	1509	4	115	125	
3	4024	tr|R7VT28|R7VT28_COLLI	Mucin-5AC	K.TTSGVIEGTSAAFGNTWK.T	N	51.15	1825.885	18	11.4	913.96	2	8.73	1522	2	598	615	
3	4024	tr|R7VT28|R7VT28_COLLI	Mucin-5AC	K.SNYVSPSILQR.Q	Y	48.74	1262.662	11	-3.2	632.3362	2	7.49	1222	1	36	46	
3	4024	tr|R7VT28|R7VT28_COLLI	Mucin-5AC	K.SPYEDFNIQIRR.T	N	46.04	1536.768	12	-0.1	513.2634	3	7.79	1298	2	115	126	
3	4024	tr|R7VT28|R7VT28_COLLI	Mucin-5AC	R.GLEGC(+57.02)YPHC(+57.02)PK.N	N	44.9	1316.564	11	-2.6	659.2877	2	5.44	787	4	1215	1225	Carbamidomethylation
3	4024	tr|R7VT28|R7VT28_COLLI	Mucin-5AC	R.VC(+57.02)STWGNFHFK.T	N	44.23	1381.624	11	-0.9	461.5481	3	7.89	1322	4	82	92	Carbamidomethylation
3	4024	tr|R7VT28|R7VT28_COLLI	Mucin-5AC	R.TPSIC(+57.02)PLFC(+57.02)DYYNPQGEC(+57.02)EWHYKPC(+57.02)GAPC(+57.02)MK.T	N	42.5	3864.596	31	-61.6	967.0968	4	10.84	1972	2	1170	1200	Carbamidomethylation
3	4024	tr|R7VT28|R7VT28_COLLI	Mucin-5AC	R.TPGGKMPFQIR.S	N	41.7	1230.654	11	-2.2	411.2245	3	7.39	1198	2	999	1009	
3	4024	tr|R7VT28|R7VT28_COLLI	Mucin-5AC	K.TC(+57.02)NNPSGNC(+57.02)V(sub L)HELRGLEGC(+57.02)YPHC(+57.02)PK.N	N	37.62	2955.263	25	2	592.0611	5	6.69	1032	3	1201	1225	Carbamidomethylation; Mutation
3	4024	tr|R7VT28|R7VT28_COLLI	Mucin-5AC	K.Q(-17.03)C(+57.02)SIITSEVFAK.C	N	36.96	1364.665	12	49.7	683.3735	2	10.15	1834	2	1107	1118	Pyro-glu from Q; Carbamidomethylation
3	4024	tr|R7VT28|R7VT28_COL	Mucin-5AC	R.SLSEPDVTC(+57.02)ST(sub I)K.F	N	36.18	1322.602	12	0.9	662.3091	2	5.71	830	1	737	748	Carbamidomethylation; Mutation

		LI															
3	4024	tr|R7VT28|R7VT28_COLLI	Mucin-5AC	K.GVLLTGWR.S	N	32.58	900.5181	8	5.8	451.269	2	8.29	1418	2	700	707	
3	4024	tr|R7VT28|R7VT28_COLLI	Mucin-5AC	R.AAGK(sub M)EVC(+57.02)QHPK.E	Y	31.36	1223.608	11	-0.8	408.8763	3	0.75	103	1	1623	1633	Carbamidomethylation; Mutation
3	4024	tr|R7VT28|R7VT28_COLLI	Mucin-5AC	K.TC(+57.02)NNPSGNC(+57.02)V(sub L)HELR.G	N	28.54	1656.71	14	2.2	553.2451	3	4.59	663	2	1201	1214	Carbamidomethylation; Mutation
3	4024	tr|R7VT28|R7VT28_COLLI	Mucin-5AC	K.MPFQIR.S	N	24.55	790.416	6	-0.9	396.2149	2	7.59	1250	2	1004	1009	
4	4027	tr|A0A1D5NVH7|A0A1D5NVH7_CHICK	Mucin-5AC	R.Q(-17.03)C(+57.02)AHAGGQPLNWR.T	N	69	1476.668	13	-1.3	739.3403	2	6.77	1053	2	312	324	Pyro-glu from Q; Carbamidomethylation
4	4027	tr|A0A1D5NVH7|A0A1D5NVH7_CHICK	Mucin-5AC	R.SQSVVGNVLEFANSWK.V	N	68.76	1763.884	16	1.4	882.9506	2	13.65	2567	5	1045	1060	
4	4027	tr|A0A1D5NVH7|A0A1D5NVH7_CHICK	Mucin-5AC	E.YTYNVDSC(+57.02)QPTC(+57.02)R.S	N	64.29	1662.677	13	0.4	832.3459	2	5.9	864	2	705	717	Carbamidomethylation
4	4027	tr|A0A1D5NVH7|A0A1D5NVH7_CHICK	Mucin-5AC	K.QC(+57.02)SIITSEVFAK.C	N	62.07	1381.691	12	11.6	691.8608	2	8.25	1407	2	1088	1099	Carbamidomethylation
4	4027	tr|A0A1D5NVH7|A0A1D5NVH7_CHICK	Mucin-5AC	R.VITENIPC(+57.02)GTTGTTC(+57.02)SK.S	N	61.05	1837.855	17	1.6	919.9363	2	6.38	958	4	940	956	Carbamidomethylation
4	4027	tr|A0A1D5NVH7|A0A1D5NVH7_CHICK	Mucin-5AC	K.SC(+57.02)QTLDMEC(+57.02)YK.T	N	55.62	1433.563	11	0.7	717.7891	2	6.52	992	2	820	830	Carbamidomethylation
4	4027	tr|A0A1D5NVH7|A0A1D5NVH7_CHICK	Mucin-5AC	K.SPYEDFNIQIR.R	N	53.73	1380.667	11	2.4	691.3426	2	8.66	1509	4	106	116	
4	4027	tr|A0A1D5NVH7|A0A1D5NVH7_CHICK	Mucin-5AC	K.TTSGVIEGTSAAFGNTWK.T	N	51.15	1825.885	18	11.4	913.96	2	8.73	1522	2	579	596	
4	4027	tr|A0A1D5NVH7|A0A1D5NVH7_CHICK	Mucin-5AC	K.SPYEDFNIQIRR.T	N	46.04	1536.768	12	-0.1	513.2634	3	7.79	1298	2	106	117	
4	4027	tr|A0A1D5NVH7|A0A1D5NVH7_CHICK	Mucin-5AC	R.GLEGC(+57.02)YPHC(+57.02)PK.N	N	44.9	1316.564	11	-2.6	659.2877	2	5.44	787	4	1196	1206	Carbamidomethylation
4	4027	tr|A0A1D5NVH7|A0A1D5NVH7_CHICK	Mucin-5AC	R.VC(+57.02)STWGNFHFK.N	N	44.23	1381.624	11	-0.9	461.5481	3	7.89	1322	4	73	83	Carbamidomethylation
4	4027	tr|A0A1D5NVH7|A0A1D5NVH7_CHICK	Mucin-5AC	R.TPSIC(+57.02)PLFC(+57.02)DYYNPQGEC(+57.02)EWHYKPC(+57.02)GAPC(+57.02)MK.T	N	42.5	3864.596	31	-61.6	967.0968	4	10.84	1972	2	1151	1181	Carbamidomethylation

4	4027	tr|A0A1D5NVH7|A0A1D5NVH7_CHICK	Mucin-5AC	K.Q(-17.03)C(+57.02)SIITSEVFAK.C	N	36.96	1364.665	12	49.7	683.3735	2	10.15	1834	2	1088	1099	Pyro-glu from Q; Carbamidomethylation
4	4027	tr|A0A1D5NVH7|A0A1D5NVH7_CHICK	Mucin-5AC	S.FKMC(+57.02)LNYR.I	N	32.36	1130.537	8	0.2	377.8528	3	7.2	1152	1	1680	1687	Carbamidomethylation
4	4027	tr|A0A1D5NVH7|A0A1D5NVH7_CHICK	Mucin-5AC	K.MC(+57.02)LNYR.I	N	29.9	855.3731	6	1.8	428.6946	2	6.04	889	2	1682	1687	Carbamidomethylation
4	4027	tr|A0A1D5NVH7|A0A1D5NVH7_CHICK	Mucin-5AC	I.TFENPC(+57.02)TLSIEND(+57.02)K(+42.01)YAQHWC(+57.02)GLLSDTTGPFAEC(+57.02)HSTVNPEVYQK.N	Y	27.05	5242.338	44	-2.6	1311.589	4	12.04	2230	1	607	650	Carbamidomethylation; Carbamidomethylation (DHKE X@N-term); Acetylation (K)
4	4027	tr|A0A1D5NVH7|A0A1D5NVH7_CHICK	Mucin-5AC	E.MPFQIR.S	N	24.55	790.416	6	-0.9	396.2149	2	7.59	1250	2	985	990	
4	4027	tr|A0A1D5NVH7|A0A1D5NVH7_CHICK	Mucin-5AC	I.TFENPC(+57.02)TLW(sub S)IENDKYAQHWC(+57.02)GLLSDTTGPFAEC(+57.02)HSTVNPEVYQK.N	Y	22.94	5242.354	44	-7.4	1311.586	4	12.06	2233	1	607	650	Carbamidomethylation; Mutation
7	4032	tr|R0LBT0|R0LBT0_ANAPL	Mucin-5AC	K.SLKYTYNVDSC(+57.02)QPTC(+57.02)R.S	N	77.4	1990.888	16	0.3	664.6367	3	6.29	938	4	658	673	Carbamidomethylation
7	4032	tr|R0LBT0|R0LBT0_ANAPL	Mucin-5AC	R.Q(-17.03)C(+57.02)AHAGGQPLNWR.T	N	69	1476.668	13	-1.3	739.3403	2	6.77	1053	2	268	280	Pyro-glu from Q; Carbamidomethylation
7	4032	tr|R0LBT0|R0LBT0_ANAPL	Mucin-5AC	R.SQSVVGNVLEFANSWK.V	N	68.76	1763.884	16	1.4	882.9506	2	13.65	2567	5	1001	1016	
7	4032	tr|R0LBT0|R0LBT0_ANAPL	Mucin-5AC	K.YTYNVDSC(+57.02)QPTC(+57.02)R.S	N	64.29	1662.677	13	0.4	832.3459	2	5.9	864	2	661	673	Carbamidomethylation
7	4032	tr|R0LBT0|R0LBT0_ANAPL	Mucin-5AC	K.QC(+57.02)SIITSEVFAK.C	N	62.07	1381.691	12	11.6	691.8608	2	8.25	1407	2	1044	1055	Carbamidomethylation
7	4032	tr|R0LBT0|R0LBT0_ANAPL	Mucin-5AC	R.VITENIPC(+57.02)GTTGTTC(+57.02)SK.S	N	61.05	1837.855	17	1.6	919.9363	2	6.38	958	4	896	912	Carbamidomethylation
7	4032	tr|R0LBT0|R0LBT0_ANAPL	Mucin-5AC	K.SC(+57.02)QTLDMEC(+57.02)YK.T	N	55.62	1433.563	11	0.7	717.7891	2	6.52	992	2	776	786	Carbamidomethylation
7	4032	tr|R0LBT0|R0LBT0_ANAPL	Mucin-5AC	K.TTSGVIEGTSAAFGNTWK.T	N	51.15	1825.885	18	11.4	913.96	2	8.73	1522	2	535	552	
7	4032	tr|R0LBT0|R0LBT0_ANAPL	Mucin-5AC	R.GLEGC(+57.02)YPHC(+57.02)PK.N	N	44.9	1316.564	11	-2.6	659.2877	2	5.44	787	4	1152	1162	Carbamidomethylation
7	4032	tr|R0LBT0|R0LBT0_ANAPL	Mucin-5AC	R.VC(+57.02)STWGNFHFK.N	N	44.23	1381.624	11	-0.9	461.5481	3	7.89	1322	4	29	39	Carbamidomethylation
7	4032	tr|R0LBT0|R0LBT0_AN	Mucin-5AC	R.TPSIC(+57.02)PLFC(+57.02)DYYNPQGEC(+57.02)EWHYK	N	42.5	3864.596	31	-61.6	967.0968	4	10.8	1972	2	1107	113	Carbamidomethylation

		APL		PC(+57.02)GAPC(+57.02)MK.T								4				7	
7	4032	tr|R0LBT0|R0LBT0_ANAPL	Mucin-5AC	K.VFLGNYELVLSDGRSD(-18.01)VIQR.T	Y	38.7	2261.18	20	38.7	754.7632	3	11.08	2025	2	916	935	Dehydration
7	4032	tr|R0LBT0|R0LBT0_ANAPL	Mucin-5AC	K.Q(-17.03)C(+57.02)SIITSEVFAK.C	N	36.96	1364.665	12	49.7	683.3735	2	10.15	1834	2	1044	1055	Pyro-glu from Q; Carbamidomethylation
7	4032	tr|R0LBT0|R0LBT0_ANAPL	Mucin-5AC	E.MPFQIR.S	N	24.55	790.416	6	-0.9	396.2149	2	7.59	1250	2	941	946	
7	4033	tr|U3IV20|U3IV20_ANAPL	Mucin-5AC	K.SLKYTYNVDSC(+57.02)QPTC(+57.02)R.S	N	77.4	1990.888	16	0.3	664.6367	3	6.29	938	4	714	729	Carbamidomethylation
7	4033	tr|U3IV20|U3IV20_ANAPL	Mucin-5AC	R.Q(-17.03)C(+57.02)AHAGGQPLNWR.T	N	69	1476.668	13	-1.3	739.3403	2	6.77	1053	2	324	336	Pyro-glu from Q; Carbamidomethylation
7	4033	tr|U3IV20|U3IV20_ANAPL	Mucin-5AC	R.SQSVVGNVLEFANSWK.V	N	68.76	1763.884	16	1.4	882.9506	2	13.65	2567	5	1057	1072	
7	4033	tr|U3IV20|U3IV20_ANAPL	Mucin-5AC	K.YTYNVDSC(+57.02)QPTC(+57.02)R.S	N	64.29	1662.677	13	0.4	832.3459	2	5.9	864	2	717	729	Carbamidomethylation
7	4033	tr|U3IV20|U3IV20_ANAPL	Mucin-5AC	K.QC(+57.02)SIITSEVFAK.C	N	62.07	1381.691	12	11.6	691.8608	2	8.25	1407	2	1100	1111	Carbamidomethylation
7	4033	tr|U3IV20|U3IV20_ANAPL	Mucin-5AC	R.VITENIPC(+57.02)GTTGTTC(+57.02)SK.S	N	61.05	1837.855	17	1.6	919.9363	2	6.38	958	4	952	968	Carbamidomethylation
7	4033	tr|U3IV20|U3IV20_ANAPL	Mucin-5AC	K.SC(+57.02)QTLDMEC(+57.02)YK.T	N	55.62	1433.563	11	0.7	717.7891	2	6.52	992	2	832	842	Carbamidomethylation
7	4033	tr|U3IV20|U3IV20_ANAPL	Mucin-5AC	K.TTSGVIEGTSAAFGNTWK.T	N	51.15	1825.885	18	11.4	913.96	2	8.73	1522	2	591	608	
7	4033	tr|U3IV20|U3IV20_ANAPL	Mucin-5AC	R.GLEGC(+57.02)YPHC(+57.02)PK.N	N	44.9	1316.564	11	-2.6	659.2877	2	5.44	787	4	1208	1218	Carbamidomethylation
7	4033	tr|U3IV20|U3IV20_ANAPL	Mucin-5AC	R.VC(+57.02)STWGNFHFK.N	N	44.23	1381.624	11	-0.9	461.5481	3	7.89	1322	4	85	95	Carbamidomethylation
7	4033	tr|U3IV20|U3IV20_ANAPL	Mucin-5AC	R.TPSIC(+57.02)PLFC(+57.02)DYYNPQGEC(+57.02)EWHYKPC(+57.02)GAPC(+57.02)MK.T	N	42.5	3864.596	31	-61.6	967.0968	4	10.84	1972	2	1163	1193	Carbamidomethylation
7	4033	tr|U3IV20|U3IV20_ANAPL	Mucin-5AC	K.VFLGNYELVLSDGRSD(-18.01)VIQR.T	Y	38.7	2261.18	20	38.7	754.7632	3	11.08	2025	2	972	991	Dehydration
7	4033	tr|U3IV20|U3IV20_ANAPL	Mucin-5AC	K.Q(-17.03)C(+57.02)SIITSEVFAK.C	N	36.96	1364.665	12	49.7	683.3735	2	10.15	1834	2	1100	1111	Pyro-glu from Q; Carbamidomethylation
7	4033	tr|U3IV20|U3IV20_ANAPL	Mucin-5AC	E.MPFQIR.S	N	24.55	790.416	6	-0.9	396.2149	2	7.59	1250	2	997	1002	

9	4036	tr|A0A093BIT2|A0A093BIT2_CHAPE	Lysyl oxidase 3	R.GWGNSDC(+57.02)SHEEDAGVIC(+57.02)KDER.I	N	79.46	2419.976	21	-0.2	606.001	4	6.01	884	4	24	44	Carbamidomethylation
9	4036	tr|A0A093BIT2|A0A093BIT2_CHAPE	Lysyl oxidase 3	R.MGQGTGPIHLNEVQC(+57.02)LGTEK.S	N	75.22	2168.035	20	5.5	723.6897	3	7.93	1332	3	250	269	Carbamidomethylation
9	4036	tr|A0A093BIT2|A0A093BIT2_CHAPE	Lysyl oxidase 3	R.VVC(+57.02)GMMGFPAEKK.V	N	63.43	1452.693	13	-5.1	485.2357	3	7.37	1194	2	107	119	Carbamidomethylation
9	4036	tr|A0A093BIT2|A0A093BIT2_CHAPE	Lysyl oxidase 3	R.VVC(+57.02)GMMGFPAEK.K	N	60.75	1324.598	12	0.9	663.3068	2	7.87	1319	2	107	118	Carbamidomethylation
9	4036	tr|A0A093BIT2|A0A093BIT2_CHAPE	Lysyl oxidase 3	R.ELGFGSAKEALTGAR.M	N	57.69	1505.784	15	-1.3	502.9345	3	7.77	1294	2	235	249	
9	4036	tr|A0A093BIT2|A0A093BIT2_CHAPE	Lysyl oxidase 3	R.IWLDNVNC(+57.02)AGGEK.S	N	51.45	1474.688	13	-59.7	738.307	2	7.69	1272	4	3	15	Carbamidomethylation
9	4036	tr|A0A093BIT2|A0A093BIT2_CHAPE	Lysyl oxidase 3	K.SIGDC(+57.02)KHRGWGNSDC(+57.02)SHEEDAGVIC(+57.02)KDER.I	N	47.52	3373.426	29	-0.3	675.6922	5	5.74	833	2	16	44	Carbamidomethylation
9	4036	tr|A0A093BIT2|A0A093BIT2_CHAPE	Lysyl oxidase 3	R.GWGN(+.98)SDC(+57.02)SHEEDAGVIC(+57.02)KDER.I	N	45.2	2420.96	21	2.5	606.2487	4	6.17	913	2	24	44	Deamidation (NQ); Carbamidomethylation
9	4036	tr|A0A093BIT2|A0A093BIT2_CHAPE	Lysyl oxidase 3	R.SSEWGTIC(+57.02)DDRWNLQSASVVC(+57.02)R.E	N	42.81	2625.17	22	0.7	876.0645	3	17.34	3265	3	213	234	Carbamidomethylation
9	4036	tr|A0A093BIT2|A0A093BIT2_CHAPE	Lysyl oxidase 3	R.YKDGWAQIC(+57.02)DQGWDSH(sub R)NSR.V	Y	37.37	2321.987	19	-4.6	581.5014	4	7.47	1220	4	88	106	Carbamidomethylation; Mutation
9	4036	tr|A0A093BIT2|A0A093BIT2_CHAPE	Lysyl oxidase 3	R.MGQGTGPIHLN(+.98)EVQC(+57.02)LGTEK.S	N	36.75	2169.02	20	6.8	724.0187	3	8.21	1400	2	250	269	Deamidation (NQ); Carbamidomethylation
9	4036	tr|A0A093BIT2|A0A093BIT2_CHAPE	Lysyl oxidase 3	K.SLWSC(+57.02)PYR.N	Y	32.53	1067.486	8	-2.5	534.7488	2	7.51	1228	2	270	277	Carbamidomethylation
9	4036	tr|A0A093BIT2|A0A093BIT2_CHAPE	Lysyl oxidase 3	W.GNSDC(+57.02)SHEEDAGVIC(+57.02)KDER.I	N	22.94	2176.875	19	0.4	726.6326	3	6.09	898	1	26	44	Carbamidomethylation
10	4037	tr|H0ZGZ6|H0ZGZ6_TAEGU	Mucin-5AC	K.SLKYTYNVDSC(+57.02)QPTC(+57.02)R.S	N	77.4	1990.888	16	0.3	664.6367	3	6.29	938	4	370	385	Carbamidomethylation
10	4037	tr|H0ZGZ6|H0ZGZ6_TAEGU	Mucin-5AC	K.YTYNVDSC(+57.02)QPTC(+57.02)R.S	N	64.29	1662.677	13	0.4	832.3459	2	5.9	864	2	373	385	Carbamidomethylation
10	4037	tr|H0ZGZ6|H0ZGZ6_TAEGU	Mucin-5AC	K.QC(+57.02)SIITSEVFAK.C	N	62.07	1381.691	12	11.6	691.8608	2	8.25	1407	2	758	769	Carbamidomethylation

10	4037	tr|H0ZGZ6|H0ZGZ6_TAEGU	Mucin-5AC	K.AWAQKQC(+57.02)SIITSEVFAK.C	N	61.8	1965.998	17	2.7	656.3418	3	8.51	1475	2	753	769	Carbamidomethylation
10	4037	tr|H0ZGZ6|H0ZGZ6_TAEGU	Mucin-5AC	R.VITENIPC(+57.02)GTTGTTC(+57.02)SK.S	N	61.05	1837.855	17	1.6	919.9363	2	6.38	958	4	610	626	Carbamidomethylation
10	4037	tr|H0ZGZ6|H0ZGZ6_TAEGU	Mucin-5AC	K.SC(+57.02)QTLDMEC(+57.02)YK.T	N	55.62	1433.563	11	0.7	717.7891	2	6.52	992	2	490	500	Carbamidomethylation
10	4037	tr|H0ZGZ6|H0ZGZ6_TAEGU	Mucin-5AC	K.TTSGVIEGTSAAFGNTWK.T	N	51.15	1825.885	18	11.4	913.96	2	8.73	1522	2	247	264	
10	4037	tr|H0ZGZ6|H0ZGZ6_TAEGU	Mucin-5AC	R.TPGGKMPFQIR.S	N	41.7	1230.654	11	-2.2	411.2245	3	7.39	1198	2	650	660	
10	4037	tr|H0ZGZ6|H0ZGZ6_TAEGU	Mucin-5AC	K.Q(-17.03)C(+57.02)SIITSEVFAK.C	N	36.96	1364.665	12	49.7	683.3735	2	10.15	1834	2	758	769	Pyro-glu from Q; Carbamidomethylation
10	4037	tr|H0ZGZ6|H0ZGZ6_TAEGU	Mucin-5AC	R.SLSEPDVTC(+57.02)ST(sub I)K.F	N	36.18	1322.602	12	0.9	662.3091	2	5.71	830	1	386	397	Carbamidomethylation; Mutation
10	4037	tr|H0ZGZ6|H0ZGZ6_TAEGU	Mucin-5AC	K.MPFQIR.S	N	24.55	790.416	6	-0.9	396.2149	2	7.59	1250	2	655	660	
10	4037	tr|H0ZGZ6|H0ZGZ6_TAEGU	Mucin-5AC	K.KIVSFQ(+.98)SVVK.N	Y	22.55	1134.665	10	-13	568.3323	2	8.64	1503	1	164	173	Deamidation (NQ)
11	4048	tr|A0A093GK45|A0A093GK45_PICPB	Lysyl oxidase 3	R.HLGFVAAAGWAHSAK.Y	Y	83.13	1521.784	15	-2.6	508.2673	3	7.55	1237	2	85	99	
11	4048	tr|A0A093GK45|A0A093GK45_PICPB	Lysyl oxidase 3	H.VVC(+57.02)GMMGFPAEKK.V	N	63.43	1452.693	13	-5.1	485.2357	3	7.37	1194	2	211	223	Carbamidomethylation
11	4048	tr|A0A093GK45|A0A093GK45_PICPB	Lysyl oxidase 3	H.VVC(+57.02)GMMGFPAEK.K	N	60.75	1324.598	12	0.9	663.3068	2	7.87	1319	2	211	222	Carbamidomethylation
11	4048	tr|A0A093GK45|A0A093GK45_PICPB	Lysyl oxidase 3	R.ELGFGSAKEALTGAR.M	N	57.69	1505.784	15	-1.3	502.9345	3	7.77	1294	2	346	360	
11	4048	tr|A0A093GK45|A0A093GK45_PICPB	Lysyl oxidase 3	R.IWLDNVNC(+57.02)AGGEK.S	N	51.45	1474.688	13	-59.7	738.307	2	7.69	1272	4	107	119	Carbamidomethylation
11	4048	tr|A0A093GK45|A0A093GK45_PICPB	Lysyl oxidase 3	H.W(+14.02)GLVC(+57.02)GEGWGTLEAMVAC(+57.02)R.Q	N	35.88	2164.986	19	3.2	722.6714	3	14.67	2763	2	443	461	Methylation; Carbamidomethylation
11	4048	tr|A0A093GK45|A0A093GK45_PICPB	Lysyl oxidase 3	H.WGLVC(+57.02)GE(+14.02)GWGTLEAMVAC(+57.02)R.Q	N	33.71	2164.986	19	0.3	1083.5	2	14.7	2769	1	443	461	Carbamidomethylation; Methyl ester
11	4048	tr|A0A093GK45|A0A093GK45_PICPB	Lysyl oxidase 3	R.C(+57.02)NIPYMGYET(+13.03)LIR.L	Y	30.38	1641.801	13	41.8	821.9419	2	10.27	1858	2	405	417	Carbamidomethylation; Michael addition with methylamine

13	4060	tr|A0A093GFU4|A0A093GFU4_PICPB	Mucin-5AC	R.SQSVVGNVLEFANSWK.V	N	68.76	1763.884	16	1.4	882.9506	2	13.65	2567	5	216	231	
13	4060	tr|A0A093GFU4|A0A093GFU4_PICPB	Mucin-5AC	K.QC(+57.02)SIITSEVFAK.C	N	62.07	1381.691	12	11.6	691.8608	2	8.25	1407	2	259	270	Carbamidomethylation
13	4060	tr|A0A093GFU4|A0A093GFU4_PICPB	Mucin-5AC	K.AWAQKQC(+57.02)SIITSEVFAK.C	N	61.8	1965.998	17	2.7	656.3418	3	8.51	1475	2	254	270	Carbamidomethylation
13	4060	tr|A0A093GFU4|A0A093GFU4_PICPB	Mucin-5AC	R.VITENIPC(+57.02)GTTGTTC(+57.02)SK.S	N	61.05	1837.855	17	1.6	919.9363	2	6.38	958	4	110	126	Carbamidomethylation
13	4060	tr|A0A093GFU4|A0A093GFU4_PICPB	Mucin-5AC	K.GGC(+57.02)IAPEDC(+57.02)PC(+57.02)VHN(+.98)GNFYNPGESIR.V	Y	37.35	2820.169	25	0.5	941.0641	3	7.96	1340	1	19	43	Carbamidomethylation; Deamidation (NQ)
13	4060	tr|A0A093GFU4|A0A093GFU4_PICPB	Mucin-5AC	K.Q(-17.03)C(+57.02)SIITSEVFAK.C	N	36.96	1364.665	12	49.7	683.3735	2	10.15	1834	2	259	270	Pyro-glu from Q; Carbamidomethylation
13	4060	tr|A0A093GFU4|A0A093GFU4_PICPB	Mucin-5AC	K.MPFQIR.S	N	24.55	790.416	6	-0.9	396.2149	2	7.59	1250	2	156	161	
14	4069	tr|U3KBI8|U3KBI8_FICAL	Mucin-5AC isoform X2	K.IISSC(+57.02)PQMAHHWIVDDNK.N	Y	51.31	2150.004	18	-5.1	538.5054	4	7.39	1199	2	359	376	Carbamidomethylation
14	4069	tr|U3KBI8|U3KBI8_FICAL	Mucin-5AC isoform X2	R.VYIDNYYC(+57.02)DAK.D	N	47.96	1422.613	11	0.2	712.3137	2	6.89	1082	2	238	248	Carbamidomethylation
14	4069	tr|U3KBI8|U3KBI8_FICAL	Mucin-5AC isoform X2	K.DC(+57.02)QEC(+57.02)VC(+57.02)DKNTLKVK(+27.99).C	Y	30.3	1923.849	15	7.7	481.9732	4	5.37	777	2	542	556	Carbamidomethylation; Formylation
14	4069	tr|U3KBI8|U3KBI8_FICAL	Mucin-5AC isoform X2	MC(+57.02)LNYR.I	N	29.9	855.3731	6	1.8	428.6946	2	6.04	889	2	1	6	Carbamidomethylation
14	4069	tr|U3KBI8|U3KBI8_FICAL	Mucin-5AC isoform X2	K.SILIFYK.S	N	27.55	882.5215	7	1.2	442.2686	2	8.71	1517	1	256	262	
14	4069	tr|U3KBI8|U3KBI8_FICAL	Mucin-5AC isoform X2	R.C(+57.02)QPVVC(+57.02)D(+14.02)TYC(+57.02)PLGYK(+43.99)YTVEPGQC(+57.02)C(+57.02)GTC(+57.02)K.A	Y	27.27	3457.422	28	13.6	692.501	5	6.42	967	1	670	697	Carbamidomethylation; Methyl ester; Carboxylation (DKW)
14	4069	tr|U3KBI8|U3KBI8_FICAL	Mucin-5AC isoform X2	R.GVC(+57.02)IDWR.G	N	27.02	904.4225	7	-2.5	453.2174	2	7.43	1208	2	454	460	Carbamidomethylation
14	4069	tr|U3KBI8|U3KBI8_FICAL	Mucin-5AC isoform X2	R.C(+57.02)QPVVC(+57.02)D(+14.02)TYC(+57.02)PLGYKYTVE(+43.99)PGQC(+57.02)C(+57.02)GTC(+57.02)K.A	Y	26.34	3457.422	28	12.6	865.3735	4	6.44	975	1	670	697	Carbamidomethylation; Methyl ester; Carboxylation (E)
14	4069	tr|U3KBI8|U3KBI8_FICAL	Mucin-5AC isoform X2	K.GC(+57.02)VFDGC(+57.02)R.I	N	25.25	969.3796	8	0.2	485.6972	2	5.24	758	1	425	432	Carbamidomethylation

14	4069	tr|U3KBI8|U3KBI8_FICAL	Mucin-5AC isoform X2	R.WPGEKWTKDCQEC(+57.02)VC(+57.02)DKNTLK.V	Y	22.53	2624.182	21	-4.9	657.0496	4	5.87	859	1	534	554	Carbamidomethylation
15	4095	tr|G1N931|G1N931_MELGA	Mucin-5AC	K.NQD(+14.02)QRGSFKMC(+57.02)LNYR.I	Y	33.3	1929.894	15	17.6	483.4892	4	6.44	972	2	118	132	Methyl ester; Carbamidomethylation
15	4095	tr|G1N931|G1N931_MELGA	Mucin-5AC	S.FKMC(+57.02)LNYR.I	N	32.36	1130.537	8	0.2	377.8528	3	7.2	1152	1	125	132	Carbamidomethylation
15	4095	tr|G1N931|G1N931_MELGA	Mucin-5AC	K.NQD(+14.02)QRGSFKMC(+57.02)LNYRIR.V	Y	31.02	2199.079	17	19.9	440.8318	5	6.91	1089	1	118	134	Methyl ester; Carbamidomethylation
15	4095	tr|G1N931|G1N931_MELGA	Mucin-5AC	K.N(+14.02)QDQRGSFKMC(+57.02)LNYRIR.V	Y	30.42	2199.079	17	20.4	440.832	5	6.93	1093	1	118	134	Methylation; Carbamidomethylation
15	4095	tr|G1N931|G1N931_MELGA	Mucin-5AC	K.MC(+57.02)LNYR.I	N	29.9	855.3731	6	1.8	428.6946	2	6.04	889	2	127	132	Carbamidomethylation
15	4095	tr|G1N931|G1N931_MELGA	Mucin-5AC	K.SIIIFYK.T	N	27.55	882.5215	7	1.2	442.2686	2	8.71	1517	1	387	393	
15	4095	tr|G1N931|G1N931_MELGA	Mucin-5AC	R.GVC(+57.02)IDWR.G	N	27.02	904.4225	7	-2.5	453.2174	2	7.43	1208	2	585	591	Carbamidomethylation
15	4095	tr|G1N931|G1N931_MELGA	Mucin-5AC	K.GC(+57.02)VFDGC(+57.02)R.I	N	25.25	969.3796	8	0.2	485.6972	2	5.24	758	1	556	563	Carbamidomethylation
16	4071	tr|A0A091I517|A0A091I517_CALAN	Hypothetical protein N300_06305	R.VYIDNYYC(+57.02)DAK.D	N	47.96	1422.613	11	0.2	712.3137	2	6.89	1082	2	92	102	Carbamidomethylation
16	4071	tr|A0A091I517|A0A091I517_CALAN	Hypothetical protein N300_06305	K.LIWSEIFADC(+57.02)HS(-2.02)VIPPEPFFKGC(+57.02)VFDGC(+57.02)R.I	Y	37.1	3480.609	29	12.2	1161.225	3	14.65	2760	4	258	286	Carbamidomethylation; 2-amino-3-oxo-butanoic_acid
16	4071	tr|A0A091I517|A0A091I517_CALAN	Hypothetical protein N300_06305	K.SIIIFYK.S	N	27.55	882.5215	7	1.2	442.2686	2	8.71	1517	1	110	116	
16	4071	tr|A0A091I517|A0A091I517_CALAN	Hypothetical protein N300_06305	R.GVC(+57.02)IDWR.G	N	27.02	904.4225	7	-2.5	453.2174	2	7.43	1208	2	308	314	Carbamidomethylation
16	4071	tr|A0A091I517|A0A091I517_CALAN	Hypothetical protein N300_06305	K.GC(+57.02)VFDGC(+57.02)R.I	N	25.25	969.3796	8	0.2	485.6972	2	5.24	758	1	279	286	Carbamidomethylation
16	4071	tr|A0A091I517|A0A091I517_CALAN	Hypothetical protein N300_06305	G.DNK(+70.04)VEVIPTHC(+57.02)PPVK.E	N	23.97	1801.94	15	7.5	451.4955	4	6.48	982	1	10	24	Crotonaldehyde; Carbamidomethylation
17	4081	tr|A0A0Q3SEH9|A0A0Q3	Hypothetical protein	K.C(+57.02)KPVIC(+57.02)DTYC(+57.02)P(+15.99)LGYKYT	Y	63.8	2281.058	18	-13	571.2644	4	6.65	1022	4	378	395	Carbamidomethylation; Hydroxylation

		SEH9_AMAAE	AAES_28655	K.K													
17	4081	tr|A0A0Q3SEH9|A0A0Q3SEH9_AMAAE	Hypothetical protein AAES_28655	K.C(+57.02)KPVIC(+57.02)DTYC(+57.02)P(+15.99)LGYK.Y	Y	52.93	1888.852	15	-18.9	630.6128	3	6.63	1018	2	378	392	Carbamidomethylation; Hydroxylation
17	4081	tr|A0A0Q3SEH9|A0A0Q3SEH9_AMAAE	Hypothetical protein AAES_28655	R.VC(+57.02)STWGNFHFK.T	N	44.23	1381.624	11	-0.9	461.5481	3	7.89	1322	4	572	582	Carbamidomethylation
17	4081	tr|A0A0Q3SEH9|A0A0Q3SEH9_AMAAE	Hypothetical protein AAES_28655	K.SIIIFYK.S	N	27.55	882.5215	7	1.2	442.2686	2	8.71	1517	1	91	97	
17	4081	tr|A0A0Q3SEH9|A0A0Q3SEH9_AMAAE	Hypothetical protein AAES_28655	K.GC(+57.02)VFDGC(+57.02)R.I	N	25.25	969.3796	8	0.2	485.6972	2	5.24	758	1	260	267	Carbamidomethylation
18	4092	tr|A0A093PIM5|A0A093PIM5_9PASS	Acidic mammalian chitinase	A.YVLTC(+57.02)YFTNWAQYRPGLGK.Y	Y	55.67	2336.141	19	0	779.7209	3	12.37	2299	2	16	34	Carbamidomethylation
18	4092	tr|A0A093PIM5|A0A093PIM5_9PASS	Acidic mammalian chitinase	K.TLLAIGGWNFGTAK.F	N	45.97	1447.782	14	0.7	724.8989	2	12.06	2235	3	86	99	
18	4092	tr|A0A093PIM5|A0A093PIM5_9PASS	Acidic mammalian chitinase	N.EGKYPLIS(+14.02)TLKK.G	N	28.33	1389.823	12	5.1	348.4648	4	6.71	1039	3	368	379	Methylation
18	4092	tr|A0A093PIM5|A0A093PIM5_9PASS	Acidic mammalian chitinase	K.YPLIT(sub S)TLKK.G	N	24.4	1075.664	9	3.6	359.5633	3	7.24	1164	1	371	379	Mutation
18	4092	tr|A0A093PIM5|A0A093PIM5_9PASS	Acidic mammalian chitinase	K.YPLIS(+14.02)TLKK.G	N	22.66	1075.664	9	3.5	359.5632	3	7.22	1158	1	371	379	Methylation
19	4080	tr|A0A091T9Y4|A0A091T9Y4_PHALP	Mucin-5AC	K.FGNNTEGQC(+57.02)GTC(+57.02)TNNKLDEC(+57.02)RLPSGK.V	N	35.64	2956.286	26	0.2	740.079	4	6.15	908	2	187	212	Carbamidomethylation
19	4080	tr|A0A091T9Y4|A0A091T9Y4_PHALP	Mucin-5AC	K.LIWSE(sub K)IFAEC(+57.02)HAVIPPEPFFK.G	Y	34.7	2529.277	21	-0.4	844.0992	3	14.86	2800	4	258	278	Carbamidomethylation; Mutation
19	4080	tr|A0A091T9Y4|A0A091T9Y4_PHALP	Mucin-5AC	K.SIIIFYK.F	N	27.55	882.5215	7	1.2	442.2686	2	8.71	1517	1	110	116	
19	4080	tr|A0A091T9Y4|A0A091T9Y4_PHALP	Mucin-5AC	R.GVC(+57.02)IDWR.G	N	27.02	904.4225	7	-2.5	453.2174	2	7.43	1208	2	308	314	Carbamidomethylation
19	4080	tr|A0A091T9Y4|A0A091T9Y4_PHALP	Mucin-5AC	G.DNK(+70.04)VEVIPTHC(+57.02)PPVK.E	N	23.97	1801.94	15	7.5	451.4955	4	6.48	982	1	10	24	Crotonaldehyde; Carbamidomethylation
20	4096	tr|A0A1D5PU28|A0A1D5PU28_CHICK	Mucin-5AC	K.SC(+57.02)PAFN(+.98)PDLC(+57.02)EPDN(+.98)IQLSDDGC(+57.02)C(+57.02)R.V	Y	46.35	2841.099	24	-3.5	948.0368	3	7.57	1243	1	929	952	Carbamidomethylation; Deamidation (NQ)

20	4096	tr|A0A1D5PU28|A0A1D5PU28_CHICK	Mucin-5AC	K.SC(+57.02)PAFNPDLC(+57.02)EPDN(+.98)IQ(+.98)LSDDGC(+57.02)C(+57.02)R.V	Y	42.17	2841.099	24	-0.3	948.0399	3	7.55	1239	1	929	952	Carbamidomethylation; Deamidation (NQ)
20	4096	tr|A0A1D5PU28|A0A1D5PU28_CHICK	Mucin-5AC	S.FKMC(+57.02)LNYR.I	N	32.36	1130.537	8	0.2	377.8528	3	7.2	1152	1	173	180	Carbamidomethylation
20	4096	tr|A0A1D5PU28|A0A1D5PU28_CHICK	Mucin-5AC	MC(+57.02)LNYR.I	N	29.9	855.3731	6	1.8	428.6946	2	6.04	889	2	1	6	Carbamidomethylation
20	4096	tr|A0A1D5PU28|A0A1D5PU28_CHICK	Mucin-5AC	K.SIIIFYK.S	N	27.55	882.5215	7	1.2	442.2686	2	8.71	1517	1	443	449	
20	4096	tr|A0A1D5PU28|A0A1D5PU28_CHICK	Mucin-5AC	R.GVC(+57.02)IDWR.G	N	27.02	904.4225	7	-2.5	453.2174	2	7.43	1208	2	641	647	Carbamidomethylation
20	4096	tr|A0A1D5PU28|A0A1D5PU28_CHICK	Mucin-5AC	K.GC(+57.02)VFDGC(+57.02)R.I	N	25.25	969.3796	8	0.2	485.6972	2	5.24	758	1	612	619	Carbamidomethylation
22	4108	tr|A0A091TEI1|A0A091TEI1_NESNO	Acidic mammalian chitinase	R.GSPAQDKTLFTVLVKEMVAAFEQEAQ.Q	Y	56.96	2836.432	26	13.2	710.1246	4	16.81	3162	4	138	163	
22	4108	tr|A0A091TEI1|A0A091TEI1_NESNO	Acidic mammalian chitinase	R.GSPAQDKTLFTVLVK.E	Y	56.56	1602.898	15	41.6	535.3289	3	9.59	1703	3	138	152	
22	4108	tr|A0A091TEI1|A0A091TEI1_NESNO	Acidic mammalian chitinase	R.GSPAQDKTLFTVLVKEMVAAFEQEAQQVNKPRLM(-29.99).V	Y	33.28	3772.982	34	-48.3	944.2073	4	16.82	3165	1	138	171	Homoserine
22	4108	tr|A0A091TEI1|A0A091TEI1_NESNO	Acidic mammalian chitinase	K.TLFTVLVK.E	N	29.69	919.5742	8	30.8	460.8085	2	9.96	1789	2	145	152	
23	4058	tr|A0A093BFV9|A0A093BFV9_CHAPE	Acidic mammalian chitinase	K.EMVAAFEQEAR.Q	Y	51.18	1279.587	11	-0.4	640.8004	2	7.26	1167	2	143	153	
23	4058	tr|A0A093BFV9|A0A093BFV9_CHAPE	Acidic mammalian chitinase	K.TLLAIGGWNFGTAK.F	N	45.97	1447.782	14	0.7	724.8989	2	12.06	2235	3	74	87	
23	4058	tr|A0A093BFV9|A0A093BFV9_CHAPE	Acidic mammalian chitinase	K.LLVGFPTYGR.T	Y	40.33	1121.623	10	4.7	561.8215	2	9.34	1650	2	237	246	
23	4058	tr|A0A093BFV9|A0A093BFV9_CHAPE	Acidic mammalian chitinase	K.TLFTVLVK.E	N	29.69	919.5742	8	30.8	460.8085	2	9.96	1789	2	135	142	
24	4070	tr|A0A093F6E7|A0A093F6E7_TYTAL	Acidic mammalian chitinase	K.TLLAIGGWNFGTAK.F	N	45.97	1447.782	14	0.7	724.8989	2	12.06	2235	3	80	93	
24	4070	tr|A0A093F6E7|A0A093F	Acidic mammalian chitinase	K.GNEWVGYDNIK.S	N	42	1293.599	11	-8.8	647.801	2	7.43	1207	2	318	328	

		6E7_TYTAL															
24	4070	tr|A0A093F6E7|A0A093F6E7_TYTAL	Acidic mammalian chitinase	K.LLVGFPTYGHNFNLQNPAD(+14.02)TAVGAPATGPGPAGPYTR.Q	Y	39.07	3751.875	37	8.9	938.9843	4	12.37	2298	2	248	284	Methyl ester
24	4070	tr|A0A093F6E7|A0A093F6E7_TYTAL	Acidic mammalian chitinase	K.TLFTVLVK.E	N	29.69	919.5742	8	30.8	460.8085	2	9.96	1789	2	141	148	
25	4072	tr|H0ZGX3|H0ZGX3_TAEGU	Mucin-5AC	R.VYIDNYYC(+57.02)DAK.D	N	47.96	1422.613	11	0.2	712.3137	2	6.89	1082	2	92	102	Carbamidomethylation
25	4072	tr|H0ZGX3|H0ZGX3_TAEGU	Mucin-5AC	K.SIIIFYK.S	N	27.55	882.5215	7	1.2	442.2686	2	8.71	1517	1	110	116	
25	4072	tr|H0ZGX3|H0ZGX3_TAEGU	Mucin-5AC	R.GVC(+57.02)IDWR.G	N	27.02	904.4225	7	-2.5	453.2174	2	7.43	1208	2	308	314	Carbamidomethylation
25	4072	tr|H0ZGX3|H0ZGX3_TAEGU	Mucin-5AC	K.GC(+57.02)VFDGC(+57.02)R.I	N	25.25	969.3796	8	0.2	485.6972	2	5.24	758	1	279	286	Carbamidomethylation
25	4072	tr|H0ZGX3|H0ZGX3_TAEGU	Mucin-5AC	R.N(+42.01)VTLTC(+57.02)SD(+21.98)GTSLDHSYTYVEK.C	Y	24.57	2453.067	21	35.8	491.6382	5	6.49	985	1	693	713	Acetylation (N-term); Carbamidomethylation; Sodium adduct
25	4073	tr|H0ZGW8|H0ZGW8_TAEGU	Mucin-5AC	R.VYIDNYYC(+57.02)DAK.D	N	47.96	1422.613	11	0.2	712.3137	2	6.89	1082	2	92	102	Carbamidomethylation
25	4073	tr|H0ZGW8|H0ZGW8_TAEGU	Mucin-5AC	K.SIIIFYK.S	N	27.55	882.5215	7	1.2	442.2686	2	8.71	1517	1	110	116	
25	4073	tr|H0ZGW8|H0ZGW8_TAEGU	Mucin-5AC	R.GVC(+57.02)IDWR.G	N	27.02	904.4225	7	-2.5	453.2174	2	7.43	1208	2	308	314	Carbamidomethylation
25	4073	tr|H0ZGW8|H0ZGW8_TAEGU	Mucin-5AC	K.GC(+57.02)VFDGC(+57.02)R.I	N	25.25	969.3796	8	0.2	485.6972	2	5.24	758	1	279	286	Carbamidomethylation
25	4073	tr|H0ZGW8|H0ZGW8_TAEGU	Mucin-5AC	R.N(+42.01)VTLTC(+57.02)SD(+21.98)GTSLDHSYTYVEK.C	Y	24.57	2453.067	21	35.8	491.6382	5	6.49	985	1	696	716	Acetylation (N-term); Carbamidomethylation; Sodium adduct
26	4132	tr|A0A091NM19|A0A091NM19_APAVI	Ovoinhibitor	R.TEIDGHVLVAC(+57.02)PR.I	Y	67.17	1465.735	13	1	733.8754	2	6.98	1102	4	76	88	Carbamidomethylation
26	4132	tr|A0A091NM19|A0A091NM19_APAVI	Ovoinhibitor	R.YQ(sub R)RTEIDGHVLVAC(+57.02)PR.I	Y	42.02	1912.958	16	1.9	479.2476	4	6.75	1047	2	73	88	Carbamidomethylation; Mutation
26	4132	tr|A0A091NM19|A0A091NM19_APAVI	Ovoinhibitor	E.IDGHVLVAC(+57.02)PR.I	Y	26.16	1235.644	11	-0.4	618.8292	2	7.02	1112	1	78	88	Carbamidomethylation

27	4079	tr|A0A091T2D6|A0A091T2D6_9AVES	Hypothetical protein N334_09374	K.YHGC(+57.02)VSPAPVEMN(sub T)YC(+57.02)EGSC(+57.02)DAYSR.Y	Y	36.61	2808.104	24	-12.9	937.0297	3	7.35	1188	1	643	666	Carbamidomethylation; Mutation
27	4079	tr|A0A091T2D6|A0A091T2D6_9AVES	Hypothetical protein N334_09375	K.FGNNTEGQC(+57.02)GTC(+57.02)TNNKLDEC(+57.02)RLPSGK.I	N	35.64	2956.286	26	0.2	740.079	4	6.15	908	2	187	212	Carbamidomethylation
27	4079	tr|A0A091T2D6|A0A091T2D6_9AVES	Hypothetical protein N334_09376	K.SIIIFYK.S	N	27.55	882.5215	7	1.2	442.2686	2	8.71	1517	1	110	116	
27	4079	tr|A0A091T2D6|A0A091T2D6_9AVES	Hypothetical protein N334_09377	R.GVC(+57.02)IDWR.G	N	27.02	904.4225	7	-2.5	453.2174	2	7.43	1208	2	307	313	Carbamidomethylation
27	4079	tr|A0A091T2D6|A0A091T2D6_9AVES	Hypothetical protein N334_09378	K.GC(+57.02)VFDGC(+57.02)R.I	N	25.25	969.3796	8	0.2	485.6972	2	5.24	758	1	278	285	Carbamidomethylation
28	4280	tr|H0ZM61|H0ZM61_TAEGU	Deleted in malignant brain tumors 1 protein	E.TITYSNVIK.V	Y	27.32	1037.576	9	0.1	519.7952	2	6.89	1085	1	180	188	
28	4280	tr|H0ZM61|H0ZM61_TAEGU	Deleted in malignant brain tumors 1 protein	R.NYPD(sub N)NANC(+57.02)VWEIQVKN(sub S)NFR.V	Y	25.42	2380.102	19	15.2	596.0417	4	8.18	1392	1	20	38	Carbamidomethylation; Mutation
28	4280	tr|H0ZM61|H0ZM61_TAEGU	Deleted in malignant brain tumors 1 protein	R.NYPD(sub N)NANC(+57.02)VWEIQVK.S	Y	24.62	1848.846	15	21.1	617.3024	3	8	1350	2	20	34	Carbamidomethylation; Mutation
28	4280	tr|H0ZM61|H0ZM61_TAEGU	Deleted in malignant brain tumors 1 protein	R.NYPND(sub N)ANC(+57.02)VWEIQVK.S	Y	22.54	1848.846	15	22.9	925.4517	2	8.08	1370	1	20	34	Carbamidomethylation; Mutation
29	4088	tr|A0A093JL69|A0A093JL69_STRCA	45 kDa calcium-binding protein	R.WYQADNPPPDLLLNEEEFLSFLHPEHSR.G	Y	68.62	3392.61	28	-0.4	849.1594	4	14.96	2818	2	174	201	
29	4088	tr|A0A093JL69|A0A093JL69_STRCA	45 kDa calcium-binding protein	R.AVDPDGDGHVSWDEYKVK.F	Y	55.37	2015.922	18	1.3	504.9885	4	6.96	1098	2	118	135	
29	4087	tr|A0A093GZT0|A0A093GZT0_PICPB	45 kDa calcium-binding protein	R.WYQADNPPPDLLLNEEEFLSFLHPEHSR.G	Y	68.62	3392.61	28	-0.4	849.1594	4	14.96	2818	2	174	201	
29	4087	tr|A0A093GZT0|A0A093GZT0_PICPB	45 kDa calcium-binding protein	R.AVDPDGDGHVSWDEYKVK.F	Y	55.37	2015.922	18	1.3	504.9885	4	6.96	1098	2	118	135	
29	4086	tr|A0A091JRH3|A0A091JRH3_9AVES	45 kDa calcium-binding protein	R.WYQADNPPPDLLLNEEEFLSFLHPEHSR.G	Y	68.62	3392.61	28	-0.4	849.1594	4	14.96	2818	2	174	201	
29	4086	tr|A0A091JRH3|A0A091JRH3_9AVES	45 kDa calcium-binding protein	R.AVDPDGDGHVSWDEYKVK.F	Y	55.37	2015.922	18	1.3	504.9885	4	6.96	1098	2	118	135	
29	4085	tr|A0A093Q7F3|A0A093Q7F3_9PASS	45 kDa calcium-binding protein	R.WYQADNPPPDLLLNEEEFLSFLHPEHSR.G	Y	68.62	3392.61	28	-0.4	849.1594	4	14.96	2818	2	174	201	

29	4085	tr|A0A093Q7F3|A0A093Q7F3_9PASS	45 kDa calcium-binding protein	R.AVDPDGDGHVSWDEYKVK.F	Y	55.37	2015.922	18	1.3	504.9885	4	6.96	1098	2	118	135	
30	4101	tr|A0A093IYD2|A0A093IYD2_PICPB	Acidic mammalian chitinase	K.GNEWVGYDNIK.S	N	42	1293.599	11	-8.8	647.801	2	7.43	1207	2	245	255	
30	4101	tr|A0A093IYD2|A0A093IYD2_PICPB	Acidic mammalian chitinase	K.EMVAAFEQEAK.E	Y	38.8	1251.58	11	1.9	626.7987	2	7.11	1134	2	76	86	
31	4307	tr|A0A091P1K5|A0A091P1K5_HALAL	Lysosomal-trafficking regulator	L.LVQFAFR.E	Y	23.04	879.4966	7	1.3	440.7562	2	7.98	1342	2	2351	2357	
31	4310	tr|U3KGE0|U3KGE0_FICAL	Lysosomal-trafficking regulator	L.LVQFAFR.E	Y	23.04	879.4966	7	1.3	440.7562	2	7.98	1342	2	3440	3446	
31	4322	tr|A0A1D5NWU9|A0A1D5NWU9_CHICK	Lysosomal-trafficking regulator	L.LVQFAFR.E	Y	23.04	879.4966	7	1.3	440.7562	2	7.98	1342	2	1489	1495	
31	4325	tr|A0A093FWF9|A0A093FWF9_PICPB	Lysosomal-trafficking regulator	L.LVQFAFR.E	Y	23.04	879.4966	7	1.3	440.7562	2	7.98	1342	2	2331	2337	
31	4326	tr|A0A091LIV9|A0A091LIV9_CATAU	Lysosomal-trafficking regulator	L.LVQFAFR.E	Y	23.04	879.4966	7	1.3	440.7562	2	7.98	1342	2	2348	2354	
31	4327	tr|A0A093F2B5|A0A093F2B5_TYTAL	Lysosomal-trafficking regulator	L.LVQFAFR.E	Y	23.04	879.4966	7	1.3	440.7562	2	7.98	1342	2	2349	2355	
31	4333	tr|A0A091W1W3|A0A091W1W3_OPIHO	Lysosomal-trafficking regulator	L.LVQFAFR.E	Y	23.04	879.4966	7	1.3	440.7562	2	7.98	1342	2	2352	2358	
31	4332	tr|A0A087R6Y7|A0A087R6Y7_APTFO	Lysosomal-trafficking regulator	L.LVQFAFR.E	Y	23.04	879.4966	7	1.3	440.7562	2	7.98	1342	2	2352	2358	
31	4331	tr|A0A091PAF4|A0A091PAF4_LEPDC	Lysosomal-trafficking regulator	L.LVQFAFR.E	Y	23.04	879.4966	7	1.3	440.7562	2	7.98	1342	2	2352	2358	
31	4330	tr|A0A093LET3|A0A093LET3_FULGA	Lysosomal-trafficking regulator	L.LVQFAFR.E	Y	23.04	879.4966	7	1.3	440.7562	2	7.98	1342	2	2352	2358	
31	4329	tr|A0A0A0AJN3|A0A0A0AJN3_CHAVO	Lysosomal-trafficking regulator	L.LVQFAFR.E	Y	23.04	879.4966	7	1.3	440.7562	2	7.98	1342	2	2352	2358	
31	4328	tr|A0A091T8Q1|A0A091T8Q1_PHALP	Lysosomal-trafficking regulator	L.LVQFAFR.E	Y	23.04	879.4966	7	1.3	440.7562	2	7.98	1342	2	2352	2358	
31	4336	tr|A0A091VSX4|A0A091VSX4_NIPNI	Lysosomal-trafficking regulator	L.LVQFAFR.E	Y	23.04	879.4966	7	1.3	440.7562	2	7.98	1342	2	2353	2359	

31	4335	tr|A0A091SJ61|A0A091SJ61_9AVES	Lysosomal-trafficking regulator	L.LVQFAFR.E	Y	23.04	879.4966	7	1.3	440.7562	2	7.98	1342	2	2353	2359	
31	4334	tr|A0A093P913|A0A093P913_PYGAD	Lysosomal-trafficking regulator	L.LVQFAFR.E	Y	23.04	879.4966	7	1.3	440.7562	2	7.98	1342	2	2353	2359	
31	4337	tr|A0A091MNM3|A0A091MNM3_9PASS	Lysosomal-trafficking regulator	L.LVQFAFR.E	Y	23.04	879.4966	7	1.3	440.7562	2	7.98	1342	2	2357	2363	
31	4338	tr|A0A091RFP2|A0A091RFP2_MERNU	Lysosomal-trafficking regulator	L.LVQFAFR.E	Y	23.04	879.4966	7	1.3	440.7562	2	7.98	1342	2	2358	2364	
31	4342	tr|A0A0Q3PLA9|A0A0Q3PLA9_AMAAE	Lysosomal-trafficking regulator	L.LVQFAFR.E	Y	23.04	879.4966	7	1.3	440.7562	2	7.98	1342	2	3395	3401	
31	4343	tr|A0A1D5PA68|A0A1D5PA68_CHICK	Lysosomal-trafficking regulator	L.LVQFAFR.E	Y	23.04	879.4966	7	1.3	440.7562	2	7.98	1342	2	3432	3438	
31	4344	tr|R0JM22|R0JM22_ANAPL	Lysosomal-trafficking regulator	L.LVQFAFR.E	Y	23.04	879.4966	7	1.3	440.7562	2	7.98	1342	2	3436	3442	
32	4089	tr|A0A0Q3XB34|A0A0Q3XB34_AMAAE	Lysyl oxidase 3	R.ELGFGSAKEALTGAR.M	N	57.69	1505.784	15	-1.3	502.9345	3	7.77	1294	2	139	153	
32	4089	tr|A0A0Q3XB34|A0A0Q3XB34_AMAAE	Lysyl oxidase 3	R.VEVAVGAGAGEQPR.W	Y	49.8	1338.689	14	0.4	670.3521	2	5.89	862	2	222	235	
33	4348	tr|A0A091N6E4|A0A091N6E4_9PASS	Ovoinhibitor	R.NTKTGEE(sub A)IGACPFILR.E	Y	25.79	1747.893	16	52	874.9991	2	11.76	2168	2	272	287	Mutation
34	4218	tr|A0A094MEI7|A0A094MEI7_ANTCR	Ovoinhibitor	G.QIMAC(+57.02)TMIYDPVC(+57.02)GTDGVTYASEC(+57.02)TLC(+57.02)AHNLEHR.T	Y	36.95	3972.703	34	75.3	994.2579	4	11.01	2007	2	344	377	Carbamidomethylation
35	4357	tr|A0A093BE17|A0A093BE17_CHAPE	Deleted in malignant brain tumors 1 protein	R.KSPSVYLKC(+57.02)EFVVC(+57.02)Q(sub R)A(sub T)YDYA(sub H)SR.C	Y	27.19	2669.262	22	25	668.3394	4	8.14	1382	1	80	101	Carbamidomethylation; Mutation
36	4241	tr|U3JHL5|U3JHL5_FICAL	78 kDa glucose-regulated protein/ Heat shock protein 70kDa	K.SQIFSTASDNQPTVTIK.V	Y	33.66	1835.927	17	6.6	918.9766	2	8.27	1412	2	449	465	
36	4240	tr|H0ZAB3|H0ZAB3_TAEGU	79 kDa glucose-regulated protein/ Heat shock protein 70kDa	K.SQIFSTASDNQPTVTIK.V	Y	33.66	1835.927	17	6.6	918.9766	2	8.27	1412	2	448	464	

36	4239	tr|A0PA15|A0PA15_COTJA	80 kDa glucose-regulated protein/ Heat shock protein 70kDa	K.SQIFSTASDNQPTVTIK.V	Y	33.66	1835.927	17	6.6	918.9766	2	8.27	1412	2	446	462	
36	4238	tr|A0ZT13|A0ZT13_COTJA	81 kDa glucose-regulated protein/ Heat shock protein 70kDa	K.SQIFSTASDNQPTVTIK.V	Y	33.66	1835.927	17	6.6	918.9766	2	8.27	1412	2	446	462	
36	4237	tr|A0A091F8D2|A0A091F8D2_CORBR	82 kDa glucose-regulated protein/ Heat shock protein 70kDa	K.SQIFSTASDNQPTVTIK.V	Y	33.66	1835.927	17	6.6	918.9766	2	8.27	1412	2	447	463	
36	4236	tr|A0A091KV08|A0A091KV08_9GRUI	83 kDa glucose-regulated protein/ Heat shock protein 70kDa	K.SQIFSTASDNQPTVTIK.V	Y	33.66	1835.927	17	6.6	918.9766	2	8.27	1412	2	414	430	
36	4235	tr|A0A093QLZ7|A0A093QLZ7_9PASS	84 kDa glucose-regulated protein/ Heat shock protein 70kDa	K.SQIFSTASDNQPTVTIK.V	Y	33.66	1835.927	17	6.6	918.9766	2	8.27	1412	2	407	423	
36	4234	tr|U3I640|U3I640_ANAPL	85 kDa glucose-regulated protein/ Heat shock protein 70kDa	K.SQIFSTASDNQPTVTIK.V	Y	33.66	1835.927	17	6.6	918.9766	2	8.27	1412	2	406	422	
36	4233	tr|A0A091V9R8|A0A091V9R8_OPIHO	86 kDa glucose-regulated protein/ Heat shock protein 70kDa	K.SQIFSTASDNQPTVTIK.V	Y	33.66	1835.927	17	6.6	918.9766	2	8.27	1412	2	407	423	
36	4232	tr|A0A091VTR8|A0A091VTR8_NIPNI	87 kDa glucose-regulated protein/ Heat shock protein 70kDa	K.SQIFSTASDNQPTVTIK.V	Y	33.66	1835.927	17	6.6	918.9766	2	8.27	1412	2	407	423	
36	4231	tr|A0A091HVD4|A0A091HVD4_CALAN	88 kDa glucose-regulated protein/ Heat shock protein 70kDa	K.SQIFSTASDNQPTVTIK.V	Y	33.66	1835.927	17	6.6	918.9766	2	8.27	1412	2	407	423	
36	4230	tr|A0A087R4J8|A0A087R4J8_APTFO	89 kDa glucose-regulated protein/ Heat shock protein 70kDa	K.SQIFSTASDNQPTVTIK.V	Y	33.66	1835.927	17	6.6	918.9766	2	8.27	1412	2	407	423	
36	4229	tr|A0A093J3B2|A0A093J3B2_PICPB	90 kDa glucose-regulated protein/ Heat shock protein 70kDa	K.SQIFSTASDNQPTVTIK.V	Y	33.66	1835.927	17	6.6	918.9766	2	8.27	1412	2	407	423	
36	4228	tr|A0A093EHT4|A0A093EHT4_TYTAL	91 kDa glucose-regulated protein/ Heat shock protein 70kDa	K.SQIFSTASDNQPTVTIK.V	Y	33.66	1835.927	17	6.6	918.9766	2	8.27	1412	2	407	423	
36	4227	tr|A0A091LT36|A0A091LT36_CARIC	92 kDa glucose-regulated protein/ Heat shock protein 70kDa	K.SQIFSTASDNQPTVTIK.V	Y	33.66	1835.927	17	6.6	918.9766	2	8.27	1412	2	407	423	
36	4226	tr|A0A091H8K7|A0A091	93 kDa glucose-regulated protein/ Heat shock protein	K.SQIFSTASDNQPTVTIK.V	Y	33.66	1835.927	17	6.6	918.9766	2	8.27	1412	2	407	423	

		H8K7_9AVES	70kDa														
36	4225	tr|A0A093CJ49|A0A093CJ49_9AVES	94 kDa glucose-regulated protein/ Heat shock protein 70kDa	K.SQIFSTASDNQPTVTIK.V	Y	33.66	1835.927	17	6.6	918.9766	2	8.27	1412	2	407	423	
36	4224	tr|A0A093HUL5|A0A093HUL5_STRCA	95 kDa glucose-regulated protein/ Heat shock protein 70kDa	K.SQIFSTASDNQPTVTIK.V	Y	33.66	1835.927	17	6.6	918.9766	2	8.27	1412	2	407	423	
36	4223	tr|A0A091MLL1|A0A091MLL1_9PASS	96 kDa glucose-regulated protein/ Heat shock protein 70kDa	K.SQIFSTASDNQPTVTIK.V	Y	33.66	1835.927	17	6.6	918.9766	2	8.27	1412	2	407	423	
36	4222	tr|A0A091U752|A0A091U752_PHORB	97 kDa glucose-regulated protein/ Heat shock protein 70kDa	K.SQIFSTASDNQPTVTIK.V	Y	33.66	1835.927	17	6.6	918.9766	2	8.27	1412	2	396	412	
36	4221	tr|A0A093J4G2|A0A093J4G2_EURHL	98 kDa glucose-regulated protein/ Heat shock protein 70kDa	K.SQIFSTASDNQPTVTIK.V	Y	33.66	1835.927	17	6.6	918.9766	2	8.27	1412	2	393	409	
36	4220	tr|G1N8R5|G1N8R5_MELGA	99 kDa glucose-regulated protein/ Heat shock protein 70kDa	K.SQIFSTASDNQPTVTIK.V	Y	33.66	1835.927	17	6.6	918.9766	2	8.27	1412	2	407	423	
37	4248	tr|A0A093TKC6|A0A093TKC6_PHACA	Nucleobindin-2	R.LVTLEEFLR.A	Y	27.89	1118.634	9	27.1	560.3392	2	12.2	2264	2	312	320	
37	4249	tr|U3ISH1|U3ISH1_ANAPL	Nucleobindin-2	R.LVTLEEFLR.A	Y	27.89	1118.634	9	27.1	560.3392	2	12.2	2264	2	320	328	
37	4259	tr|A0A093GVR1|A0A093GVR1_PICPB	Nucleobindin-2	R.LVTLEEFLR.A	Y	27.89	1118.634	9	27.1	560.3392	2	12.2	2264	2	313	321	
37	4261	tr|A0A093IF41|A0A093IF41_FULGA	Nucleobindin-2	R.LVTLEEFLR.A	Y	27.89	1118.634	9	27.1	560.3392	2	12.2	2264	2	312	320	
37	4260	tr|A0A091TQN7|A0A091TQN7_PHALP	Nucleobindin-2	R.LVTLEEFLR.A	Y	27.89	1118.634	9	27.1	560.3392	2	12.2	2264	2	312	320	
37	4262	tr|A0A091SAC3|A0A091SAC3_NESNO	Nucleobindin-2	R.LVTLEEFLR.A	Y	27.89	1118.634	9	27.1	560.3392	2	12.2	2264	2	312	320	
37	4250	tr|A0A091HNJ7|A0A091HNJ7_CALAN	Nucleobindin-2	R.LVTLEEFLR.A	Y	27.89	1118.634	9	27.1	560.3392	2	12.2	2264	2	311	319	
37	4274	tr|A0A091PFA1|A0A091PFA1_LEPDC	Nucleobindin-2	R.LVTLEEFLR.A	Y	27.89	1118.634	9	27.1	560.3392	2	12.2	2264	2	312	320	

37	4273	tr|A0A0A0AZD6|A0A0A0AZD6_CHAVO	Nucleobindin-2	R.LVTLEEFLR.A	Y	27.89	1118.634	9	27.1	560.3392	2	12.2	2264	2	312	320	
37	4272	tr|A0A091HJ71|A0A091HJ71_BUCRH	Nucleobindin-2	R.LVTLEEFLR.A	Y	27.89	1118.634	9	27.1	560.3392	2	12.2	2264	2	312	320	
37	4271	tr|F1NGB1|F1NGB1_CHICK	Nucleobindin-2 isoform X1	R.LVTLEEFLR.A	Y	27.89	1118.634	9	27.1	560.3392	2	12.2	2264	2	312	320	
37	4270	tr|A0A091VMW6|A0A091VMW6_NIPNI	Nucleobindin-2	R.LVTLEEFLR.A	Y	27.89	1118.634	9	27.1	560.3392	2	12.2	2264	2	312	320	
37	4269	tr|A0A094KJ55|A0A094KJ55_ANTCR	Nucleobindin-2	R.LVTLEEFLR.A	Y	27.89	1118.634	9	27.1	560.3392	2	12.2	2264	2	312	320	
37	4268	tr|A0A094L6H8|A0A094L6H8_9AVES	Nucleobindin-2	R.LVTLEEFLR.A	Y	27.89	1118.634	9	27.1	560.3392	2	12.2	2264	2	312	320	
37	4267	tr|A0A093PSK0|A0A093PSK0_9PASS	Nucleobindin-2	R.LVTLEEFLR.A	Y	27.89	1118.634	9	27.1	560.3392	2	12.2	2264	2	312	320	
37	4266	tr|H0ZEB8|H0ZEB8_TAEGU	Nucleobindin-2	R.LVTLEEFLR.A	Y	27.89	1118.634	9	27.1	560.3392	2	12.2	2264	2	312	320	
37	4265	tr|A0A091ED95|A0A091ED95_CORBR	Nucleobindin-2	R.LVTLEEFLR.A	Y	27.89	1118.634	9	27.1	560.3392	2	12.2	2264	2	312	320	
37	4264	tr|Q5ZHR1|Q5ZHR1_CHICK	Nucleobindin-2 precursor	R.LVTLEEFLR.A	Y	27.89	1118.634	9	27.1	560.3392	2	12.2	2264	2	312	320	
37	4263	tr|A0A091L2T7|A0A091L2T7_9GRUI	Nucleobindin-2	R.LVTLEEFLR.A	Y	27.89	1118.634	9	27.1	560.3392	2	12.2	2264	2	312	320	
37	4255	tr|A0A093CUP2|A0A093CUP2_9AVES	Nucleobindin-2	R.LVTLEEFLR.A	Y	27.89	1118.634	9	27.1	560.3392	2	12.2	2264	2	312	320	
37	4254	tr|A0A091GCH4|A0A091GCH4_9AVES	Nucleobindin-2	R.LVTLEEFLR.A	Y	27.89	1118.634	9	27.1	560.3392	2	12.2	2264	2	312	320	
37	4253	tr|A0A093JDZ9|A0A093JDZ9_EURHL	Nucleobindin-2	R.LVTLEEFLR.A	Y	27.89	1118.634	9	27.1	560.3392	2	12.2	2264	2	312	320	
37	4252	tr|A0A087RK71|A0A087RK71_APTFO	Nucleobindin-2	R.LVTLEEFLR.A	Y	27.89	1118.634	9	27.1	560.3392	2	12.2	2264	2	312	320	
37	4251	tr|R0LG94|R0LG94_ANAPL	Nucleobindin-2	R.LVTLEEFLR.A	Y	27.89	1118.634	9	27.1	560.3392	2	12.2	2264	2	312	320	
37	4275	tr|A0A091U6D8|A0A091U6D8_PHORB	Nucleobindin-2	R.LVTLEEFLR.A	Y	27.89	1118.634	9	27.1	560.3392	2	12.2	2264	2	312	320	
37	4256	tr|A0A093HG29|A0A093	Nucleobindin-2	R.LVTLEEFLR.A	Y	27.89	1118.634	9	27.1	560.3392	2	12.2	2264	2	312	320	

		HG29_STRCA															
37	4276	tr|A0A091IWJ1|A0A091IWJ1_9AVES	Nucleobindin-2	R.LVTLEEFLR.A	Y	27.89	1118.634	9	27.1	560.3392	2	12.2	2264	2	312	320	
37	4277	tr|G1N538|G1N538_MELGA	Nucleobindin-2	R.LVTLEEFLR.A	Y	27.89	1118.634	9	27.1	560.3392	2	12.2	2264	2	316	324	
37	4278	tr|U3JDE6|U3JDE6_FICAL	Nucleobindin-2	R.LVTLEEFLR.A	Y	27.89	1118.634	9	27.1	560.3392	2	12.2	2264	2	325	333	
37	4257	tr|A0A0Q3X4D7|A0A0Q3X4D7_AMAAE	Nucleobindin-2	R.LVTLEEFLR.A	Y	27.89	1118.634	9	27.1	560.3392	2	12.2	2264	2	358	366	
38	4286	tr|A0A0A0AR29|A0A0A0AR29_CHAVO	RGM domain family member B	K.ITIIFK.S	Y	25.33	733.4738	6	3.2	367.7453	2	8.33	1427	2	176	181	
39	4285	tr|A0A091U916|A0A091U916_PHORB	Calcineurin-like phosphoesterase domain-containing protein 1	L.VFVSGNHDIGNTPTK.E	Y	24.95	1584.79	15	28.1	793.4243	2	24.38	4323	1	98	112	
41	4242	tr|A0A091V887|A0A091V887_NIPNI	Ovoinhibitor	V.IGDHVLVAC(+57.02)PR.I	Y	31.03	1235.644	11	2.2	618.8308	2	7	1108	1	78	88	Carbamidomethylation
42	4279	tr|A0A093QEZ4|A0A093QEZ4_9PASS	Ovoinhibitor	K.SIVIDC(+57.02)SK.Y	Y	27.48	920.4637	8	1	461.2396	2	5.55	804	1	65	72	Carbamidomethylation
44	4297	tr|A0A091XAE4|A0A091XAE4_OPIHO	Zona pellucida sperm-binding protein 2	K.AFAFVSGDK.A	Y	23.28	940.4654	9	-51.9	471.2155	2	6.2	918	1	565	573	
44	4299	tr|F1NNU1|F1NNU1_CHICK	Zona pellucida sperm-binding protein 2	K.AFAFVSGDK.A	Y	23.28	940.4654	9	-51.9	471.2155	2	6.2	918	1	574	582	
44	4298	tr|Q2PGY2|Q2PGY2_CHICK	Zona pellucida A	K.AFAFVSGDK.A	Y	23.28	940.4654	9	-51.9	471.2155	2	6.2	918	1	574	582	
44	4300	tr|Q5CZI6|Q5CZI6_CHICK	Zona pellucida protein	K.AFAFVSGDK.A	Y	23.28	940.4654	9	-51.9	471.2155	2	6.2	918	1	614	622	
47	4172	tr|A0A091M1K5|A0A091M1K5_CARIC	Neuropilin and tolloid-like 1	R.DGPFGFSPIIGR.F	Y	44.09	1261.646	12	-30.4	631.8109	2	9.87	1770	1	98	109	

47	4173	tr|A0A1D5PQM2|A0A1D5PQM2_CHICK	Neuropilin and tolloid-like protein 1 isoform X2	R.DGPFGFSPIIGR.F	Y	44.09	1261.646	12	-30.4	631.8109	2	9.87	1770	1	105	116	
47	4174	tr|A0A093FGT3|A0A093FGT3_TYTAL	Neuropilin and tolloid-like 1	R.DGPFGFSPIIGR.F	Y	44.09	1261.646	12	-30.4	631.8109	2	9.87	1770	1	32	43	
47	4175	tr|A0A087QND6|A0A087QND6_APTFO	Neuropilin and tolloid-like 1	R.DGPFGFSPIIGR.F	Y	44.09	1261.646	12	-30.4	631.8109	2	9.87	1770	1	32	43	
47	4176	tr|R0LMR2|R0LMR2_ANAPL	Neuropilin and tolloid-like protein 1	R.DGPFGFSPIIGR.F	Y	44.09	1261.646	12	-30.4	631.8109	2	9.87	1770	1	79	90	
47	4177	tr|A0A091JZC9|A0A091JZC9_COLST	Neuropilin and tolloid-like 1	R.DGPFGFSPIIGR.F	Y	44.09	1261.646	12	-30.4	631.8109	2	9.87	1770	1	79	90	
47	4196	tr|A0A093FW41|A0A093FW41_GAVST	Neuropilin and tolloid-like 1	R.DGPFGFSPIIGR.F	Y	44.09	1261.646	12	-30.4	631.8109	2	9.87	1770	1	98	109	
47	4195	tr|A0A091SKD1|A0A091SKD1_9GRUI	Neuropilin and tolloid-like 1	R.DGPFGFSPIIGR.F	Y	44.09	1261.646	12	-30.4	631.8109	2	9.87	1770	1	98	109	
47	4194	tr|A0A099Z9Q6|A0A099Z9Q6_TINGU	Neuropilin and tolloid-like 1	R.DGPFGFSPIIGR.F	Y	44.09	1261.646	12	-30.4	631.8109	2	9.87	1770	1	98	109	
47	4193	tr|A0A091ICA8|A0A091ICA8_CALAN	Neuropilin and tolloid-like 1	R.DGPFGFSPIIGR.F	Y	44.09	1261.646	12	-30.4	631.8109	2	9.87	1770	1	98	109	
47	4192	tr|A0A091JE74|A0A091JE74_9AVES	Neuropilin and tolloid-like 1	R.DGPFGFSPIIGR.F	Y	44.09	1261.646	12	-30.4	631.8109	2	9.87	1770	1	98	109	
47	4191	tr|A0A0A0ARN5|A0A0A0ARN5_CHAVO	Neuropilin and tolloid-like 1	R.DGPFGFSPIIGR.F	Y	44.09	1261.646	12	-30.4	631.8109	2	9.87	1770	1	98	109	
47	4190	tr|A0A093GYX1|A0A093GYX1_PICPB	Neuropilin and tolloid-like 1	R.DGPFGFSPILGR.F	Y	44.09	1261.646	12	-30.4	631.8109	2	9.87	1770	1	98	109	
47	4189	tr|A0A093IPZ4|A0A093IPZ4_EURHL	Neuropilin and tolloid-like 1	R.DGPFGFSPIIGR.F	Y	44.09	1261.646	12	-30.4	631.8109	2	9.87	1770	1	98	109	
47	4188	tr|A0A091F3F2|A0A091F3F2_CORBR	Neuropilin and tolloid-like 1	R.DGPFGFSPIIGR.F	Y	44.09	1261.646	12	-30.4	631.8109	2	9.87	1770	1	98	109	
47	4187	tr|A0A093QEM7|A0A093QEM7_9PASS	Neuropilin and tolloid-like 1	R.DGPFGFSPIIGR.F	Y	44.09	1261.646	12	-30.4	631.8109	2	9.87	1770	1	98	109	
47	4186	tr|H0ZFW8|H0ZFW8_TAEGU	Neuropilin and tolloid-like 1	R.DGPFGFSPILGR.F	Y	44.09	1261.646	12	-30.4	631.8109	2	9.87	1770	1	98	109	
47	4185	tr|A0A093BGU1|A0A093BGU1_CHAPE	Neuropilin and tolloid-like 1	R.DGPFGFSPIIGR.F	Y	44.09	1261.646	12	-30.4	631.8109	2	9.87	1770	1	98	109	
47	4184	tr|A0A091WRF1|A0A091	Neuropilin and tolloid-like 1	R.DGPFGFSPIIGR.F	Y	44.09	1261.646	12	-30.4	631.8109	2	9.87	1770	1	98	109	

		WRF1_NIPNI															
47	4183	tr|A0A091WHV3|A0A091WHV3_OPIHO	Neuropilin and tolloid-like 1	R.DGPFGFSPIIGR.F	Y	44.09	1261.646	12	-30.4	631.8109	2	9.87	1770	1	98	109	
47	4182	tr|A0A093HHJ2|A0A093HHJ2_STRCA	Neuropilin and tolloid-like 1	R.DGPFGFSPIIGR.F	Y	44.09	1261.646	12	-30.4	631.8109	2	9.87	1770	1	98	109	
47	4181	tr|A0A093NAE4|A0A093NAE4_PYGAD	Neuropilin and tolloid-like 1	R.DGPFGFSPIIGR.F	Y	44.09	1261.646	12	-30.4	631.8109	2	9.87	1770	1	98	109	
47	4180	tr|A0A091TLD0|A0A091TLD0_9AVES	Neuropilin and tolloid-like 1	R.DGPFGFSPIIGR.F	Y	44.09	1261.646	12	-30.4	631.8109	2	9.87	1770	1	97	108	
47	4179	tr|A0A091Q239|A0A091Q239_LEPDC	Neuropilin and tolloid-like 1	R.DGPFGFSPIIGR.F	Y	44.09	1261.646	12	-30.4	631.8109	2	9.87	1770	1	97	108	
47	4178	tr|A0A091G4C9|A0A091G4C9_9AVES	Neuropilin and tolloid-like 1	R.DGPFGFSPIIGR.F	Y	44.09	1261.646	12	-30.4	631.8109	2	9.87	1770	1	97	108	
47	4199	tr|U3IQM0|U3IQM0_ANAPL	Neuropilin and tolloid-like protein 1 isoform X1	R.DGPFGFSPIIGR.F	Y	44.09	1261.646	12	-30.4	631.8109	2	9.87	1770	1	108	119	
47	4198	tr|G1N880|G1N880_MELGA	Neuropilin and tolloid-like 1	R.DGPFGFSPIIGR.F	Y	44.09	1261.646	12	-30.4	631.8109	2	9.87	1770	1	107	118	
47	4197	tr|A0A0Q3TPW3|A0A0Q3TPW3_AMAAE	Neuropilin and tolloid-like protein 1	R.DGPFGFSPIIGR.F	Y	44.09	1261.646	12	-30.4	631.8109	2	9.87	1770	1	105	116	

Supplementary File 2

Protein Group	Protein ID	Protein Accession	Protein Name	Peptide	Unique	-10lgP	Mass	Length	ppm	m/z	z	RT	Scan	#Spec	Start	End	PTM
1	4026	tr|H0ZGY9|H0ZGY9_TAEGU	Mucin-5AC	R.EC(+57.02)HC(+57.02)TYEGETYAPGASFSSK.C	N	70.1	2279.91	20	0.5	760.9777	3	6.56	986	2	393	412	Carbamidomethylation
1	4026	tr|H0ZGY9|H0ZGY9_TAEGU	Mucin-5AC	K.SLKYTYNVDSC(+57.02)QPTC(+57.02)R.S	N	64.5	1990.888	16	0.2	664.6367	3	6.4	949	2	707	722	Carbamidomethylation
1	4026	tr|H0ZGY9|H0ZGY9_TAEGU	Mucin-5AC	K.LC(+57.02)DSNEFTVLGDIHK.C	N	63.74	1746.825	15	1.8	583.2832	3	8.26	1396	2	463	477	Carbamidomethylation
1	4026	tr|H0ZGY9|H0ZGY9_TAEGU	Mucin-5AC	K.TTSGVIEGTSAAFGNTWK.T	N	59.64	1825.885	18	2.1	913.9515	2	8.77	1509	2	584	601	
1	4026	tr|H0ZGY9|H0ZGY9_TAEGU	Mucin-5AC	S.GPNQGDFETYQHIR.A	Y	58.8	1660.759	14	1.8	831.3885	2	6.51	974	4	1618	1631	
1	4026	tr|H0ZGY9|H0ZGY9_TAEGU	Mucin-5AC	R.VITENIPC(+57.02)GTTGTTC(+57.02)SK.S	N	57.19	1837.855	17	2.3	919.9369	2	6.47	965	4	945	961	Carbamidomethylation
1	4026	tr|H0ZGY9|H0ZGY9_TAEGU	Mucin-5AC	R.Q(-17.03)C(+57.02)AHAGGQPLNWR.T	N	55.91	1476.668	13	2.5	739.3431	2	6.91	1064	2	317	329	Pyro-glu from Q; Carbamidomethylation
1	4026	tr|H0ZGY9|H0ZGY9_TAEGU	Mucin-5AC	R.VC(+57.02)STWGNFHFK.T	N	43.07	1381.624	11	1.2	461.5491	3	7.68	1254	2	78	88	Carbamidomethylation
1	4026	tr|H0ZGY9|H0ZGY9_TAEGU	Mucin-5AC	K.QC(+57.02)SIITSEVFAK.C	N	39.34	1381.691	12	1.1	691.8536	2	8.16	1370	1	1093	1104	Carbamidomethylation
1	4026	tr|H0ZGY9|H0ZGY9_TAEGU	Mucin-5AC	K.FKMC(+57.02)LNYK(+27.99).I	Y	35.06	1130.525	8	10.4	377.853	3	7.2	1136	2	1682	1689	Carbamidomethylation; Formylation
1	4026	tr|H0ZGY9|H0ZGY9_TAEGU	Mucin-5AC	K.Q(+41.03)IEC(+57.02)QAEDYPDVAIQQVGQVVQC(+57.02)DVHFGLVC(+57.02)K.N	Y	32.03	3772.765	32	13.2	1258.612	3	13.38	2516	2	1643	1674	Amidination of lysines or N-terminal amines with methyl acetimidate; Carbamidomethylation
1	4026	tr|H0ZGY9|H0ZGY9_TAEGU	Mucin-5AC	N.Q(-17.03)GDFETYQHIR.A	N	31.43	1375.616	11	1.8	688.8163	2	7.14	1121	1	1621	1631	Pyro-glu from Q
1	4026	tr|H0ZGY9|H0ZGY9_TAEGU	Mucin-5AC	S.GPNQ(+.98)GDFETYQHIR.A	Y	31.14	1661.743	14	4.6	554.9243	3	6.67	1008	1	1618	1631	Deamidation (NQ)
1	4026	tr|H0ZGY9|H0ZGY9_TAEGU	Mucin-5AC	S.GPN(+.98)QGDFETYQHIR.A	Y	29.69	1661.743	14	4.4	554.9242	3	6.64	1003	1	1618	1631	Deamidation (NQ)

1	4026	tr|H0ZGY9|H0ZGY9_TAEGU	Mucin-5AC	S.GPNQGDFETYQH(+57.02)IR.A	Y	28.69	1717.781	14	0.9	573.6014	3	6.45	959	2	1618	1631	Carbamidomethylation (DHKE X@N-term)
1	4026	tr|H0ZGY9|H0ZGY9_TAEGU	Mucin-5AC	R.QPM(+15.99)(subK)QIEC(+57.02)QAEDYPDVAIQQVGQVVQC(+57.02)DVHFGLVC(+57.02)K.N	Y	28.1	4103.885	35	29	1027.008	4	15.84	3001	3	1640	1674	Oxidation (M); Carbamidomethylation; Mutation
1	4026	tr|H0ZGY9|H0ZGY9_TAEGU	Mucin-5AC	P.NQ(+192.06)GDFETYQHIR.A	Y	25.7	1698.749	12	-20.1	425.6859	4	6.52	975	1	1620	1631	Heptose
1	4026	tr|H0ZGY9|H0ZGY9_TAEGU	Mucin-5AC	K.MPFQIR.S	N	24.44	790.416	6	1	396.2157	2	7.44	1196	2	990	995	
1	4026	tr|H0ZGY9|H0ZGY9_TAEGU	Mucin-5AC	S.GPNQGD(+37.96)FETYQHIR.A	Y	22.02	1698.715	14	-3	425.6848	4	6.49	971	1	1618	1631	Replacement of proton by potassium
1	4026	tr|H0ZGY9|H0ZGY9_TAEGU	Mucin-5AC	R.QPKQIECQF(subA)EDYPDVAIQQVGQVVQC(+57.02)DVHFGLVC(+57.02)K.N	Y	21	4103.954	35	9.7	1027.006	4	15.71	2976	1	1640	1674	Carbamidomethylation; Mutation
2	4070	tr|A0A093F6E7|A0A093F6E7_TYTAL	Acidic mammalian chitinase	R.QYQFDGLDIDWEYPGSR.G	N	64.5	2087.922	17	2.2	1044.971	2	12.24	2280	4	117	133	
2	4070	tr|A0A093F6E7|A0A093F6E7_TYTAL	Acidic mammalian chitinase	K.GNEWVGYDNIK.S	N	51.64	1293.599	11	-1.6	647.8057	2	7.32	1163	2	318	328	
2	4070	tr|A0A093F6E7|A0A093F6E7_TYTAL	Acidic mammalian chitinase	N.EWVGYDNIK.S	N	43.23	1122.535	9	0.7	562.275	2	7.22	1138	2	320	328	
2	4070	tr|A0A093F6E7|A0A093F6E7_TYTAL	Acidic mammalian chitinase	K.TLLAIGGWNFGTAK.F	N	42.63	1447.782	14	0.2	724.8986	2	12	2228	16	80	93	
2	4070	tr|A0A093F6E7|A0A093F6E7_TYTAL	Acidic mammalian chitinase	Y.FTNWAQYRPGLGK.F	N	41.91	1536.784	13	1.9	513.2695	3	7.58	1228	2	16	28	
2	4070	tr|A0A093F6E7|A0A093F6E7_TYTAL	Acidic mammalian chitinase	F.TNWAQYRPGLGK.F	N	34.54	1389.715	12	1.2	695.8658	2	7.03	1094	4	17	28	
2	4070	tr|A0A093F6E7|A0A093F6E7_TYTAL	Acidic mammalian chitinase	K.YPLITTLK.N	N	32.83	947.5692	8	1	474.7923	2	7.93	1313	2	365	372	
2	4070	tr|A0A093F6E7|A0A093F6E7_TYTAL	Acidic mammalian chitinase	K.LLVGFPTYGHNFNLQNPAD(+14.02)TAVGAPATGPGPAGPYTR.Q	Y	25.34	3751.875	37	66.2	939.038	4	12.4	2313	1	248	284	Methyl ester
2	4070	tr|A0A093F6E7|A0A093F6E7_TYTAL	Acidic mammalian chitinase	K.TLFTVLVK.E	N	23.05	919.5742	8	-34.5	460.7785	2	9.63	1713	2	141	148	
2	4070	tr|A0A093F6E7|A0A093F6E7_TYTAL	Acidic mammalian chitinase	A.IGGWNFGTAK.F	N	21.19	1049.529	10	0.6	525.7723	2	7.69	1256	1	84	93	
2	4070	tr|A0A093F6E7|A0A093F	Acidic mammalian chitinase	N.TGENSPLYK.G	N	19.12	1007.492	9	3.7	504.7	2	4.67	675	1	210	218	

		6E7_TYTAL								553							
3	4058	tr|A0A093BFV9|A0A093BFV9_CHAPE	Acidic mammalian chitinase	K.EMVAAFEQEAR.Q	Y	54.98	1279.587	11	-0.6	640.8002	2	7.18	1131	2	143	153	
3	4058	tr|A0A093BFV9|A0A093BFV9_CHAPE	Acidic mammalian chitinase	K.TLLAIGGWNFGTAK.F	N	42.63	1447.782	14	0.2	724.8986	2	12	2228	16	74	87	
3	4058	tr|A0A093BFV9|A0A093BFV9_CHAPE	Acidic mammalian chitinase	Y.FTNWAQYRPGLGK.F	N	41.91	1536.784	13	1.9	513.2695	3	7.58	1228	2	10	22	
3	4058	tr|A0A093BFV9|A0A093BFV9_CHAPE	Acidic mammalian chitinase	K.LLVGFPTYGR.T	N	41.63	1121.623	10	42.7	561.8429	2	9.2	1609	4	237	246	
3	4058	tr|A0A093BFV9|A0A093BFV9_CHAPE	Acidic mammalian chitinase	F.TNWAQYRPGLGK.F	N	34.54	1389.715	12	1.2	695.8658	2	7.03	1094	4	11	22	
3	4058	tr|A0A093BFV9|A0A093BFV9_CHAPE	Acidic mammalian chitinase	R.GSPPQAKTM(sub L)FTVLVKEMVAAFEQEAR.Q	Y	29.11	2864.456	26	8.4	717.1274	4	17.13	3239	3	128	153	Mutation
3	4058	tr|A0A093BFV9|A0A093BFV9_CHAPE	Acidic mammalian chitinase	A.VAAGLSTIQAGYEIAELGK.Y	N	25.54	1890.01	19	72.8	946.081	2	10.86	1986	2	166	184	
3	4058	tr|A0A093BFV9|A0A093BFV9_CHAPE	Acidic mammalian chitinase	K.TLFTVLVK.E	N	23.05	919.5742	8	-34.5	460.7785	2	9.63	1713	2	135	142	
3	4058	tr|A0A093BFV9|A0A093BFV9_CHAPE	Acidic mammalian chitinase	A.IGGWNFGTAK.F	N	21.19	1049.529	10	0.6	525.7723	2	7.69	1256	1	78	87	
5	4024	tr|R7VT28|R7VT28_COLLI	Mucin-5AC	K.TFDGDIFYFPGIC(+57.02)NYIFASNC(+57.02)K.S	Y	68.83	2648.172	22	0.6	1325.094	2	15.3	2896	4	93	114	Carbamidomethylation
5	4024	tr|R7VT28|R7VT28_COLLI	Mucin-5AC	R.SQSVVGNVLEFANSWK.V	N	67.59	1763.884	16	2.3	882.9515	2	13.67	2575	4	1064	1079	
5	4024	tr|R7VT28|R7VT28_COLLI	Mucin-5AC	K.TTSGVIEGTSAAFGNTWK.T	N	59.64	1825.885	18	2.1	913.9515	2	8.77	1509	2	598	615	
5	4024	tr|R7VT28|R7VT28_COLLI	Mucin-5AC	R.VITENIPC(+57.02)GTTGTTC(+57.02)SK.S	N	57.19	1837.855	17	2.3	919.9369	2	6.47	965	4	959	975	Carbamidomethylation
5	4024	tr|R7VT28|R7VT28_COLLI	Mucin-5AC	R.Q(-17.03)C(+57.02)AHAGGQPLNWR.T	N	55.91	1476.668	13	2.5	739.3431	2	6.91	1064	2	321	333	Pyro-glu from Q; Carbamidomethylation
5	4024	tr|R7VT28|R7VT28_COLLI	Mucin-5AC	K.SPYEDFNIQIR.R	N	51.89	1380.667	11	3.1	691.3431	2	8.68	1489	2	115	125	
5	4024	tr|R7VT28|R7VT28_COL	Mucin-5AC	R.THC(+57.02)VSGC(+57.02)VC(+57.02)PHNQVLDGK.G	N	48.46	2066.908	18	1.9	517.7	4	5.66	820	2	850	867	Carbamidomethylation

		LI								354							
5	4024	tr|R7VT28|R7VT28_COLLI	Mucin-5AC	K.SNYVSPSILQR.Q	Y	45.65	1262.662	11	0.5	632.3385	2	7.42	1190	2	36	46	
5	4024	tr|R7VT28|R7VT28_COLLI	Mucin-5AC	R.VC(+57.02)STWGNFHFK.T	N	43.07	1381.624	11	1.2	461.5491	3	7.68	1254	2	82	92	Carbamidomethylation
5	4024	tr|R7VT28|R7VT28_COLLI	Mucin-5AC	K.QC(+57.02)SIITSEVFAK.C	N	39.34	1381.691	12	1.1	691.8536	2	8.16	1370	1	1107	1118	Carbamidomethylation
5	4024	tr|R7VT28|R7VT28_COLLI	Mucin-5AC	K.GVLLTGWR.S	N	30.19	900.5181	8	3.1	451.2677	2	8.18	1375	2	700	707	
5	4024	tr|R7VT28|R7VT28_COLLI	Mucin-5AC	R.SQSVVGNVLEFAN(+.98)SWK.V	N	28.32	1764.868	16	65.4	883.4991	2	11.43	2109	1	1064	1079	Deamidation (NQ)
5	4024	tr|R7VT28|R7VT28_COLLI	Mucin-5AC	K.MPFQIR.S	N	24.44	790.416	6	1	396.2157	2	7.44	1196	2	1004	1009	
5	4024	tr|R7VT28|R7VT28_COLLI	Mucin-5AC	R.GLE(+57.02)GCYPHC(+57.02)PK.N	N	20.12	1316.564	11	1.8	439.8628	3	5.45	789	1	1215	1225	Carbamidomethylation (DHKE X@N-term); Carbamidomethylation
11	4025	tr|A0A0Q3U2A7|A0A0Q3U2A7_AMAAE	Mucin-5AC	R.SQSVVGNVLEFANSWK.V	N	67.59	1763.884	16	2.3	882.9515	2	13.67	2575	4	854	869	
11	4025	tr|A0A0Q3U2A7|A0A0Q3U2A7_AMAAE	Mucin-5AC	R.VITENIPC(+57.02)GTTGTTC(+57.02)SK.S	N	57.19	1837.855	17	2.3	919.9369	2	6.47	965	4	749	765	Carbamidomethylation
11	4025	tr|A0A0Q3U2A7|A0A0Q3U2A7_AMAAE	Mucin-5AC	R.AEKFPNIPLKDLGQK.V	Y	53.24	1696.951	15	4.2	425.2469	4	7.89	1306	3	1195	1209	
11	4025	tr|A0A0Q3U2A7|A0A0Q3U2A7_AMAAE	Mucin-5AC	K.SPYEDFNIQIR.R	N	51.89	1380.667	11	3.1	691.3431	2	8.68	1489	2	115	125	
11	4025	tr|A0A0Q3U2A7|A0A0Q3U2A7_AMAAE	Mucin-5AC	K.THC(+57.02)VSGC(+57.02)VC(+57.02)PHNQVLDGK.G	N	48.46	2066.908	18	1.9	517.7354	4	5.66	820	2	640	657	Carbamidomethylation
11	4025	tr|A0A0Q3U2A7|A0A0Q3U2A7_AMAAE	Mucin-5AC	R.VC(+57.02)STWGNFHFK.T	N	43.07	1381.624	11	1.2	461.5491	3	7.68	1254	2	82	92	Carbamidomethylation
11	4025	tr|A0A0Q3U2A7|A0A0Q3U2A7_AMAAE	Mucin-5AC	K.QC(+57.02)SIITSEVFAK.C	N	39.34	1381.691	12	1.1	691.8536	2	8.16	1370	1	897	908	Carbamidomethylation
11	4025	tr|A0A0Q3U2A7|A0A0Q3U2A7_AMAAE	Mucin-5AC	K.GVLLTGWR.S	N	30.19	900.5181	8	3.1	451.2677	2	8.18	1375	2	490	497	
11	4025	tr|A0A0Q3U2A7|A0A0Q3U2A7_AMAAE	Mucin-5AC	R.SQSVVGNVLEFAN(+.98)SWK.V	N	28.32	1764.868	16	65.4	883.4991	2	11.43	2109	1	854	869	Deamidation (NQ)

11	4025	tr|A0A0Q3U2A7|A0A0Q3U2A7_AMAAE	Mucin-5AC	K.MPFQIR.S	N	24.44	790.416	6	1	396.2157	2	7.44	1196	2	794	799	
11	4025	tr|A0A0Q3U2A7|A0A0Q3U2A7_AMAAE	Mucin-5AC	R.GLE(+57.02)GCYPHC(+57.02)PK.N	N	20.12	1316.564	11	1.8	439.8628	3	5.45	789	1	1005	1015	Carbamidomethylation (DHKE X@N-term); Carbamidomethylation
15	4035	tr|A0A0A0B371|A0A0A0B371_CHAVO	Lysyl oxidase 3	R.IPGFKDSNVIETEQSHVEEVR.L	Y	72.54	2412.192	21	-0.1	805.0712	3	7.63	1241	3	66	86	
15	4035	tr|A0A0A0B371|A0A0A0B371_CHAVO	Lysyl oxidase 4	R.GWGNSDC(+57.02)SHEEDAGVIC(+57.02)KDER.I	N	67.54	2419.976	21	1.4	606.002	4	6.07	886	2	45	65	Carbamidomethylation
15	4035	tr|A0A0A0B371|A0A0A0B371_CHAVO	Lysyl oxidase 5	R.RQLPVTEGIVEVR.Y	Y	64.1	1494.852	13	2.1	499.2923	3	7.5	1211	4	96	108	
15	4035	tr|A0A0A0B371|A0A0A0B371_CHAVO	Lysyl oxidase 6	K.DSNVIETEQSHVEEVR.L	Y	61.72	1869.87	16	0	624.2974	3	6.76	1028	1	71	86	
15	4035	tr|A0A0A0B371|A0A0A0B371_CHAVO	Lysyl oxidase 7	R.VVC(+57.02)GMMGFPAEK.K	N	55.56	1324.598	12	1.1	663.3069	2	7.8	1284	2	128	139	Carbamidomethylation
15	4035	tr|A0A0A0B371|A0A0A0B371_CHAVO	Lysyl oxidase 8	R.QLPVTEGIVEVR.Y	Y	48.73	1338.751	12	-0.1	670.3826	2	8.24	1391	2	97	108	
15	4035	tr|A0A0A0B371|A0A0A0B371_CHAVO	Lysyl oxidase 9	R.IWLDNVNC(+57.02)AGGEK.S	N	46.64	1474.688	13	2.9	738.3531	2	7.5	1210	2	24	36	Carbamidomethylation
15	4035	tr|A0A0A0B371|A0A0A0B371_CHAVO	Lysyl oxidase 10	R.GWGN(+.98)SDC(+57.02)SHEEDAGVIC(+57.02)KDER.I	N	45.43	2420.96	21	3.7	606.2495	4	6.2	908	3	45	65	Deamidation (NQ); Carbamidomethylation
17	4108	tr|A0A091TEI1|A0A091TEI1_NESNO	Acidic mammalian chitinase	R.GSPAQDKTLFTVLVK.E	Y	59.82	1602.898	15	-0.8	535.3062	3	9.33	1639	9	138	152	
17	4108	tr|A0A091TEI1|A0A091TEI1_NESNO	Acidic mammalian chitinase	R.GSPAQDKTLFTVLVKEMVAAFEQEAQ.Q	Y	55.01	2836.432	26	13.6	946.4974	3	17.04	3219	3	138	163	
17	4108	tr|A0A091TEI1|A0A091TEI1_NESNO	Acidic mammalian chitinase	S.EWVGYDNIK.S	N	43.23	1122.535	9	0.7	562.275	2	7.22	1138	2	319	327	
17	4108	tr|A0A091TEI1|A0A091TEI1_NESNO	Acidic mammalian chitinase	K.YPLITTLK.N	N	32.83	947.5692	8	1	474.7923	2	7.93	1313	2	364	371	
17	4108	tr|A0A091TEI1|A0A091TEI1_NESNO	Acidic mammalian chitinase	R.GSPAQDKTLFTVLVKEMVAAFEQEAQ(+28.03).Q	Y	26.44	2864.463	26	6.5	955.8345	3	17.16	3243	1	138	163	Ethylation
17	4108	tr|A0A091TEI1|A0A091TEI1_NESNO	Acidic mammalian chitinase	K.TLFTVLVK.E	N	23.05	919.5742	8	-34.5	460.7785	2	9.63	1713	2	145	152	

18	7544	tr|A0A0A0AQX5|A0A0A0AQX5_CHAVO	Acidic mammalian chitinase	R.QYQFDGLDLDWEYPGSR.G	N	64.5	2087.922	17	2.2	1044.971	2	12.24	2280	4	117	133	
18	7544	tr|A0A0A0AQX5|A0A0A0AQX5_CHAVO	Acidic mammalian chitinase	K.EWVGYDNIK.S	N	43.23	1122.535	9	0.7	562.275	2	7.22	1138	2	320	328	
18	7544	tr|A0A0A0AQX5|A0A0A0AQX5_CHAVO	Acidic mammalian chitinase	Y.FTNWAQYRPGLGK.F	N	41.91	1536.784	13	1.9	513.2695	3	7.58	1228	2	16	28	
18	7544	tr|A0A0A0AQX5|A0A0A0AQX5_CHAVO	Acidic mammalian chitinase	F.TNWAQYRPGLGK.F	N	34.54	1389.715	12	1.2	695.8658	2	7.03	1094	4	17	28	
18	7544	tr|A0A0A0AQX5|A0A0A0AQX5_CHAVO	Acidic mammalian chitinase	K.YPLITTLK.N	N	32.83	947.5692	8	1	474.7923	2	7.93	1313	2	365	372	
18	7544	tr|A0A0A0AQX5|A0A0A0AQX5_CHAVO	Acidic mammalian chitinase	K.G(+42.01)KEWVGYDNIK.S	Y	22.29	1349.662	11	11.6	450.8997	3	7.14	1119	1	318	328	Acetylation (N-term)
18	7544	tr|A0A0A0AQX5|A0A0A0AQX5_CHAVO	Acidic mammalian chitinase	K.EWL(sub V)GYDNIK.S	N	20.62	1136.55	9	0.9	569.2829	2	7.58	1230	1	320	328	Mutation
18	7544	tr|A0A0A0AQX5|A0A0A0AQX5_CHAVO	Acidic mammalian chitinase	N.TGENSPLYK.G	N	19.12	1007.492	9	3.7	504.7553	2	4.67	675	1	210	218	
19	4037	tr|H0ZGZ6|H0ZGZ6_TAEGU	Mucin-5AC	K.SLKYTYNVDSC(+57.02)QPTC(+57.02)R.S	N	64.5	1990.888	16	0.2	664.6367	3	6.4	949	2	370	385	Carbamidomethylation
19	4037	tr|H0ZGZ6|H0ZGZ6_TAEGU	Mucin-5AC	K.TTSGVIEGTSAAFGNTWK.T	N	59.64	1825.885	18	2.1	913.9515	2	8.77	1509	2	247	264	
19	4037	tr|H0ZGZ6|H0ZGZ6_TAEGU	Mucin-5AC	R.VITENIPC(+57.02)GTTGTTC(+57.02)SK.S	N	57.19	1837.855	17	2.3	919.9369	2	6.47	965	4	610	626	Carbamidomethylation
19	4037	tr|H0ZGZ6|H0ZGZ6_TAEGU	Mucin-5AC	K.QC(+57.02)SIITSEVFAK.C	N	39.34	1381.691	12	1.1	691.8536	2	8.16	1370	1	758	769	Carbamidomethylation
19	4037	tr|H0ZGZ6|H0ZGZ6_TAEGU	Mucin-5AC	K.KIVSFQ(+.98)SVVK.N	Y	26.02	1134.665	10	-15.4	379.2231	3	8.44	1434	4	164	173	Deamidation (NQ)
19	4037	tr|H0ZGZ6|H0ZGZ6_TAEGU	Mucin-5AC	K.MPFQIR.S	N	24.44	790.416	6	1	396.2157	2	7.44	1196	2	655	660	
19	4037	tr|H0ZGZ6|H0ZGZ6_TAEGU	Mucin-5AC	K.KIVSFQ(+.98)SVVK(+42.01)NSR(+14.02).T	Y	20.85	1547.867	13	16.8	516.9716	3	10.26	1855	1	164	176	Deamidation (NQ); Acetylation (K); Methyl ester
22	4036	tr|A0A093BIT2|A0A093B	Lysyl oxidase 3	R.GWGNSDC(+57.02)SHEEDAGVIC(+57.02)KDER.I	N	67.54	2419.976	21	1.4	606.0	4	6.07	886	2	24	44	Carbamidomethylation

		IT2_CHAPE								02							
22	4036	tr|A0A093BIT2|A0A093BIT2_CHAPE	Lysyl oxidase 3	R.VVC(+57.02)GMMGFPAEK.K	N	55.56	1324.598	12	1.1	663.3069	2	7.8	1284	2	107	118	Carbamidomethylation
22	4036	tr|A0A093BIT2|A0A093BIT2_CHAPE	Lysyl oxidase 3	R.IWLDNVNC(+57.02)AGGEK.S	N	46.64	1474.688	13	2.9	738.3531	2	7.5	1210	2	3	15	Carbamidomethylation
22	4036	tr|A0A093BIT2|A0A093BIT2_CHAPE	Lysyl oxidase 3	R.GWGN(+.98)SDC(+57.02)SHEEDAGVIC(+57.02)KDER.I	N	45.43	2420.96	21	3.7	606.2495	4	6.2	908	3	24	44	Deamidation (NQ); Carbamidomethylation
22	4036	tr|A0A093BIT2|A0A093BIT2_CHAPE	Lysyl oxidase 3	R.YKDGWAQIC(+57.02)DQGWDSH(sub R)NSR.V	Y	34.82	2321.987	19	-2.3	581.5027	4	7.36	1173	4	88	106	Carbamidomethylation; Mutation
22	4036	tr|A0A093BIT2|A0A093BIT2_CHAPE	Lysyl oxidase 3	K.SLWSC(+57.02)PYR.N	Y	21.97	1067.486	8	-0.3	534.7501	2	7.4	1185	1	270	277	Carbamidomethylation
25	4132	tr|A0A091NM19|A0A091NM19_APAVI	Ovoinhibitor	R.TEIDGHVLVAC(+57.02)PR.I	Y	66.32	1465.735	13	0.8	489.5859	3	6.99	1084	4	76	88	Carbamidomethylation
25	4132	tr|A0A091NM19|A0A091NM19_APAVI	Ovoinhibitor	R.YQ(sub R)RTEIDGHVLVAC(+57.02)PR.I	Y	42.9	1912.958	16	1.2	479.2473	4	6.85	1050	2	73	88	Carbamidomethylation; Mutation
25	4132	tr|A0A091NM19|A0A091NM19_APAVI	Ovoinhibitor	E.IDGHVLVAC(+57.02)PR.I	Y	29.09	1235.644	11	1.5	618.8304	2	7.05	1100	1	78	88	Carbamidomethylation
25	4132	tr|A0A091NM19|A0A091NM19_APAVI	Ovoinhibitor	L.SPVC(+57.02)GTDGITYDNEC(+57.02)GIC(+57.02)AHNGK(+149.03)H.G	Y	25.71	2810.131	24	4.9	937.722	3	6.81	1041	2	154	177	Carbamidomethylation; Benzyl isothiocyanate
26	4072	tr|H0ZGX3|H0ZGX3_TAEGU	Mucin-5AC	R.VYIDNYYC(+57.02)DAK.D	N	45.91	1422.613	11	-0.2	712.3134	2	6.95	1073	2	92	102	Carbamidomethylation
26	4072	tr|H0ZGX3|H0ZGX3_TAEGU	Mucin-5AC	T.C(+57.02)QPVIC(+57.02)DTYC(+57.02)P(+15.99)LGYK.Y	Y	34.29	1888.816	15	1.3	630.6133	3	6.76	1030	2	530	544	Carbamidomethylation; Hydroxylation
26	4072	tr|H0ZGX3|H0ZGX3_TAEGU	Mucin-5AC	R.GVC(+57.02)IDWR.G	N	26.67	904.4225	7	-0.4	453.2184	2	7.36	1176	1	308	314	Carbamidomethylation
26	4072	tr|H0ZGX3|H0ZGX3_TAEGU	Mucin-5AC	R.N(+42.01)VTLTC(+57.02)SDGTSLD(+21.98)HSYTYVEK.C	Y	23.83	2453.067	21	38.8	491.6397	5	6.59	991	1	693	713	Acetylation (N-term); Carbamidomethylation; Sodium adduct
26	4073	tr|H0ZGW8|H0ZGW8_TAEGU	Mucin-5AC	R.VYIDNYYC(+57.02)DAK.D	N	45.91	1422.613	11	-0.2	712.3134	2	6.95	1073	2	92	102	Carbamidomethylation
26	4073	tr|H0ZGW8|H0ZGW8_TAEGU	Mucin-5AC	T.C(+57.02)QPVIC(+57.02)DTYC(+57.02)P(+15.99)LGYK.Y	Y	34.29	1888.816	15	1.3	630.6133	3	6.76	1030	2	533	547	Carbamidomethylation; Hydroxylation
26	4073	tr|H0ZGW8|H0ZGW8_TA	Mucin-5AC	R.GVC(+57.02)IDWR.G	N	26.67	904.4225	7	-0.4	453.2	2	7.36	1176	1	308	314	Carbamidomethylation

		EGU								184							
26	4073	tr|H0ZGW8|H0ZGW8_TAEGU	Mucin-5AC	R.N(+42.01)VTLTC(+57.02)SDGTSLD(+21.98)HSYTYVEK.C	Y	23.83	2453.067	21	38.8	491.6397	5	6.59	991	1	696	716	Acetylation (N-term); Carbamidomethylation; Sodium adduct
27	4048	tr|A0A093GK45|A0A093GK45_PICPB	Lysyl oxidase 3	H.VVC(+57.02)GMMGFPAEK.K	N	55.56	1324.598	12	1.1	663.3069	2	7.8	1284	2	211	222	Carbamidomethylation
27	4048	tr|A0A093GK45|A0A093GK45_PICPB	Lysyl oxidase 3	R.IWLDNVNC(+57.02)AGGEK.S	N	46.64	1474.688	13	2.9	738.3531	2	7.5	1210	2	107	119	Carbamidomethylation
27	4048	tr|A0A093GK45|A0A093GK45_PICPB	Lysyl oxidase 3	R.C(+57.02)NIPYMGYET(+13.03)LIR.L	Y	22.71	1641.801	13	42	821.9421	2	10.14	1828	1	405	417	Carbamidomethylation; Michael addition with methylamine
28	4071	tr|A0A091I517|A0A091I517_CALAN	Hypothetical protein N300_06305	R.VYIDNYYC(+57.02)DAK.D	N	45.91	1422.613	11	-0.2	712.3134	2	6.95	1073	2	92	102	Carbamidomethylation
28	4071	tr|A0A091I517|A0A091I517_CALAN	Hypothetical protein N300_06305	K.LIWSEIFADC(+57.02)HS(-2.02)VIPPEPFFK.G	Y	41.14	2529.24	21	16.1	844.1009	3	14.82	2798	2	258	278	Carbamidomethylation; 2-amino-3-oxo-butanoic_acid
28	4071	tr|A0A091I517|A0A091I517_CALAN	Hypothetical protein N300_06305	R.GVC(+57.02)IDWR.G	N	26.67	904.4225	7	-0.4	453.2184	2	7.36	1176	1	308	314	Carbamidomethylation
29	4096	tr|A0A1D5PU28|A0A1D5PU28_CHICK	Mucin-5AC	K.SC(+57.02)PAFN(+.98)PDLC(+57.02)EPDN(+.98)IQLSDDGC(+57.02)C(+57.02)R.V	Y	44.38	2841.099	24	6.5	948.0463	3	7.48	1206	1	929	952	Carbamidomethylation; Deamidation (NQ)
29	4096	tr|A0A1D5PU28|A0A1D5PU28_CHICK	Mucin-5AC	S.Q(-17.03)GDFETYQHIR.A	N	31.43	1375.616	11	1.8	688.8163	2	7.14	1121	1	112	122	Pyro-glu from Q
29	4096	tr|A0A1D5PU28|A0A1D5PU28_CHICK	Mucin-5AC	MC(+57.02)LNYR.I	N	29.76	855.3731	6	1	428.6942	2	6.06	883	1	1	6	Carbamidomethylation
29	4096	tr|A0A1D5PU28|A0A1D5PU28_CHICK	Mucin-5AC	R.AAGKEVC(+57.02)H(sub Q)QPK.Q	N	27.2	1223.608	11	0.3	408.8767	3	0.81	112	1	123	133	Carbamidomethylation; Mutation
29	4096	tr|A0A1D5PU28|A0A1D5PU28_CHICK	Mucin-5AC	R.GVC(+57.02)IDWR.G	N	26.67	904.4225	7	-0.4	453.2184	2	7.36	1176	1	641	647	Carbamidomethylation
30	7556	tr|A0A099ZAP5|A0A099ZAP5_TINGU	78 kDa glucose-regulated protein/ Heat shock protein 70kDa	K.SQIFSTASDNQPTVTIK.V	Y	29.09	1835.927	17	-3.7	918.9671	2	8.18	1373	4	407	423	
30	4240	tr|H0ZAB3|H0ZAB3_TAEGU	78 kDa glucose-regulated protein/ Heat shock protein 70kDa	K.SQIFSTASDNQPTVTIK.V	Y	29.09	1835.927	17	-3.7	918.9671	2	8.18	1373	4	448	464	

30	4239	tr|A0PA15|A0PA15_COTJA	78 kDa glucose-regulated protein/ Heat shock protein 70kDa	K.SQIFSTASDNQPTVTIK.V	Y	29.09	1835.927	17	-3.7	918.9671	2	8.18	1373	4	446	462	
30	4238	tr|A0ZT13|A0ZT13_COTJA	78 kDa glucose-regulated protein/ Heat shock protein 70kDa	K.SQIFSTASDNQPTVTIK.V	Y	29.09	1835.927	17	-3.7	918.9671	2	8.18	1373	4	446	462	
30	4237	tr|A0A091F8D2|A0A091F8D2_CORBR	78 kDa glucose-regulated protein/ Heat shock protein 70kDa	K.SQIFSTASDNQPTVTIK.V	Y	29.09	1835.927	17	-3.7	918.9671	2	8.18	1373	4	447	463	
30	4236	tr|A0A091KV08|A0A091KV08_9GRUI	78 kDa glucose-regulated protein/ Heat shock protein 70kDa	K.SQIFSTASDNQPTVTIK.V	Y	29.09	1835.927	17	-3.7	918.9671	2	8.18	1373	4	414	430	
30	4235	tr|A0A093QLZ7|A0A093QLZ7_9PASS	78 kDa glucose-regulated protein/ Heat shock protein 70kDa	K.SQIFSTASDNQPTVTIK.V	Y	29.09	1835.927	17	-3.7	918.9671	2	8.18	1373	4	407	423	
30	4234	tr|U3I640|U3I640_ANAPL	78 kDa glucose-regulated protein/ Heat shock protein 70kDa	K.SQIFSTASDNQPTVTIK.V	Y	29.09	1835.927	17	-3.7	918.9671	2	8.18	1373	4	406	422	
30	4233	tr|A0A091V9R8|A0A091V9R8_OPIHO	78 kDa glucose-regulated protein/ Heat shock protein 70kDa	K.SQIFSTASDNQPTVTIK.V	Y	29.09	1835.927	17	-3.7	918.9671	2	8.18	1373	4	407	423	
30	4232	tr|A0A091VTR8|A0A091VTR8_NIPNI	78 kDa glucose-regulated protein/ Heat shock protein 70kDa	K.SQIFSTASDNQPTVTIK.V	Y	29.09	1835.927	17	-3.7	918.9671	2	8.18	1373	4	407	423	
30	4231	tr|A0A091HVD4|A0A091HVD4_CALAN	78 kDa glucose-regulated protein/ Heat shock protein 70kDa	K.SQIFSTASDNQPTVTIK.V	Y	29.09	1835.927	17	-3.7	918.9671	2	8.18	1373	4	407	423	
30	4230	tr|A0A087R4J8|A0A087R4J8_APTFO	78 kDa glucose-regulated protein/ Heat shock protein 70kDa	K.SQIFSTASDNQPTVTIK.V	Y	29.09	1835.927	17	-3.7	918.9671	2	8.18	1373	4	407	423	
30	4229	tr|A0A093J3B2|A0A093J3B2_PICPB	78 kDa glucose-regulated protein/ Heat shock protein 70kDa	K.SQIFSTASDNQPTVTIK.V	Y	29.09	1835.927	17	-3.7	918.9671	2	8.18	1373	4	407	423	
30	4228	tr|A0A093EHT4|A0A093EHT4_TYTAL	78 kDa glucose-regulated protein/ Heat shock protein 70kDa	K.SQIFSTASDNQPTVTIK.V	Y	29.09	1835.927	17	-3.7	918.9671	2	8.18	1373	4	407	423	
30	4227	tr|A0A091LT36|A0A091LT36_CARIC	78 kDa glucose-regulated protein/ Heat shock protein 70kDa	K.SQIFSTASDNQPTVTIK.V	Y	29.09	1835.927	17	-3.7	918.9671	2	8.18	1373	4	407	423	
30	4226	tr|A0A091H8K7|A0A091	78 kDa glucose-regulated protein/ Heat shock protein	K.SQIFSTASDNQPTVTIK.V	Y	29.09	1835.927	17	-3.7	918.9	2	8.18	1373	4	407	423	

		H8K7_9AVES	70kDa							671							
30	4224	tr|A0A093HUL5|A0A093HUL5_STRCA	78 kDa glucose-regulated protein/ Heat shock protein 70kDa	K.SQIFSTASDNQPTVTIK.V	Y	29.09	1835.927	17	-3.7	918.9671	2	8.18	1373	4	407	423	
30	4222	tr|A0A091U752|A0A091U752_PHORB	78 kDa glucose-regulated protein/ Heat shock protein 70kDa	K.SQIFSTASDNQPTVTIK.V	Y	29.09	1835.927	17	-3.7	918.9671	2	8.18	1373	4	396	412	
30	4221	tr|A0A093J4G2|A0A093J4G2_EURHL	78 kDa glucose-regulated protein/ Heat shock protein 70kDa	K.SQIFSTASDNQPTVTIK.V	Y	29.09	1835.927	17	-3.7	918.9671	2	8.18	1373	4	393	409	
30	4220	tr|G1N8R5|G1N8R5_MELGA	78 kDa glucose-regulated protein/ Heat shock protein 70kDa	K.SQIFSTASDNQPTVTIK.V	Y	29.09	1835.927	17	-3.7	918.9671	2	8.18	1373	4	407	423	
32	7659	tr|A0A1D5PXD0|A0A1D5PXD0_CHICK	Selenocysteine-specific elongation factor isoform X1	T.ITLLFK.R	Y	23.68	733.4738	6	3.2	367.7453	2	8.2	1380	4	560	565	
33	4357	tr|A0A093BE17|A0A093BE17_CHAPE	Deleted in malignant brain tumors 1 protein	K.SPSVYLK.C	Y	23.79	792.4381	7	0.6	397.2266	2	5.91	860	1	81	87	
33	4357	tr|A0A093BE17|A0A093BE17_CHAPE	Deleted in malignant brain tumors 1 protein	R.KSPSVYLK.C	Y	22.78	920.5331	8	-0.3	461.2737	2	5.14	743	1	80	87	
34	4086	tr|A0A091JRH3|A0A091JRH3_9AVES	45 kDa calcium-binding protein	R.WYQADNPPPDLLLNEEEFLSFLHPEHSR.G	Y	71.1	3392.61	28	0	849.1598	4	14.85	2804	2	174	201	
34	7551	tr|A0A091TMS0|A0A091TMS0_PHALP	45 kDa calcium-binding protein	R.WYQADNPPPDLLLNEEEFLSFLHPEHSR.G	Y	71.1	3392.61	28	0	849.1598	4	14.85	2804	2	174	201	
34	7550	tr|A0A091NEX0|A0A091NEX0_APAVI	45 kDa calcium-binding protein	R.WYQADNPPPDLLLNEEEFLSFLHPEHSR.G	Y	71.1	3392.61	28	0	849.1598	4	14.85	2804	2	174	201	
34	7549	tr|A0A091PAL6|A0A091PAL6_LEPDC	45 kDa calcium-binding protein	R.WYQADNPPPDLLLNEEEFLSFLHPEHSR.G	Y	71.1	3392.61	28	0	849.1598	4	14.85	2804	2	174	201	
34	4119	tr|A0A093C625|A0A093C625_9AVES	45 kDa calcium-binding protein	R.WYQADNPPPDLLLNEEEFLSFLHPEHSR.G	Y	71.1	3392.61	28	0	849.1598	4	14.85	2804	2	174	201	
34	7552	tr|A0A091H4Q9|A0A091H4Q9_BUCRH	45 kDa calcium-binding protein	R.WYQADNPPPDLLLNEEEFLSFLHPEHSR.G	Y	71.1	3392.61	28	0	849.1598	4	14.85	2804	2	174	201	
34	7548	tr|A0A099Z957|A0A099Z957_TINGU	45 kDa calcium-binding protein	R.WYQADNPPPDLLLNEEEFLSFLHPEHSR.G	Y	71.1	3392.61	28	0	849.1598	4	14.85	2804	2	174	201	

34	4126	tr|A0A0A0AQY4|A0A0A0AQY4_CHAVO	45 kDa calcium-binding protein	R.WYQADNPPPDLLLNEEEFLSFLHPEHSR.G	Y	71.1	3392.61	28	0	849.1598	4	14.85	2804	2	174	201	
34	4131	tr|A0A091J9Q7|A0A091J9Q7_CALAN	45 kDa calcium-binding protein	R.WYQADNPPPDLLLNEEEFLSFLHPEHSR.G	Y	71.1	3392.61	28	0	849.1598	4	14.85	2804	2	180	207	
34	4130	tr|A0A093IV46|A0A093IV46_EURHL	45 kDa calcium-binding protein	R.WYQADNPPPDLLLNEEEFLSFLHPEHSR.G	Y	71.1	3392.61	28	0	849.1598	4	14.85	2804	2	174	201	
34	4129	tr|A0A091L3N9|A0A091L3N9_CATAU	45 kDa calcium-binding protein	R.WYQADNPPPDLLLNEEEFLSFLHPEHSR.G	Y	71.1	3392.61	28	0	849.1598	4	14.85	2804	2	174	201	
34	4128	tr|A0A091M3R6|A0A091M3R6_CARIC	45 kDa calcium-binding protein	R.WYQADNPPPDLLLNEEEFLSFLHPEHSR.G	Y	71.1	3392.61	28	0	849.1598	4	14.85	2804	2	174	201	
34	4127	tr|A0A091WMT3|A0A091WMT3_OPIHO	45 kDa calcium-binding protein	R.WYQADNPPPDLLLNEEEFLSFLHPEHSR.G	Y	71.1	3392.61	28	0	849.1598	4	14.85	2804	2	174	201	
34	4125	tr|A0A091UV24|A0A091UV24_NIPNI	45 kDa calcium-binding protein	R.WYQADNPPPDLLLNEEEFLSFLHPEHSR.G	Y	71.1	3392.61	28	0	849.1598	4	14.85	2804	2	174	201	
34	4124	tr|A0A087VP14|A0A087VP14_BALRE	45 kDa calcium-binding protein	R.WYQADNPPPDLLLNEEEFLSFLHPEHSR.G	Y	71.1	3392.61	28	0	849.1598	4	14.85	2804	2	174	201	
34	4123	tr|A0A087QSB0|A0A087QSB0_APTFO	45 kDa calcium-binding protein	R.WYQADNPPPDLLLNEEEFLSFLHPEHSR.G	Y	71.1	3392.61	28	0	849.1598	4	14.85	2804	2	174	201	
34	4122	tr|A0A091N2G3|A0A091N2G3_9PASS	45 kDa calcium-binding protein	R.WYQADNPPPDLLLNEEEFLSFLHPEHSR.G	Y	71.1	3392.61	28	0	849.1598	4	14.85	2804	2	174	201	
34	4121	tr|A0A093P6L7|A0A093P6L7_PYGAD	45 kDa calcium-binding protein	R.WYQADNPPPDLLLNEEEFLSFLHPEHSR.G	Y	71.1	3392.61	28	0	849.1598	4	14.85	2804	2	174	201	
34	4120	tr|A0A091S825|A0A091S825_MERNU	45 kDa calcium-binding protein	R.WYQADNPPPDLLLNEEEFLSFLHPEHSR.G	Y	71.1	3392.61	28	0	849.1598	4	14.85	2804	2	174	201	
34	4118	tr|A0A091FU09|A0A091FU09_9AVES	45 kDa calcium-binding protein	R.WYQADNPPPDLLLNEEEFLSFLHPEHSR.G	Y	71.1	3392.61	28	0	849.1598	4	14.85	2804	2	174	201	
34	4117	tr|A0A093D128|A0A093D128_TAUER	45 kDa calcium-binding protein	R.WYQADNPPPDLLLNEEEFLSFLHPEHSR.G	Y	71.1	3392.61	28	0	849.1598	4	14.85	2804	2	174	201	
34	4116	tr|A0A091R7C3|A0A091R7C3_9GRUI	45 kDa calcium-binding protein	R.WYQADNPPPDLLLNEEEFLSFLHPEHSR.G	Y	71.1	3392.61	28	0	849.1598	4	14.85	2804	2	174	201	
34	4115	tr|A0A091KSZ2|A0A091KSZ2_9GRUI	45 kDa calcium-binding protein	R.WYQADNPPPDLLLNEEEFLSFLHPEHSR.G	Y	71.1	3392.61	28	0	849.1598	4	14.85	2804	2	109	136	
34	4114	tr|A0A091PRV2|A0A091PRV2_HALAL	45 kDa calcium-binding protein	R.WYQADNPPPDLLLNEEEFLSFLHPEHSR.G	Y	71.1	3392.61	28	0	849.1598	4	14.85	2804	2	109	136	
34	4113	tr|A0A091UH75|A0A091	45 kDa calcium-binding protein	R.WYQADNPPPDLLLNEEEFLSFLHPEHSR.G	Y	71.1	3392.61	28	0	849.1	4	14.8	2804	2	104	131	

		UH75_PHORB								598		5					
34	4112	tr|A0A094KP97|A0A094KP97_9AVES	45 kDa calcium-binding protein	R.WYQADNPPPDLLLNEEEFLSFLHPEHSR.G	Y	71.1	3392.61	28	0	849.1598	4	14.85	2804	2	102	129	
34	4111	tr|A0A094KKK3|A0A094KKK3_ANTCR	45 kDa calcium-binding protein	R.WYQADNPPPDLLLNEEEFLSFLHPEHSR.G	Y	71.1	3392.61	28	0	849.1598	4	14.85	2804	2	11	38	
34	4088	tr|A0A093JL69|A0A093JL69_STRCA	45 kDa calcium-binding protein	R.WYQADNPPPDLLLNEEEFLSFLHPEHSR.G	Y	71.1	3392.61	28	0	849.1598	4	14.85	2804	2	174	201	
34	4087	tr|A0A093GZT0|A0A093GZT0_PICPB	45 kDa calcium-binding protein	R.WYQADNPPPDLLLNEEEFLSFLHPEHSR.G	Y	71.1	3392.61	28	0	849.1598	4	14.85	2804	2	174	201	
34	4085	tr|A0A093Q7F3|A0A093Q7F3_9PASS	45 kDa calcium-binding protein	R.WYQADNPPPDLLLNEEEFLSFLHPEHSR.G	Y	71.1	3392.61	28	0	849.1598	4	14.85	2804	2	174	201	
35	4172	tr|A0A091M1K5|A0A091M1K5_CARIC	Neuropilin and tolloid-like 1	R.DGPFGFSPIIGR.F	Y	39.08	1261.646	12	-30.9	631.8105	2	9.6	1706	2	98	109	
35	4173	tr|A0A1D5PQM2|A0A1D5PQM2_CHICK	Neuropilin and tolloid-like protein 1 isoform X2	R.DGPFGFSPIIGR.F	Y	39.08	1261.646	12	-30.9	631.8105	2	9.6	1706	2	105	116	
35	4174	tr|A0A093FGT3|A0A093FGT3_TYTAL	Neuropilin and tolloid-like 1	R.DGPFGFSPIIGR.F	Y	39.08	1261.646	12	-30.9	631.8105	2	9.6	1706	2	32	43	
35	4175	tr|A0A087QND6|A0A087QND6_APTFO	Neuropilin and tolloid-like 1	R.DGPFGFSPIIGR.F	Y	39.08	1261.646	12	-30.9	631.8105	2	9.6	1706	2	32	43	
35	4176	tr|R0LMR2|R0LMR2_ANAPL	Neuropilin and tolloid-like 1	R.DGPFGFSPIIGR.F	Y	39.08	1261.646	12	-30.9	631.8105	2	9.6	1706	2	79	90	
35	4177	tr|A0A091JZC9|A0A091JZC9_COLST	Neuropilin and tolloid-like 1	R.DGPFGFSPIIGR.F	Y	39.08	1261.646	12	-30.9	631.8105	2	9.6	1706	2	79	90	
35	4180	tr|A0A091TLD0|A0A091TLD0_9AVES	Neuropilin and tolloid-like 1	R.DGPFGFSPIIGR.F	Y	39.08	1261.646	12	-30.9	631.8105	2	9.6	1706	2	97	108	
35	4179	tr|A0A091Q239|A0A091Q239_LEPDC	Neuropilin and tolloid-like 1	R.DGPFGFSPIIGR.F	Y	39.08	1261.646	12	-30.9	631.8105	2	9.6	1706	2	97	108	
35	4178	tr|A0A091G4C9|A0A091G4C9_9AVES	Neuropilin and tolloid-like 1	R.DGPFGFSPIIGR.F	Y	39.08	1261.646	12	-30.9	631.8105	2	9.6	1706	2	97	108	
35	4196	tr|A0A093FW41|A0A093FW41_GAVST	Neuropilin and tolloid-like 1	R.DGPFGFSPIIGR.F	Y	39.08	1261.646	12	-30.9	631.8105	2	9.6	1706	2	98	109	
35	4195	tr|A0A091SKD1|A0A091SKD1_9GRUI	Neuropilin and tolloid-like 1	R.DGPFGFSPIIGR.F	Y	39.08	1261.646	12	-30.9	631.8105	2	9.6	1706	2	98	109	

35	4194	tr|A0A099Z9Q6|A0A099Z9Q6_TINGU	Neuropilin and tolloid-like 1	R.DGPFGFSPIIGR.F	Y	39.08	1261.646	12	-30.9	631.8105	2	9.6	1706	2	98	109	
35	4193	tr|A0A091ICA8|A0A091ICA8_CALAN	Neuropilin and tolloid-like 1	R.DGPFGFSPIIGR.F	Y	39.08	1261.646	12	-30.9	631.8105	2	9.6	1706	2	98	109	
35	4192	tr|A0A091JE74|A0A091JE74_9AVES	Neuropilin and tolloid-like 1	R.DGPFGFSPIIGR.F	Y	39.08	1261.646	12	-30.9	631.8105	2	9.6	1706	2	98	109	
35	4191	tr|A0A0A0ARN5|A0A0A0ARN5_CHAVO	Neuropilin and tolloid-like 1	R.DGPFGFSPIIGR.F	Y	39.08	1261.646	12	-30.9	631.8105	2	9.6	1706	2	98	109	
35	4190	tr|A0A093GYX1|A0A093GYX1_PICPB	Neuropilin and tolloid-like 1	R.DGPFGFSPILGR.F	Y	39.08	1261.646	12	-30.9	631.8105	2	9.6	1706	2	98	109	
35	4189	tr|A0A093IPZ4|A0A093IPZ4_EURHL	Neuropilin and tolloid-like 1	R.DGPFGFSPIIGR.F	Y	39.08	1261.646	12	-30.9	631.8105	2	9.6	1706	2	98	109	
35	4188	tr|A0A091F3F2|A0A091F3F2_CORBR	Neuropilin and tolloid-like 1	R.DGPFGFSPIIGR.F	Y	39.08	1261.646	12	-30.9	631.8105	2	9.6	1706	2	98	109	
35	4187	tr|A0A093QEM7|A0A093QEM7_9PASS	Neuropilin and tolloid-like 1	R.DGPFGFSPIIGR.F	Y	39.08	1261.646	12	-30.9	631.8105	2	9.6	1706	2	98	109	
35	4186	tr|H0ZFW8|H0ZFW8_TAEGU	Neuropilin and tolloid-like 1	R.DGPFGFSPILGR.F	Y	39.08	1261.646	12	-30.9	631.8105	2	9.6	1706	2	98	109	
35	4185	tr|A0A093BGU1|A0A093BGU1_CHAPE	Neuropilin and tolloid-like 1	R.DGPFGFSPIIGR.F	Y	39.08	1261.646	12	-30.9	631.8105	2	9.6	1706	2	98	109	
35	4184	tr|A0A091WRF1|A0A091WRF1_NIPNI	Neuropilin and tolloid-like 1	R.DGPFGFSPIIGR.F	Y	39.08	1261.646	12	-30.9	631.8105	2	9.6	1706	2	98	109	
35	4183	tr|A0A091WHV3|A0A091WHV3_OPIHO	Neuropilin and tolloid-like 1	R.DGPFGFSPIIGR.F	Y	39.08	1261.646	12	-30.9	631.8105	2	9.6	1706	2	98	109	
35	4182	tr|A0A093HHJ2|A0A093HHJ2_STRCA	Neuropilin and tolloid-like 1	R.DGPFGFSPIIGR.F	Y	39.08	1261.646	12	-30.9	631.8105	2	9.6	1706	2	98	109	
35	4181	tr|A0A093NAE4|A0A093NAE4_PYGAD	Neuropilin and tolloid-like 1	R.DGPFGFSPIIGR.F	Y	39.08	1261.646	12	-30.9	631.8105	2	9.6	1706	2	98	109	
35	4199	tr|U3IQM0|U3IQM0_ANAPL	Neuropilin and tolloid-like 1	R.DGPFGFSPIIGR.F	Y	39.08	1261.646	12	-30.9	631.8105	2	9.6	1706	2	108	119	
35	4198	tr|G1N880|G1N880_MELGA	Neuropilin and tolloid-like 1	R.DGPFGFSPIIGR.F	Y	39.08	1261.646	12	-30.9	631.8105	2	9.6	1706	2	107	118	
35	4197	tr|A0A0Q3TPW3|A0A0Q3TPW3_AMAAE	Neuropilin and tolloid-like 1	R.DGPFGFSPIIGR.F	Y	39.08	1261.646	12	-30.9	631.8105	2	9.6	1706	2	105	116	

36	4245	tr|A0A091FRV3|A0A091FRV3_9AVES	Hypothetical protein N303_00190	V.KCKPVVCDTYC(+57.02)PEGYKYTK.Q	Y	28.95	2281.058	19	2.3	571.2731	4	6.74	1026	1	523	541	Carbamidomethylation
36	4245	tr|A0A091FRV3|A0A091FRV3_9AVES	Hypothetical protein N303_00190	R.GVC(+57.02)IDWR.Q	N	26.67	904.4225	7	-0.4	453.2184	2	7.36	1176	1	308	314	Carbamidomethylation
37	4089	tr|A0A0Q3XB34|A0A0Q3XB34_AMAAE	Lysyl oxidase 3	R.VEVAVGAGAGEQPR.W	Y	39.63	1338.689	14	-0.6	670.3514	2	5.91	859	2	222	235	
38	4080	tr|A0A091T9Y4|A0A091T9Y4_PHALP	Hypothetical protein N335_00594	R.GVC(+57.02)IDWR.G	N	26.67	904.4225	7	-0.4	453.2184	2	7.36	1176	1	308	314	Carbamidomethylation
38	4080	tr|A0A091T9Y4|A0A091T9Y4_PHALP	Hypothetical protein N335_00594	K.LIWSKIFE(sub A)ECHAVIPPEPFFK.G	Y	21.69	2529.313	21	-14.2	844.0996	3	15.4	2916	1	258	278	Mutation
39	7630	tr|A0A091SIR2|A0A091SIR2_9GRUI	Hyaluronan mediated motility receptor	K.RLEQEIQSQALELAQMEEKLK.G	Y	21.99	2513.316	21	-20.4	629.3234	4	11.91	2208	1	325	345	
40	4280	tr|H0ZM61|H0ZM61_TAEGU	Deleted in malignant brain tumors 1 protein	E.TITYSNVIK.V	Y	20.32	1037.576	9	1.2	519.7957	2	6.93	1070	1	180	188	
40	4280	tr|H0ZM61|H0ZM61_TAEGU	Deleted in malignant brain tumors 1 protein	R.NYPD(sub N)NANC(+57.02)VWEIQVK.S	Y	19.58	1848.846	15	19.7	617.3016	3	7.91	1309	1	20	34	Carbamidomethylation; Mutation
40	4280	tr|H0ZM61|H0ZM61_TAEGU	Deleted in malignant brain tumors 1 protein	Q.SPFYPR.N	Y	19.1	765.3809	6	1.6	383.6984	2	5.75	833	1	14	19	
41	7554	tr|U3JPD6|U3JPD6_FICAL	Collagen alpha-2(V) chain	I.DPNQGC(+57.02)VEDAIK.V	Y	28.15	1344.598	12	8.1	673.3116	2	7.99	1329	2	1120	1131	Carbamidomethylation
41	7555	tr|H0ZL50|H0ZL50_TAEGU	Collagen alpha-2(V) chain	I.DPNQGC(+57.02)VEDAIK.V	Y	28.15	1344.598	12	8.1	673.3116	2	7.99	1329	2	1278	1289	Carbamidomethylation
41	7557	tr|G3UP25|G3UP25_MELGA	Collagen alpha-2(V) chain	I.DPNQGC(+57.02)VEDAIK.V	Y	28.15	1344.598	12	8.1	673.3116	2	7.99	1329	2	193	204	Carbamidomethylation
41	7558	tr|G3URW1|G3URW1_MELGA	Collagen alpha-2(V) chain	I.DPNQGC(+57.02)VEDAIK.V	Y	28.15	1344.598	12	8.1	673.3116	2	7.99	1329	2	248	259	Carbamidomethylation
41	7559	tr|R7VT76|R7VT76_COLLI	Collagen alpha-2(V) chain	I.DPNQGC(+57.02)VEDAIK.V	Y	28.15	1344.598	12	8.1	673.3116	2	7.99	1329	2	1278	1289	Carbamidomethylation
41	7560	tr|R0LNH9|R0LNH9_AN	Collagen alpha-2(V) chain	I.DPNQGC(+57.02)VEDAIK.V	Y	28.15	1344.598	12	8.1	673.3	2	7.99	1329	2	1284	1295	Carbamidomethylation

		APL								116							
41	7561	tr|U3IL67|U3IL67_ANAPL	Collagen alpha-2(V) chain	I.DPNQGC(+57.02)VEDAIK.V	Y	28.15	1344.598	12	8.1	673.3116	2	7.99	1329	2	1310	1321	Carbamidomethylation
41	7563	tr|A0A1D5P6W1|A0A1D5P6W1_CHICK	Collagen alpha-2(V) chain isoform X3	I.DPNQGC(+57.02)VEDAIK.V	Y	28.15	1344.598	12	8.1	673.3116	2	7.99	1329	2	1316	1327	Carbamidomethylation
41	7562	tr|G1N2W3|G1N2W3_MELGA	Collagen alpha-2(V) chain isoform X3	I.DPNQGC(+57.02)VEDAIK.V	Y	28.15	1344.598	12	8.1	673.3116	2	7.99	1329	2	1312	1323	Carbamidomethylation
42	7565	tr|U3IA51|U3IA51_ANAPL	Keratin type II cytoskeletal 75	R.SLDLDSIIAEVK.A	Y	25.63	1301.708	12	40.1	651.8873	2	12.5	2335	1	283	294	
42	7564	tr|R0J8L6|R0J8L6_ANAPL	Keratin type II cytoskeletal 75	R.SLDLDSIIAEVK.A	Y	25.63	1301.708	12	40.1	651.8873	2	12.5	2335	1	282	293	
42	7566	tr|H9H0B7|H9H0B7_MELGA	Keratin, type II cytoskeletal 4-like	R.SLDLDSIIAEVK.A	Y	25.63	1301.708	12	40.1	651.8873	2	12.5	2335	1	70	81	
42	7567	tr|H9H0B6|H9H0B6_MELGA	Keratin, type II cytoskeletal 4-like	R.SLDLDSIIAEVK.A	Y	25.63	1301.708	12	40.1	651.8873	2	12.5	2335	1	118	129	
42	7568	tr|A0A093GRA7|A0A093GRA7_PICPB	Keratin type II cytoskeletal 75	R.SLDLDSIIAEVK.A	Y	25.63	1301.708	12	40.1	651.8873	2	12.5	2335	1	230	241	
42	7569	tr|A0A091MSU7|A0A091MSU7_9PASS	Keratin type II cytoskeletal 75	R.SLDLDSIIAEVK.A	Y	25.63	1301.708	12	40.1	651.8873	2	12.5	2335	1	240	251	
42	7571	tr|U3JP96|U3JP96_FICAL	Keratin, type II cytoskeletal 4-like	R.SLDLDSIIAEVK.A	Y	25.63	1301.708	12	40.1	651.8873	2	12.5	2335	1	275	286	
42	7570	tr|H0Z0C5|H0Z0C5_TAEGU	Keratin, type II cytoskeletal 4-like	R.SLDLDSIIAEVK.A	Y	25.63	1301.708	12	40.1	651.8873	2	12.5	2335	1	273	284	
42	7572	tr|U3JP95|U3JP95_FICAL	Keratin, type II cytoskeletal 4-like	R.SLDLDSIIAEVK.A	Y	25.63	1301.708	12	40.1	651.8873	2	12.5	2335	1	300	311	
42	7573	tr|U3IFQ5|U3IFQ5_ANAPL	Keratin, type II cytoskeletal 4-like	R.SLDLDSIIAEVK.A	Y	25.63	1301.708	12	40.1	651.8873	2	12.5	2335	1	331	342	
42	7574	tr|U3JPW5|U3JPW5_FICAL	Keratin, type II cytoskeletal cochleal-like	R.SLDLDSIIAEVK.A	Y	25.63	1301.708	12	40.1	651.8873	2	12.5	2335	1	347	358	
43	4429	tr|U3J1Y3|U3J1Y3_ANAPL	Protein lin-9 homolog isoform X1	L.QSPITDSDPLLGQSSWK.N	Y	20.6	1857.911	17	-10.6	620.3043	3	8.24	1388	1	308	324	
43	4427	tr|A0A091F4A8|A0A091F	Protein lin-9 (Fragment)	L.QSPITDSDPLLGQSSWK.N	Y	20.6	1857.911	17	-10.6	620.3	3	8.24	1388	1	297	313	

		4A8_CORBR								043							
43	4426	tr|A0A091IE25|A0A091IE25_CALAN	Protein lin-9 (Fragment)	L.QSPLTDSDPLLGQSSWK.N	Y	20.6	1857.911	17	-10.6	620.3043	3	8.24	1388	1	297	313	
43	4424	tr|A0A091MQ05|A0A091MQ05_9PASS	Protein lin-9 (Fragment)	L.QSPITDSDPLLGQSSWK.N	Y	20.6	1857.911	17	-10.6	620.3043	3	8.24	1388	1	297	313	
43	4423	tr|H0Z1D7|H0Z1D7_TAEGU	Protein lin-9	L.QSPITDSDPLLGQSSWK.N	Y	20.6	1857.911	17	-10.6	620.3043	3	8.24	1388	1	297	313	
43	4422	tr|A0A093EQ52|A0A093EQ52_TYTAL	Protein lin-9	L.QSPITDSDPLLGQSSWK.N	Y	20.6	1857.911	17	-10.6	620.3043	3	8.24	1388	1	297	313	
43	4414	tr|A0A091H8T7|A0A091H8T7_9AVES	Protein lin-9	L.QSPITDSDPLLGQSSWK.N	Y	20.6	1857.911	17	-10.6	620.3043	3	8.24	1388	1	297	313	
43	4413	tr|A0A091VS37|A0A091VS37_NIPNI	Protein lin-9	L.QSPITDSDPLLGQSSWK.N	Y	20.6	1857.911	17	-10.6	620.3043	3	8.24	1388	1	297	313	
43	4411	tr|A0A093PYF4|A0A093PYF4_9PASS	Protein lin-9	L.QSPITDSDPLLGQSSWK.S	Y	20.6	1857.911	17	-10.6	620.3043	3	8.24	1388	1	297	313	
43	4410	tr|R0K4G2|R0K4G2_ANAPL	Lin-9-like protein	L.QSPITDSDPLLGQSSWK.N	Y	20.6	1857.911	17	-10.6	620.3043	3	8.24	1388	1	287	303	
43	4409	tr|U3KAS0|U3KAS0_FICAL	Protein lin-9 homolog isoform X2	L.QSPITDSDPLLGQSSWK.N	Y	20.6	1857.911	17	-10.6	620.3043	3	8.24	1388	1	256	272	
43	4408	tr|R7VWM6|R7VWM6_COLLI	Lin-9 like protein	L.QSPITDSDPLLGQSSWK.S	Y	20.6	1857.911	17	-10.6	620.3043	3	8.24	1388	1	215	231	
43	4404	tr|A0A093IZM7|A0A093IZM7_FULGA	Protein lin-9	L.QSPITDSDPLLGQSSWK.N	Y	20.6	1857.911	17	-10.6	620.3043	3	8.24	1388	1	297	313	
44	7584	tr|A0A093GEW7|A0A093GEW7_PICPB	Fibronectin type III domain-containing protein 3B	R.APSLSFLSDAR.V	Y	21.98	1162.598	11	81.2	582.3536	2	10.31	1866	1	771	781	
44	7631	tr|A0A091VQQ8|A0A091VQQ8_NIPNI	Fibronectin type III domain-containing protein 3B	R.APSLSFLSDAR.V	Y	21.98	1162.598	11	81.2	582.3536	2	10.31	1866	1	788	798	
45	7648	tr|L1IJ368|L1IJ368_GUITH	Hypothetical protein GUITHDRAFT_110997	A.QATSVSWNDDWGITTSK.W	Y	20.37	1894.87	17	-9.1	948.4335	2	6.35	938	1	34	50	
46	307	tr|U3K2X6|U3K2X6_FICAL	Protein bassoon	R.HHREYDRHSGSSR.H	Y	21.58	1622.741	13	25.5	406.7029	4	18.41	3460	1	3522	3534	

47	4261	tr|A0A093IF41|A0A093IF41_FULGA	Nucleobindin-2	K.LHDVNNDGFLDEQELEALFTKELEK.V	Y	50.3	2945.429	25	6	737.369	4	13.89	2621	1	252	276	
48	7635	tr|A0A091UL69|A0A091UL69_PHALP	Putative threonine--tRNA ligase 2 cytoplasmic	R.NFTEVVSPNIFNSKLWEASGHWQHYSENMFSFEIEK.E	Y	21.65	4331.006	36	35.5	867.2392	5	27.78	4890	1	318	353	
49	7651	tr|A0A091HMJ8|A0A091HMJ8_BUCRH	Integrator complex subunit 1	R.RDSAETAR.S	Y	20.92	904.4362	8	-15.8	453.2182	2	7.38	1178	1	1239	1246	

Chapter 7

Discussion, general conclusion, future works and recommendations

7.1 Discussion

7.1.1 Possible links between EBN protein and effects seen in NSC and animal studies

In Chapter 6, some proteins identified from the proteomic analysis of EBN were suggested to be involved in the neuroprotective effects of EBN on PD neuronal cell model as studied in Chapter 3. Here, it is speculated that some proteins from the EBN may be associated with the neurotrophic effects of EBN seen in the study with NSC model (Chapter 4) and neuroprotective effects of EBN seen in the animal studies (Chapter 5).

EBN was found to contain proteins with a variety of neurotrophic functions. Protein lin-9 regulates cell proliferation by modulating the expression of genes involved in mitosis and cytokinesis (Esterlechner et al., 2013, Osterloh et al., 2007). The presence of this protein in EBN might explain the proliferative outcome of EBN-treated NE4C neural stem cell in Chapter 4. INTS1 protein, discovered only in the water extract of EBN, might play a role in directing neuronal migration. Knock-down of integrator complex subunit 1 *in vivo* has been shown to affect cortical neuronal patterning in mouse embryonic brain. Hence it is hypothesized that INTS1 may be present in EBN to affect migration behavior of the NSC as seen in Chapter 4 (van den Berg et al., 2017). Hyaluronan mediated motility receptor is a protein bound to hyaluronan to coordinate cell migration as well as neurite extension in neuron, therefore it is likely to have contributed to translocation and neuronal differentiation in EBN-treated NE4C neural stem cell (Nagy et al., 1995). On top of that, the presence of RGMB protein in raw EBN powder is likely to contribute to neurogenesis in NE4C cell model due to its potential in promoting neurite extension and axonal growth through BMP signalling (Ma, 2011). The sole presence of this protein in S1 (trypsin-treated crude EBN extract) explains the findings in Chapter 4 whereby S1 promoted neuronal differentiation

more efficiently than S2 (trypsin-treated water extract of EBN), indicating higher neurotrophic effect in S1 comparing to S2.

Proteomic analysis of EBN also revealed the exclusive presence of selenocysteine-specific elongation factor with potential ROS-reducing effect in water extract of EBN. Selenocysteine-specific elongation factor is an essential mediator in the biosynthesis of selenoproteins, one of which includes the GPX family (Dubey and Copeland, 2016). In Chapter 5, it was found that expression of GPX1 protein in substantia nigra of EBN-treated PD mouse model was elevated as compared to untreated PD mice, which is likely attributed to enhanced synthesis of selenoprotein glutathione peroxidase in the mice brain via EBN supplementation. With that, EBN treatment could have led to efficient sequestration of cell-damaging peroxides and ROS, prevented lipid peroxidation and inflammatory response from activated microglia, and eventually resulted in preservation of dopaminergic neuron in the substantia nigra of 6-OHDA-injected mice (Pillai et al., 2014). The presence of selenocysteine-specific elongation factor in water extract of EBN explains the higher expression of GPX1 in the substantia nigra of S2-treated mice.

7.1.2 Rationale of using EBN as a nutraceutical option for PD

Current therapies for PD are mostly symptomatic and therefore dopamine-based. However, long term dopaminergic medication often results in wearing-off phenomenon, whereas non-motor symptoms appearing in late stage PD are mostly refractory to dopaminergic therapy (Jenner, 2015). Also, invasive procedures like deep brain stimulation is not suitable for elderly, associated with risk of surgery complications and development of neuropsychiatric side effects (Burn and Troster, 2004). Since PD is a disease in the deep brain and due to its complicated pathogenesis, any of these conventional treatments are still

far from being a stand-alone approach to PD management and often need to couple to other therapy to achieve optimum results. They also failed to counteract the progressive degenerative nature of the disease. The purpose of neuroprotective therapy is to apply treatment at early stage of the disease to delay disease progression. For instance, it has been shown in clinical studies that Chinese herb formulas as an adjunct improved both motor and non-motor complications of PD, and reduced the use of dopaminergic medication and events of dyskinesia due to its multi-target neuroprotective mechanisms (Zeng, 2017). Currently many studies are focusing on reducing oxidative stress, inhibiting excitotoxicity, providing trophic support, enhancing mitochondrial functionality, counteracting inflammation and preventing apoptosis (Fahn and Sulzer, 2004).

Meanwhile, natural product has raised public's interest in the treatment of many health complications, including PD (Mythri et al., 2012). Since EBN contains proteins which might possess neuroprotective and neurotrophic effects, EBN may be explored as a nutraceutical for PD treatment and achieve a disease-modifying outcome in PD. Ultimately, the present study expanded the research on EBN so that evidence-based medicinal value may be established for this food product in the future.

7.1.3 Protein across blood brain barrier?

Due to hydrophobicity nature and molecular weight, macromolecule like proteins has limited permeability through the tight junctions on blood-brain-barrier (BBB). In Chapter 6, proteomics analysis showed that all trypsin-digested peptides from EBN were less than 6kDa, and 94% of them are smaller than 3kDa. Since EBN samples used in current study were trypsin-digested to resemble the biological digestion process whereby large proteins are broken down to smaller peptides, it is not surprising to predict that some of the bioactive

peptides described above may cross the BBB in the animal model by transmembrane diffusion as the largest substance found to date to cross the BBB weighed up to 7kDa (Banks, 2009). Assimilation of the peptides into the brain may also be achieved by receptor-mediated transcytosis (Laterra et al., 1999). For instance, RGMB as part of the plasma membrane receptor has the highest expression level in the brain (Mouse ENCODE transcriptome data), implying an active state of RGMB homeostasis, hence RGMB trafficking might be up-regulated at the BBB. Passage of bioactive proteins in EBN through BBB may be evaluated in the future for optimization of drug delivery.

7.2 General conclusion of the study

In summary, it has been successfully demonstrated that EBN extracts confer neuroprotection in 6-OHDA-challenged SH-SY5Y cell model. Particularly, S1 demonstrated neuroprotective potential by improving cell viability while S2 inhibited oxidative stress and caspase-3 activation. Both the EBN extracts were able to attenuate apoptosis of the neurons due to 6-OHDA-induced oxidative stress. EBN was also shown to possess neurotrophic effects on NSCs by regulating proliferation, migration and neuronal differentiation. The potential of EBN in neurogenesis might be of medical importance in the treatment of aging-related neurodegenerative disorders. Additionally, oral supplementation of EBN was demonstrated to be beneficial to PD mouse model by restoring motor function, preserving dopaminergic neuron, improving expression of antioxidant glutathione peroxidase 1 and ameliorating expression of activated microglia in the substantia nigra following 6-OHDA injection. Lipid peroxidation and nitric oxide formation in 6-OHDA-treated SH-SY5Y cell were reduced by EBN treatment. Lastly, protein analysis of EBN extracts has identified bioactive proteins with potential role in immunity, extracellular matrix formation, neurodevelopment, cell survival and apoptosis, cell proliferation and migration, antioxidation

as well as common cellular processes. The antioxidant activities of both crude and water extracts of EBN were studied as well. Some of the proteins found in EBN were speculated to be linked to the neuroprotective and neurotrophic effects of EBN reported in the Chapter 3 to 6 in this thesis, and mainly attributed to antioxidant and anti-inflammatory properties of EBN, which might differ following different extraction methods.

7.3 Future works and recommendations

7.3.1 Purification of bioactive compound and characterization of novel compound

Our study has successfully demonstrated the neuroprotective and neurotrophic effects of EBN in the form of crude extract and water extract, followed by a comprehensive protein profiling which revealed a list of proteins possessing various functions. It is recommended to subject the EBN extracts to further fractionation using preparative high-performance liquid chromatography. The elute may be purified multiple times, cleaned-up and concentrated for further analyses.

Using the principle of bioassay-guided isolation, fractions may be tested on cell lines and animal models for direct elucidation of their bioactivities. The methodology used in the studies in Chapter 3-6 may be repeated with purified sample in order to screen for pure compound which exerts neuroprotective and neurotrophic effects similar to the current findings reported in this thesis. Compound which shows peak on the chromatogram may be identified by comparing its retention time to the literature. Nonetheless, compound unidentified at this stage may be further characterized with the use of elemental techniques such as X-ray crystallography, which will be useful for finding out the structure of crystallisable component in the lyophilized pure compound isolated from EBN (Deschamps, 2010). In case of liquid EBN sample, ultraviolet–visible spectroscopy, nuclear magnetic

resonance (NMR), Fourier-transform infrared spectroscopy and mass spectrometry may be employed. In particular, tandem mass spectrometry will generate a wealth of information about the compound including molecular formula, mass and mass-to-charge ratio (Kaklamanos et al., 2012). These data may also be correlated with NMR data, which includes information on number of carbon atoms, hydrogen atoms, nitrogen atoms or phosphorous atoms, which allows reconstruction of the molecule architecture. These technologies will help to elucidate the structure, elemental make-up and physical properties of the novel compound (Forseth and Schroeder, 2011).

Interestingly, a concept known as bioactive molecular networking was recently proposed to identify candidate molecules directly from fractionated bioactive extracts (Nothias et al., 2018). Molecular networking is a tandem mass spectrometry (MS/MS) data organizational method recently introduced in high-throughput drug discovery. This approach is advantageous in the sense that it avoids repeated discovery of molecules previously identified by enabling dereplication of molecules using molecular networking prior to isolation of the compounds. It is also possible to reveal potentially bioactive molecules using bioactivity score prediction, which is calculated based on the relative abundance of a molecule in the fraction and the bioactivity level of the fraction (Quinn et al., 2017).

Molecular networking is a versatile algorithm to illustrate chemical relationship between MS/MS spectra and has contributed extensively towards the development of the database called Global Natural Products Social Molecular Networking (GNPS) (Wang et al., 2016). GNPS on the other hand, may be utilized for search of molecules with similar spectral information in the molecular network, hence allowing the identification of analogues and novel compounds for potential therapeutic application (Nothias et al., 2018). Using this

approach, Nothias et al. successfully isolated novel and effective antiviral compound from a previously investigated extract of *Euphorbia dendroides* where the bioactive diterpene esters were not discovered following a classical bioassay-guided fractionation procedure (Esposito et al., 2016). Novel neuroprotective and neurotrophic compounds in EBN sample may be predicted using such strategy. Compound identified from this stage may be explored as drug lead in the treatment of neurodegenerative diseases.

7.3.2 Study on alternative PD model

PD pathology does not only reflect in degeneration of nigrostriatal dopaminergic neuron but also includes intraneuronal deposition of Lewy bodies inclusion, which results from aggregation of α-synuclein protein. Neurotoxin-induced models of PD, including those treated with 6-OHDA, MPTP and rotenone and paraquat were established based on mechanisms thought to be involved in pathogenesis of PD (Potashkin et al., 2011). However, the use of these models falls short to absence of Lewy bodies, which renders them a model that does not sufficiently address Lewy bodies as one of the major pathologies in PD (Lane and Dunnett, 2008).

Presence of Lewy bodies in neurons is an important pathological hallmark in PD hence EBN should be tested against Lewy body pathology using various models to broaden our understanding of its neuroprotective and neurotrophic potentials in counteracting the formation of Lewy bodies in PD. With the advent of genetic engineering, α-synuclein transgenesis with either wild-type or A53T mutation has been shown to approximate Lewy bodies formation in mice (Giasson et al., 2002). The transgenic A53T α-synuclein mouse model develops progressive motor failure and filamentous Lewy bodies-like inclusions in

several brain areas (Tsika et al., 2010). Whether EBN is able to restore motor function by modulating Lewy bodies deposition in the neurons is worth investigating.

Another model that may be used for the study of effect of EBN on PD is the Smad3 deficiency mouse, which features selective postnatal neurodegeneration of midbrain dopaminergic neurons, MAO-mediated catabolism of dopamine in the striatum, oxidative stress, and loss of trophic and astrocytic support to dopaminergic neurons (Tapia-Gonzalez et al., 2011). Notably, it has been suggested that there is a link between α-synuclein aggregates and cognitive impairment observed in demented PD patients as Lewy bodies are detected in the hippocampus, the brain region for learning and memory acquisition, of PD patients. Smad3 deficiency not only induces distribution of α-synuclein inclusions similar to the human Lewy bodies, but it also abolishes the induction of long-term potentiation in the dentate gyrus (Tapia-Gonzalez et al., 2013). These characteristics of Smad3 deficiency model emphasizes that it is a model which combines features such as neurodegeneration, inhibition of neurogenesis of the dentate gyrus, α-synuclein aggregation, loss of trophic support and decline of cognitive function (Giráldez-Pérez et al., 2014). It is therefore an alternative PD animal model that allows us to probe into the effect of EBN in various pathological aspects of PD hence validating its nutraceutical potential for the treatment of PD.

7.4 References

BANKS, W. A. 2009. Characteristics of compounds that cross the blood-brain barrier. *BMC Neurology,* 9**,** S3-S3.

BURN, D. J. & TROSTER, A. I. 2004. Neuropsychiatric complications of medical and surgical therapies for Parkinson's disease. *J Geriatr Psychiatry Neurol,* 17**,** 172-80.

DESCHAMPS, J. R. 2010. X-ray crystallography of chemical compounds. *Life Sci,* 86**,** 585-9.

DUBEY, A. & COPELAND, P. R. 2016. The Selenocysteine-Specific Elongation Factor Contains Unique Sequences That Are Required for Both Nuclear Export and Selenocysteine Incorporation. *PLoS One,* 11**,** e0165642.

ESPOSITO, M., NOTHIAS, L.-F., NEDEV, H., GALLARD, J.-F., LEYSSEN, P., RETAILLEAU, P., COSTA, J., ROUSSI, F., IORGA, B. I., PAOLINI, J. & LITAUDON, M. 2016. Euphorbia dendroides Latex as a Source of Jatrophane Esters: Isolation, Structural Analysis, Conformational Study, and Anti-CHIKV Activity. *Journal of Natural Products,* 79**,** 2873-2882.

ESTERLECHNER, J., REICHERT, N., ILTZSCHE, F., KRAUSE, M., FINKERNAGEL, F. & GAUBATZ, S. 2013. LIN9, a Subunit of the DREAM Complex, Regulates Mitotic Gene Expression and Proliferation of Embryonic Stem Cells. *PLOS ONE,* 8**,** e62882.

FAHN, S. & SULZER, D. 2004. Neurodegeneration and Neuroprotection in Parkinson Disease.

FORSETH, R. R. & SCHROEDER, F. C. 2011. NMR-spectroscopic analysis of mixtures: from structure to function. *Current opinion in chemical biology,* 15**,** 38-47.

GIASSON, B. I., DUDA, J. E., QUINN, S. M., ZHANG, B., TROJANOWSKI, J. Q. & LEE, V. M. 2002. Neuronal alpha-synucleinopathy with severe movement disorder in mice expressing A53T human alpha-synuclein. *Neuron,* 34**,** 521-33.

GIRÁLDEZ-PÉREZ, R. M., ANTOLÍN-VALLESPÍN, M., MUÑOZ, M. D. & SÁNCHEZ-CAPELO, A. 2014. Models of α-synuclein aggregation in Parkinson's disease. *Acta Neuropathologica Communications,* 2**,** 176.

JENNER, P. 2015. Treatment of the later stages of Parkinson's disease – pharmacological approaches now and in the future. *Translational Neurodegeneration,* 4**,** 3.

KAKLAMANOS, G., APREA, E. & THEODORIDIS, G. 2012. Chapter 9 - Mass Spectrometry. *Chemical Analysis of Food: Techniques and Applications.* Boston: Academic Press.

LANE, E. & DUNNETT, S. 2008. Animal models of Parkinson's disease and L-dopa induced dyskinesia: how close are we to the clinic? *Psychopharmacology (Berl),* 199**,** 303-12.

LATERRA, J., KEEP, R., BETZ, L. A. & GOLDSTEIN., G. W. 1999. Blood—Brain Barrier. *Basic Neurochemistry: Molecular, Cellular and Medical Aspects. .* 6th ed. Philadelphia: Lippincott-Raven.

MYTHRI, R. B., HARISH, G. & BHARATH, M. M. 2012. Therapeutic potential of natural products in Parkinson's disease. *Recent Pat Endocr Metab Immune Drug Discov,* 6**,** 181-200.

NAGY, J. I., HACKING, J., FRANKENSTEIN, U. N. & TURLEY, E. A. 1995. Requirement of the hyaluronan receptor RHAMM in neurite extension and motility as demonstrated in primary neurons and neuronal cell lines. *J Neurosci,* 15**,** 241-52.

NOTHIAS, L. F., NOTHIAS-ESPOSITO, M., DA SILVA, R., WANG, M., PROTSYUK, I., ZHANG, Z., SARVEPALLI, A., LEYSSEN, P., TOUBOUL, D., COSTA, J., PAOLINI, J., ALEXANDROV, T., LITAUDON, M. & DORRESTEIN, P. C. 2018. Bioactivity-Based Molecular Networking for the Discovery of Drug Leads in Natural Product Bioassay-Guided Fractionation. *J Nat Prod,* 81**,** 758-767.

OSTERLOH, L., VON EYSS, B., SCHMIT, F., REIN, L., HÜBNER, D., SAMANS, B., HAUSER, S. & GAUBATZ, S. 2007. The human synMuv-like protein LIN-9 is required for transcription of G2/M genes and for entry into mitosis. *The EMBO Journal,* 26**,** 144-157.

PILLAI, R., UYEHARA-LOCK, J. H. & BELLINGER, F. P. 2014. Selenium and selenoprotein function in brain disorders. *IUBMB Life,* 66**,** 229-39.

POTASHKIN, J. A., BLUME, S. R. & RUNKLE, N. K. 2011. Limitations of Animal Models of Parkinson's Disease. *Parkinson's Disease,* 2011**,** 658083.

QUINN, R. A., NOTHIAS, L.-F., VINING, O., MEEHAN, M., ESQUENAZI, E. & DORRESTEIN, P. C. 2017. Molecular Networking As a Drug Discovery, Drug Metabolism, and Precision Medicine Strategy. *Trends in Pharmacological Sciences,* 38**,** 143-154.

TAPIA-GONZALEZ, S., GIRALDEZ-PEREZ, R. M., CUARTERO, M. I., CASAREJOS, M. J., MENA, M. A., WANG, X. F. & SANCHEZ-CAPELO, A. 2011. Dopamine and alpha-synuclein dysfunction in Smad3 null mice. *Mol Neurodegener,* 6**,** 72.

TAPIA-GONZALEZ, S., MUNOZ, M. D., CUARTERO, M. I. & SANCHEZ-CAPELO, A. 2013. Smad3 is required for the survival of proliferative intermediate progenitor cells in the dentate gyrus of adult mice. *Cell Commun Signal,* 11**,** 93.

TSIKA, E., MOYSIDOU, M., GUO, J., CUSHMAN, M., GANNON, P., SANDALTZOPOULOS, R., GIASSON, B. I., KRAINC, D., ISCHIROPOULOS, H. & MAZZULLI, J. R. 2010. Distinct region-specific alpha-synuclein oligomers in A53T transgenic mice: implications for neurodegeneration. *J Neurosci,* 30**,** 3409-18.

VAN DEN BERG, D. L. C., AZZARELLI, R., OISHI, K., MARTYNOGA, B., URBÁN, N., DEKKERS, D. H. W., DEMMERS, J. A. & GUILLEMOT, F. 2017. Nipbl Interacts

with Zfp609 and the Integrator Complex to Regulate Cortical Neuron Migration. *Neuron,* 93**,** 348-361.

WANG, M., CARVER, J. J., PHELAN, V. V., SANCHEZ, L. M., GARG, N., PENG, Y., NGUYEN, D. D., WATROUS, J., KAPONO, C. A., LUZZATTO-KNAAN, T., PORTO, C., BOUSLIMANI, A., MELNIK, A. V., MEEHAN, M. J., LIU, W. T., CRUSEMANN, M., BOUDREAU, P. D., ESQUENAZI, E., SANDOVAL-CALDERON, M., KERSTEN, R. D., PACE, L. A., QUINN, R. A., DUNCAN, K. R., HSU, C. C., FLOROS, D. J., GAVILAN, R. G., KLEIGREWE, K., NORTHEN, T., DUTTON, R. J., PARROT, D., CARLSON, E. E., AIGLE, B., MICHELSEN, C. F., JELSBAK, L., SOHLENKAMP, C., PEVZNER, P., EDLUND, A., MCLEAN, J., PIEL, J., MURPHY, B. T., GERWICK, L., LIAW, C. C., YANG, Y. L., HUMPF, H. U., MAANSSON, M., KEYZERS, R. A., SIMS, A. C., JOHNSON, A. R., SIDEBOTTOM, A. M., SEDIO, B. E., KLITGAARD, A., LARSON, C. B., P, C. A. B., TORRES-MENDOZA, D., GONZALEZ, D. J., SILVA, D. B., MARQUES, L. M., DEMARQUE, D. P., POCIUTE, E., O'NEILL, E. C., BRIAND, E., HELFRICH, E. J. N., GRANATOSKY, E. A., GLUKHOV, E., RYFFEL, F., HOUSON, H., MOHIMANI, H., KHARBUSH, J. J., ZENG, Y., VORHOLT, J. A., KURITA, K. L., CHARUSANTI, P., MCPHAIL, K. L., NIELSEN, K. F., VUONG, L., ELFEKI, M., TRAXLER, M. F., ENGENE, N., KOYAMA, N., VINING, O. B., BARIC, R., SILVA, R. R., MASCUCH, S. J., TOMASI, S., JENKINS, S., MACHERLA, V., HOFFMAN, T., AGARWAL, V., WILLIAMS, P. G., DAI, J., NEUPANE, R., GURR, J., RODRIGUEZ, A. M. C., LAMSA, A., ZHANG, C., DORRESTEIN, K., DUGGAN, B. M., ALMALITI, J., ALLARD, P. M., PHAPALE, P., et al. 2016. Sharing and community curation of mass spectrometry data with Global Natural Products Social Molecular Networking. *Nat Biotechnol,* 34**,** 828-837.

ZENG, B. Y. 2017. Effect and Mechanism of Chinese Herbal Medicine on Parkinson's Disease. *Int Rev Neurobiol,* 135**,** 57-76.

PUBLICATION

YEW, M. Y., KOH, R. Y., CHYE, S. M., OTHMAN, I. & NG, K. Y. 2014. Edible bird's nest ameliorates oxidative stress-induced apoptosis in SH-SY5Y human neuroblastoma cells. *BMC Complementary and Alternative Medicine,* 14**,** 391.

APPENDIX

Yew et al. BMC Complementary and Alternative Medicine 2014, 14:391
http://www.biomedcentral.com/1472-6882/14/391

BMC Complementary & Alternative Medicine

RESEARCH ARTICLE Open Access

Edible bird's nest ameliorates oxidative stress-induced apoptosis in SH-SY5Y human neuroblastoma cells

Mei Yeng Yew[1], Rhun Yian Koh[2], Soi Moi Chye[2], Iekhsan Othman[1] and Khuen Yen Ng[1*]

Abstract

Background: Parkinson's disease (PD) is the second most common neurodegenerative disorder affecting the senile population with manifestation of motor disability and cognitive impairment. Reactive oxygen species (ROS) is implicated in the progression of oxidative stress-related apoptosis and cell death of the midbrain dopaminergic neurons. Its interplay with mitochondrial functionality constitutes an important aspect of neuronal survival in the perspective of PD. Edible bird's nest (EBN) is an animal-derived natural food product made of saliva secreted by swiftlets from the *Aerodamus* genus. It contains bioactive compounds which might confer neuroprotective effects to the neurons. Hence this study aims to investigate the neuroprotective effect of EBN extracts in the neurotoxin-induced *in vitro* PD model.

Methods: EBN was first prepared into pancreatin-digested crude extract and water extract. *In vitro* PD model was generated by exposing SH-SY5Y cells to neurotoxin 6-hydroxydopamine (6-OHDA). Cytotoxicity of the extracts on SH-SY5Y cells was tested using MTT assay. Then, microscopic morphological and nuclear examination, cell viability test and ROS assay were performed to assess the protective effect of EBN extracts against 6-OHDA-induced cellular injury. Apoptotic event was later analysed with Annexin V-propidium iodide flow cytometry. To understand whether the mechanism underlying the neuroprotective effect of EBN was mediated via mitochondrial or caspase-dependent pathway, mitochondrial membrane potential (MMP) measurement and caspase-3 quantification were carried out.

Results: Cytotoxicity results showed that crude EBN extract did not cause SH-SY5Y cell death at concentrations up to 75 μg/ml while the maximum non-toxic dose (MNTD) of water extract was double of that of crude extract. Morphological observation and nuclear staining suggested that EBN treatment reduced the level of 6-OHDA-induced apoptotic changes in SH-SY5Y cells. MTT study further confirmed that cell viability was better improved with crude EBN extract. However, water extract exhibited higher efficacy in ameliorating ROS build up, early apoptotic membrane phosphatidylserine externalization as well as inhibition of caspase-3 cleavage. None of the EBN treatment had any effect on MMP.

Conclusions: Current findings suggest that EBN extracts might confer neuroprotective effect against 6-OHDA-induced degeneration of dopaminergic neurons, particularly through inhibition of apoptosis. Thus EBN may be a viable nutraceutical option to protect against oxidative stress-related neurodegenerative disorders such as PD.

Keywords: Edible bird's nest, Apoptosis, SH-SY5Y, 6-OHDA, Neurodegenerative disorder, Parkinson's disease, Neuroprotection

* Correspondence: ng.khuen.yen@monash.edu
[1]Jeffrey Cheah School of Medicine & Health Sciences, Monash University Malaysia, Selangor, Malaysia
Full list of author information is available at the end of the article

BioMed Central

© 2014 Yew et al.; licensee BioMed Central Ltd. This is an Open Access article distributed under the terms of the Creative Commons Attribution License (http://creativecommons.org/licenses/by/4.0), which permits unrestricted use, distribution, and reproduction in any medium, provided the original work is properly credited. The Creative Commons Public Domain Dedication waiver (http://creativecommons.org/publicdomain/zero/1.0/) applies to the data made available in this article, unless otherwise stated.

Background

Parkinson's disease (PD) is an age-related progressive neurodegenerative disease with estimated worldwide prevalence approaching 9 million of people over the age of 50 by 2030 [1]. Pathologically, there is loss of dopaminergic neurons in the substantia nigra which subsequently causes dopamine depletion in the striatum [2]. Abnormal aggregation of α-synuclein known as Lewy bodies is also detected in surviving neurons [3]. Dopamine depletion ultimately leads to deterioration of motor functions whereby the patients are often manifested with clinical signs such as tremor, rigidity and slow responsiveness [4].

Several hypotheses including neuroinflammation, mitochondrial dysfunction, failure of ubiquitin-proteasome system and proteinopathy have been proposed to explain the neurodegeneration events in PD [5,6]. Amongst those, oxidative stress-related apoptosis has been implicated in the pathogenesis of neurodegenerative diseases. Oxidative stress is caused by the production and accumulation of excessive partially reduced reactive oxygen species (ROS) within the cell, which attacks electron-rich biological molecules such as DNA, protein and lipid to affect cellular functions [7]. ROS is generated as a part of normal cellular metabolism. In the cells with high oxygen-utilizing capacity such as the neurons, however, greater amount of highly reactive oxygen radical is being produced which renders these cells more vulnerable to oxidative damages [8]. In PD, substantial post-mortem studies noted that impaired mitochondrial function and ROS build up are two events linked to apoptotic episode in dopaminergic neurons [6,9]. Experimental models of PD which are generated through the use of mitochondrial complex I activity-inhibiting and ROS-inducing neurotoxins are able to recapitulate the pathological features in PD, further reinforces that ROS introduction is critically involved in the disease [10]. Therefore the brain requires an effective antioxidant system to counteract the impact of ROS, as well as an anti-apoptotic mechanism to maintain the neuronal integrity.

Edible bird nest (EBN) is natural food product made from saliva of the swiftlets of the genus *Aerodramus* (or *Collocalia).* Numerous *in vitro* and *in vivo* researches have shown that administration of EBN was able to boost immunity, promote cell division and proliferation, neutralize influenza activity as well as improve osteoporosis [11-14]. Studies have shown that EBN contains the bioactive compound sialic acid [15-17]. Furthermore, EBN may also contain epidermal growth factor (EGF) because EGF-like activity was detected in protein fractions partially purified from EBN extract. In fact, sialic acid and EGF are neurotrophic factors known to promote neuron and brain development [18-21]. On the other hand, animal saliva was previously found to contain vascular endothelial growth factor and melatonin [22,23]. These compounds are powered with anti-apoptotic and antioxidant properties [24,25]. As apoptosis and oxidative stress have been suggested as crucial events in neurodegeneration, EBN, the salivary secretion of swiftlets, may have neuroprotective relevance in the therapeutic context of PD. Nevertheless no scientific investigation has been conducted thus far to confirm this. Hence this study aimed to investigate the neuroprotective effect of EBN.

Methods

Preparation of EBN extracts

Raw EBN from the swiftlet of *Aerodamus* genus collected from bird's nest farm in Perak, Malaysia was kindly provided by a local EBN distributor Yew Kee Pte Ltd. Cleaning was carried out by first soaking the unprocessed EBN in ultrapure water until softened and protein strands became slightly loosened. Dirt and feathers were removed manually by forceps. Cleaned EBN was subsequently oven-dried at 50°C before being grounded into fine powder. A portion of cleaned EBN was kept for water extraction whereby the EBN was first soaked in cold distilled water for 48 hours followed by boiling at 100°C for 30 minutes. The solution mixture was filtered and the filtrate was freeze-dried with freeze dryer (EYELA Freeze Dryer FOU 2100) to obtain EBN water extract powder.

Traditionally, a bird's nest soup was prepared by double-boiling the cleaned EBN strands with water until softened, whereby sugar is often added to enrich the taste. In the current study, however, both raw EBN and its water extracts were prepared by enzymatic digestion using method adopted from Guo *et al.* [13]. Pancreatin digestion was performed as numerous studies have suggested that proteolytic breakdown of EBN produced greater bioactivities when compared to the undigested EBN [13,14]. This additional step of enzymatic hydrolysis is suggested to enhance solubilisation of bioactive compounds, which subsequently leading to cellular assimilation. Briefly, raw EBN and water extract powder dissolved in ultrapure water at 2.5% (w/v) were digested with pancreatin (final concentration 0.5 mg/ml) (Sigma Aldrich, USA) in a 45°C water bath for 4 hours at pH 8.5- 9.0. Pancreatin enzyme was then deactivated at 90°C for 5 minutes. The mixtures were then filtered and freeze-dried to obtain the final crude and water EBN extracts, which were denoted as S1 and S2 respectively. Finally, products were dissolved in dimethyl sulphoxide (DMSO) (Sigma Aldrich, USA) as a stock of 50 mg/ml and sonicated until the powder was fully solubilized. Then the EBN solutions were centrifuged at 3000 rpm for 10 minutes to precipitate the undissolved EBN particles. The supernatant was collected and stored at -20°C for future use.

Neuronal cell culture

Human neuroblastoma cells SH-SY5Y was purchased from the American Type Culture Collection (ATCC no.

CRL-2266) and cultured in complete medium prepared from Dulbecco's Modified Eagle's Medium (Gibco, UK) supplemented with 10% fetal bovine serum (Gibco, UK). The cells were maintained at 37°C humidified incubator with 5% CO_2 for 2-3 days until 70% confluent. Cell collection was carried out by rinsing the cells with phosphate-buffered saline (PBS) (Biobasic, Canada) followed by addition of trypsin-EDTA (Gibco, UK) to detach the cells. The action of trypsin was later neutralized with complete medium and cells were harvested by centrifugation at 1500 rpm for 5 minutes. The cells were then sub-cultured into new tissue culture flask or plated for assays.

Determination of maximum non-toxic dose (MNTD) and effect of the EBN extracts on 6-OHDA-induced cytotoxicity

Cytotoxic test was performed with tetrazolium reduction assay using 3-(4, 5-dimethylthiazol-2-yl)-2, 5-diphenyltetrazolium bromide (MTT) reagent (Sigma Aldrich, USA). Cells were first seeded onto 96-well plate at a density of 4×10^4 cells/well with complete medium, which then was replaced by serum-free medium for treatment in the next day. Cytotoxic effect of both crude and water EBN extracts on SH-SY5Y cells was tested across a wide range of concentrations from 0 to 500 μg/ml. DMSO, which was used to dissolve the extracts, was included as vehicle control. After 48 hours incubation, MTT solution was added into the culture to a final concentration of 0.5 mg/ml. After 4 hours incubation at 37°C, the medium was removed and replaced with equal volume of DMSO to dissolve the purple formazan crystal. Absorbance of the solution was measured spectrophotometrically with microplate reader (DynexOpsys MR 24100) at 570 nm and was compared to control to be presented in percentage of cell viability or toxicity. MNTD and ½ MNTD of EBN extracts were determined from graph plotted.

To determine the effect of EBN extracts on SH-SY5Y intoxicated with neurotoxin, cells were pre-treated with EBN extracts at MNTD and ½ MNTD for 24 hours followed by co-incubation with 100 μM 6-OHDA for another 24 hours. Upon completion of treatment, MTT assay was performed to determine the cell viability. All test assays followed the same treatment whereby DMSO alone (0.5% v/v) was used as vehicle control.

Morphological examination

Apoptotic cells experiencing damage in the nuclei are featured by cell shrinkage, membrane blebbing and presence of apoptotic bodies [26]. In order to perform morphological study, cells were first grown in 60 mm culture dish and treated accordingly whereby groups such as vehicle control, 6-OHDA, S1 MNTD + 6-OHDA and S2 MNTD + 6-OHDA were included. Then, cell morphology was examined under bright field inverted microscope (Nikon Eclipse T*i*, Japan). In addition to that, nuclear staining was performed with Hoechst staining. Treated cells were fixed with 4% paraformaldehyde for 15 minutes before stained with Hoechst 33258 (1 μg/ml) (Sigma Aldrich, USA) for 15-20 minutes. Nuclear changes were examined under fluorescence excitation using the same microscope for features such as chromatin condensation, DNA fragmentation and cell shrinkage. Photomicrographs were taken using attaching camera.

Intracellular reactive oxygen species (ROS) level measurement

Intracellular ROS production was assessed with 2′, 7′-dichlorofluorescein diacetate (DCFH-DA) fluorescent probe. Cells were seeded into 12-well plate at a density of 1.5×10^5 cells/well. Upon completion of treatment, cells were collected and washed before added with 40 μM DCFH-DA (Sigma Aldrich, USA) working solution in 96-well black plate. Fluorescence reading was taken at 0, 10, 20 and 30 minutes with fluorescence microplate reader using excitation and emission wavelengths of 485 nm and 535 nm (Tecan, Austria). The fluorescence readings were then normalized to the respective cell number to give relative value of DCF fluorescence unit. Fold change in ROS production of the treated groups was determined by comparing to the untreated control.

Apoptosis analysis

The procedure was performed with Annexin V-FITC Apoptosis Detection Kit (BD Pharmingen, USA) using a modified protocol by Rieger *et al.* [27]. Briefly, upon completion of treatments, cells were harvested and washed with binding buffer. Cells were counted to obtain a final concentration of 1×10^6 cells/ml. Then Annexin V and propidium iodide (PI) were added and incubated in dark for 15 minutes. After washing, cell suspension was fixed with 1% formaldehyde for 10 minutes on ice. Subsequently, washing was performed twice with binding buffer followed by addition of RNase (EMD Biosciences, USA) which then incubated for 15 minutes at 37°C. Finally, samples were washed and ready for analysis with FACSCalibur flow cytometer (BD Biosciences, USA) and the software Cell Quest Pro.

Mitochondrial membrane potential measurement

Mitochondrial membrane potential (MMP or $\Delta\Psi m$) is an important indicator of mitochondrial functionality. Apoptosis through mitochondrial-mediated pathway can be assessed by performing MMP assay using MitoScreen kit (BD Pharmingen, USA) according to the protocols provided. Briefly, cells were collected by trypsinization and centrifugation. Washing with PBS was carried out and cells were counted to obtain a final concentration of 1×10^6 cells/ml. Working staining solution was prepared

from the JC-1 powdered dye and assay buffer at a ratio of 1:99, which was then added to the cells. Incubation was carried out at 37°C in 5% CO_2 incubator for 15 minutes. Cells were washed twice in assay buffer before analyzed with flow cytometer. Mitochondrial depolarization is indicated by a decrease in the red JC aggregates/green JC monomer fluorescence intensity ratio.

Caspase-3 detection

Caspase-3 is a proteolytic enzyme activated during apoptosis. It was detected using FITC active caspase-3 apoptosis kit (BD Pharmingen, USA) according to the protocol provided. Cells were first collected by trypsinization and centrifugation. Then, cells were washed with PBS twice and resuspended in BD Cytofix/ Cytoperm™ fixation and permeabilization solution at 1×10^6 cells/0.5 ml. Subsequently cells were incubated on ice for 20 minutes. Fixation solution was discarded after centrifugation and cells were washed twice with 0.5 ml of BD Perm/Wash™ buffer. A hundred microliters of BD Perm/Wash™ buffer and 20 μl of FITC anti-active caspase-3 antibody were added to each sample and incubated for 30 minutes at room temperature. Then, cells were washed with 1 ml of BD Perm/Wash™ buffer. Finally cells were resuspended in 0.5 ml of the same buffer and transferred to FACS tube for flow cytometry analysis.

Statistical analysis

Data was collected as triplicate from at least 3 independent experiments. The results were expressed as mean ± standard deviation. Statistical significance was assessed with Student's t-test. P value <0.05 was considered significant.

Results & Discussion

Cytotoxic profile of EBN extracts (S1 and S2)

Toxicity study was first performed with addition of EBN extracts to SH-SY5Y cells to determine the concentration-wide effect as well as MNTDs of the extracts on neuronal culture. MNTD is the maximal dose just below the threshold for cell toxicity that demonstrates no cytotoxic effect. Half of the MNTD value was also determined in order to study the effect of EBN treatment at lower concentration.

In the graph of cytotoxicity percentage in SH-SY5Y cells against EBN extract concentration (Figure 1), it was found that there was an increasing trend of cytotoxicity along with the concentration. However, cell death was not evident at concentration below 100 μg/ml for S1 and 200 μg/ml for S2. MNTDs are the concentrations at which cytotoxicity starts to become evident (where line touches x-axis). As determined from the graph, MNTDs were 76.25 ± 16.52 μg/ml for S1 and 150 ± 36.06 μg/ml for S2. Meanwhile the ½ MNTDs were 38.13 μg/ml and 75 μg/ml for S1 and S2, respectively. Overall the cytotoxicity of S1 was double as much as the cytotoxicity of S2. Such discrepancy could be due to varying methods employed in preparing the two extracts. In fact, compound solubility and stability are major factors that contribute to varied activities in different extracts [28]. S2 was extracted with water thus one might expect the resulting sample to contain only water-soluble substances. Also, high temperature applied during the water extraction process might have affected the potency of proteins within the EBN, possibly through denaturation. Based on the observations, it is likely that the water-soluble substances possess less cytotoxic effect comparing to S1, the crude EBN extract.

EBN extracts prevent 6-OHDA-induced apoptotic changes in SH-SY5Y cells

A number of cellular morphological changes including cytoplasmic condensation resulting in reduced cell size, plasma membrane undulations or blebbing, condensation of chromatin at nuclear periphery, dilatation of endoplasmic reticulum and formation of apoptotic bodies represent the typical characteristics of apoptosis [29,30]. In the present study, changes in cellular morphology of SH-SY5Y upon different treatments were assessed by microscopic examination. Untreated SH-SY5Y cells had a distinctive neuronal shape with typical long neurite outgrowth. In addition, cell membrane was intact and there were minimal dead cells (Figure 2A). Nuclear staining with DNA-binding fluorescent dye Hoechst 33258 showed homogenously stained regular rounded nuclei in control cells (Figure 2E). However, when incubated with 100 μM 6-OHDA (an optimum concentration determined from our studies earlier; Data not shown), cell death was made evident by the presence of shiny, floating and round-shaped cells under bright field microscopy (Figure 2B). Shrinking cells which gradually lost their elongated neuronal shape and have shrunken in size were also detected (yellow arrow in Figure 2B). Meanwhile, increased number of bright fluorescent nuclei indicative of chromatin condensation (white arrow in Figure 2F), as well as nuclear fragmentation (red arrow in Figure 2F) were apparent after Hoechst staining. Smaller asymmetrical nuclei were also seen as a result of cell shrinkage (green arrow in Figure 2F). These features altogether suggest that 6-OHDA-induced SH-SY5Y cell death was likely to be mediated through apoptosis. This finding is supported by previous study which concluded that the selective catecholaminergic neurotoxin induces oxidative stress-associated cell death primarily through apoptosis [31].

Nonetheless, pre-treatment with S1 or S2 for 24 hours prior to the addition of 6-OHDA conferred protection to SH-SY5Y cells by reducing cell death in the culture (Figure 2C-D). In addition, the nuclear apoptotic changes induced by 6-OHDA were less noted in the cells after pre-treatment with S1 and S2 (Figure 2G-H), suggesting that

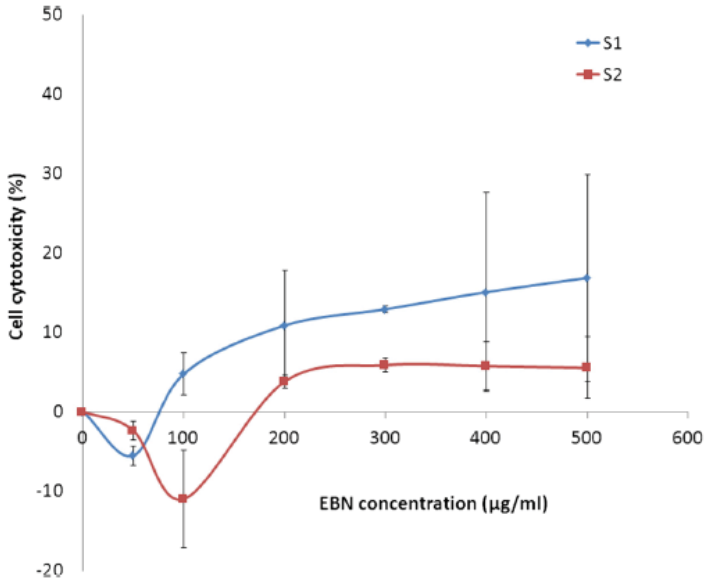

Figure 1 Cytotoxic effect of EBN extracts on SH-SY5Y cells. Cytotoxicity percentage of SH-SY5Y cells upon 48 hours treatment with either S1 or S2 was tested across a wide range of concentration from 0 to 500 µg/ml and MTT assay was carried out. Maximum non-toxic dose was then determined from the graph. The data shown are means ± S.D. of three independent experiments performed in triplicates.

EBN may be effective in reversing the cytotoxic effect of 6-OHDA.

S1 improves cell viability in 6-OHDA-challenged SH-SY5Y cells

To quantify the cell viability from those observed in the morphological study, MTT assay was performed. Upon challenge with 100 µM 6-OHDA for 24 hours, cell viability decreased significantly to about 40% of that of control (Figure 3). Pre-treatment with EBN extracts followed by co-incubation with 6-OHDA generally did not improve cell viability except in the cells treated with S1 at respective MNTD. About 20% increase in the cell viability was observed under that treatment as compared to the 6-OHDA group. This could be due to mitogenic property of S1 that promoted cell growth, as made evident by a study by Zainal Abidin *et al.* which shows that EBN promoted cell division in rabbit corneal keratocytes [32]. Moreover, acid hydrolysates of EBN have been shown to promote proliferation of human colonic adenocarcinoma (Caco-2) cells [33]. The same report also pointed out that sialic acid treatment alone induced significant Caco-2 proliferation. Taken together the finding by Yagi *et al.* which showed that sialic acid was present in EBN, it is suggested that sialic acid could be the bioactive compound that we are interested in [17].

On the contrary, S2 in overall did not prevent cell death, which may be explained by the lower activity associated with the water extract discussed earlier. Meanwhile, EBN treatment alone for 48 hours did not affect cell survival, indicating that EBN treatments at MNTDs were non-cytotoxic to SH-SY5Y cells.

S2 attenuates ROS build up in 6-OHDA-challenged SH-SY5Y cells

The overall oxidative status in SH-SY5Y cells was assessed with the DCFH-DA assay. Figure 4 showed that ROS was maintained at basal level when SH-SY5Y cells were treated with EBN extracts alone, indicating that EBN alone did not induce oxidative stress within the cell. Furthermore, S2 caused significant drop in ROS production suggesting the protective role of EBN as a free radical species scavenger.

Intracellular ROS production was augmented by 4 fold upon 6-OHDA exposure when compared to control group. Pre-treatment with S1 at high dose (MNTD) did not restore ROS to the basal level, but instead promoted intracellular ROS build up twice as much as the level of that in cell treated with 6-OHDA alone. This could be due to the presence of reactive compounds in S1 which prompted the generation of extra free radical in cells on top of the existing oxidative load, for example a 66 kDa major allergen protein in EBN [34]. As allergenic immune reaction is often linked to increased intracellular ROS production, this putative protein possesses homology to a domain of an ovoinhibitor precursor in chicken could possibly be the contributor of intracellular ROS load in S1-treated SH-SY5Y cells [35,36].

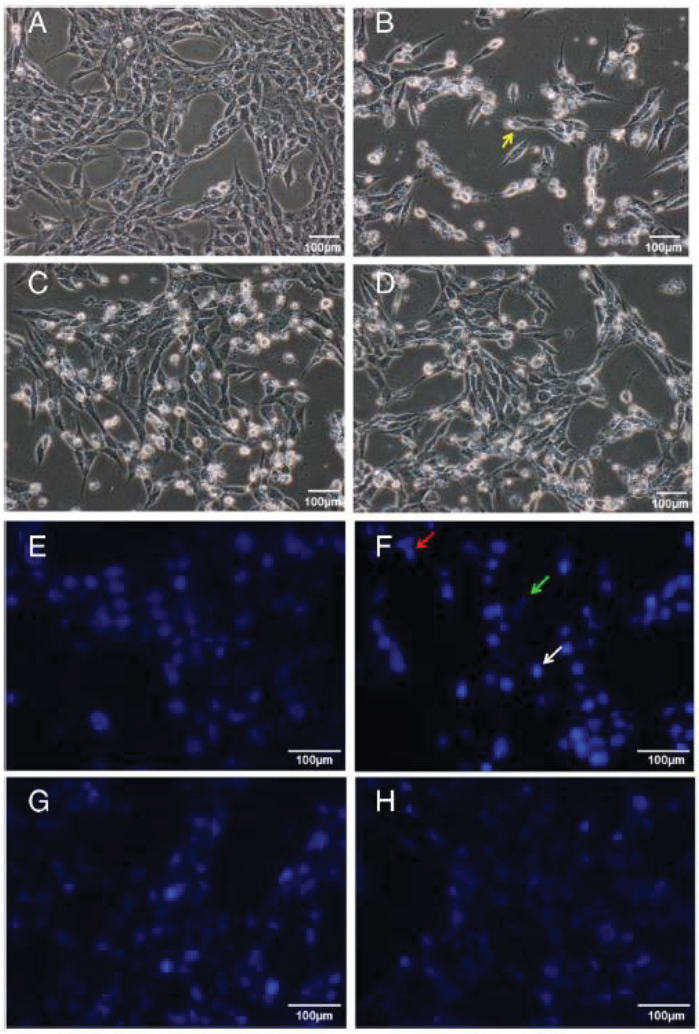

Figure 2 Effect of EBN extracts on morphological and nuclear changes of 6-OHDA-challenged SH-SY5Y cells. Microscopic images were taken after 48 hours of treatment. Figures **A-D** are bright field images while Figures **E-H** are fluorescent images taken after Hoechst 33258 staining. Figures **A** and **E**: control group; Figures **B** and **F**: 6-OHDA group; Figures **C** and **G**: S1 MNTD + 6-OHDA-treated group; Figures **D** and **H**: S2 MNTD + 6-OHDA-treated group. Cell shrinkage is indicated by cell losing its distinctive neuronal shape and has becomes smaller in size (yellow arrow in Figure 2B), DNA fragmentation is indicated by cluster of nuclei fragments (red arrow in Figure 2F), shrunken cell is indicated by smaller and distorted nuclei (green arrow in Figure 2F) while nuclear chromatin condensation is indicated by brightly fluorescent nuclei (white arrow in Figure 2F).

Meanwhile, ROS production was significantly attenuated to sub-control level by S2 treatment, in which high dose seemed to suppress ROS production better than low dose. These findings suggest that the water-soluble compounds in S2 could be more effective in scavenging intracellular ROS if present in high dose, whereas in crude extract high dose would do the opposite effect. The difference in activities of S1 and S2 can be inferred from the different methods used in extract preparation. Although both extracts derived from the same raw material, solubility and solvent accessibility of bioactive compounds in crude and water extracts may affect their chemical properties and hence, the bioactivities. In particular, water extraction method involves heat treatment at 100°C and therefore may modify tertiary conformational structure of the native EBN protein. This manipulation could possibly uncover the nucleophilic amino acid residues that present in the protein core, such as cysteine's sulfhydryl groups [37]. These amino acid residues are free radical scavenger because they are

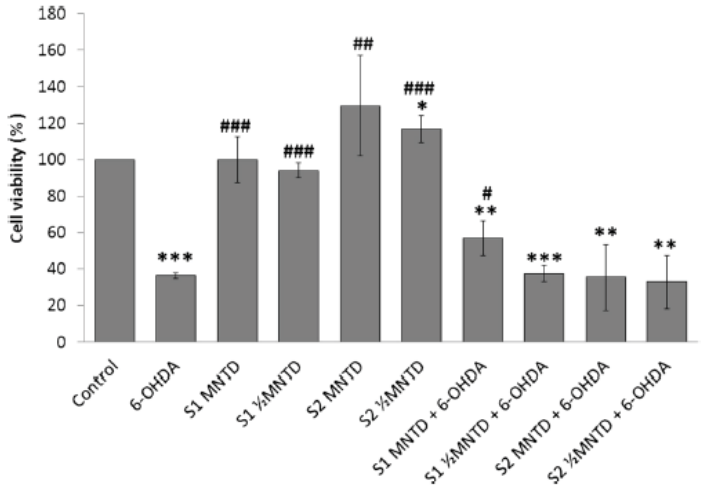

Figure 3 Effect of EBN extracts on 6-OHDA-challenged SH-SY5Y cell viability. Cell viability was assessed with MTT assay and data shown are means ± S.D. of three independent experiments performed in triplicates. *P < 0.05; **P < 0.01; ***P < 0.001 versus untreated control cells while #P < 0.05, ##P < 0.01; ###P < 0.001 versus 6-OHDA treated cells.

oxidized preferentially to the membrane phospholipids. S2 may therefore possess higher antioxidant potential than S1 because of greater solvent exposure of free radical scavenging amino acid residues as a result of heat-assisted protein denaturation.

Generally, reduction of ROS level would ameliorate oxidative stress-related cellular damage and cell death, but this was not observed in the present study. Results from ROS measurement when put together with MTT results raised an intriguing question because S1 had successfully improved cell viability although it triggered ROS generation. One explanation for this is that S1 could have initiated cytoprotective mechanism other than direct ROS-scavenging, such as the promotion of antioxidant defense system through nuclear erythroid 2-related factor 2 - antioxidant responsive element (Nrf2-ARE) signaling [38]. It has been suggested that exogenous protein can act through Nrf2-ARE signaling pathway to induce expression of endogenous antioxidant enzymes [39]. In fact, ARE activation have been demonstrated to be protective against *in vitro* cell death induced by dopamine and 6-OHDA, likely due to enhanced expression of the antioxidant proteins such as glutathione S-transferase A2, heme oxygenase-1 and NAD(P)H quinoneoxidoreductase 1 [40-42]. Interestingly, Nrf2-ARE activation is a redox-sensitive process thus this process can be triggered in response to intracellular oxidative changes, as seen in the action of apomorphine whereby ROS produced by the drug

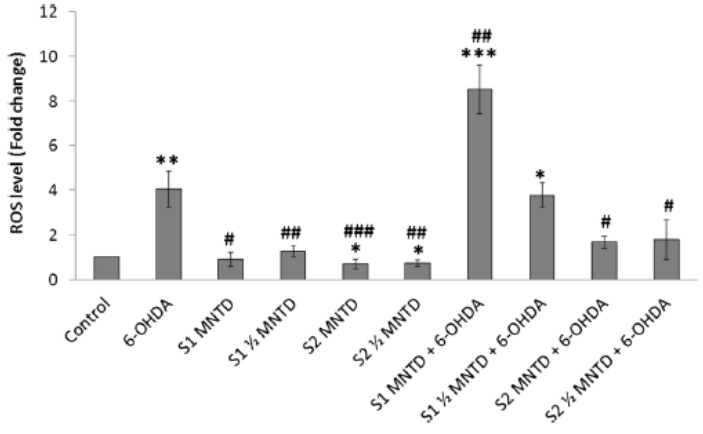

Figure 4 Effect of EBN extracts on intracellular reactive oxygen species (ROS) production in 6-OHDA-challenged SH-SY5Y cells. Intracellular ROS levels of treated groups were assessed with DCFH-DA assay and data shown are means ± S.D. of three independent experiments performed in triplicates. *P < 0.05; **P < 0.01; ***P < 0.001 versus untreated control cells while #P < 0.05, ##P < 0.01; ###P < 0.001 versus 6-OHDA treated cells.

itself acts as Nrf2-ARE pathway activator [43,44]. Therefore, it is possible that S1, in the presence of ROS, generates signals that initialize molecular changes to result in cytoprotection and hence improved cell viability. However, further works should be done to confirm the role of these members of the intracellular antioxidant response system in the neuroprotective mechanism of S1. Investigations on expression of the antioxidant genes or proteins, and nuclear translocation of Nrf2 protein could be performed in the future.

EBN extracts reduce early apoptotic event in 6-OHDA-challenged SH-SY5Y cells

Apoptotic event was investigated by Annexin V-PI double staining method to identify the mode of cell death. Several previous reports showed that apoptosis of dopaminergic neurons was found to increase with 6-OHDA-induced oxidative stress [45-48]. In this assay, cells residing at different stages of apoptosis upon exposure to 6-OHDA were identified by differential staining of membrane phosphatidylserine and DNA, whereby cells are grouped and represented in dot plot as healthy (lower left quadrant), early apoptotic (lower right quadrant), late apoptotic (upper right quadrant) and necrotic (upper left quadrant) ones. Early apoptosis, represented by cell stained positively with Annexin V due to phosphatidylserine translocation towards outer membrane surface followed by loss of membrane integrity, was found to be the major cell death mechanism in cell treated with 6-OHDA for 24 hours. It accounted for about 30% of the cell population (Figure 5B, lower right quadrant), which is in concordance with other reports [49,50].

Generally EBN treatment alone did not stimulate apoptotic event (Figure 5D-F), but it effectively reduced early apoptotic injury in cells challenged with 6-OHDA (Figure 5H-J). The results suggest that EBN is a potential neuroprotective agent which acts by inhibiting apoptosis. However, S1 treatment increased the percentage of apoptotic population in normal culture (Figure 5C) and did not reduced the early apoptosis induced by 6-OHDA (Figure 5G) when given at MNTD. Such findings imply that high dose of crude extract did not improve apoptosis and could have itself contributed to apoptosis in SH-SY5Y cells, despite the fact that MNTD used for S1 treatment had been pre-determined as non-toxic. The apoptosis-inducing nature of S1 at MNTD may be related to the elevated intracellular ROS produced as determined from the DCFH-DA assay previously.

EBN extracts did not improve mitochondrial dysfunction in 6-OHDA-challenged SH-SY5Y cells

Mitochondrial dysfunction as defined by collapse in MMP is an early and critical event in cellular apoptosis. In fact, the opening of mitochondrial transition pore

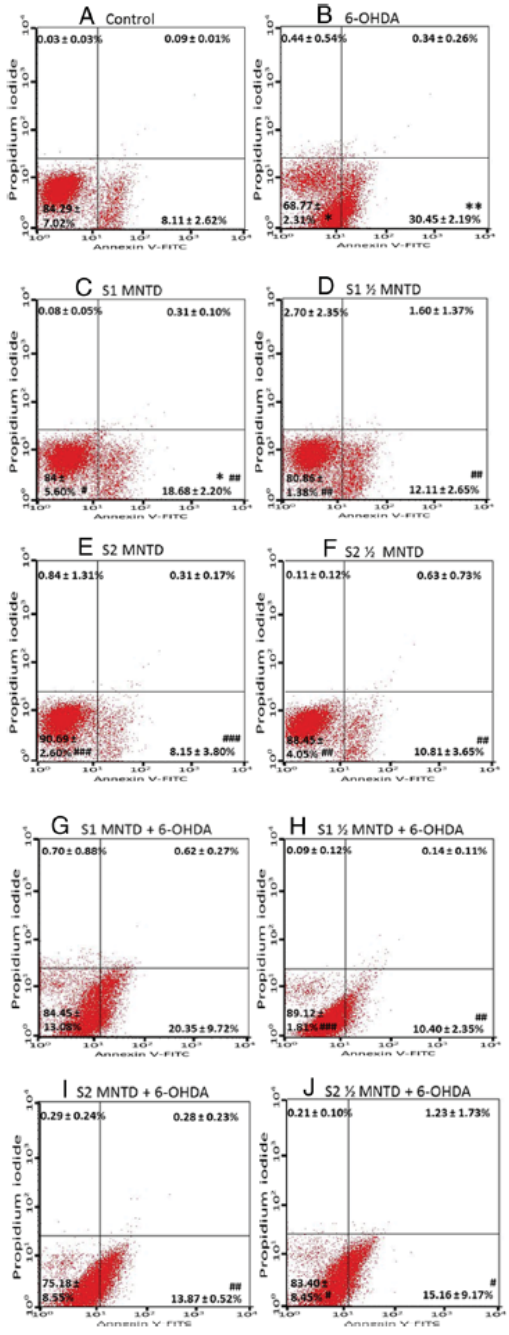

Figure 5 Effect of EBN extracts on 6-OHDA-induced apoptosis in SH-SY5Y cells. Cells treated with EBN extracts for 48 hours were analyzed by Annexin V-propidium iodide double staining. Representative plots of propidium iodide versus Annexin V-FITC fluorescence signals are shown **(A-J)**. Results shown are the mean ± S.D. of three independent experiments. *P < 0.05; **P < 0.01 versus untreated control cells while #P < 0.05, ##P < 0.01; ###P < 0.001 versus 6-OHDA treated cells.

upon different stimuli precedes the depolarization of mitochondrial potential, subsequently leading to increased mitochondrial permeability and thus the efflux of pro-apoptotic factors such as cytochrome c and procaspases [51]. The MMP in SH-SY5Y cells was measured in order to study the alteration in mitochondrial activity during apoptosis. In the present study, MMP of SH-SY5Y cells dropped drastically to 27% of that in control when the cell was exposed to 100 μM 6-OHDA for 24 hours (Figure 6). Although the action through which 6-OHDA induces cytotoxicity in neuronal cell lines such as SH-SY5Y and PC12 has been linked to ROS outburst, literature is available to show that failure of cellular respiratory complex may be the direct cause of apoptosis. Gomez- Lazaro *et al.* found that mitochondrial fragmentation constitutes early event in mitochondrial dysfunction and eventually cell death of SH-SY5Y. The author further revealed that 6-OHDA-induced SH-SY5Y cell death was reversible by blockage of the mitochondrial fission activity [51]. Taken together, the findings support the indispensable role of mitochondrial integrity in SH-SY5Y cells' survival. In fact, studies have successfully demonstrated neuroprotection against apoptosis via restoration of mitochondrial functionality by natural products, such as the herbal medicine Chunghyuldan, which ameliorated PD-like behavioral symptoms by preserving dopaminergic neurons in the nigrostriatal region of PD mice model [52].

Yet, mitochondrial functionality in the intoxicated cell was not improved with EBN treatment in the present study. There was no significant difference in MMPs between the EBN-co-treated and 6-OHDA groups. Therefore, the cell-promoting effect of S1 seen in MTT assay may be not related to resuscitation of MMP in 6-OHDA-challenged SH-SY5Y cells. Although 6-OHDA-induced cytotoxicity is mainly associated with mitochondrial respiratory dysfunction, an opposite mitochondrial-independent pathway is as well indicated in a number of studies [53,54]. As such, involvement of non-mitochondrial mechanism may be implicated in the neuroprotection conferred by the EBN crude extract.

Notably, EBN treatment alone was shown to bring down the level of MMP significantly, indicating that the addition of foreign compound to the SH-SY5Y culture could affect the mitochondrial status. Still, treatment with EBN extracts alone for 48 hours did not exhibit any detrimental effect on the SH-SY5Y's cell viability and oxidative status.

S2 inhibits cleavage of caspase-3 in 6-OHDA-challenged SH-SY5Y cells

Caspase-3 is the executioner protein of the apoptotic process and remains as inactive procaspase until it is being cleaved by activated initiator caspases such as caspase-8 or caspase-9. Its activation leads to downstream mechanisms which involve poly(ADP-ribose) polymerase-mediated DNA cleavage and breakdown of proteins essential for maintenance of cytoskeletal structure. Eventually, activation of caspase-3 results in DNA fragmentation and apoptosis [55].

Elevated active caspase-3 level was detected in SH-SY5Y cells treated with 6-OHDA, which was 7.8% as compared to 3.5% in control (Figure 7). However, S2 at ½ MNTD managed to attenuate caspase-3 activation in the cell. This explains the parallel reduction in early apoptotic population by S2 at ½ MNTD as seen from

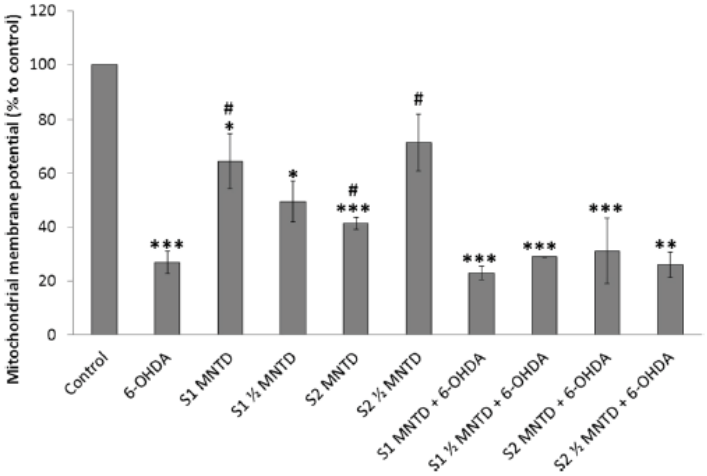

Figure 6 Effect of EBN extracts on mitochondrial membrane potential (MMP) in 6-OHDA-challenged SH-SY5Y cells. MMP was assessed with mitochondria-selective JC-1 dye and results shown are the mean ± S.D. for three independent experiments. *P < 0.05; **P < 0.01 versus untreated control cells while #P < 0.05 versus 6-OHDA treated cells.

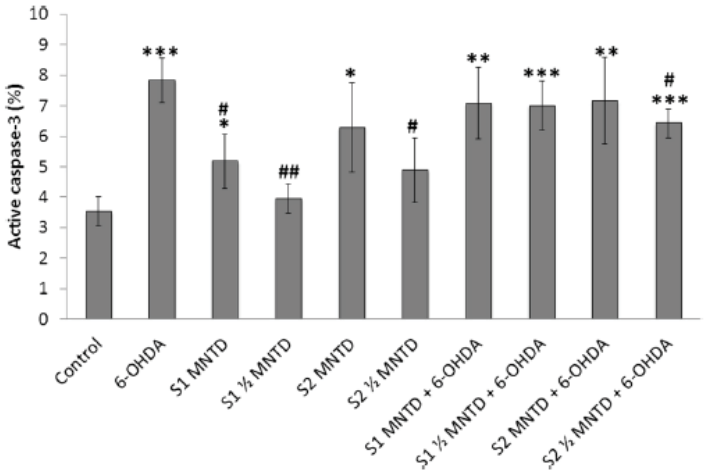

Figure 7 Effect of EBN extracts on cleavage of caspase-3 in SH-SY5Y cells challenged with 6-OHDA. The release of active caspase-3 into cytosol was assessed by immunostaining using FITC-conjugated antibody and results were generated from flow cytometry. Results shown are the mean ± S.D. of three independent experiments. **P < 0.05; **P < 0.01 versus untreated control cells while #P < 0.05, ##P < 0.01versus 6-OHDA treated cells.

Annexin V-PI analysis, thus consolidates the role of caspase-3 activation in the process of 6-OHDA-induced SH-SY5Y apoptosis [56].

Caspase-3 can be activated through two machineries, namely the mitochondria-related apoptosis protease-activating factor-1/caspase-9/caspase-3 cascade, and Fas-associated adapter protein/caspase-8/caspase-3 cascade which is the extrinsic apoptotic pathway [57]. Based on the observation from MMP assay in which S2 failed to resuscitate mitochondrial depolarization in SH-SY5Y cells challenged with 6-OHDA, it is likely that S2 inhibited caspase-3 through modulation of the extrinsic pathway which has little relation to the mitochondrial activity. However, future study is warranted to investigate the involvement of extrinsic pathway in S2-mediated neuroprotection. For EBN treatment only, both S1 and S2 when given at MNTD induced release of active caspase-3, signifying that high dose of the extracts may trigger early apoptosis event and hence lower concentrations should be used for the treatment.

Remarks on discordance between cytotoxicity and apoptotic parameters

Current finding showed that S1 treatment at MNTD improved SH-SY5Y cell viability despite being unable to prevent apoptosis and restore ROS and caspase-3 to basal level. On the contrary, S2 treatment has successfully attenuated ROS development and reduced apoptosis and caspase-3 release, yet it failed to reverse cytotoxic effect of 6-OHDA. This is intriguing as cytotoxicity is positively associated with apoptotic event, oxidative stress and caspase-3 activation. However, it is worth mentioning that cytotoxicity can be mediated by several different cell death mechanisms. Other than apoptosis, cell death can also be orchestrated by autophagy and necrosis [58]. Under such circumstances, cells are likely to either slowly sequestrated and then degraded by autolysomes through autophagy, or undergo necrosis upon activation of death domain receptors on cell surface. Cytotoxicity is thus attributed, but not exclusively, to apoptosis parameters such as externalization of phosphatidylserine on plasma membrane and activation of caspase signaling cascade. Meanwhile caspase-dependent cell death mechanism has often been described as cardinal to 6-OHDA-induced apoptosis in SH-SY5Y cells, it is proposed that another caspase-independent mechanism may also exist in a cell death scenario [59]. Such claim is supported by literatures, stating that in dying cells, caspase inhibition alone does not necessary grant full resuscitation from apoptosis but may switch cell death to alternative autophagic or necrotic modes instead [60,61]. In fact, dysregulation of autophagic response in the neurons has been linked to PD incidence [62] and autophagic changes in SH-SY5Y cells are inducible with 6-OHDA treatment [63]. On the other hand, oxidative burst from 6-OHDA could contribute to membrane rupture and therefore necrosis in neurons too [64]. Considering that autophagy or other cell death mechanisms could be activated and participated in regulating cell death in our PD cell model, hence it is indefinite that inhibition of apoptosis or caspase activation by S2 treatment would see corresponding decrease in cell death or cytotoxicity. This may partly explain the failure of S2 extract to counteract cytotoxicity due to 6-OHDA exposure regardless of its ability to attenuate apoptosis and caspase-3 cleavage.

Conclusions

It has been successfully demonstrated that EBN extracts confer neuroprotection in 6-OHDA-challenged SH-SY5Y cell model. Particularly, S1 demonstrated neuroprotective potential by improving cell viability while S2 inhibited oxidative stress and caspase-3 activation. Both the EBN extracts shown to inhibit apoptosis. Further investigation is needed to identify and elaborate the properties of the bioactive compounds in EBN that are responsible for the neuroprotective benefits. In summary, the present study suggests that EBN may be effective in the treatment of neurodegenerative diseases where oxidative stress plays a causal role.

Abbreviations

6-OHDA: 6-hydroxydopamine; ARE: Antioxidant responsive element; Caco-2: Human colonic adenocarcinoma; DCF-DA: 2′ 7′-dichlorofluorescein diacetate; DMSO: Dimethyl sulphoxide; EBN: Edible bird's nest; EGF: Epidermal growth factor; MMP: Mitochondrial membrane potential; MNTD: Maximum non-toxic dose; MTT: 3-(4 5-dimethylthiazol-2-yl)-2, 5-diphenyltetrazolium bromide; Nrf2: nuclear erythroid 2-related factor 2; PBS: Phosphate-buffered saline; PD: Parkinson's disease; PI: Propidium iodide; ROS: Reactive oxygen species; SH-SY5Y: Human neuroblastoma cell.

Competing interests

The authors declare that they have no competing interests.

Authors' contributions

MYY carried out the study, performed the statistical analysis and penned the manuscript. RYK, SMC and KYN were involved in the design of the study, coordination of the experiment and revision of the manuscript. IO was involved in the design of the study and revision of the manuscript. All authors read and approved the final manuscript.

Acknowledgements

This study was supported by Exploratory Research Grant Scheme fund 2011 ERGS/1/2011/SKK/MUSM/03/3 from Ministry of Higher Education of Malaysia. The authors would also like to thank Dr Lim Chooi Ling for her guidance in preparing the EBN water extract.

Author details

[1]Jeffrey Cheah School of Medicine & Health Sciences, Monash University Malaysia, Selangor, Malaysia. [2]Department of Human Biology, School of Medicine, International Medical University, Kuala Lumpur, Malaysia.

Received: 25 April 2014 Accepted: 1 October 2014
Published: 13 October 2014

References

1. Dorsey ER, Constantinescu R, Thompson JP, Biglan KM, Holloway RG, Kieburtz K, Marshall FJ, Ravina BM, Schifitto G, Siderowf A, Tanner CM: **Projected number of people with Parkinson disease in the most populous nations, 2005 through 2030.** *Neurology* 2007, **68**(5):384–386.
2. Dauer W, Przedborski S: **Parkinson's disease: mechanisms and models.** *Neuron* 2003, **39**(6):889–909.
3. Przedborski S: **Pathogenesis of nigral cell death in Parkinson's disease.** *Parkinsonism Relat Disord* 2005, **11**(Suppl 1):S3–S7.
4. Snyder CH, Adler CH: **The patient with Parkinson's disease: part I-treating the motor symptoms; part II-treating the nonmotor symptoms.** *J Am Acad Nurse Pract* 2007, **19**(4):179–197.
5. Schulz JB: **Mechanisms of neurodegeneration in idiopathic Parkinson's disease.** *Parkinsonism Relat Disord* 2007, **13**(Suppl 3):S306–S308.
6. Melo A, Monteiro L, Lima RM, Oliveira DM, Cerqueira MD, El-Bacha RS: **Oxidative stress in neurodegenerative diseases: mechanisms and therapeutic perspectives.** *Oxid Med Cell Longev* 2011, **2011**:467180.
7. Farooqui T, Farooqui AA: **Lipid-mediated oxidative stress and inflammation in the pathogenesis of Parkinson's disease.** *Parkinsons Dis* 2011, **2011**:247467.
8. Gandhi S, Abramov AY: **Mechanism of Oxidative Stress in Neurodegeneration.** *Oxid Med Cell Longev* 2012, **2012**:11.
9. Mounsey RB, Teismann P: **Mitochondrial dysfunction in Parkinson's disease: pathogenesis and neuroprotection.** *Parkinsons Dis* 2010, **2011**:617472.
10. Bové J, Prou D, Perier C, Przedborski S: **Toxin-induced models of Parkinson's disease.** *Neurotherapeutics* 2005, **2**(3):484–494.
11. Ng MH, Chan KH, Kong YC: **Potentiation of mitogenic response by extracts of the swiftlet's (Collocalia) nest.** *Biochem Int* 1986, **13**(3):521–531.
12. Kong YC, Keung WM, Yip TT, Ko KM, Tsao SW, Ng MH: **Evidence that epidermal growth factor is present in swiftlet's (Collocalia) nest.** *Comp Biochem Physiol B, Comparative biochemistry* 1987, **87**(2):221–226.
13. Guo CT, Takahashi T, Bukawa W, Takahashi N, Yagi H, Kato K, Hidari KI, Miyamoto D, Suzuki T, Suzuki Y: **Edible bird's nest extract inhibits influenza virus infection.** *Antiviral Res* 2006, **70**(3):140–146.
14. Matsukawa N, Matsumoto M, Bukawa W, Chiji H, Nakayama K, Hara H, Tsukahara T: **Improvement of bone strength and dermal thickness due to dietary edible bird's nest extract in ovariectomized rats.** *Biosci Biotechnol Biochem* 2011, **75**(3):590–592.
15. Pozsgay V, Jennings H, Kasper DL: **4,8-anhydro-N-acetylneuraminic acid. Isolation from edible bird's nest and structure determination.** *Eur J Biochem* 1987, **162**(2):445–450.
16. Wieruszeski JM, Michalski JC, Montreuil J, Strecker G, Peter-Katalinic J, Egge H, van Halbeek H, Mutsaers JH, Vliegenthart JF: **Structure of the monosialyl oligosaccharides derived from salivary gland mucin glycoproteins of the Chinese swiftlet (genus Collocalia). Characterization of novel types of extended core structure, Gal beta(1——3)[GlcNAc beta(1——6)] GalNAc alpha(1——3)GalNAc(-ol), and of chain termination, [Gal alpha(1——4)] 0-1[Gal beta(1——4)]2Gl.** *J Biol Chem* 1987, **262**(14):6650–6657.
17. Yagi H, Yasukawa N, Yu SY, Guo CT, Takahashi N, Takahashi T, Bukawa W, Suzuki T, Khoo KH, Suzuki Y, Kato K: **The expression of sialylated high-antennary N-glycans in edible bird's nest.** *Carbohydr Res* 2008, **343**(8):1373–1377.
18. Schneider JS, Sendek S, Daskalakis C, Cambi F: **GM1 ganglioside in Parkinson's disease: Results of a five year open study.** *J Neurol Sci* 2010, **292**(1–2):45–51.
19. Wang B: **Molecular mechanism underlying sialic acid as an essential nutrient for brain development and cognition.** *Adv Nutr (Bethesda, Md)* 2012, **3**(3):465S–472S.
20. O'Keeffe GC, Tyers P, Aarsland D, Dalley JW, Barker RA, Caldwell MA: **Dopamine-induced proliferation of adult neural precursor cells in the mammalian subventricular zone is mediated through EGF.** *Proc Natl Acad Sci U S A* 2009, **106**(21):8754–8759.
21. Ninomiya M, Yamashita T, Araki N, Okano H, Sawamoto K: **Enhanced neurogenesis in the ischemic striatum following EGF-induced expansion of transit-amplifying cells in the subventricular zone.** *Neurosci Lett* 2006, **403**(1–2):63–67.
22. Voultsios A, Kennaway DJ, Dawson D: **Salivary melatonin as a circadian phase marker: validation and comparison to plasma melatonin.** *J Biol Rhythms* 1997, **12**(5):457–466.
23. Pammer J, Weninger W, Mildner M, Burian M, Wojta J, Tschachler E: **Vascular endothelial growth factor is constitutively expressed in normal human salivary glands and is secreted in the saliva of healthy individuals.** *J Pathol* 1998, **186**(2):186–191.
24. Falk T, Yue X, Zhang S, McCourt AD, Yee BJ, Gonzalez RT, Sherman SJ: **Vascular endothelial growth factor-B is neuroprotective in an in vivo rat model of Parkinson's disease.** *Neurosci Lett* 2011, **496**(1):43–47.
25. Mehraein F, Talebi R, Jameie B, Joghataie MT, Madjd Z: **Neuroprotective effect of exogenous melatonin on dopaminergic neurons of the substantia nigra in ovariectomized rats.** *Iran Biomed J* 2011, **15**(1–2):44–50.
26. Ossola B, Kaarainen TM, Raasmaja A, Mannisto PT: **Time-dependent protective and harmful effects of quercetin on 6-OHDA-induced toxicity in neuronal SH-SY5Y cells.** *Toxicology* 2008, **250**(1):1–8.
27. Rieger AM, Nelson KL, Konowalchuk JD, Barreda DR: **Modified Annexin V/Propidium Iodide Apoptosis Assay For Accurate Assessment of Cell Death.** *JoVE* 2011, **50**:e2597.
28. Lopes AP, Bagatela BS, Rosa PC, Nanayakkara DN, Carlos Tavares Carvalho J, Maistro EL, Bastos JK, Perazzo FF: **Antioxidant and cytotoxic effects of**

crude extract, fractions and 4-nerolidylcathecol from aerial parts of Pothomorphe umbellata L. (Piperaceae). *BioMed research international* 2013, **2013**:206581.
29. Hacker G: **The morphology of apoptosis.** *Cell Tissue Res* 2000, **301**(1):5–17.
30. Ziegler U, Groscurth P: **Morphological features of cell death.** *Physiology* 2004, **19**(3):124–128.
31. Tobón-Velasco JC, Limón-Pacheco JH, Orozco-Ibarra M, Macías-Silva M, Vázquez-Victorio G, Cuevas E, Ali SF, Cuadrado A, Pedraza-Chaverrí J, Santamaría A: **6-OHDA-induced apoptosis and mitochondrial dysfunction are mediated by early modulation of intracellular signals and interaction of Nrf2 and NF-κB factors.** *Toxicology* 2013, **304**:109–119.
32. Zainal Abidin F, Hui CK, Luan NS, Mohd Ramli ES, Hun LT, Abd Ghafar N: **Effects of edible bird's nest (EBN) on cultured rabbit corneal keratocytes.** *BMC Complement Altern Med* 2011, **11**:94.
33. A AR, WN WM: **Effect of edible bird's nest on cell proliferation and tumor necrosis factor-alpha (TNF-α) release in vitro.** *Int Food Res J* 2011, **18**:1123–1127.
34. Goh DLM, Chua KY, Chew FT, Liang RCMY, Seow TK, Ou KL, Yi FC, Lee BW: **Immunochemical characterization of edible bird's nest allergens.** *J Allergy Clin Immunol* 2001, **107**(6):1082–1088.
35. Zuo L, Otenbaker NP, Rose BA, Salisbury KS: **Molecular mechanisms of reactive oxygen species-related pulmonary inflammation and asthma.** *Mol Immunol* 2013, **56**(1–2):57–63.
36. Boldogh I, Bacsi A, Choudhury BK, Dharajiya N, Alam R, Hazra TK, Mitra S, Goldblum RM, Sur S: **ROS generated by pollen NADPH oxidase provide a signal that augments antigen-induced allergic airway inflammation.** *J Clin Invest* 2005, **115**(8):2169–2179.
37. Elias RJ, Kellerby SS, Decker EA: **Antioxidant activity of proteins and peptides.** *Crit Rev Food Sci Nutr* 2008, **48**(5):430–441.
38. Johnson JA, Johnson DA, Kraft AD, Calkins MJ, Jakel RJ, Vargas MR, Chen PC: **The Nrf2-ARE pathway: an indicator and modulator of oxidative stress in neurodegeneration.** *Ann N Y Acad Sci* 2008, **1147**:61–69.
39. Erdmann K, Grosser N, Schipporeit K, Schröder H: **The ACE Inhibitory Dipeptide Met-Tyr Diminishes Free Radical Formation in Human Endothelial Cells via Induction of Heme Oxygenase-1 and Ferritin.** *J Nutr* 2006, **136**(8):2148–2152.
40. Jakel RJ, Kern JT, Johnson DA, Johnson JA: **Induction of the protective antioxidant response element pathway by 6-hydroxydopamine in vivo and in vitro.** *Toxicol Sci* 2005, **87**(1):176–186.
41. Hara H, Ohta M, Ohta K, Kuno S, Adachi T: **Increase of antioxidative potential by tert-butylhydroquinone protects against cell death associated with 6-hydroxydopamine-induced oxidative stress in neuroblastoma SH-SY5Y cells.** *Brain Res Mol Brain Res* 2003, **119**(2):125–131.
42. Nguyen T, Nioi P, Pickett CB: **The Nrf2-Antioxidant response element signaling pathway and its activation by oxidative stress.** *J Biol Chem* 2009, **284**(20):13291–13295.
43. Singh S, Vrishni S, Singh BK, Rahman I, Kakkar P: **Nrf2-ARE stress response mechanism: a control point in oxidative stress-mediated dysfunctions and chronic inflammatory diseases.** *Free Radic Res* 2010, **44**(11):1267–1288.
44. Hara H, Ohta M, Adachi T: **Apomorphine protects against 6-hydroxydopamine-induced neuronal cell death through activation of the Nrf2-ARE pathway.** *J Neurosci Res* 2006, **84**(4):860–866.
45. Lotharius J, Dugan LL, O'Malley KL: **Distinct mechanisms underlie neurotoxin-mediated cell death in cultured dopaminergic neurons.** *J Neurosci* 1999, **19**(4):1284–1293.
46. Choi WS, Yoon SY, Oh TH, Choi EJ, O'Malley KL, Oh YJ: **Two distinct mechanisms are involved in 6-hydroxydopamine- and MPP + -induced dopaminergic neuronal cell death: role of caspases, ROS, and JNK.** *J Neurosci Res* 1999, **57**(1):86–94.
47. Holtz WA, Turetzky JM, Jong YJ, O'Malley KL: **Oxidative stress-triggered unfolded protein response is upstream of intrinsic cell death evoked by parkinsonian mimetics.** *J Neurochem* 2006, **99**(1):54–69.
48. Bernstein AI, Garrison SP, Zambetti GP, O'Malley KL: **6-OHDA generated ROS induces DNA damage and p53- and PUMA-dependent cell death.** *J Biol Chem* 2011, **6**(1):2.
49. Wei L, Sun C, Lei M, Li G, Yi L, Luo F, Li Y, Ding L, Liu Z, Li S, Xu P: **Activation of Wnt/beta-catenin pathway by exogenous Wnt1 protects SH-SY5Y cells against 6-hydroxydopamine toxicity.** *J Mol Neurosci* 2013, **49**(1):105–115.
50. Ikeda Y, Tsuji S, Satoh A, Ishikura M, Shirasawa T, Shimizu T: **Protective effects of astaxanthin on 6-hydroxydopamine-induced apoptosis in human neuroblastoma SH-SY5Y cells.** *J Neurochem* 2008, **107**(6):1730–1740.
51. Gomez-Lazaro M, Bonekamp NA, Galindo MF, Jordan J, Schrader M: **6-Hydroxydopamine (6-OHDA) induces Drp1-dependent mitochondrial fragmentation in SH-SY5Y cells.** *Free Radic Biol Med* 2008, **44**(11):1960–1969.
52. Kim HG, Ju MS, Kim DH, Hong J, Cho SH, Cho KH, Park W, Lee EH, Kim SY, Oh MS: **Protective effects of Chunghyuldan against ROS-mediated neuronal cell death in models of Parkinson's disease.** *Basic Clin Pharmacol Toxicol* 2010, **107**(6):958–964.
53. Storch A, Kaftan A, Burkhardt K, Schwarz J: **6-Hydroxydopamine toxicity towards human SH-SY5Y dopaminergic neuroblastoma cells: independent of mitochondrial energy metabolism.** *J Neural Transm* 2000, **107**(3):281–293.
54. Giordano S, Lee J, Darley-Usmar VM, Zhang J: **Distinct Effects of Rotenone, 1-methyl-4-phenylpyridinium and 6-hydroxydopamine on Cellular Bioenergetics and Cell Death.** *PLoS One* 2012, **7**(9):e44610.
55. Chang HY, Yang X: **Proteases for cell suicide: functions and regulation of caspases.** *Microbiol Mol Biol Rev* 2000, **64**(4):821–846.
56. Ossola B, Lantto TA, Puttonen KA, Tuominen RK, Raasmaja A, Männistö PT: **Minocycline protects SH-SY5Y cells from 6-hydroxydopamine by inhibiting both caspase-dependent and -independent programmed cell death.** *J Neurosci Res* 2012, **90**(3):682–690.
57. MacKenzie SH, Clark AC: **Death by caspase dimerization.** *Adv Exp Med Biol* 2012, **747**:55–73.
58. Nikoletopoulou V, Markaki M, Palikaras K, Tavernarakis N: **Crosstalk between apoptosis, necrosis and autophagy.** *Biochim Biophys Acta (BBA) - Molecular Cell Research* 2013, **1833**(12):3448–3459.
59. Kroemer G, Galluzzi L, Vandenabeele P, Abrams J, Alnemri ES, Baehrecke EH, Blagosklonny MV, El-Deiry WS, Golstein P, Green DR, Hengartner M, Knight RA, Kumar S, Lipton SA, Malomi W, Nuñez G, Peter ME, Tschopp J, Yuan J, Piacentini M, Zhivotovsky B, Melino G: **Classification of cell death: recommendations of the Nomenclature Committee on Cell Death 2009.** *Cell Death Differ* 2009, **16**(1):3–11.
60. Chipuk JE, Green DR: **Do inducers of apoptosis trigger caspase-independent cell death?** *Nat Rev Mol Cell Biol* 2005, **6**(3):268–275.
61. Golstein P, Kroemer G: **Redundant cell death mechanisms as relics and backups.** *Cell Death Differ* 2005, **12**(Suppl 2):1490–1496.
62. Cheung ZH, Ip NY: **The emerging role of autophagy in Parkinson's disease.** *Mol Brain* 2009, **2**:29.
63. Solesio ME, Saez-Atienzar S, Jordan J, Galindo MF: **Characterization of mitophagy in the 6-hydoxydopamine Parkinson's disease model.** *Toxicol Sci* 2012, **129**(2):411–420.
64. Chao J, Li H, Cheng K-W, Yu M-S, Chang RC-C, Wang M: **Protective effects of pinostilbene, a resveratrol methylated derivative, against 6-hydroxydopamine-induced neurotoxicity in SH-SY5Y cells.** *J Nutr Biochem* 2010, **21**(6):482–489.

doi:10.1186/1472-6882-14-391
Cite this article as: Yew *et al.*: Edible bird's nest ameliorates oxidative stress-induced apoptosis in SH-SY5Y human neuroblastoma cells. *BMC Complementary and Alternative Medicine* 2014 **14**:391.

Submit your next manuscript to BioMed Central and take full advantage of:

- **Convenient online submission**
- **Thorough peer review**
- **No space constraints or color figure charges**
- **Immediate publication on acceptance**
- **Inclusion in PubMed, CAS, Scopus and Google Scholar**
- **Research which is freely available for redistribution**

Submit your manuscript at
www.biomedcentral.com/submit

BioMed Central